LTV ASTRONAUTICS DIVISION
Ling-Temco-Vought, Inc.
P. O. Box 6267
Dallas, Texas 75222

TITLE

STUDY TO DETERMINE THE EFFECTS ON THE SCOUT VEHICLE STRUCTURE DUE TO UNCONVENTIONAL VEHICLE-SPACECRAFT CONFIGURATIONS

SUBMITTED UNDER
Task Order 4

REPORT NO.	DATED
23.175	20 November 1964
PROJECT	CONTRACT NO.
Scout	NAS1-3899

Scout Engineering
PREPARED

H. C. Scott
REVIEWED
H. C. Scott

C. D. Buehrle

G. Tarnower
APPROVED
G. Tarnower

REV.	DATE	REV. BY	PAGES AFFECTED	REMARKS
				ENCLOSURE (2) TO
				LTV LETTER NO.
				3-15000/4L-4440

3-52715

TABLE OF CONTENTS

Summary 1.1

Conclusions 1.2

Introduction 1.4

Weights 2.0

Loads and Dynamics 3.0

Structures 4.0

Stability and Control 5.0

Vehicle Design 6.0

Vehicle Performance 7.0

Thermal Analysis 8.0

References. 9.0

Summary

Under Contract NAS1-3899 Task Order 4, Ling-Temco-Vought Astronautics Division has been authorized to conduct a study "To Determine the Effects on the Scout Vehicle Structure Due to Unconventional Vehicle-Spacecraft Configurations."

For this study, a Scout Vehicle composed of the following motor stack was used:

First Stage	Algol IIB
Second Stage	Castor II
Third Stage	ABL X-259

Two (2) basic vehicle configurations were studied. These are:

Case I-A — 300 pound conical re-entry payload mounted in a current 34" diameter--25 Station Heatshield.

Case II-A — A 150 inch length 5° half angle conical payload which weighs 300, 400, 500 and 600 pounds.

A more detailed description of the payloads, weights, weight distribution, stiffness and center of gravity locations are presented in reference (a), as well as, in the individual sections of this report.

Conclusions

As a result of this study program, it is concluded that payloads representing an unconventional vehicle-spacecraft configuration, as defined by reference (a), can be flown on the Scout Vehicle with only small changes made to the present Scout production hardware.

STABILITY AND CONTROL

In order to provide the necessary H_2O_2 to satisfy the long second stage coast required to meet the desired re-entry trajectories for payloads of Cases I-A and II-A, an added deadband switching capability must be incorporated in the guidance and control system. With the incorporation of this additional switching function, no additional H_2O_2 tankage will be required. A complete description of this required change is presented in Section 5.0 of this report.

STRUCTURAL

For the Case I-A Configuration (with existing Scout heatshield) no structural changes to the vehicle are required. Also sufficient structural static tests have been conducted to demonstrate the Scout structural integrity for this configuration.

For the Case II-A Configuration, all structural analysis was based on the 600-pound weight configuration. A new Scout transition section will be required between the present Scout spin bearing and the payload. A detailed description of this new transition section is presented in Sections 4.0 and 6.0 of this report. Since this section is new, a complete qualification program will be required to demonstrate its integrity. It is recommended that this new transition section and the payload be qualified to the Scout design criteria under one complete test program.

GENERAL

This study was based on the use of a Castor II motor. To date, temperature data on the Castor II nozzle is preliminary and all analyses presented in Section 8.0 of this report were based on this preliminary data. It must be recognized that a final review of the Castor II nozzle temperature and its effect on the vehicle must be made after firm nozzle temperatures are established. Based on the results of data available, it does not appear that Castor II nozzle temperatures will have a significant effect on the present Scout hardware.

Based on the present available data, no changes in the Scout Ground Support Equipment (GSE) are anticipated. However, it must be noted that no consideration has been given to the physical handling of payloads, (GFE) for either Case I-A or II-A and no electrical interface has been provided between the vehicle and its payload.

This complete study has been based on Nominal Scout Motor performance data as presented in Section 7.0. Since the study uses Nominal Motor Performance data and must be updated for final motor performance at the time of actual motor assignment to a vehicle, the small changes in preliminary weights (discussed in Section 2.0) and vehicle drag configuration (discussed in Sections 5.0 and 7.0) will have no significant effects on the results of this study and are well within the state-of-the-art currently being used on the Scout Vehicle.

INTRODUCTION

Under Task Order 4 to Contract NAS1-3899, a study was conducted to "Determine the Effects on the Scout Vehicle Structure Due to Unconventional Vehicle-Spacecraft Configurations."

This study has been conducted using the criteria presented in the Statement of Work (reference (a)) in conjunction with the existing Scout Vehicle and philosophy. Maximum use has been made of Scout design data, studies, tests and flight test data during this study. At present, work is progressing on the basic Scout Vehicle to review some of the critical items that are defined in this study. However, this study was based on currently available information and represents changes required to the Scout Vehicle on the present state-of-the-art.

This study was conducted by the sections of the Engineering Department that are associated with the Scout Vehicle and is presented by the individual sections of responsibility. Each of these individual sections contains an introduction to that section and a description of the work accomplished.

STUDY

UNCONVENTIONAL VEHICLE - SPACECRAFT CONFIGURATION

WEIGHTS

Prepared by

E. S. Baker

E. S. Baker

Reviewed by

R. R. Siedell

R. R. Siedell

2.0 WEIGHTS

This section presents the weight, c.g. and mass moment of inertia for two unconventional vehicles, Case I A and Case II A-2.

These vehicles are based on a typical Scout vehicle, except the fourth stage motor has been omitted. Nominal weight data for the following motors were used for both Case I A and Case II A-2 Vehicles.

Antares	X 259
Castor	XM 33
Algol	II B

The Case I A Vehicle detail weight breakdown is presented on pages 2.2 through 2.8. Center of gravity and moment of inertia data are shown on page 2.9. The configuration includes a 300 pound payload and a 34" - 25" nose cone heat shield.

The Case II A-2 Vehicle detail weight breakdown is presented on pages 2.10 through 2.16. There are four configurations consisting of a 300, 400, 500, and 600 pound payload.

Vehicle stage weight, center of gravity and moment of inertia for the various payloads are shown on pages 2.17 through 2.20. All structural, loads and dynamics, stability control and trajectory analyses are based on preliminary weight data shown on pages 2.10 through 2.20.

The vehicle weights, c.g.'s and moment of inertia data shown on pages 2.21 through 2.24 reflect the current vehicle design and are included for comparison purposes to original data shown in pages 2.17 through 2.20. The weight change between the preliminary and revised vehicle weights is approximately -9.0 pounds. The effect of this weight increase on vehicle performance is discussed in Section 7.0.

UNCONVENTIONAL VEHICLE - SPACECRAFT

CASE I A

LTV ASTRONAUTICS DIVISION

Scout Vehicle Weight Report

Vehicle No.:

FOURTH STAGE WEIGHTS	Total Weight Pounds	C.G. Scout Sta.-In.	Moment Inch-Pounds
Interim Total	300.00		13305.
Interim Inert	300.00		13305.
Items:			
1. Payload and Separation System			
a. Payload (No.)	300.00	44.35	13305.
b. P/L Attach Ring	0.00		
c. Hdw - P/L Attach Ring	0.00		
d. CVC Sep Syst - Minus (b.+c.)	0.00		
e. Electrolyte	0.00		
f. Exp Bolts - P/L Sep Syst	0.00		
g. Hdw - Sep Syst to Mtr	0.00		
2. Motor and Hardware			
a. Altair (X-258) - Inert, S/N-	0.00		
b. Ign Harn	0.00		
c. Tape - Install Ign Harn	0.00		
d. Head Cap Transducer	0.00		
e. Reflective Tape or Paint	0.00		
3. Upper D			
a. Hdw - Upr D to Mtr	0.00		
b. Upr D Struct	0.00		
c. Upr D Harn	0.00		
d. Dynamic Bal Wts	0.00		
e. Ballast Wts	0.00		
Fourth Stage - Burnout	300.00	44.35	13305.
4. Consumed Weight			
a. Altair Internal - Cons	0.00		
Fourth Stage - Ignition	300.00	44.35	13305.

THIRD STAGE WEIGHTS	Total Weight Pounds	C.G. Scout Sta.-In.	Moment Inch-Pounds
Interim Total	3368.21		545223.
Interim Inert	778.21		129619.
5. Lower D Section			
1) Spin Items			
a. Sep Clamp	6.03	99.45	600.
b. Explosive Bolts	0.53	99.45	53.
c. Spin Motor - ( )	3.19	101.58	324.
d. Spin Table Structure	14.54	101.65	1478.
e. Harn + Hdw	3.50	101.55	355.
f. Ring + Hdw - Spin Brg Att	1.70	104.25	177.
g. Resistors and Clamps	0.54	101.75	55.
h. Inner Bearing Race	3.20	103.88	332.
2) Lower D			
a. Ring + Hdw - Spin to Lwr D	2.95	103.49	305.
b. Outer Bearing Race e	3.60	103.88	374.
c. Lwr D + Components	215.57	116.75	25168.
d. Electrolyte	1.82	115.75	211.
e. IRP Install + Hdw	21.42	112.35	2407.
f. Tunnel Covers	0.34	128.75	44.
g. Hdw - Tunnel Covers	0.09	128.75	12.
h. Hdw - Low D to Mtr	0.35	131.10	46.
6. Motor Section			
a. Antares (X-259) Inert, S/N	215.00	180.60	38829.
b. Fillet	0.35	191.15	67.
c. Head Cap Transducer	0.48	121.70	58.
d. Nozzle Tape	0.70	224.00	157.
e. Dome Tape	0.34	193.00	66.
f. Mtr Tunnels	6.45	157.71	1017.
g. Hdw - Mtr Tunnels	1.34	157.71	211.

THIRD STAGE WEIGHTS (Cont'd)	Total Weight Pounds	C.G. Scout Sta.-In.	Moment Inch-Pounds
6. Motor Section Cont'd.			
h. Tunnel Harn (T/M)	9.86	169.52	1671.
i. Tunnel Harn (Guid)	11.05	169.52	1873.
j. Harn + Hdw	0.79	169.52	134.
k. Dest Charges + Hdw	1.12	179.20	201.
l. Mtr Nozzle Shroud + Hdw	9.80	224.05	2196.
7. Upper C Section			
a. Hdw - Upr C to Mtr	0.86	191.95	165.
b. Upr C + Components	212.95	211.62	45064.
c. Electrolyte	0.26	215.00	56.
d. S/A + Hdw	2.10	230.83	485.
e. Static Bal Wts (225°)	1.98	203.60	403.
f. Static Bal Wts (270°)	6.50	231.40	1504.
g. Nitrogen - Remain	1.00	203.00	203.
h. Hyd Peroxide - Remain	8.50	203.00	1725.
i. Tunnel Covers	7.24	215.00	1557.
j. Hdw - Tunnel Covers	0.17	215.00	37.
Third Stage - Burnout	1078.21	132.56	142924.
8. Consumed Weight			
a. Antares Internal - Cons	2580.00	160.30	413574.
b. Hyd Peroxide - Cons	10.00	203.00	2030.
Third Stage - Ignition	3668.21	152.26	558528.

SECOND STAGE WEIGHTS

	Total Weight Pounds	C.G. Scout Sta.-In.	Moment Inch-Pounds
Interim Total	1Ø593.62		3688637.
Interim Inert	2178.12		777374.
9. Nose Cone Heat Shield			
a. Heat Shield ( )	242.ØØ	43.5Ø	1Ø527.
b. Explosives - For Actuator	Ø.Ø8	-17.ØØ	-1.
1Ø. Lower C Section			
a. Diaphragm - Lwr C to Upr C	27.5Ø	238.18	655Ø.
b. Lwr C + Components	59.93	243.22	14576.
c. Electrolyte	Ø.2Ø	244.ØØ	49.
d. S/A Unit + Hdw	2.1Ø	246.Ø2	517.
e. Tunnel Covers	3.74	245.Ø5	916.
f. Hdw - Tunnel Covers	Ø.16	245.Ø5	39.
g. Hdw - Lwr C to Mtr	2.34	253.Ø6	592.
h. Head Cap Pressure Tube	Ø.23	243.2Ø	56.
11. Motor Section			
a. Castor (XM 33) - Inert, S/N-	1386.ØØ	39Ø.43	541136.
b. Mtr Tunnels	2Ø.31	347.71	7Ø62.
c. Hdw - Mtr Tunnels	2.34	347.71	814.
d. Tunnel Harn (T/M)	2Ø.58	359.21	7393.
e. Tunnel Harn (Guid)	17.92	359.21	6437.
f. Hdw - Tunnel Harn	1.97	359.21	7Ø8.
g. Dest Charges + Hdw	1.84	338.Ø2	622.
h. Nozzle Insul Remain + Hdw	31.ØØ	473.ØØ	14663.

SECOND STAGE WEIGHTS (Cont'd)	Total Weight Pounds	C.G. Scout Sta.-In.	Moment Inch-Pounds
12. Upper B Section			
a. Hdw - Upr B to Mtr	1.53	437.56	669.
b. Upr B + Components	249.83	462.41	115524.
c. Tunnel Covers	4.42	468.ØØ	2Ø69.
d. Hdw - Tunnel Covers	Ø.1Ø	468.ØØ	47.
e. Nitrogen - Remain	7.ØØ	455.ØØ	3185.
f. Hyd Peroxide - Remain	95.ØØ	455.ØØ	43225.
Second Stage - Burnout	5846.33	228.5Ø	13359Ø2.
13. Consumed Weight			
a. Castor Internal - Cons	8321.5Ø	344.7Ø	2868421.
b. Hyd Peroxide - Cons	9Ø.ØØ	455.ØØ	4Ø95Ø.
c. Thermosorb - Cons	4.ØØ	473.ØØ	1892.
Second Stage - Ignition	14261.83	297.8Ø	4247165.

FIRST STAGE WEIGHTS	Total Weight Pounds	C.G. Scout Sta.-In.	Moment Inch-Pounds
Interim Total	24825.71		16337483.
Interim Inert	3367.71		2381200.
14. Castor Nozzle Plug	7.00	453.60	3175.
15. Lower B Section			
a. Diaphragm - Lwr B to Upr B	68.50	486.66	33336.
b. Lwr B + Components	102.39	489.92	50163.
c. Electrolyte	0.20	490.00	98.
d. S/A Unit + Hdw	2.10	492.00	1033.
e. Tunnel Covers	2.17	492.00	1068.
f. Hdw - Tunnel Covers	0.04	492.01	20.
g. Hdw - Lwr B to Mtr	0.99	495.80	491.
h. Head Cap Pressure Tube	0.25	489.90	122.
16. Hoist Ring Installation			
a. Hoist Ring	89.00	496.44	44183.
b. Hdw - Hoist Ring to Mtr	3.87	496.35	1921.
17. Motor Section			
a. Algol (II) - Inert, S/N-	2267.00	692.64	1570215.
b. Dest Charges + Hdw	3.31	646.00	2138.
c. Hdw - Tunnels to Mtr	4.89	652.10	3189.
d. Mtr Tunnels	36.25	652.10	23639.
e. Tunnel Harn (T/M)	24.48	653.05	15987.
f. Tunnel Harn (Guid)	23.29	653.05	15210.
g. Hdw - Tunnel Harn	3.31	653.05	2162.

FIRST STAGE WEIGHTS (Cont'd)	Total Weight Pounds	C.G. Scout Sta.-In.	Moment Inch-Pounds
18. Base A Section			
a. Hdw - Base A to Mtr	2.97	809.92	2405.
b. Base A + Components	721.40	841.52	607073.
c. Electrolyte	2.55	842.00	2147.
d. Tunnel Covers	1.70	815.00	1385.
e. Hdw - Tunnel Covers	0.05	815.00	41.
First Stage - Burnout	17629.54	375.98	6628365.
19. Consumed Weight			
a. Algol (II) Internal - Cons	21458.00	650.40	13956283.
First Stage - Ignition	39087.54	526.63	20584648.

300 LB. PAYLOAD

Case I A Weight, X(cg), and Moment of Inertia for Percent of Fuel Consumed

	Weight	X(cg)	Ixx Slug-Ft**2	Iyy Slug-Ft**2
Fourth Stage - Burnout	300.00	44.35	3.92	68.09
75 °/o	300.00	44.35	3.92	68.09
50 °/o	300.00	44.35	3.92	68.09
25 °/o	300.00	44.35	3.92	68.09
Fourth Stage - Ignition	300.00	44.35	3.92	68.09
Spin-up Items	333.23	50.06	4.79	89.67
Third Stage - Burnout	1078.21	132.56	25.98	1150.23
75 °/o	1725.71	143.03	47.62	1287.06
50 °/o	2373.21	147.79	64.57	1384.27
25 °/o	3020.71	150.51	76.86	1463.21
Third Stage - Ignition	3668.21	152.26	84.48	1533.41
Less N/C - H/S	5604.25	236.50	163.50	20442.33
Second Stage - Burnout	5846.33	228.50	174.41	22391.48
75 °/o	7950.20	259.58	271.89	28474.77
50 °/o	10054.08	277.65	343.50	32619.44
25 °/o	12157.95	289.47	391.57	35826.07
Second Stage - Ignition	14261.83	297.80	413.80	38504.85
First Stage - Burnout	17629.54	375.98	699.02	149991.84
75 °/o	22994.04	440.00	1081.18	226241.72
50 °/o	28358.54	479.80	1375.16	277161.56
25 °/o	33723.04	506.94	1571.17	314784.53
First Stage - Ignition	39087.54	526.63	1679.02	344592.28

UNCONVENTIONAL VEHICLE - SPACECRAFT

CASE II A-2

LTV ASTRONAUTICS DIVISION

Scout Vehicle Weight Report

Vehicle No.:

FOURTH STAGE WEIGHTS	Total Weight Pounds	C.G. Scout Sta.-In.	Moment Inch-Pounds
Interim Total	6ØØ.ØØ		1482Ø.
Interim Inert	6ØØ.ØØ		1482Ø.
Items:			
1. Payload and Separation System			
a. Payload (No.)	6ØØ.ØØ	24.7Ø	1482Ø.
b. P/L Attach Ring	Ø.ØØ		
c. Hdw - P/L Attach Ring	Ø.ØØ		
d. CVC Sep Syst - Minus (b.+c.)	Ø.ØØ		
e. Electrolyte	Ø.ØØ		
f. Exp Bolts - P/L Sep Syst	Ø.ØØ		
g. Hdw - Sep Syst to Mtr	Ø.ØØ		
2. Motor and Hardware			
a. Altair (X-258) - Inert, S/N-	Ø.ØØ		
b. Ign Harn	Ø.ØØ		
c. Tape - Install Ign Harn	Ø.ØØ		
d. Head Cap Transducer	Ø.ØØ		
e. Reflective Tape or Paint	Ø.ØØ		
3. Upper D			
a. Hdw - Upr D to Mtr	Ø.ØØ		
b. Upr D Struct	Ø.ØØ		
c. Upr D Harn	Ø.ØØ		
d. Dynamic Bal Wts	Ø.ØØ		
e. Ballast Wts	Ø.ØØ		
Fourth Stage - Burnout	6ØØ.ØØ	24.7Ø	1482Ø.
4. Consumed Weight			
a. Altair Internal - Cons	Ø.ØØ		
Fourth Stage - Ignition	6ØØ.ØØ	24.7Ø	1482Ø.

THIRD STAGE WEIGHTS	Total Weight Pounds	C.G. Scout Sta.-In.	Moment Inch-Pounds
Interim Total	3378.43		546262.
Interim Inert	788.43		130658.
5. Lower D Section			
1) Spin Items			
a. Sep Clamp	7.12	99.45	708.
b. Explosive Bolts	0.53	99.45	53.
c. Spin Motor - ( )	3.50	101.58	356.
d. Spin Table Structure	21.93	101.65	2229.
e. Harn + Hdw	3.87	101.55	393.
f. Ring + Hdw - Spin Brg Att	1.79	104.25	187.
g. Resistors and Clamps	0.55	101.75	56.
h. Inner Bearing Race	3.51	103.88	365.
2) Lower D			
a. Ring + Hdw - Spin to Lwr D	3.21	103.49	332.
b. Outer Bearing Race	3.99	103.88	414.
c. Lwr D + Components	215.57	116.75	25168.
d. Electrolyte	1.82	115.75	211.
e. IRP Install + Hdw	21.42	112.35	2407.
f. Tunnel Covers	0.34	128.75	44.
g. Hdw - Tunnel Covers	0.09	128.75	12.
h. Hdw - Low D to Mtr	0.35	131.10	46.
6. Motor Section			
a. Antares (X-259) Inert, S/N(Nom)	215.00	180.60	38829.
b. Fillet	0.35	191.15	67.
c. Head Cap Transducer	0.48	121.70	58.
d. Nozzle Tape	0.70	224.00	157.
e. Dome Tape	0.34	193.00	66.
f. Mtr Tunnels	6.45	157.71	1017.
g. Hdw - Mtr Tunnels	1.34	157.71	211.

THIRD STAGE WEIGHTS (Cont'd)	Total Weight Pounds	C.G. Scout Sta.-In.	Moment Inch-Pounds
6. Motor Section Cont'd.			
h. Tunnel Harn (T/M)	9.86	169.52	1671.
i. Tunnel Harn (Guid)	11.Ø5	169.52	1873.
j. Harn + Hdw	Ø.79	169.52	134.
k. Dest Charges + Hdw	1.12	179.2Ø	2Ø1.
l. Mtr Nozzle Shroud + Hdw	9.8Ø	224.Ø5	2196.
7. Upper C Section			
a. Hdw - Upr C to Mtr	Ø.86	191.95	165.
b. Upr C + Components	212.95	211.62	45Ø64.
c. Electrolyte	Ø.26	215.ØØ	56.
d. S/A + Hdw	2.1Ø	23Ø.83	485.
e. Static Bal Wts (225°)	1.98	2Ø3.6Ø	4Ø3.
f. Static Bal Wts (27Ø°)	6.5Ø	231.4Ø	15Ø4.
g. Nitrogen - Remain	1.ØØ	2Ø3.ØØ	2Ø3.
h. Hyd Peroxide - Remain	8.5Ø	2Ø3.ØØ	1725.
i. Tunnel Covers	7.24	215.ØØ	1557.
j. Hdw - Tunnel Covers	Ø.17	215.ØØ	37.
Third Stage - Burnout	1388.43	1Ø4.78	145478.
8. Consumed Weight			
a. Antares Internal - Cons	258Ø.ØØ	16Ø.3Ø	413574.
b. Hyd Peroxide - Cons	1Ø.ØØ	2Ø3.ØØ	2Ø3Ø.
Third Stage - Ignition	3978.43	141.Ø3	561Ø82.

SECOND STAGE WEIGHTS

	Total Weight Pounds	C.G. Scout Sta.-In.	Moment Inch-Pounds
Interim Total	10351.54		3678111.
Interim Inert	1936.04		766848.
9. Nose Cone Heat Shield			
a. Heat Shield ( )	0.00		
b. Explosives - For Actuator	0.00		
10. Lower C Section			
a. Diaphragm - Lwr C to Upr C	27.50	238.18	6550.
b. Lwr C + Components	59.93	243.22	14576.
c. Electrolyte	0.20	244.00	49.
d. S/A Unit + Hdw	2.10	246.02	517.
e. Tunnel Covers	3.74	245.05	916.
f. Hdw - Tunnel Covers	0.16	245.05	39.
g. Hdw - Lwr C to Mtr	2.34	253.06	592.
h. Head Cap Pressure Tube	0.23	243.20	56.
11. Motor Section			
a. Castor (XM 33) - Inert, S/N-	1386.00	390.43	541136.
b. Mtr Tunnels	20.31	347.71	7062.
c. Hdw - Mtr Tunnels	2.34	347.71	814.
d. Tunnel Harn (T/M)	20.58	359.21	7393.
e. Tunnel Harn (Guid)	17.92	359.21	6437.
f. Hdw - Tunnel Harn	1.97	359.21	708.
g. Dest Charges + Hdw	1.84	338.02	622.
h. Nozzle Insul Remain + Hdw	31.00	473.00	14663.

SECOND STAGE WEIGHTS (Cont'd)	Total Weight Pounds	C.G. Scout Sta.-In.	Moment Inch-Pounds
12. Upper B Section			
a. Hdw - Upr B to Mtr	1.53	437.56	669.
b. Upr B + Components	249.83	462.41	115524.
c. Tunnel Covers	4.42	468.ØØ	2Ø69.
d. Hdw - Tunnel Covers	Ø.1Ø	468.ØØ	47.
e. Nitrogen - Remain	7.ØØ	455.ØØ	3185.
f. Hyd Peroxide - Remain	95.ØØ	455.ØØ	43225.
Second Stage - Burnout	5914.47	224.52	132793Ø.
13. Consumed Weight			
a. Castor Internal - Cons	8321.5Ø	344.7Ø	2868421.
b. Hyd Peroxide - Cons	9Ø.ØØ	455.ØØ	4Ø95Ø.
c. Thermosorb - Cons	4.ØØ	473.ØØ	1892.
Second Stage - Ignition	14329.97	295.83	4239193.

FIRST STAGE WEIGHTS	Total Weight Pounds	C.G. Scout Sta.-In.	Moment Inch-Pounds
Interim Total	24825.71		16337483.
Interim Inert	3367.71		2381200.
14. Castor Nozzle Plug	7.00	453.60	3175.
15. Lower B Section			
a. Diaphragm - Lwr B to Upr B	68.50	486.66	33336.
b. Lwr B + Components	102.39	489.92	50163.
c. Electrolyte	0.20	490.00	98.
d. S/A Unit + Hdw	2.10	492.00	1033.
e. Tunnel Covers	2.17	492.00	1068.
f. Hdw - Tunnel Covers	0.04	492.01	20.
g. Hdw - Lwr B to Mtr	0.99	495.80	491.
h. Head Cap Pressure Tube	0.25	489.90	122.
16. Hoist Ring Installation			
a. Hoist Ring	89.00	496.44	44183.
b. Hdw - Hoist Ring to Mtr	3.87	496.35	1921.
17. Motor Section			
a. Algol (II) - Inert, S/N-	2267.00	692.64	1570215.
b. Dest Charges + Hdw	3.31	646.00	2138.
c. Hdw - Tunnels to Mtr	4.89	652.10	3189.
d. Mtr Tunnels	36.25	652.10	23639.
e. Tunnel Harn (T/M)	24.48	653.05	15987.
f. Tunnel Harn (Guid)	23.29	653.05	15210.
g. Hdw - Tunnel Harn	3.31	653.05	2162.

FIRST STAGE WEIGHTS (Cont'd)	Total Weight Pounds	C.G. Scout Sta.-In.	Moment Inch-Pounds
18. Base A Section			
a. Hdw - Base A to Mtr	2.97	809.92	2405.
b. Base A + Components	721.40	841.52	607073.
c. Electrolyte	2.55	842.00	2147.
d. Tunnel Covers	1.70	815.00	1385.
e. Hdw - Tunnel Covers	0.05	815.00	41.
First Stage - Burnout	17697.68	374.08	6620393.
19. Consumed Weight			
a. Algol (II) Internal - Cons	21458.00	650.40	13956283.
First Stage - Ignition	39155.68	525.51	20576676.

300 LB. PAYLOAD

Case II A-2 Weight, X(cg), and Moment of Inertia for Percent of Fuel Consumed

	Weight	X(cg)	Ixx Slug-Ft**2	Iyy Slug-Ft**2
Fourth Stage - Burnout	300.00	24.70	3.92	123.37
75 %	300.00	24.70	3.92	123.37
50 %	300.00	24.70	3.92	123.37
25 %	300.00	24.70	3.92	123.37
Fourth Stage - Ignition	300.00	24.70	3.92	123.37
Spin-up Items	342.80	34.30	5.08	171.73
Third Stage - Burnout	1088.43	126.86	26.29	1449.59
75 %	1735.93	139.39	47.94	1617.41
50 %	2383.43	145.12	64.88	1728.93
25 %	3030.93	148.40	77.17	1816.12
Third Stage - Ignition	3678.43	150.52	84.80	1891.68
Less N/C - H/S	5614.47	235.20	172.36	21202.67
Second Stage - Burnout	5614.47	235.20	172.36	21202.67
75 %	7718.34	265.39	263.19	26679.23
50 %	9822.22	282.64	329.92	30409.51
25 %	11926.09	293.81	374.79	33312.16
Second Stage - Ignition	14029.97	301.62	395.58	35754.60
First Stage - Burnout	17397.68	380.11	680.81	145104.94
75 %	22762.18	443.81	1062.96	219158.40
50 %	28126.68	483.21	1356.94	268511.15
25 %	33491.18	509.99	1552.96	304977.51
First Stage - Ignition	38855.68	529.38	1660.81	333901.62

400 LB. PAYLOAD

Case II A-2 Weight, X(cg), and Moment of Inertia

for Percent of Fuel Consumed

	Weight	X(cg)	Ixx Slug-Ft**2	Iyy Slug-Ft**2
Fourth Stage - Burnout	400.00	24.70	5.23	164.50
75 °/o	400.00	24.70	5.23	164.50
50 °/o	400.00	24.70	5.23	164.50
25 °/o	400.00	24.70	5.23	164.50
Fourth Stage - Ignition	400.00	24.70	5.23	164.50
Spin-up Items	442.80	32.13	6.39	214.39
Third Stage - Burnout	1188.43	118.26	27.60	1697.01
75 °/o	1835.93	133.15	49.24	1927.00
50 °/o	2483.43	140.27	66.19	2070.43
25 °/o	3130.93	144.44	78.48	2176.95
Third Stage - Ignition	3778.43	147.19	86.10	2265.45
Less N/C - H/S	5714.47	231.52	173.67	22183.46
Second Stage - Burnout	5714.47	231.52	173.67	22183.46
75 °/o	7818.34	262.31	264.50	27954.73
50 °/o	9922.22	280.04	331.23	31872.24
25 °/o	12026.09	291.57	376.10	34903.39
Second Stage - Ignition	14129.97	299.67	396.89	37439.25
First Stage - Burnout	17497.68	378.08	682.11	147856.91
75 °/o	22862.18	441.98	1064.27	222974.29
50 °/o	28226.68	481.59	1358.25	273073.94
25 °/o	33591.18	508.55	1554.26	310086.78
First Stage - Ignition	38955.68	528.08	1662.11	339426.12

500 LB. PAYLOAD

Case II A-2 Weight, X(cg), and Moment of Inertia

for Percent of Fuel Consumed

	Weight	X(cg)	Ixx Slug-Ft**2	Iyy Slug-Ft**2
Fourth Stage - Burnout	500.00	24.70	6.53	205.62
75 %	500.00	24.70	6.53	205.62
50 %	500.00	24.70	6.53	205.62
25 %	500.00	24.70	6.53	205.62
Fourth Stage - Ignition	500.00	24.70	6.53	205.62
Spin-up Items	542.80	30.76	7.70	256.48
Third Stage - Burnout	1288.43	111.00	28.91	1912.41
75 %	1935.93	127.54	50.55	2208.85
50 %	2583.43	135.79	67.49	2388.68
25 %	3230.93	140.74	79.79	2517.99
Third Stage - Ignition	3878.43	144.03	87.41	2622.08
Less N/C - H/S	5814.47	227.96	174.98	23131.93
Second Stage - Burnout	5814.47	227.96	174.98	23131.93
75 %	7918.34	259.31	265.80	29199.06
50 %	10022.22	277.49	332.54	33306.59
25 %	12126.09	289.37	377.41	36469.05
Second Stage - Ignition	14229.97	297.73	398.20	39100.80
First Stage - Burnout	17597.68	376.07	683.42	150578.07
75 %	22962.18	440.16	1065.58	226757.30
50 %	28326.68	479.97	1359.56	277604.80
25 %	33691.18	507.11	1555.57	315165.95
First Stage - Ignition	39055.68	526.79	1663.42	344922.54

600 LB. PAYLOAD

Case II A-2 Weight, X(cg), and Moment of Inertia

for Percent of Fuel Consumed

	Weight	X(cg)	Ixx Slug-Ft**2	Iyy Slug-Ft**2
Fourth Stage - Burnout	600.00	24.70	7.84	246.74
75 °/o	600.00	24.70	7.84	246.74
50 °/o	600.00	24.70	7.84	246.74
25 °/o	600.00	24.70	7.84	246.74
Fourth Stage - Ignition	600.00	24.70	7.84	246.74
Spin-up Items	642.80	29.82	9.01	298.28
Third Stage - Burnout	1388.43	104.78	30.21	2102.70
75 °/o	2035.93	122.49	51.86	2467.05
50 °/o	2683.43	131.65	68.80	2686.27
25 °/o	3330.93	137.26	81.09	2841.02
Third Stage - Ignition	3978.43	141.03	88.72	2962.84
Less N/C - H/S	5914.47	224.52	176.28	24049.72
Second Stage - Burnout	5914.47	224.52	176.28	24049.72
75 °/o	8018.34	256.38	267.11	30413.37
50 °/o	10122.22	275.00	333.85	34713.42
25 °/o	12226.09	287.20	378.71	38009.78
Second Stage - Ignition	14329.97	295.83	399.50	40739.74
First Stage - Burnout	17697.68	374.08	684.73	153268.94
75 °/o	23062.18	438.36	1066.89	230507.86
50 °/o	28426.68	478.37	1360.87	282104.07
25 °/o	33791.18	505.68	1556.88	320215.31
First Stage - Ignition	39155.68	525.51	1664.73	350391.09

300 LB. PAYLOAD

Revised Case II A-2 Weight, X(cg), and Moment of Inertia
for Percent of Fuel Consumed

	Weight	X(cg)	Ixx Slug-Ft**2	Iyy Slug-Ft**2
Fourth Stage - Burnout	300.00	23.25	3.92	123.37
75 %	300.00	23.25	3.92	123.37
50 %	300.00	23.25	3.92	123.37
25 %	300.00	23.25	3.92	123.37
Fourth Stage - Ignition	300.00	23.25	3.92	123.37
Spin-up Items	351.87	34.94	5.33	184.07
Third Stage - Burnout	1097.50	126.30	26.54	1469.68
75 %	1745.00	138.97	48.18	1641.15
50 %	2392.50	144.79	65.13	1754.54
25 %	3040.00	148.13	77.42	1842.86
Third Stage - Ignition	3687.50	150.30	85.04	1919.18
Less N/C - H/S	5623.54	234.92	172.61	21274.46
Second Stage - Burnout	5623.54	234.92	172.61	21274.46
75 %	7727.41	265.14	263.44	26773.62
50 %	9831.29	282.43	330.17	30518.43
25 %	11935.16	293.63	375.04	33431.10
Second Stage - Ignition	14039.04	301.47	395.83	35880.86
First Stage - Burnout	17406.75	379.94	681.05	145317.75
75 %	22771.25	443.66	1063.21	219459.21
50 %	28135.75	483.08	1357.19	268874.36
25 %	33500.25	509.87	1553.20	305386.60
First Stage - Ignition	38864.75	529.27	1661.05	334345.67

400 LB. PAYLOAD

Revised Case II A-2 Weight, X(cg), and Moment of Inertia for Percent of Fuel Consumed

	Weight	X(cg)	Ixx Slug-Ft**2	Iyy Slug-Ft**2
Fourth Stage - Burnout	400.00	23.25	5.23	164.50
75 %	400.00	23.25	5.23	164.50
50 %	400.00	23.25	5.23	164.50
25 %	400.00	23.25	5.23	164.50
Fourth Stage - Ignition	400.00	23.25	5.23	164.50
Spin-up Items	451.87	32.35	6.64	227.49
Third Stage - Burnout	1197.50	117.69	27.85	1720.86
75 %	1845.00	132.70	49.49	1955.67
50 %	2492.50	139.91	66.43	2101.72
25 %	3140.00	144.15	78.73	2209.87
Third Stage - Ignition	3787.50	146.94	86.35	2299.49
Less N/C - H/S	5723.54	231.22	173.92	22265.72
Second Stage - Burnout	5723.54	231.22	173.92	22265.72
75 %	7827.41	262.05	264.74	28061.56
50 %	9931.29	279.82	331.48	31994.91
25 %	12035.16	291.38	376.35	35037.03
Second Stage - Ignition	14139.04	299.50	397.13	37580.91
First Stage - Burnout	17506.75	377.90	682.36	148089.34
75 %	22871.25	441.82	1064.52	223298.50
50 %	28235.75	481.45	1358.50	273463.09
25 %	33600.25	508.42	1554.51	310523.64
First Stage - Ignition	38964.75	527.97	1662.36	339899.33

500 LB. PAYLOAD

Revised Case II A-2 Weight, X(cg), and Moment of Inertia for Percent of Fuel Consumed

	Weight	X(cg)	Ixx Slug-Ft**2	Iyy Slug-Ft**2
Fourth Stage - Burnout	500.00	23.25	6.53	205.62
75 °/o	500.00	23.25	6.53	205.62
50 °/o	500.00	23.25	6.53	205.62
25 °/o	500.00	23.25	6.53	205.62
Fourth Stage - Ignition	500.00	23.25	6.53	205.62
Spin-up Items	551.87	30.70	7.95	270.08
Third Stage - Burnout	1297.50	110.41	29.15	1939.65
75 °/o	1945.00	127.08	50.80	2242.07
50 °/o	2592.50	135.41	67.74	2425.29
25 °/o	3240.00	140.42	80.03	2556.76
Third Stage - Ignition	3887.50	143.76	87.66	2662.34
Less N/C - H/S	5823.54	227.65	175.22	23224.35
Second Stage - Burnout	5823.54	227.65	175.22	23224.35
75 °/o	7927.41	259.04	266.05	29318.05
50 °/o	10031.29	277.27	332.78	33442.77
25 °/o	12135.16	289.17	377.65	36617.17
Second Stage - Ignition	14239.04	297.56	398.44	39257.65
First Stage - Burnout	17606.75	375.89	683.67	150829.90
75 °/o	22971.25	440.00	1065.83	227104.73
50 °/o	28335.75	479.83	1359.80	278019.72
25 °/o	33700.25	506.98	1555.82	315630.44
First Stage - Ignition	39064.75	526.68	1663.67	345424.78

600 LB. PAYLOAD

Revised Case II A-2 Weight, X(cg), and Moment of Inertia

for Percent of Fuel Consumed

	Weight	X(cg)	Ixx Slug-Ft**2	Iyy Slug-Ft**2
Fourth Stage - Burnout	600.00	23.25	7.84	246.74
75 %	600.00	23.25	7.84	246.74
50 %	600.00	23.25	7.84	246.74
25 %	600.00	23.25	7.84	246.74
Fourth Stage - Ignition	600.00	23.25	7.84	246.74
Spin-up Items	651.87	29.56	9.25	312.22
Third Stage - Burnout	1397.50	104.18	30.46	2133.03
75 %	2045.00	122.00	52.10	2504.49
50 %	2692.50	131.25	69.05	2727.87
25 %	3340.00	136.91	81.34	2885.34
Third Stage - Ignition	3987.50	140.74	88.96	3009.06
Less N/C - H/S	5923.54	224.20	176.53	24152.00
Second Stage - Burnout	5923.54	224.20	176.53	24152.00
75 %	8027.41	256.10	267.36	30544.25
50 %	10131.29	274.76	334.09	34862.86
25 %	12235.16	287.00	378.96	38172.14
Second Stage - Ignition	14339.04	295.65	399.75	40911.58
First Stage - Burnout	17706.75	373.90	684.98	153539.98
75 %	23071.25	438.19	1067.13	230878.31
50 %	28435.75	478.22	1361.11	282544.60
25 %	33800.25	505.55	1557.12	320707.27
First Stage - Ignition	39164.75	525.39	1664.97	350922.21

"UNCONVENTIONAL VEHICLE - SPACECRAFT STUDY"

STRUCTURAL DYNAMICS

Prepared by

G. W. Kreiter

G. W. Kreiter

Reviewed by

D. C. Fritz

D. C. Fritz

SYMBOL TABLE

Symbol	Definition
$[A_A]$	Inertia Matrix of the Vehicle
$[A_B]$	Inertia Matrix of the Payload
$[E_A]$	Influence Coefficient Matrix of the Vehicle
$[K_A]$	Stiffness Matrix of the Vehicle
$[K_B]$	Stiffness Matrix of the Payload
K_S	Spin Bearing Joint Stiffness
$\{p_A\}$	Matrix of Generalized Coordinates of the Vehicle
$\{p_B\}$	Matrix of Generalized Coordinates of the Payload
$\{q_A\}$	Matrix of Generalized Displacements of the Vehicle
$\{q_B\}$	Matrix of Generalized Displacements of the Payload
$\{q_S\}$	Matrix of Generalized Displacements of the Spin Bearing
$[T_{BA}]$	Transformation Matrix Relating Displacements of the Payload to the Vehicle
T	Kinetic Energy
U	Potential Energy
$\bar{x}$	Location of Center of Gravity
x_i	Location of i^{th} Panel Point
$[\Phi_A]$	Modal Matrix of Vehicle
$[\Phi_B]$	Modal Matrix of Payload
$\{\Phi_S\}$	Modal Matrix of Spin Bearing
λ	Eigenvalues
$\{\Phi\}, \{\Pi\}$	Eigenvectors

3.0 SUMMARY

The study reported in this section was made to determine the effects on loads and vehicle dynamics of adapting the hypersonic re-entry spacecraft to the Scout vehicle. The study analyzed two types of re-entry spacecraft, the first being a 300 lb. cone shaped payload which fits inside the standard 34 inch diameter heat shield with the bumper at Station 47.7 removed. The second configuration was a 12.5 foot long cone shaped payload varying in weight from 300 to 600 pounds, which did not require a heat shield.

Areas of interest in the study for the first configuration were the coupled modes of vibration and relative clearance of vehicle and payload. The results of the study showed that clearance between the payload and heat shield is not a problem and the coupled modes and frequencies are not significantly different from those of the basic Scout vehicle.

Since the second configuration was significantly different from the basic Scout vehicle, the modes of vibration and natural frequencies of the various stages were calculated. The flight loads were also calculated. The results of this study revealed that without providing an additional load path at Station 103.7 (spin bearing), such as a Marmon clamp, the third stage bending frequencies were undesirably low. As an example, the 600 lb. payload fundamental bending frequency was 8.46 cps at third stage ignition. Therefore, to increase the stiffness, a Marmon clamp, which is torqued to limit load, is provided across the spin bearing at Station 103.7. This increases the joint stiffness sufficiently to raise the bending frequency to 13.22 cps for the above example, which is acceptable. The flight loads were found to be considerably less than the flight loads on the basic Scout vehicle, when the Marmon clamp at Station 103.7 is used. Therefore, no wind restrictions are required on this configuration.

3.1.0 Configuration I A

This configuration was basically a standard Scout vehicle, except the bumper inside the heat shield is removed and there is no fourth stage motor. The payload is a right circular cone with its forward most point at Station -11.0. Since the bumper at Station 47.7 is removed, the payload is cantilevered from the spin bearing. Consequently, the areas of most concern on this configuration are clearance and modal coupling of the vehicle and payload.

3.1.1 Basic Data

The basic data for this configuration is the same as for a Scout vehicle aft of Station 103.7. Forward of this station the payload properties are defined in the statement of work, reference A. The heat shield properties are those of a standard 34 inch diameter heat shield with nose station at -25.0. The weight and stiffness distributions are shown in Figure 3.1 and Table 3.1, respectively.

In the calculations for the coupled modes of the system, the value used for joint stiffness of the spin bearing was $.13 \times 10^8 \frac{\text{in-lb}}{\text{rad}}$. The value used for the joint stiffness with the Marmon clamp at the spin bearing was $.289 \times 10^9 \frac{\text{in-lb}}{\text{rad}}$. Both of these values were based on past experience on the Scout vehicle.

3.1.2 Modal Coupling

Consider the structure divided into two parts which are elastically uncoupled. That is, strain energy can be stored in one part without inducing deformations in the other part. Let $\{p_A\}$ be a set of generalized co-ordinates describing the configuration of the vehicle and $\{p_B\}$ be a set of generalized co-ordinates describing the configuration of the payload. Then the kinetic energy may be written as

$$T = 1/2 \{\dot{p}_A\}' [A_A] \{\dot{p}_A\} + 1/2 \{\dot{p}_B\}' [A_B] \{\dot{p}_B\} \tag{1}$$

and the strain energy may be written as

$$U = 1/2 \{p_A\}' [K_A] \{p_A\} + 1/2 \{p_B\}' [K_B] \{p_B\} \tag{2}$$

If the payload is considered as a rigid body, its displacements can be related to those of the vehicle by a geometric transformation

$$\{p_B\} = [T_{BA}] \{p_A\} \tag{3}$$

A general displacement of the payload when elastic is given by

$$\{p_B\} = [T_{BA}] \{p_A\} + [\phi_B] \{q_B\} + [\phi_S] \{q_S\} \tag{4}$$

where $[\phi_B]$ is a matrix of the modes of the payload cantilevered from the spin bearing when the vehicle is motionless and $[\phi_S]$ is the modal matrix of the spin bearing; for our case being rotation only or $\{\bar{x} - x_{Bi}\} = \{\phi_S\}$.

The total kinetic energy when the payload is rigid is

$$T = 1/2 \{\dot{p}_A\}' [A_A] \{\dot{p}_A\} + 1/2 \{\dot{p}_A\}' [T_{BA}]' [A_B] [T_{BA}] \{\dot{p}_A\}$$

$$T = 1/2 \{\dot{p}_A\}' \left([A_A] + [T_{BA}]' [A_B] [T_{BA}]\right) \{\dot{p}_A\} \tag{5}$$

The vehicle vibration modes with payload rigid are obtained from

$$[E_A] \left([A_A] + [T_{BA}]' [A_B] [T_{BA}]\right) \{\phi\} = \lambda \{\phi\} \tag{6}$$

Where $[E_A]$ is the inverse of $[K_A]$. From equation (6) the free - free modes of the vehicle can be obtained by classical methods.

We then have

$$\{P_A\} = [\phi_A]\{q_A\} \tag{7}$$

and therefore from equation (4)

$$\{P_B\} = [T_{BA}][\phi_A]\{q_A\} + [\phi_B]\{q_B\} + \{\phi_s\}\{q_s\}$$

or

$$\begin{bmatrix} \{P_A\} \\ \{P_B\} \end{bmatrix} = [\phi] \begin{bmatrix} \{q_A\} \\ \{q_B\} \\ \{q_s\} \end{bmatrix} \qquad [\phi] = \begin{bmatrix} [\phi_A] & [0] & \{0\} \\ [T_{BA}][\phi_A] & [\phi_B] & \{\phi_s\} \end{bmatrix} \tag{9}$$

The kinetic energy can then be written

$$T = 1/2 \left[\{\dot{q}_A\}' \{\dot{q}_B\}' \{\dot{q}_s\}' \right] [M] \begin{bmatrix} \{\dot{q}_A\} \\ \{\dot{q}_B\} \\ \{\dot{q}_s\} \end{bmatrix} \tag{10}$$

where

$$[M] = \begin{bmatrix} [A_A] & [0] \\ [0] & [A_B] \end{bmatrix} \tag{11}$$

Since $[T_{BA}]\{P_A\}$

represents a rigid displacement of the payload with respect to the vehicle, we must conclude that

$$[K_B][T_{BA}]\{P_A\} = \{0\}$$

or

$$[K_B][T_{BA}] = [0] \tag{12}$$

The strain energy from equation (2) can be written as

$$U = 1/2 \left[\{q_A\}' \{q_B\}' \{q_s\}' \right] [F] \begin{bmatrix} \{q_A\} \\ \{q_B\} \\ \{q_s\} \end{bmatrix} \tag{13}$$

where
$$\left[F\right]=\left[\phi\right]'\begin{bmatrix}[K_A] & [0]\\ [0] & [K_B]\end{bmatrix}\left[\phi\right]$$

Using equation (12) we conclude that

$$\left[F\right]=\begin{bmatrix}[\phi_A]'[K_A][\phi_A] & [0] & [0]\\ [0] & [\phi_B]'[K_B][\phi_B] & \{\phi_s\}'K_s\{\phi_s\}\end{bmatrix}$$

Furthermore, we know

$$[\phi_A]'[K_A][\phi_A]=\left[{}^{1}\!/\!\lambda_{Ai}\right]$$

$$[\phi_B]'[K_B][\phi_B]=\left[{}^{1}\!/\!\lambda_{Bi}\right]$$

so that the total "modal" stiffness matrix for an elastically uncoupled system is diagonal. Hence

$$\left[F\right]=\begin{bmatrix}1/\lambda_{Ai} & & \\ & 1/\lambda_{Bi} & \\ & & K_s\end{bmatrix}$$

The vibration modes of the coupled system are obtained by iterating

$$[G][M]\{\pi\}=\lambda\{\pi\} \tag{14}$$

where

$$[G]=[F]^{-1}$$

The matrix of eigenvectors to this problem are used to determine the natural vibration modes of the coupled system in the form

$$\begin{bmatrix}\{P_A\}\\ \{P_B\}\end{bmatrix}=[\phi][\pi]\{q\} \tag{15}$$

Hence the matrix of natural bending modes is simply

$$\{P\}=[\varphi]\{q\} \tag{16}$$

where

$$[\varphi]=[\phi][\pi]$$

In this study the first 4 elastic modes of the vehicle and the first 2 elastic modes of the payload along with the mode of the rigid payload hinged by the spin bearing were used in determining the modes of the coupled system. The results of these calculations are shown in Figures 3.2 to 3.5.

3.1.3 Clearance

Having the coupled modes of the system, the relative deflection of the payload and vehicle may be determined. The design criteria for the payload area is for the structure to withstand 10 g's axially and 3 g's laterally at the CG of the payload. Maximum deflection will occur when loads corresponding to this criteria are applied. If it is assumed that all the motion occurs in a single mode and that the vibrating acceleration is 3 g's at the C.G. of the payload and sinusoidial, the relative deflection may be determined as follows:

Since we have shown that

$$\{p\} = [\phi]\{q\}$$

in equation (16), the acceleration is

$$\{\ddot{p}\} = [\phi]\{\ddot{q}\} \tag{17}$$

For a single mode

$$\{\ddot{p}\} = \{\phi_i\}\ddot{q}_i$$

and for the acceleration of a single point, the C.G. of the payload for example,

$$\ddot{p}_{CG} = \phi_{CG}\,\ddot{q}_i \tag{18}$$

For displacements the expression is still valid, e.g., for points on the heat shield as well.

$$p_{H.S.} = \phi_{H.S.}\,q_i$$

or

$$p_{CG} = \phi_{CG}\,q_i \tag{19}$$

$$\frac{p_{H.S}}{p_{CG}} = \frac{\phi_{H.S.}}{\phi_{PL}}$$

Thus the relative displacement of the heat shield with respect to the C.G. of the payload is

$$p_{H.S} = p_{CG}\,\frac{\phi_{H.S.}}{\phi_{CG}} \tag{20}$$

or displacement of the payload with respect to the C.G. of the payload is

$$p_{PL} = p_{CG}\,\frac{\phi_{PL}}{\phi_{CG}} \tag{21}$$

Since the response was assumed sinusoidial

$$p_{CG} = \frac{\ddot{p}_{CG}}{\omega_j^2}$$

Where ω_j is the circular natural frequency of the j^{th} mode. Also, the $\ddot{p}_{CG}$ was assumed to be 3 g's. Substituting these expressions into equations (20) and (21) yields the expression

$$p_{H.S} = \frac{\phi_{H.S}}{\phi_{CG}}\,\frac{3g}{\omega_j^2} \tag{22}$$

and

$$P_{P.L.} = \frac{\phi_{P.L.}}{\phi_{cg}} \frac{3g}{\omega_j^2}$$

From these equations plots of the relative deflection were made and the results are shown in Figures 3.6 to 3.9. These figures show that when all the motion is considered to be in the first vibrational bending mode the relative displacement between the payload and heat shield centerline is 0.36 inches at Station -11.0. The clearance at this station is approximately 10.0 inches. If the motion is considered to be all in the fourth mode the relative displacement is 8.9 inches at Station -11.0. However, experience on the Scout vehicle has shown that, in general, most of the vibratory motion occurs in the first mode. Relative deflections at other stations are smaller than at Station -11.0 and, therefore, of less concern.

3.1.4 Loads

Flight and hoist loads were not calculated for this configuration since it was not significantly different from the basic Scout vehicle. Furthermore, the dynamic response of the payload does not appear to increase the loads significantly from those payloads which do have a bumper at Station 47.7.

3.2.0 Configuration II A-2

This configuration of the study consisted of a basic Scout vehicle aft of Station 103.7. Forward of this station a 12.5 foot cone shaped payload is attached. Since the vehicle is significantly different from the basic Scout, the vibrational bending modes and frequencies and flight loads are of interest.

3.2.1 Basic Data

For this configuration the vehicle has the following motor stack:

(1) First stage motor - Algol IIB

(2) Second stage motor - Castor II

(3) Third stage motor - X-259

The stiffness and weight distributions for this configuration are shown in Table 3.2 and Figure 3.10, respectively. The weight distribution shown is for a 600 lb. payload; however, payload weights of 300, 400, and 500 lb. were also investigated, with the weight distribution being consistent with the statement of work, reference A.

The values for the joint stiffnesses for this configuration are shown in Table 3.5. It should be pointed out that the value for the joint stiffness at Station 103.7 is shown as infinity, but calculations were made with the value for the joint stiffness of $.115 \times 10^8 \frac{\text{in-lb}}{\text{rad}}$. These latter calculations proved conclusively that a Marmon clamp must be used at this joint to ensure sufficient stiffness. The value of $.115 \times 10^8 \frac{\text{in-lb}}{\text{rad}}$ was used because it is the lowest value for spin bearing joint stiffness indicated on Scout flight records.

Aerodynamic and drag data used in the flight loads calculations are shown in Section 5.0 of this report.

3.2.2 Mode Shapes and Frequencies

The vibrational bending modes and frequencies for this configuration were calculated for the vehicle in the free - free condition. Classical methods were used to determine these mode shapes.

Figures 3.11 to 3.22 present the first and second vibration bending modes at ignition of the first, second and third stages for the 300, 400, 500, and 600 lb. payload, respectively. Table 3.3 is a summary of the natural bending frequencies for these modes.

A summary of the natural bending frequencies for the 4 payload weights when the joint stiffness for the spin bearing is assumed to be $.115 \times 10^8 \frac{\text{in-lb}}{\text{rad}}$ are shown in Table 3.4.

3.2.3 Flight Loads

The flight loads for this configuration were calculated using a flexible body dynamic response computer routine. A complete description of this routine and the necessary input data can be found in reference C. The input data includes the predicted engine performance of a nominal Algol IIB motor, the vehicle weight distribution with a 600 lb. payload, and the exact pitch program. A more detailed description of the pitch program can be found in Section 7.0 of this report. The wind profile used in these calculations is the profile shown in the Scout Specification, reference B.

The results of these calculations are shown in Figure 3.23, which reveals that the loads are considerably less than the flight loads on a Scout vehicle. These loads were calculated for a peak wind altitude of 27,000 feet and a peak wind speed of 300 ft/sec., which represent the most critical condition. Figure 3.23 shows that Station 131.1, the critical station, experiences 214,000 in-lb. maximum flight moment for a side wind. The flight allowable bending moment for this station is 392,500 in-lbs. The maximum axial loads experienced are shown in Figure 3.24.

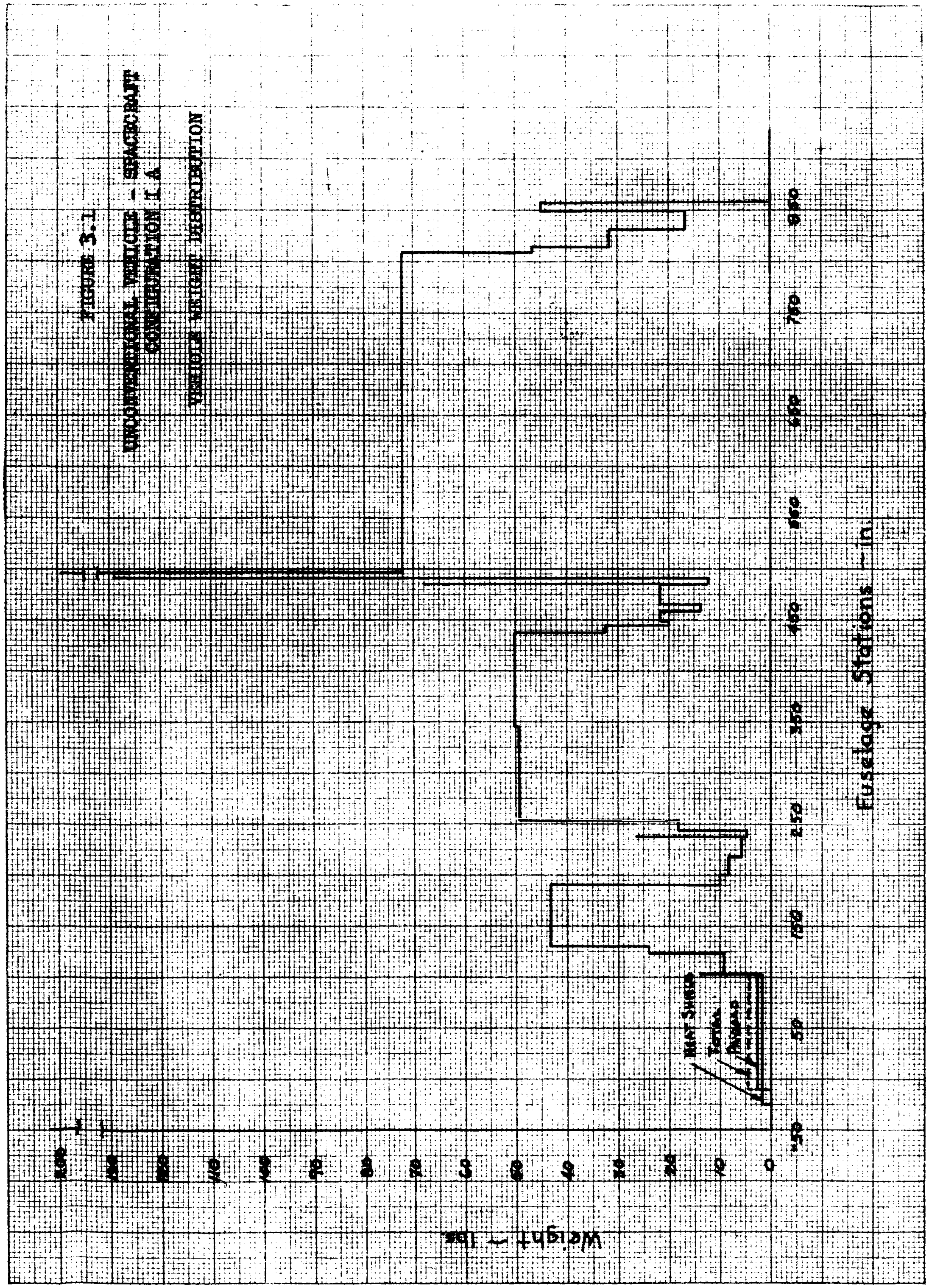
FIGURE 3.1
UNCONVENTIONAL VEHICLE - SPACECRAFT
CONFIGURATION I A
VEHICLE WEIGHT DISTRIBUTION
Heat Shield
Total
Payload
Weight ~ lbs.
Fuselage Stations ~ in.

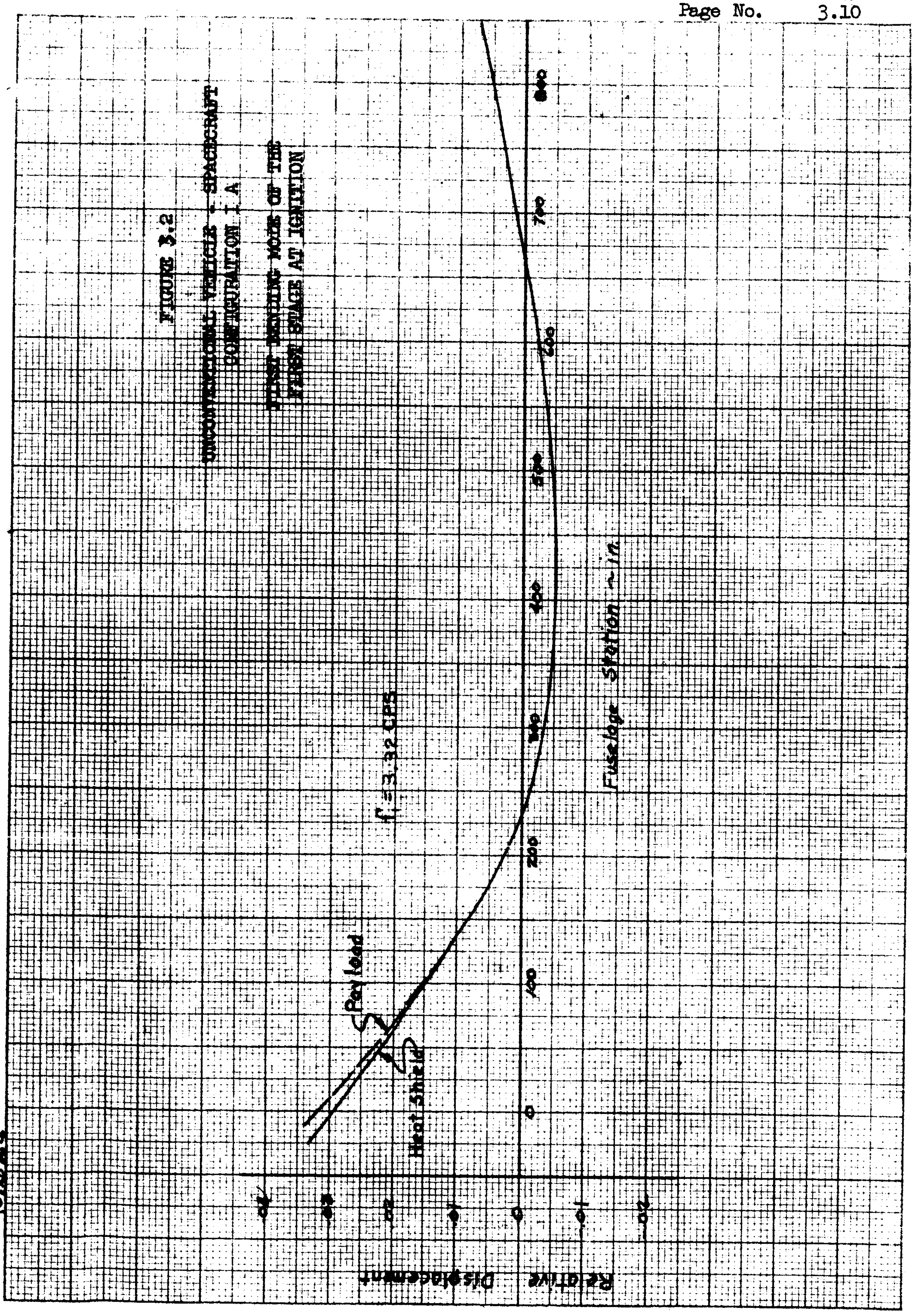

FIGURE 3.2
UNCONVENTIONAL VEHICLE - SPACECRAFT CONFIGURATION 1 A
FIRST BENDING MODE OF THE FIRST STAGE AT IGNITION

10/30/63

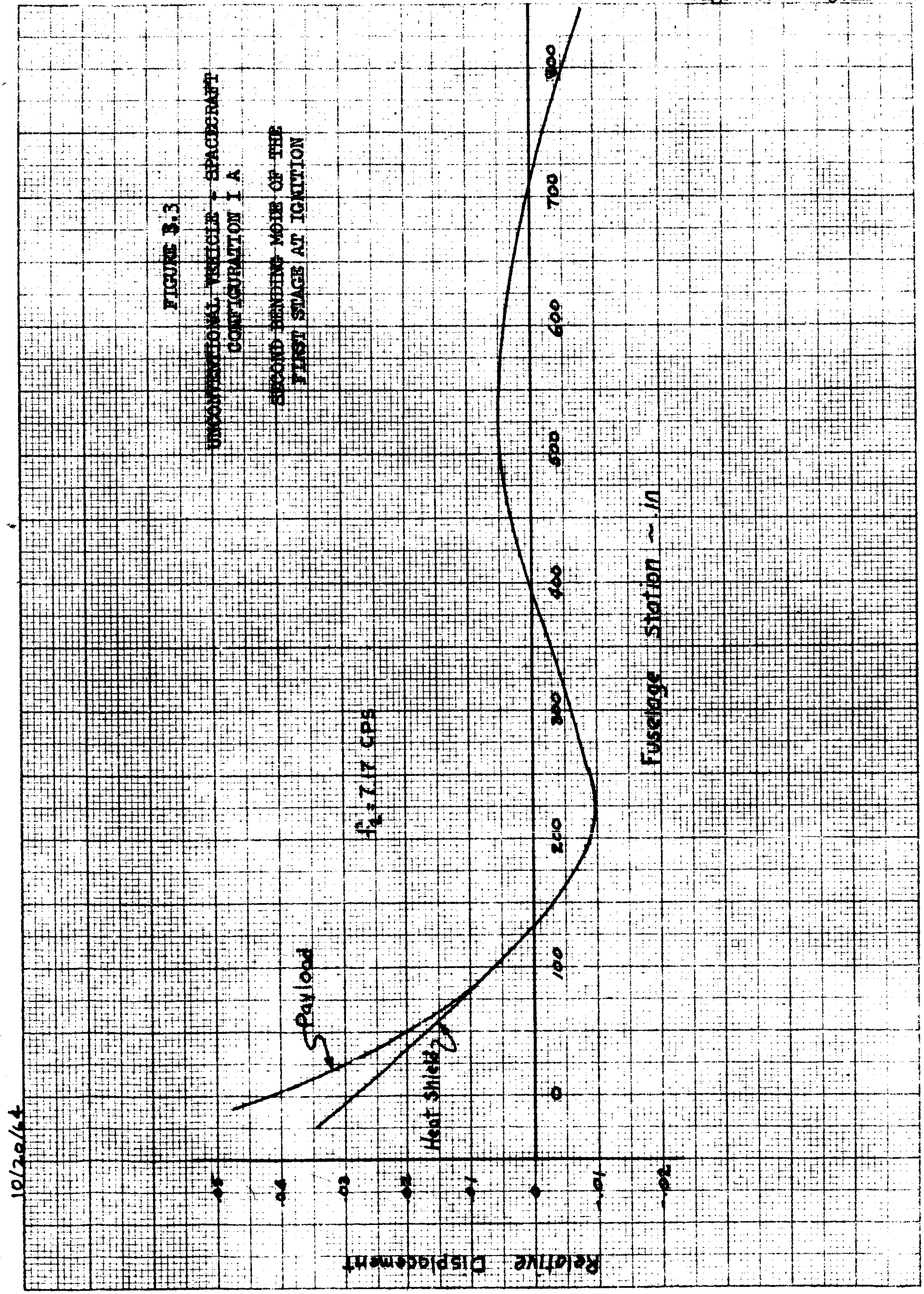
FIGURE 3.3
UNCONVENTIONAL VEHICLE - SPACECRAFT
CONFIGURATION I A
SECOND BENDING MODE OF THE
FIRST STAGE AT IGNITION
f2 = 7.17 CPS
Payload
Heat Shield
Fuselage Station ~ in
Relative Displacement
0
100
200
300
400
500
600
700
800
.5
.4
.3
.2
.1
0
-.01
-.02
10/20/64

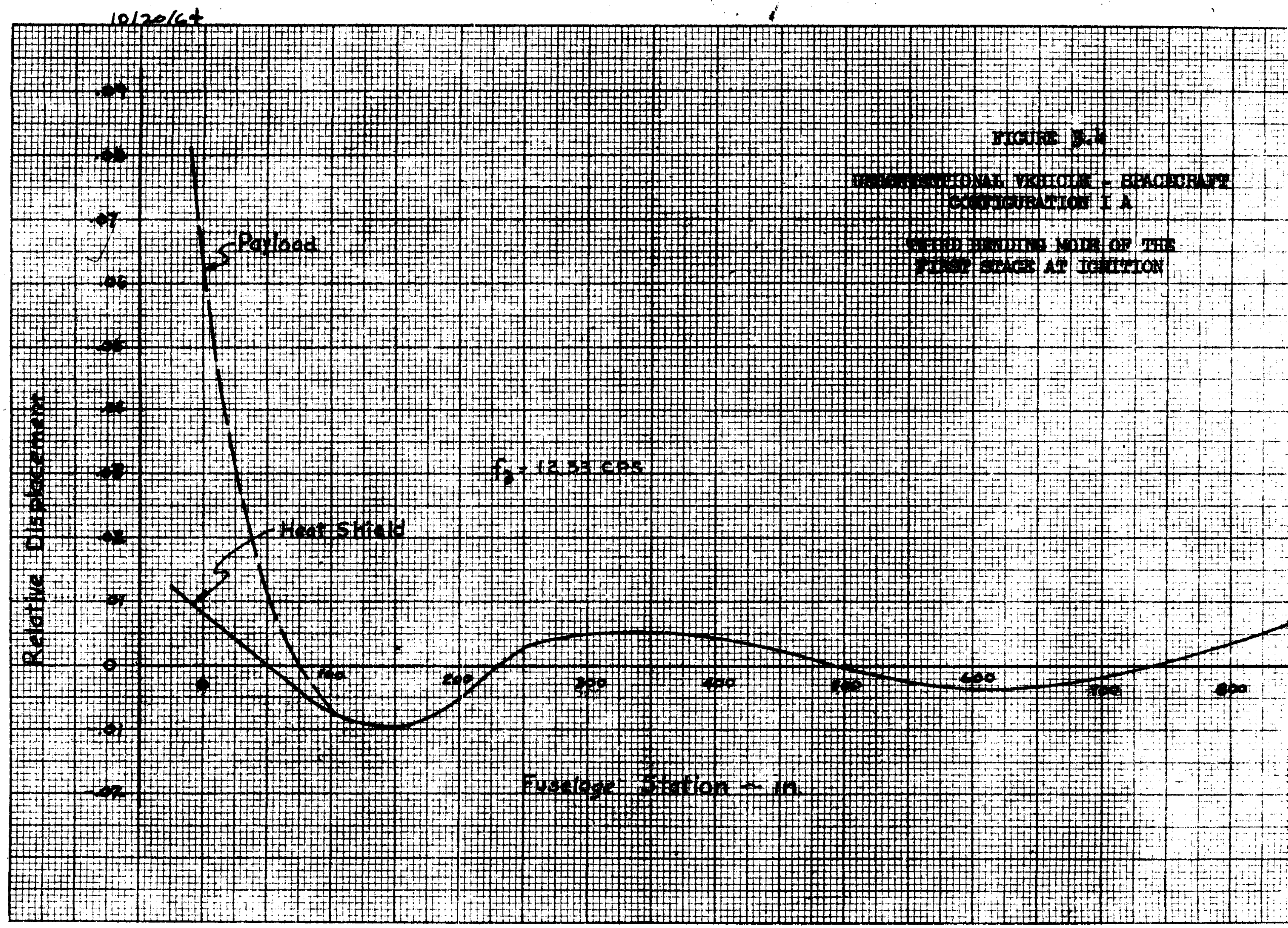
10/20/64
FIGURE B.4
UNCONVENTIONAL VEHICLE - SPACECRAFT
CONFIGURATION I A
THIRD BENDING MODE OF THE
FIRST STAGE AT IGNITION
Payload
Heat Shield
f3 = 12.33 CPS
Relative Displacement
Fusolage Station ~ in.
0
100
200
300
400
500
600
700
800
.01
-.01
-.02

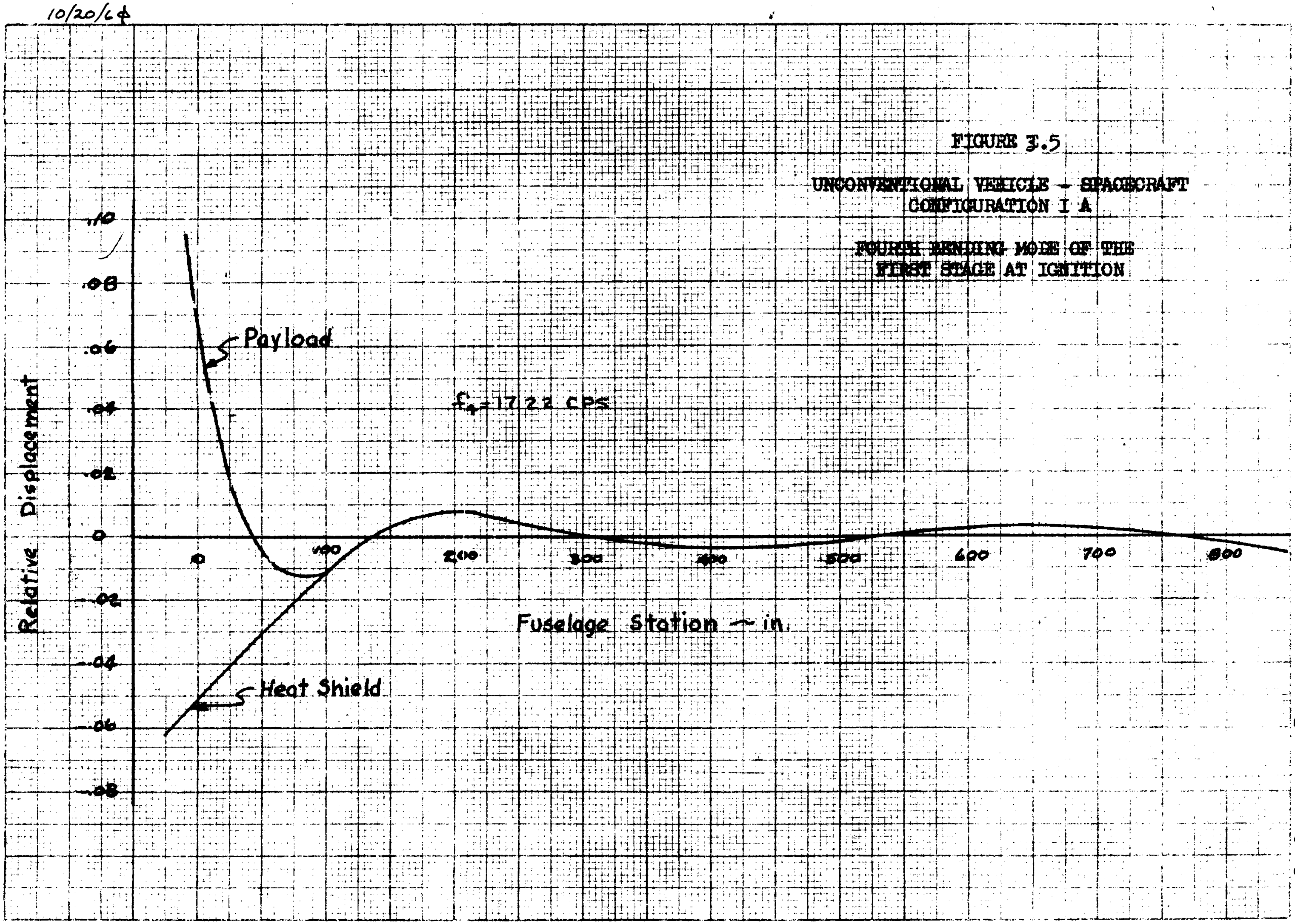

FIGURE 3.5

UNCONVENTIONAL VEHICLE - SPACECRAFT
CONFIGURATION I A

FOURTH BENDING MODE OF THE
FIRST STAGE AT IGNITION

10/20/64

FIGURE 3.6

UNCONVENTIONAL VEHICLE - SPACECRAFT
CASE IA CONFIGURATION

DISPLACEMENT OF THE PAYLOAD AND HEAT SHIELD CENTER LINES FROM THE VEHICLE CENTER LINE

CONDITIONS:
(1) 3 g Acceleration at Payload CG
(2) All Response is Sinusoidal and in the First Mode (Freq. = 3.32 cps)

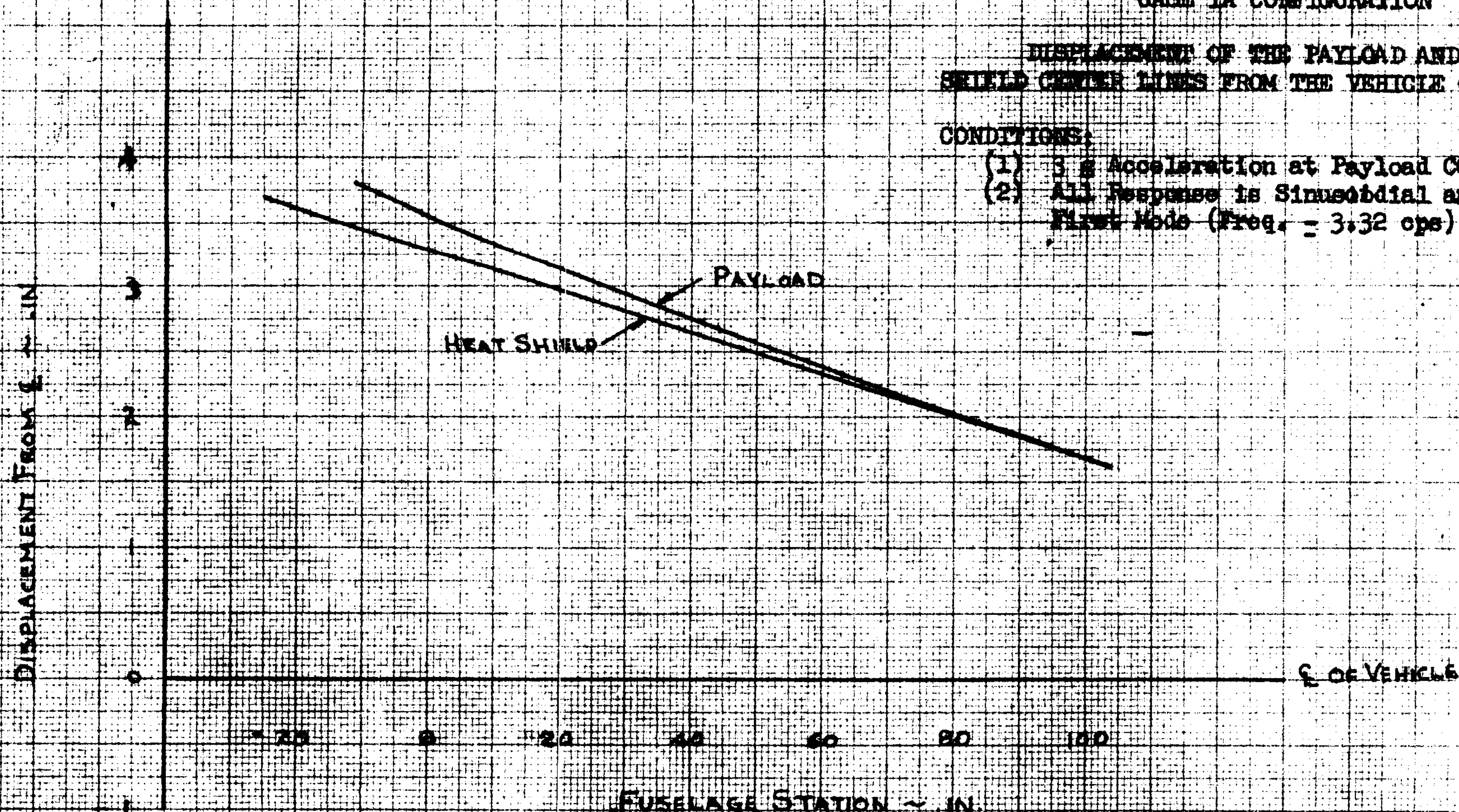

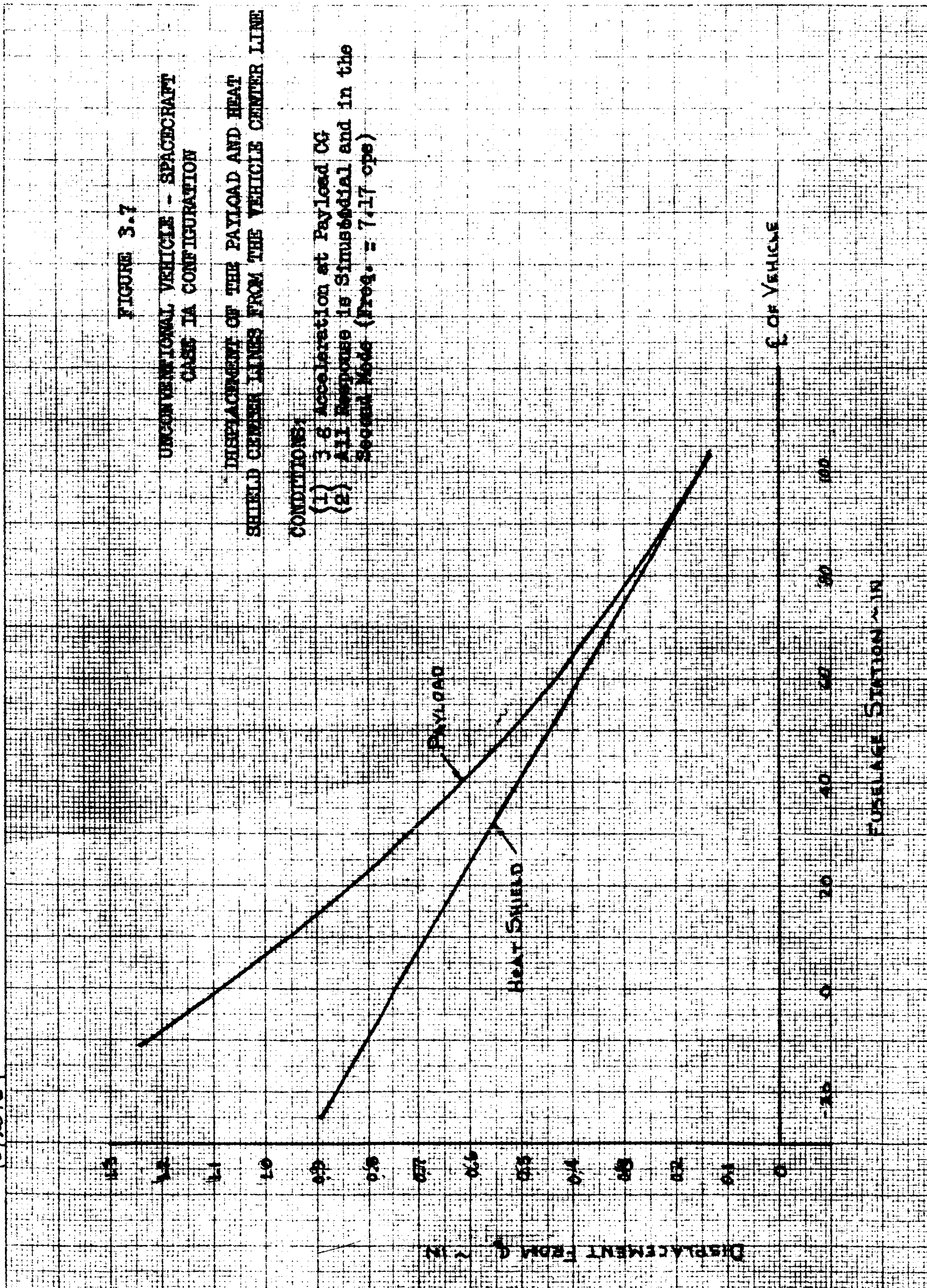

FIGURE 3.7

UNCONVENTIONAL VEHICLE - SPACECRAFT
CASE IA CONFIGURATION

DISPLACEMENT OF THE PAYLOAD AND HEAT
SHIELD CENTER LINES FROM THE VEHICLE CENTER LINE

CONDITIONS:
(1) 3 g Acceleration at Payload CG
(2) All Response is Sinusoidal and in the Second Mode (Freq. = 7.17 cps)

10/20/64

10/20/64

FIGURE 3.8

UNCONVENTIONAL VEHICLE - SPACECRAFT
CASE IA CONFIGURATION

DISPLACEMENT OF THE PAYLOAD AND HEAT SHIELD CENTER LINES FROM THE VEHICLE CENTER LINE

CONDITIONS:
(1) 3 g Acceleration at Payload CG
(2) All Response is Sinusoidial and in the Third Mode (Freq. = 12.33 cps)

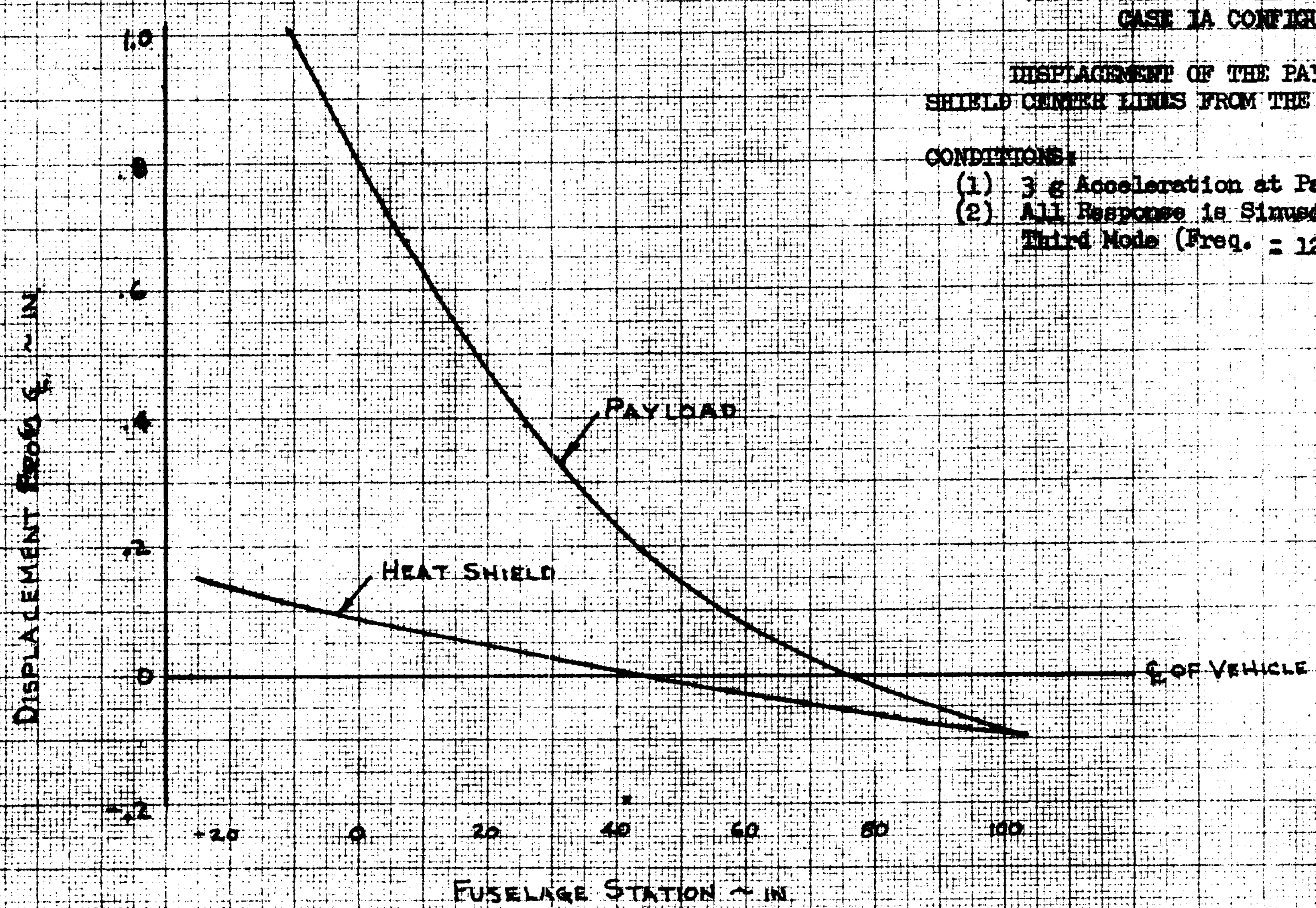

10/20/64

FIGURE 3.9

UNCONVENTIONAL VEHICLE - SPACECRAFT
CASE IA CONFIGURATION

DISPLACEMENT OF THE PAYLOAD AND HEAT
SHIELD CENTER LINES FROM THE VEHICLE CENTER LINE

CONDITIONS:
(1) 3 g Acceleration at Payload CG
(2) All Response is Sinusoidial and in the
Fourth Mode (Freq. = 17.22 cps)

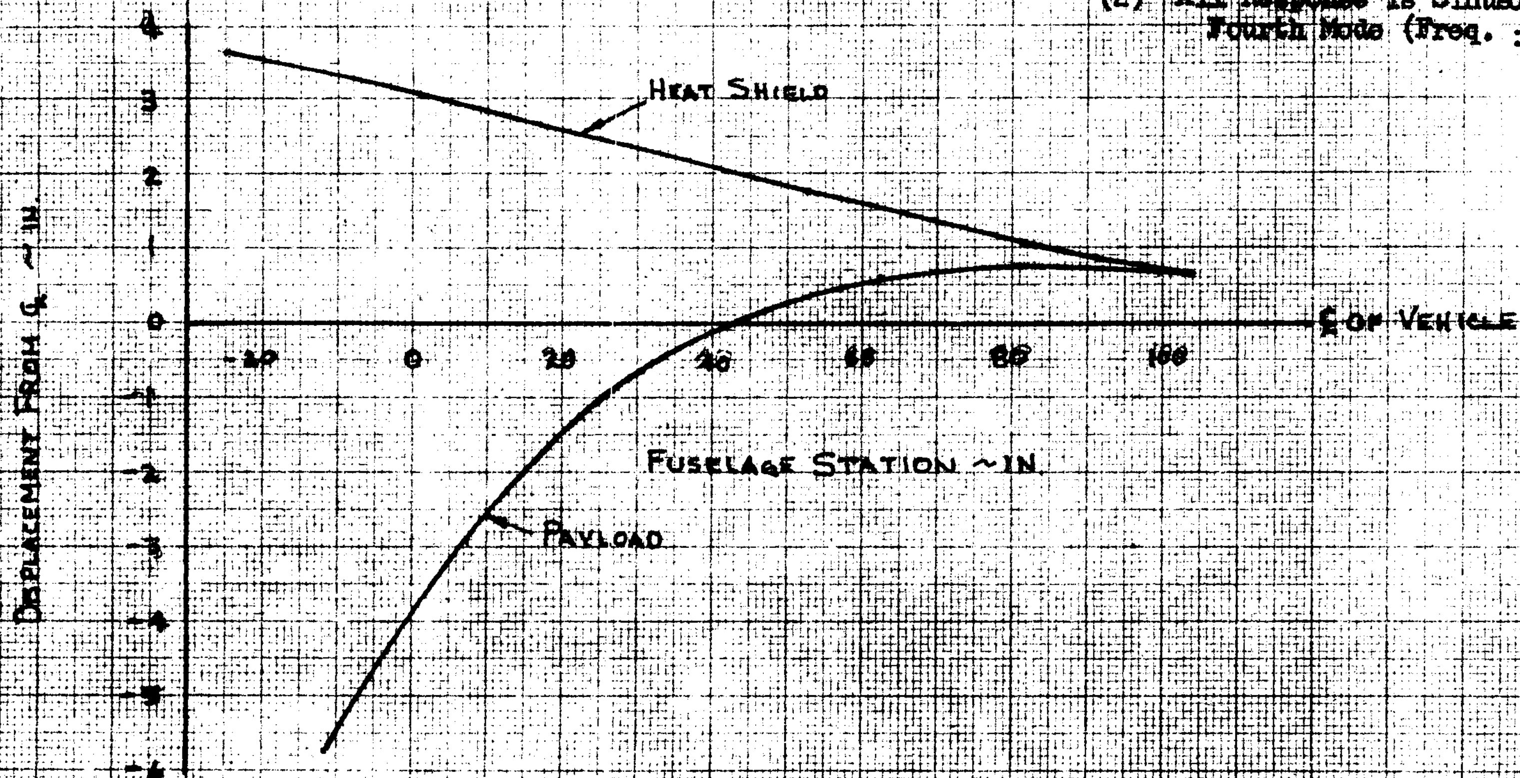

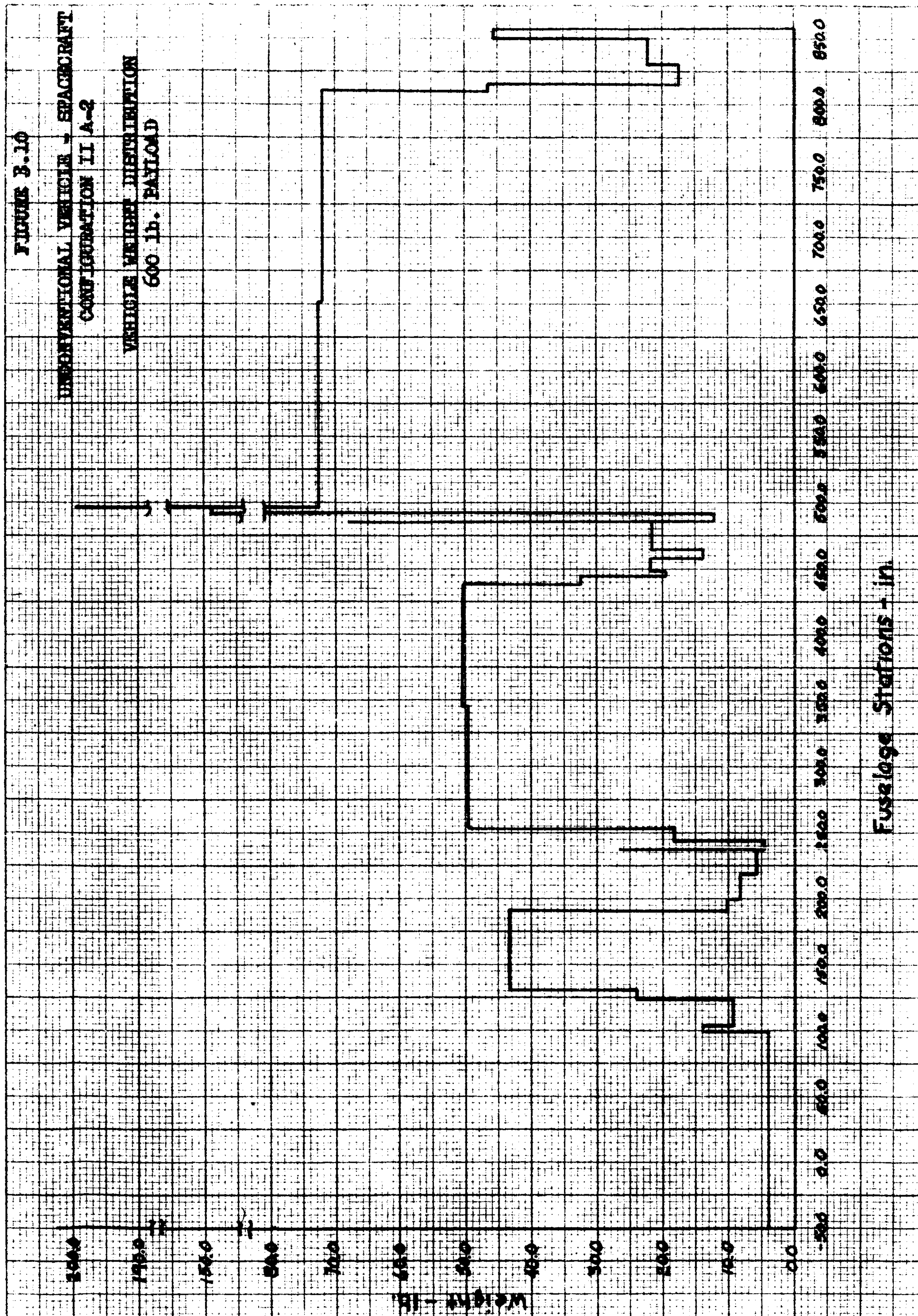
FIGURE 3.10
UNCONVENTIONAL VEHICLE - SPACECRAFT
CONFIGURATION II A-2
VEHICLE WEIGHT DISTRIBUTION
600 lb. PAYLOAD
Fuselage Stations - in.
Weight - lb.
-50.0
0.0
50.0
100.0
150.0
200.0
250.0
300.0
350.0
400.0
450.0
500.0
550.0
600.0
650.0
700.0
750.0
800.0
850.0
0.0
10.0
20.0
30.0
40.0
50.0
60.0
70.0
80.0

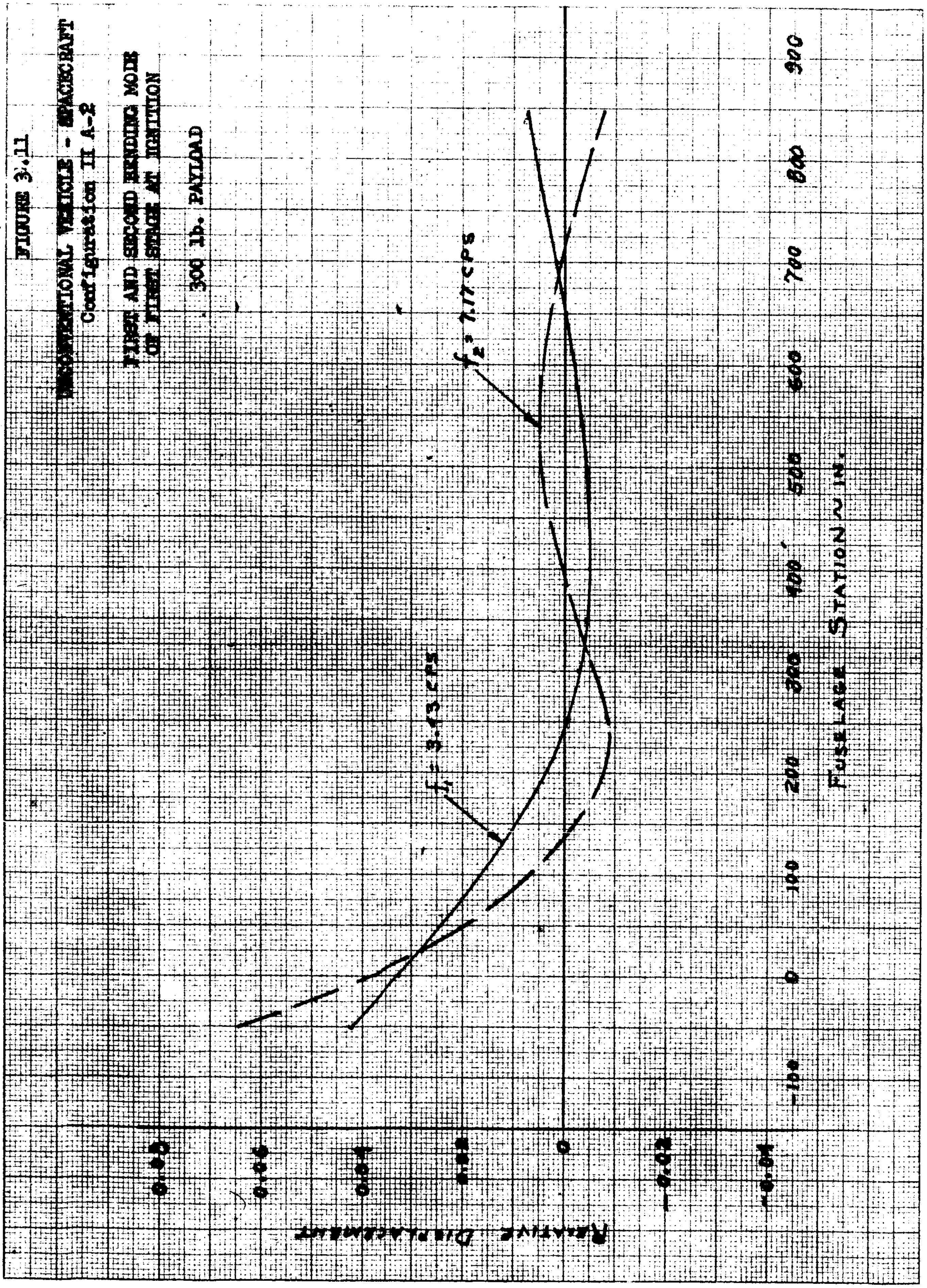

FIGURE 3.11
UNCONVENTIONAL VEHICLE - SPACECRAFT
Configuration II A-2
FIRST AND SECOND BENDING MODE
OF FIRST STAGE AT IGNITION
300 lb. PAYLOAD

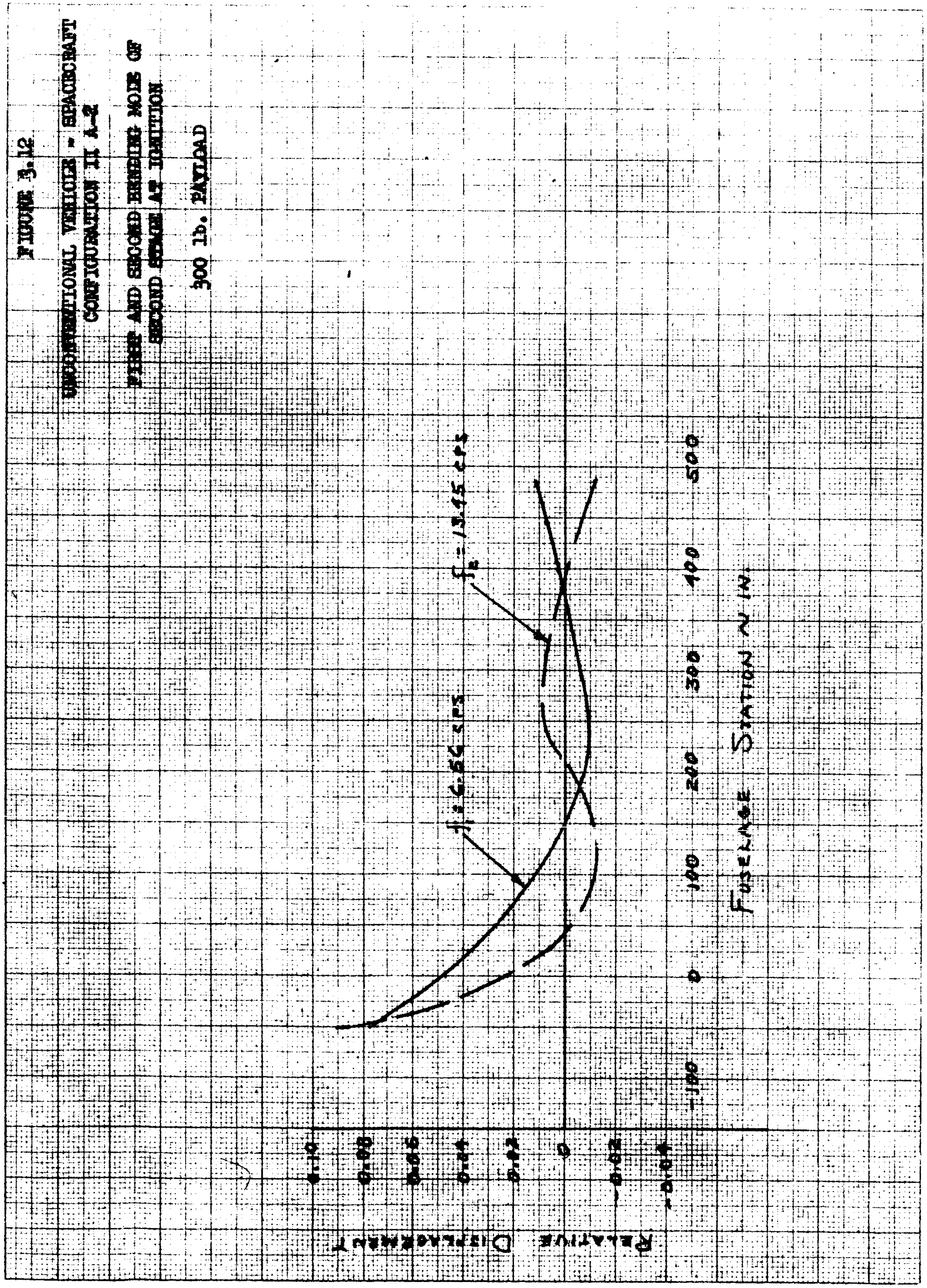

FIGURE 3.12

UNCONVENTIONAL VEHICLE - SPACECRAFT CONFIGURATION II A-2

FIRST AND SECOND BENDING MODE OF SECOND STAGE AT IGNITION

300 lb. PAYLOAD

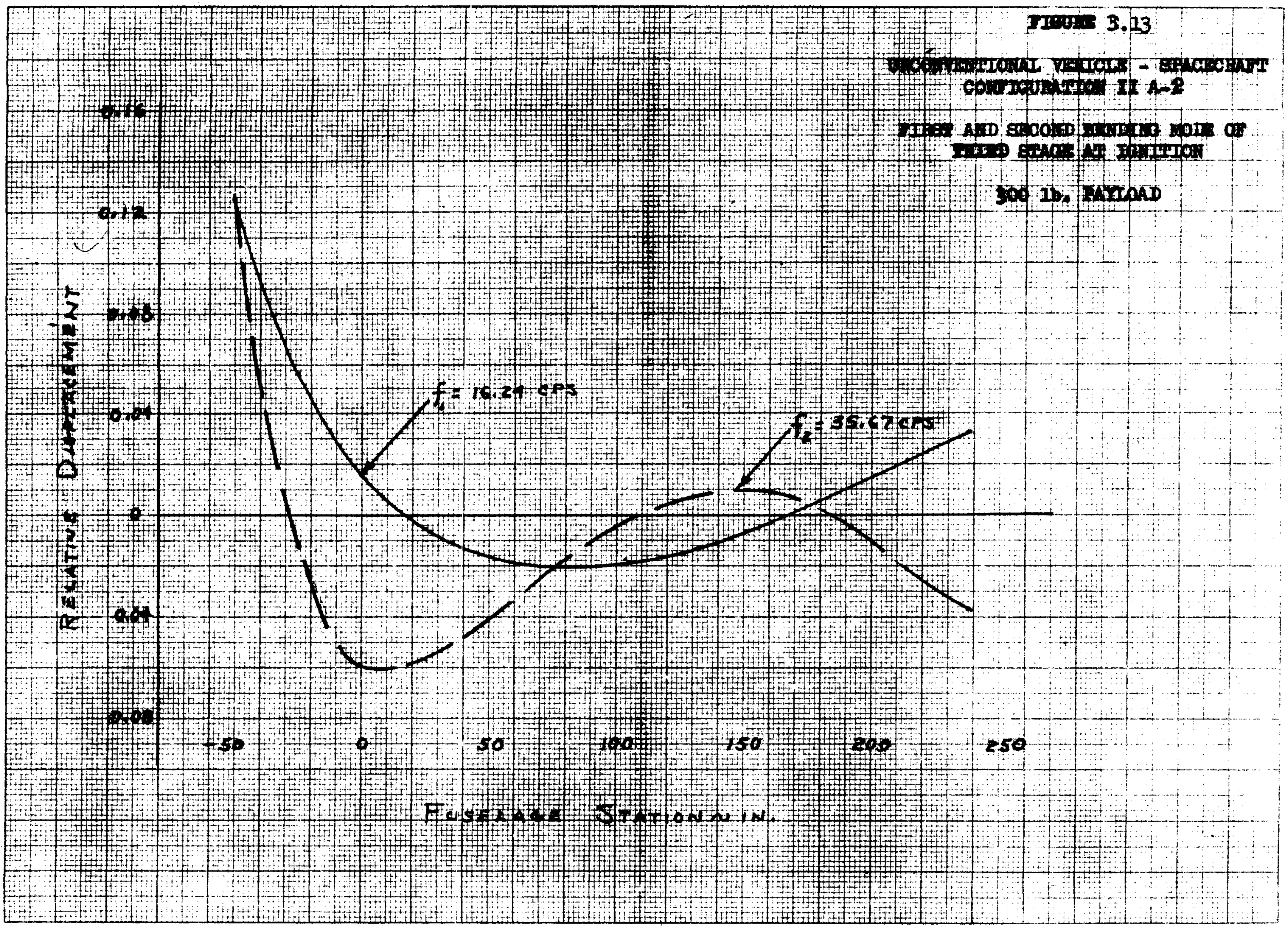

FIGURE 3.13

UNCONVENTIONAL VEHICLE - SPACECRAFT
CONFIGURATION II A-2

FIRST AND SECOND BENDING MODE OF
THIRD STAGE AT IGNITION

300 lb. PAYLOAD

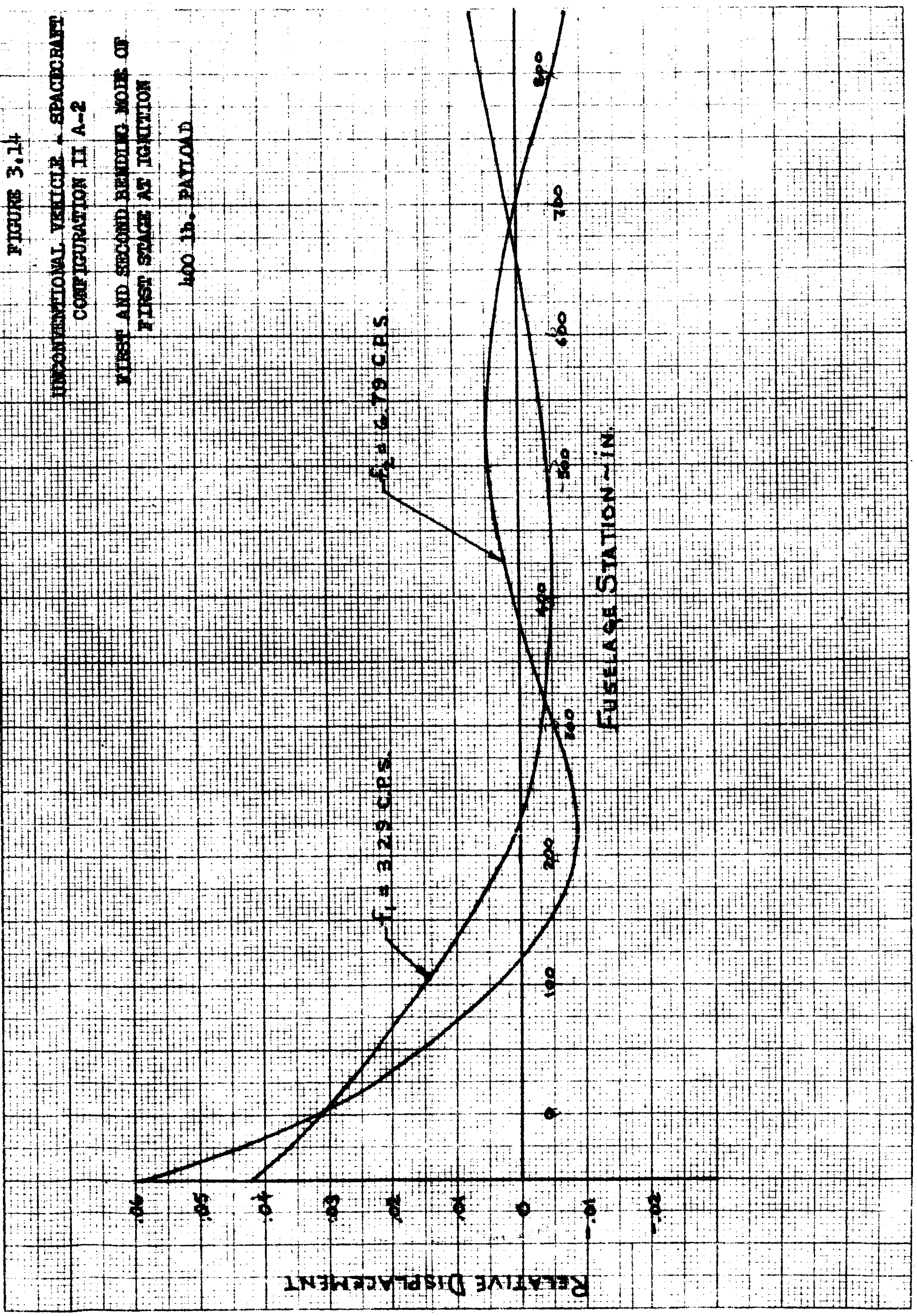
FIGURE 3.14
UNCONVENTIONAL VEHICLE - SPACECRAFT
CONFIGURATION II A-2
FIRST AND SECOND BENDING MODE OF
FIRST STAGE AT IGNITION
400 lb. PAYLOAD
f_1 = 3.29 C.P.S.
f_2 = 6.79 C.P.S.
FUSELAGE STATION ~ IN.
RELATIVE DISPLACEMENT
.06
.05
.04
.03
.02
.01
0
-.01
-.02
0
100
200
300
400
500
600
700
800

FIGURE 3.15

UNCONVENTIONAL VEHICLE - SPACECRAFT
CONFIGURATION II A-2

FIRST AND SECOND BENDING MODE OF
SECOND STAGE AT IGNITION

400 lb. PAYLOAD

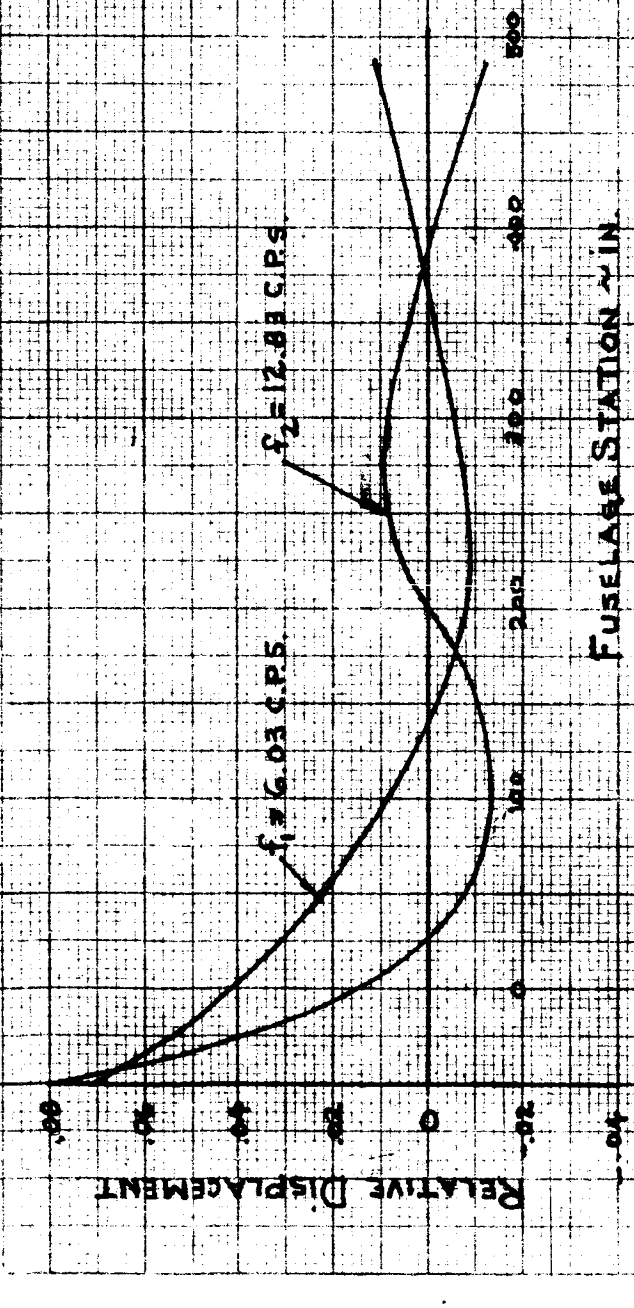

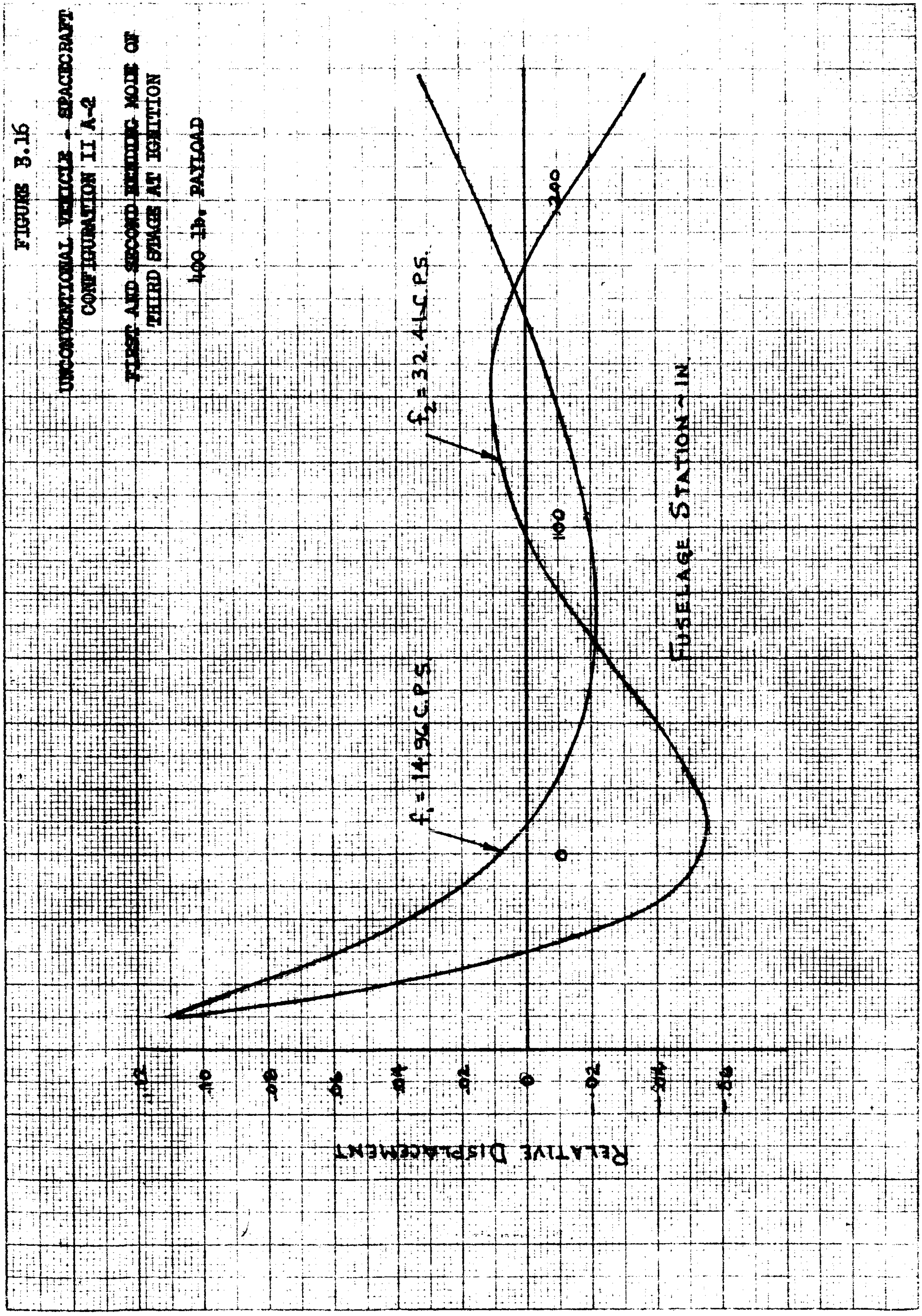

FIGURE B.16

UNCONVENTIONAL VEHICLE - SPACECRAFT CONFIGURATION II A-2

FIRST AND SECOND BENDING MODE OF THIRD STAGE AT IGNITION

400 lb. PAYLOAD

FIGURE 3.17

UNCONVENTIONAL VEHICLE - SPACECRAFT
CONFIGURATION II A-2

FIRST AND SECOND BENDING MODE OF
FIRST STAGE AT IGNITION

500 lb. PAYLOAD

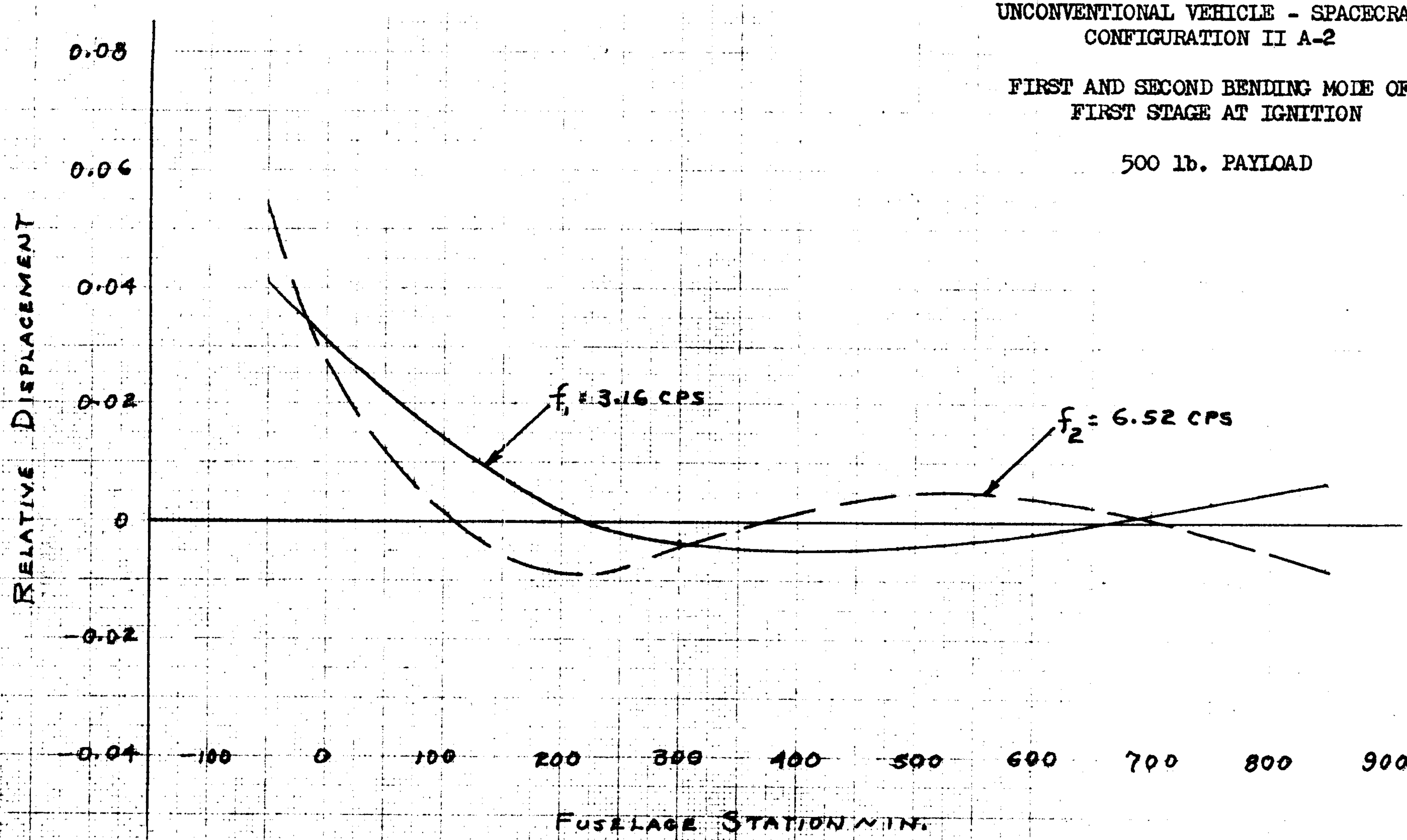

FIGURE 3.18

UNCONVENTIONAL VEHICLE - SPACECRAFT CONFIGURATION II A-2

FIRST AND SECOND BENDING MODE OF SECOND STAGE AT IGNITION

500 lb. PAYLOAD

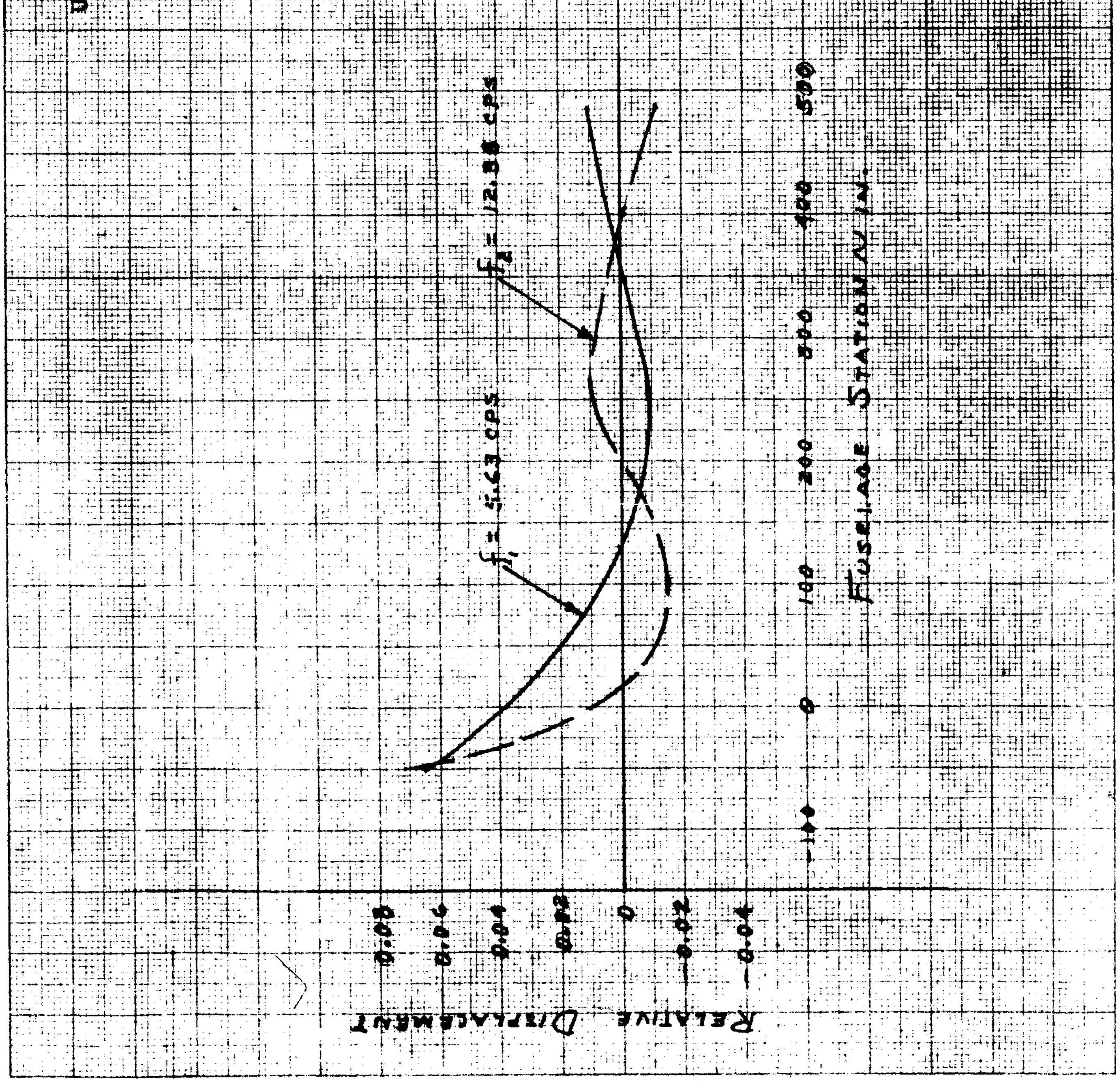

FIGURE 3.19

UNCONVENTIONAL VEHICLE - SPACECRAFT
CONFIGURATION II A-2

FIRST AND SECOND BENDING MODE OF
THIRD STAGE AT IGNITION

500 lb. PAYLOAD

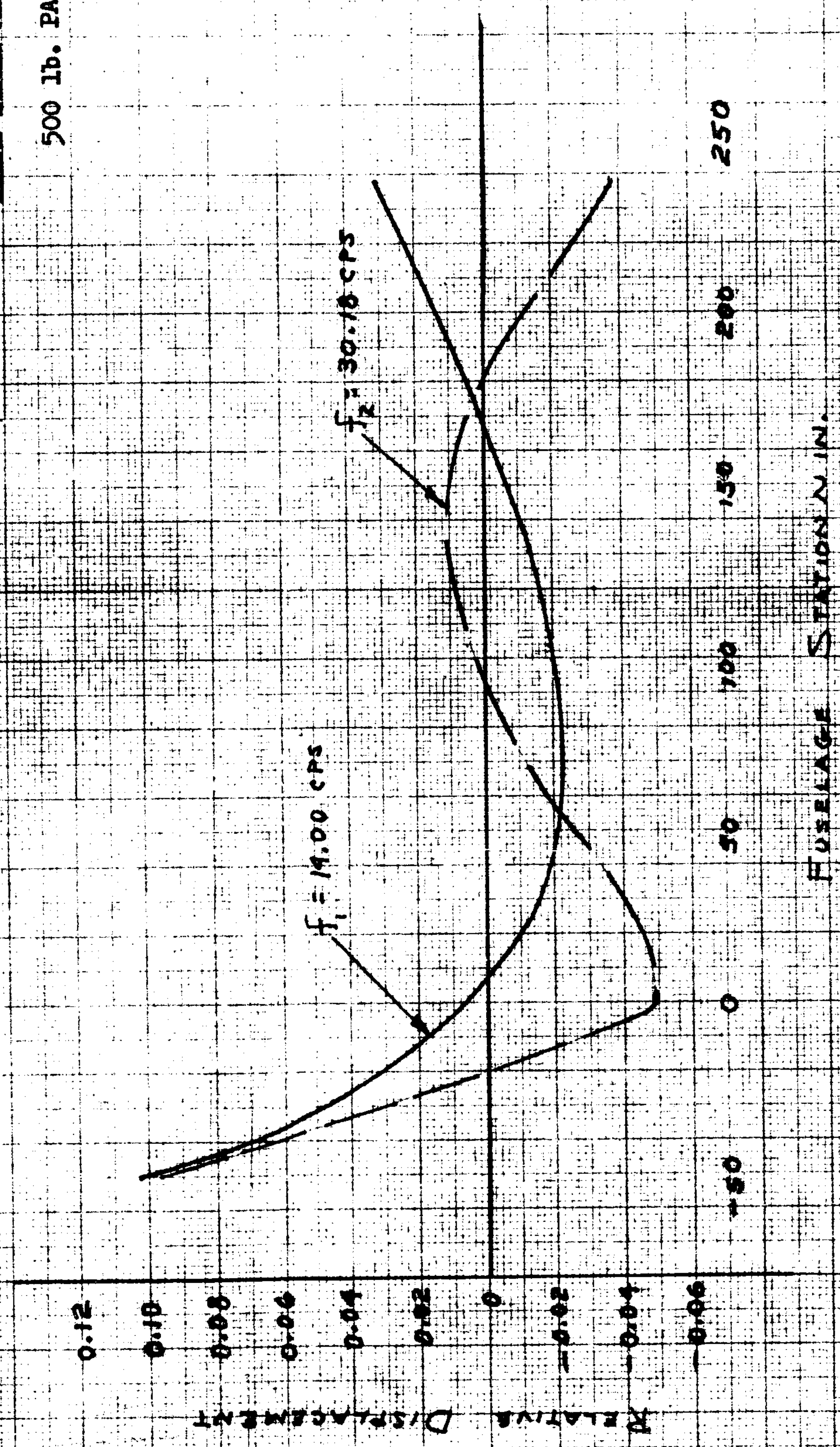

FIGURE 3.20

UNCONVENTIONAL VEHICLE - SPACECRAFT
CONFIGURATION II A-2

FIRST AND SECOND BENDING MODE OF
FIRST STAGE AT IGNITION

600 lb. PAYLOAD

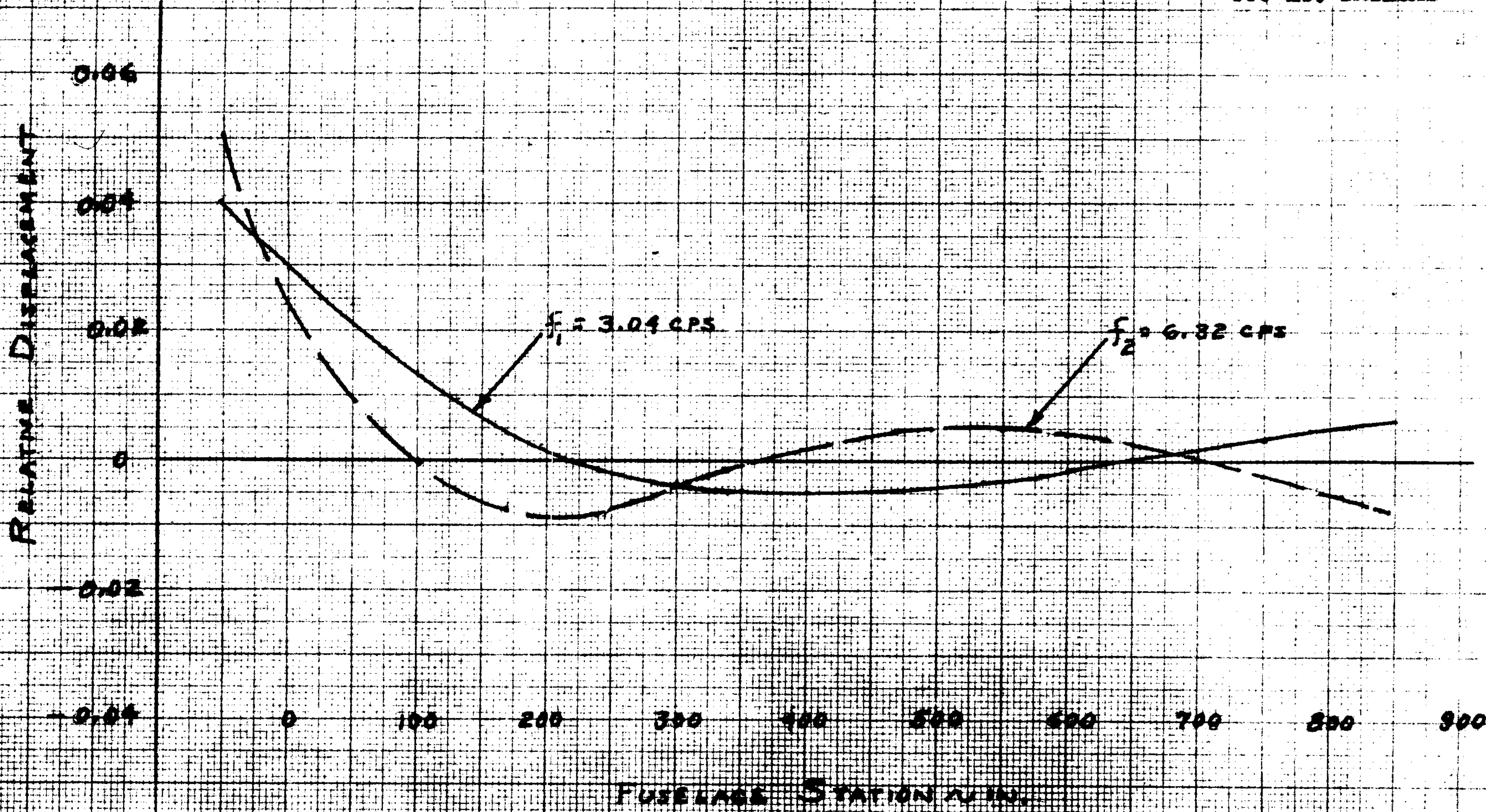

FIGURE 3.21

UNCONVENTIONAL VEHICLE - SPACECRAFT
CONFIGURATION II A-2

FIRST AND SECOND BENDING MODE OF
SECOND STAGE AT IGNITION

600 lb. PAYLOAD

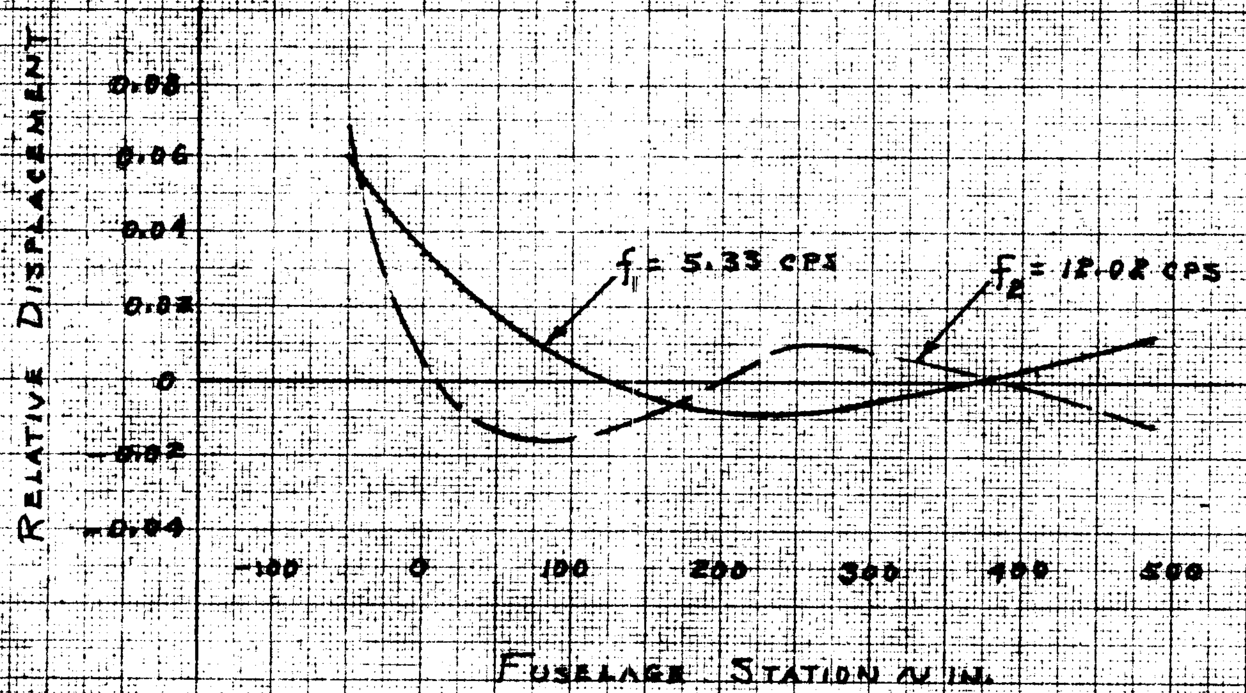

FIGURE 3.22

UNCONVENTIONAL VEHICLE - SPACECRAFT
CONFIGURATION II A-2

FIRST AND SECOND BENDING MODE OF
THIRD STAGE AT IGNITION

600 lb. PAYLOAD

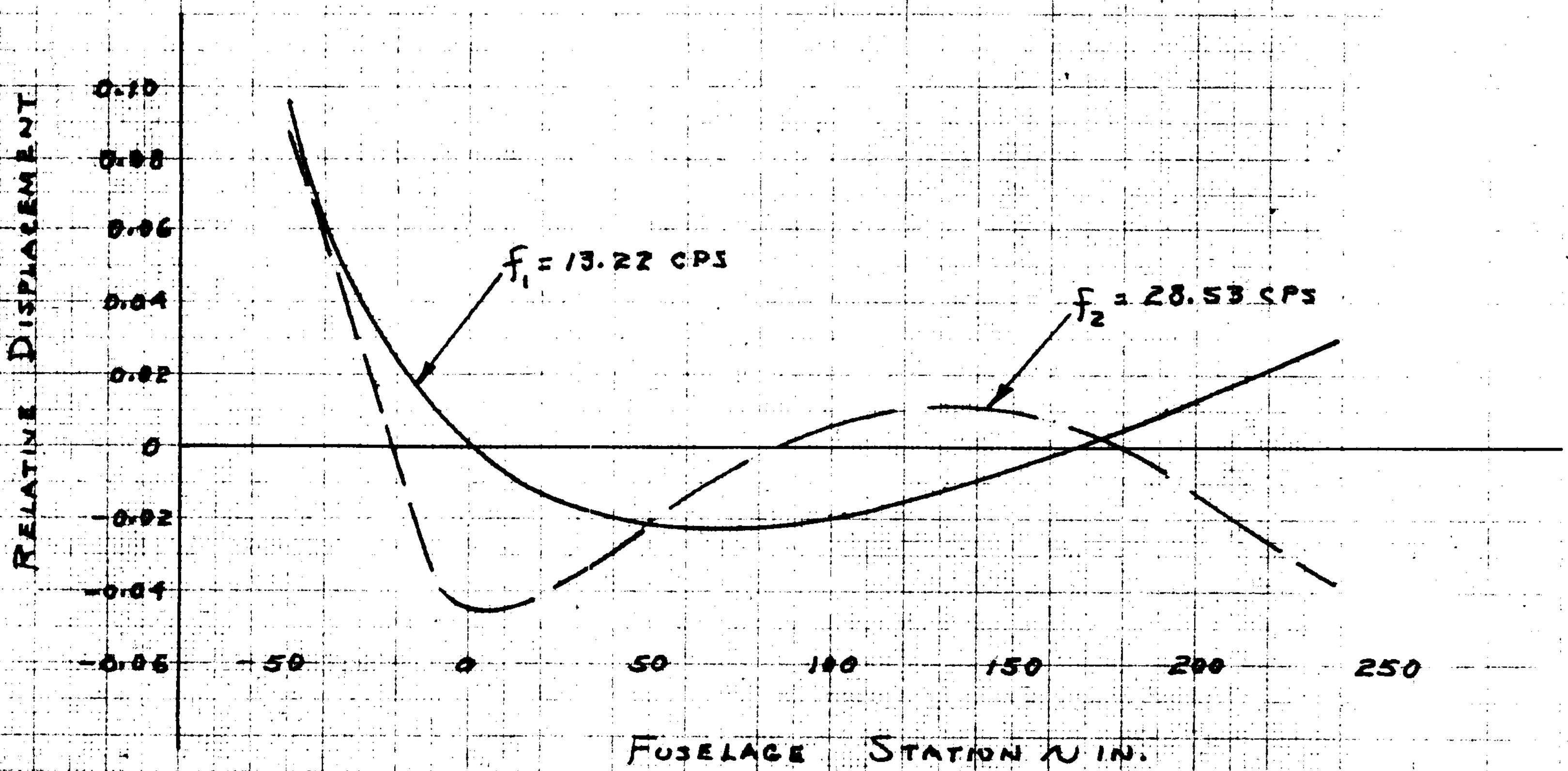

FIGURE 3.23

UNCONVENTIONAL VEHICLE - SPACECRAFT
CONFIGURATION II A-2
(12.5 Ft. Cone)

MAXIMUM BENDING MOMENT VS. FUSELAGE STATION

Payload Weight = 600 lbs.
Peak Wind Altitude = 27,000 ft.
Peak Wind Speed = 300 FPS

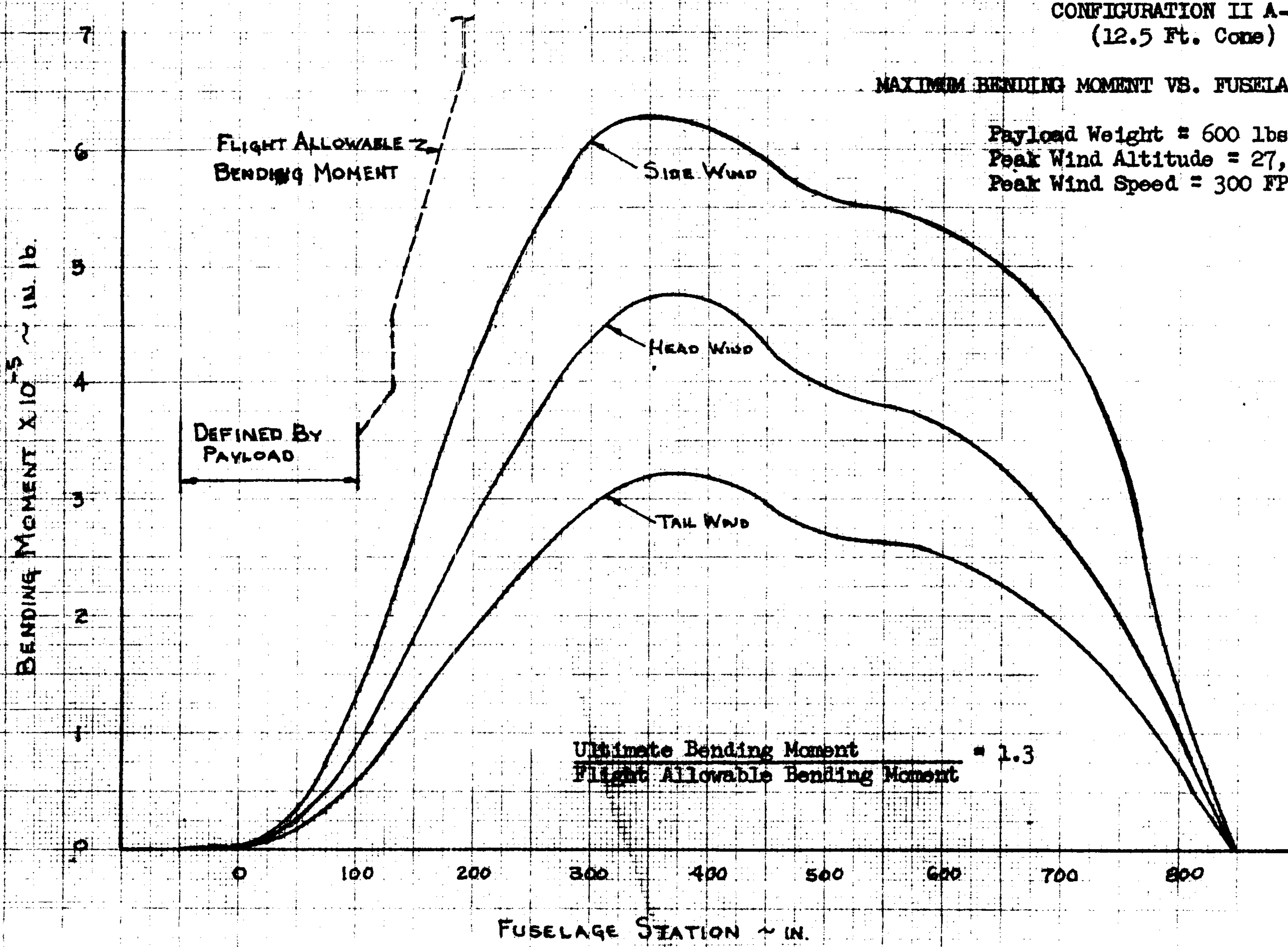

10/20/64

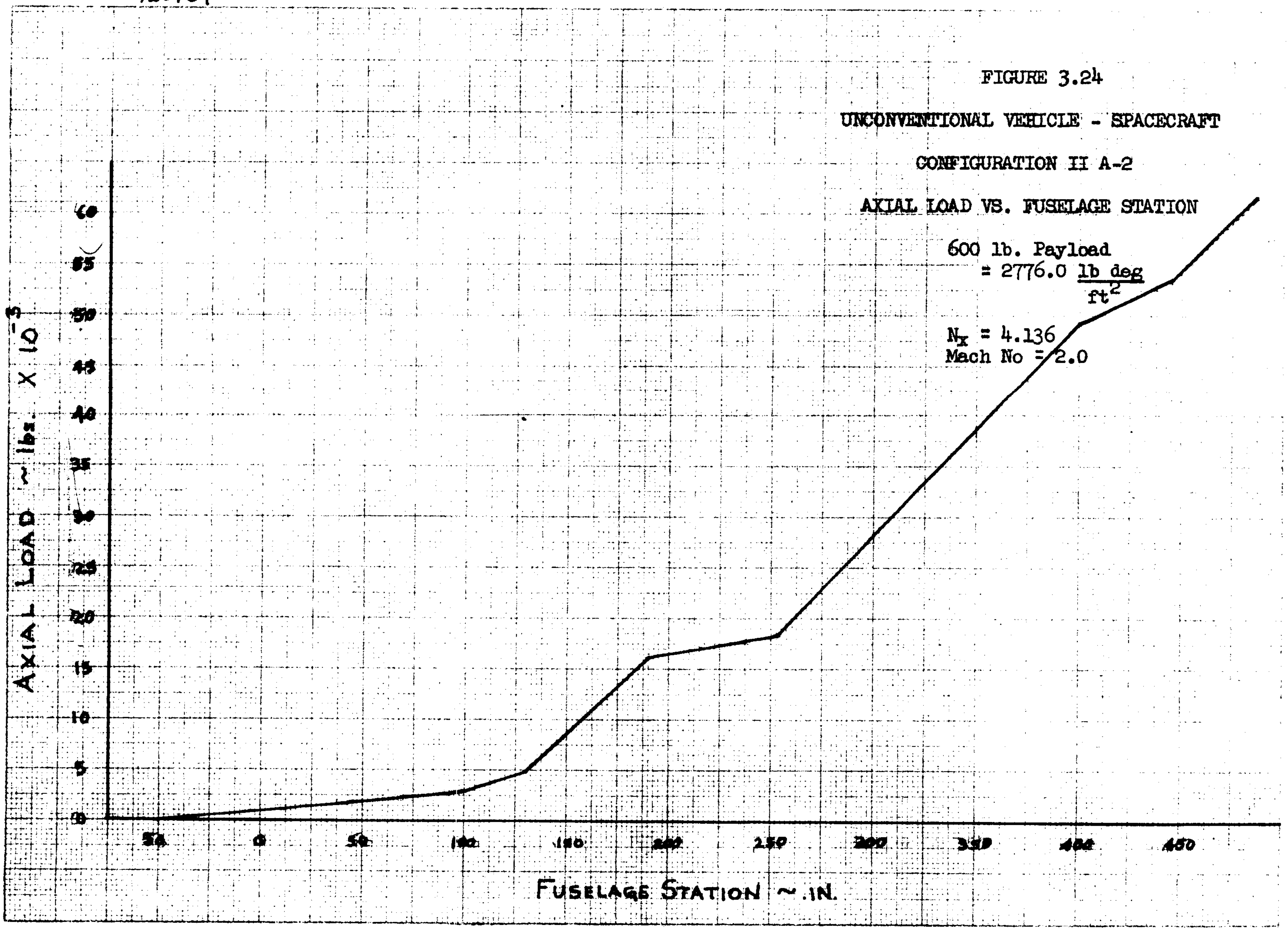

FIGURE 3.24

UNCONVENTIONAL VEHICLE - SPACECRAFT

CONFIGURATION II A-2

AXIAL LOAD VS. FUSELAGE STATION

600 lb. Payload
$= 2776.0 \frac{\text{lb deg}}{\text{ft}^2}$

$N_x = 4.136$
Mach No = 2.0

TABLE 3.1

UNCONVENTIONAL VEHICLE - SPACECRAFT

CONFIGURATION I A

VEHICLE STIFFNESS DISTRIBUTION

Station From	Station To	$EI \times 10^9$ ~ in^2 lb.		$GA \times 10^7$ ~ lb.	
-25.00	-19.30	1.22	3.68	0.967	2.900
-19.30	4.00	0.40	4.79	2.900	0.269
4.00	52.50	4.79	4.79	0.269	0.672
52.50	103.70	4.79	2.03	0.672	0.924
103.70	125.60	7.90	12.80	2.250	2.650
125.60	131.10	12.80	14.30	2.650	2.740
131.10	191.95	4.61	4.61	0.684	0.684
191.95	238.18	4.25	4.86	0.375	0.393
238.18	253.06	5.91	5.48	0.481	0.468
253.06	254.11	388.40	102.30	134.800	33.390
254.11	255.46	102.30	43.34	33.390	13.992
255.46	430.96	43.34	38.20	13.992	12.319
430.96	431.40	38.20	38.15	12.319	12.313
431.40	432.40	38.15	39.75	12.319	12.934
432.40	433.40	39.75	39.21	12.934	12.949
433.40	434.40	39.21	49.99	12.949	16.936
434.40	435.40	49.99	57.04	16.939	19.984
435.40	436.40	57.04	55.18	19.984	23.860
436.40	437.40	65.18	74.01	23.860	28.631
437.40	438.40	74.01	82.98	28.631	34.388
438.40	439.40	82.98	91.42	34.388	41.204
439.40	440.40	91.42	97.99	41.204	49.003
440.40	441.40	97.99	102.30	49.003	58.223
441.40	442.40	102.30	102.20	58.223	68.813
442.40	443.40	102.20	160.00	68.813	125.300
443.40	445.00	160.00	30.46	125.300	125.300
445.00	447.29	30.46	61.33	35.500	78.530
447.29	450.79	61.33	37.11	78.530	37.667
450.79	457.83	37.11	42.94	37.667	25.663
457.83	463.11	42.94	50.66	25.663	21.745
463.11	473.35	50.66	86.10	21.745	21.843
473.35	477.55	86.10	171.90	21.843	36.183
477.55	486.66	171.90	171.90	36.183	36.183
486.66	497.00	33.00	33.00	3.060	3.060
497.00	810.00	80.00	80.00	7.590	7.590
810.00	847.95	26.40	26.40	2.460	2.460

TABLE 3.2

UNCONVENTIONAL VEHICLE - SPACECRAFT
CONFIGURATION IIA-2

VEHICLE STIFFNESS DISTRIBUTION

Station From	Station To	$EI \times 10^9$	$EI \times 10^9$	$GA \times 10^7$ (lb)	$GA \times 10^7$ (lb)
-50.3	-38.7	0.010	0.025	0.8723	1.7446
-38.7	-26.7	0.025	0.0375	1.7446	0.6541
-26.7	-14.7	0.0375	0.0750	0.6541	0.58145
-14.7	-2.7	0.075	0.150	0.58145	0.65410
-2.7	10.0	0.150	0.300	0.6541	0.83733
10.0	22.0	0.300	0.550	0.83733	1.0659
22.0	34.0	0.550	0.900	1.0659	1.2816
34.0	46.0	0.900	1.300	1.2816	1.4172
46.0	58.0	1.300	1.800	1.4172	1.5505
58.0	70.0	1.800	2.500	1.5505	1.1637
70.0	99.7	2.500	2.500	1.1637	1.1637
99.7	103.7	4.790	2.030	0.3780	0.4620
103.7	125.6	7.900	12.800	2.2500	2.6500
125.6	131.1	12.800	14.300	2.6500	2.7400
131.1	191.95	4.610	4.610	0.6840	0.6840
191.95	238.18	4.250	4.860	0.3750	0.3930
238.18	253.06	5.910	5.480	0.4810	0.4680
253.06	254.11	388.400	102.300	134.800	33.390
254.11	255.46	102.300	43.340	33.390	13.992
255.46	430.96	43.340	38.200	13.992	12.319
430.96	431.4	38.200	38.150	12.319	12.313
431.4	432.4	38.150	39.750	12.319	12.934
432.4	433.4	39.750	39.210	12.934	12.949
433.4	434.4	39.210	49.990	12.949	16.936
434.4	435.4	49.990	57.040	16.939	19.984
435.4	436.4	57.040	65.180	19.984	23.860
436.4	437.4	65.180	74.010	23.860	28.631
437.4	438.4	74.010	82.980	28.631	34.388
438.4	439.4	82.980	91.420	34.388	41.204
439.4	440.4	91.420	97.990	41.204	49.003
440.4	441.4	97.990	102.300	49.003	58.223
441.4	442.4	102.300	102.200	58.223	68.813
442.4	443.4	102.200	160.000	68.813	125.300
443.4	445.0	160.000	30.460	125.300	125.300
445.0	447.29	30.460	61.330	35.500	78.530
447.29	450.79	61.330	37.110	78.530	37.667
450.79	457.83	37.110	42.940	37.667	25.663
457.83	463.11	42.940	50.660	25.663	21.745
463.11	473.35	50.660	86.100	21.745	21.843
473.35	477.55	86.100	171.190	21.843	36.183
477.55	487.0	171.190	171.190	36.183	36.183
487.0	497.0	33.000	33.000	3.060	3.060
497.0	810.0	80.000	80.000	7.590	7.590
810.0	847.95	26.400	26.400	2.460	2.460

TABLE 3.3

UNCONVENTIONAL VEHICLE - SPACECRAFT

SUMMARY OF BENDING FREQUENCIES

FOR CASE II A-2

$K_{SPIN\ BEARING} = \infty$

First Stage at Ignition

Payload Wt. (lb)	1st Mode CPS	2nd Mode CPS	3rd Mode CPS	4th Mode CPS
300	3.43	7.165	11.96	19.07
400	3.29	6.79	11.45	18.70
500	3.16	6.52	11.11	18.29
600	3.04	6.32	10.85	17.84

Second Stage at Ignition

Payload Wt. (lb)	1st Mode CPS	2nd Mode CPS	3rd Mode CPS	4th Mode CPS
300	6.55	13.45	26.39	41.39
400	6.03	12.83	24.27	39.74
500	5.63	12.38	22.64	38.45
600	5.32	12.02	21.36	37.34

Third Stage at Ignition

Payload Wt. (lb)	1st Mode CPS	2nd Mode CPS	3rd Mode CPS	4th Mode CPS
300	16.24	35.67	58.74	89.41
400	14.96	32.41	56.10	82.15
500	14.00	30.18	53.71	77.24
600	13.22	28.53	51.47	73.76

TABLE 3.4

UNCONVENTIONAL VEHICLE - SPACECRAFT

SUMMARY OF BENDING FREQUENCIES

FOR CASE II A-2

$$K_{SPIN\ BEARING} = 0.115 \times 10^8 \ \frac{in\ lb}{rad}$$

First Stage at Ignition

Payload Wt. (lb)	1st Mode CPS	2nd Mode CPS	3rd Mode CPS	4th Mode CPS
300	3.30	5.81	9.80	18.41
400	3.10	5.44	9.66	18.24
500	2.92	5.21	9.56	18.03
600	2.77	5.06	9.47	17.74

Second Stage at Ignition

Payload Wt. (lb)	1st Mode CPS	2nd Mode CPS	3rd Mode CPS	4th Mode CPS
300	5.10	10.73	26.35	34.29
400	4.56	10.53	24.19	32.30
500	4.20	10.38	22.32	31.27
600	3.92	10.24	20.78	30.57

Third Stage at Ignition

Payload Wt. (lb)	1st Mode CPS	2nd Mode CPS	3rd Mode CPS	4th Mode CPS
300	9.75	30.87	53.42	87.23
400	9.19	27.13	52.38	77.65
500	8.78	24.59	51.27	71.11
600	8.46	22.72	50.04	66.46

TABLE 3.5

UNCONVENTIONAL VEHICLE - SPACECRAFT

CONFIGURATION II A-2

JOINT STIFFNESS VALUES *

Joint Location in.	Joint Stiffness in lb/rad
131.1	$.31 \times 10^{10}$
191.8	$.41 \times 10^{10}$
253.0	$.19 \times 10^{10}$
445.0	$.19 \times 10^{11}$
486.6	$.292 \times 10^{10}$

*Joint Stiffness Values for those other than shown are assumed to be infinite.

STUDY

"UNCONVENTIONAL VEHICLE - SPACECRAFT CONFIGURATION"

STRUCTURAL LOADS AND STRESS ANALYSIS

Prepared by

W. E. Agan

W. E. Agan

Reviewed by

H. E. Brougham

H. E. Brougham

CONFIGURATION I A

INTRODUCTION

The purpose of this section is to present the structural loads and stress analysis for the vehicle structure required to meet the objectives of configuration I A of the statement of work, reference A.

DESCRIPTION

The schematic presented on page 4.101 shows the payload support ring which provides the load path between the payload and Scout's 23-002158 ring. The payload support ring is machined from an aluminum rolled ring forging. Continuity between the payload support ring and Scout's 23-002158 ring is maintained with a Marmon type clamp. The payload support ring is bolted to and separates with the payload.

LOADS

The payload support ring is critical for Scout's fourth stage design loads, reference B. This loading specifies a 4.5 g laterial ultimate load at the payload center of gravity varying linearly to zero at Scout Station 131 to be combined with 0 to 15 g longitudinal ultimate load. The Scout criteria used in the analysis is:

Limit load = anticipated load on structure
Yield load = 1.15 x Limit load
Ultimate load = 1.5 x Limit load

In accordance with the statement of work (reference A), the payload used in configuration I A weighs 300 pounds and its center of gravity is at one-half the cone length.

ANALYSIS

The stress analysis of the payload support ring is presented on pages 4.102 - .106. Payload separation velocity is presented on page 4.107 using the existing Scout spring separation system. System efficiency was assumed to be 80%. As noted on page 4.101, the payload is required to provide a shear lip to transfer the shear load from the payload to the payload support ring.

SUMMARY OF RESULTS

Item	Margin of Safety	With Respect To	Ref. Page
Payload Support Ring	High	Bolt Tension	4.102
	+0.10	Bolt Cutout Bending	.103
	High	Panel Compression Yield	.104
	+0.10	Ring Torsion	.105

Item	Subject	Ref. Page
Payload Support Ring	Torque Bolt at Sta. 98.25 to 25 in-lbs.	4.103
	Torque Marmon Clamp Bolt at Sta. 99.7 to 81 in-lbs.	.105
	Payload Separation Velocity = 2.17 fps.	.107

UNCONVENTIONAL VEHICLE

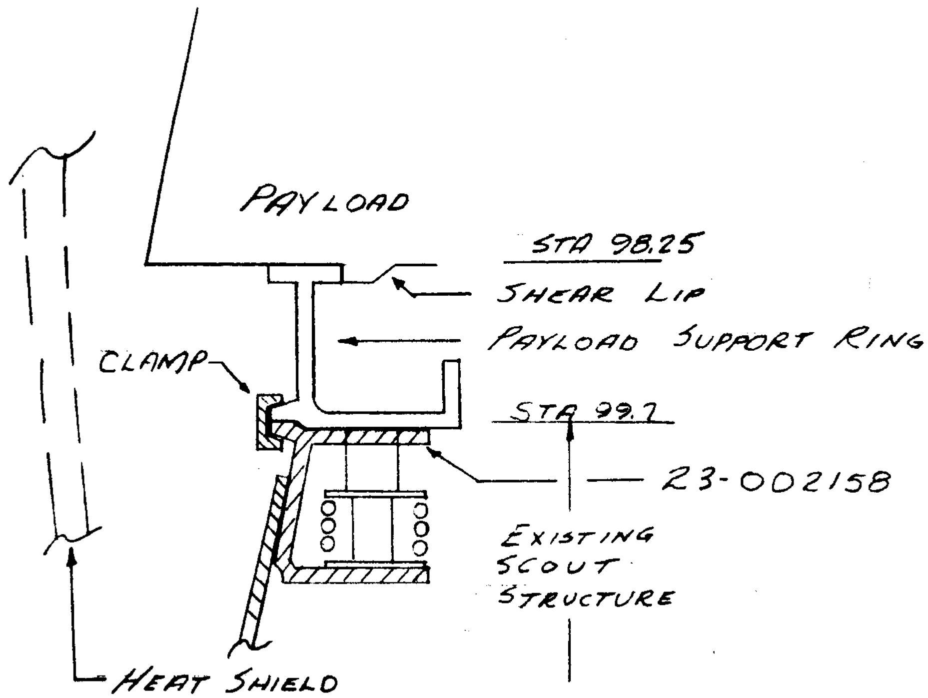

LOADS ULT

PAYLOAD WEIGHT = 300 lbs
PAYLOAD C.G. = SCOUT STA 44.35
REF. PG. 2.2

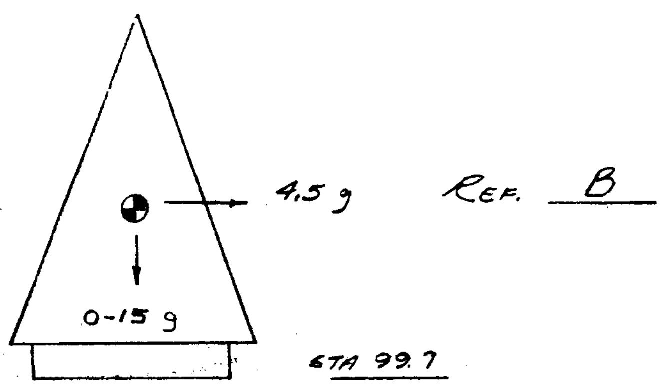

ULT LOADS

PAYLOAD SUPPORT RING

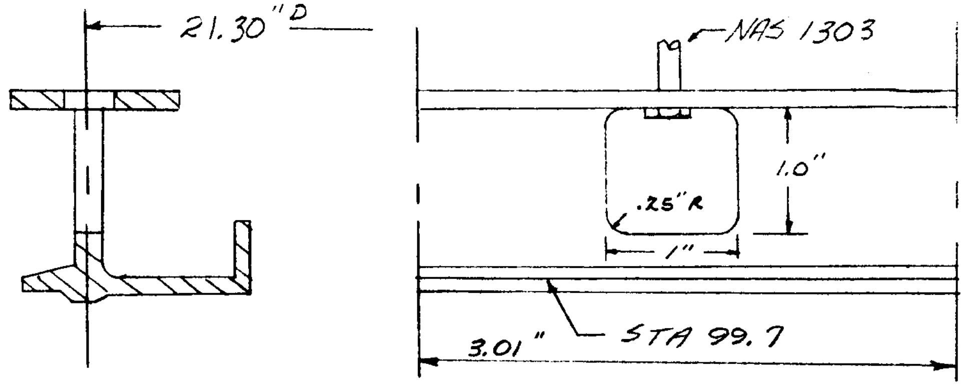

MAT'L: 2014-T6 ALUM FORGING $F_{TU} = 65,000$ psi REF. K

$M_{99.7} = 300(4.5)(99.7 - 44.35) = 74,600$ in-lbs

$P_{99.7} = 0$ lbs (MIN) $P_{99.7} = 300(15) = 4500$ lbs (MAX)

REF. PG. 4.101

THERE ARE FOUR (4) 5.20 in SPIN MOTOR CUTOUTS BETWEEN STA 99.7 AND 103.81

RUNNING LOADS

$f = \frac{MR}{2890t}$ $\quad ft = w_m = \frac{MR}{2890}$

$w_m = \frac{74,600\,(10.65)}{2890} = \pm 275$ #/in

$f = P/48.2t$ $\quad ft = w_p = P/48.2$

$w_p = \frac{4500}{48.2} = 93.5$ #/in

$w_{t\,MAX} = 275$ #/in

$w_{c\,MAX} = 368.5$ #/in

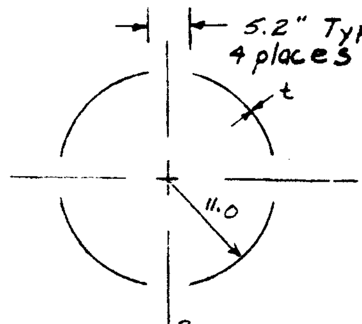

$I = \pi R^3 t - 2Ad^2$

$I = 2890\,t$

$A = 48.2\,t$

BOLTS

NAS 1303 24-REQUIRED

TENSION ALL. = 3620 lbs REF. NATIONAL STANDARD ASSOCIATION

BOLT SPACE = $\pi(21.3)/24 = 2.79$ in

BOLT LOAD = $2.79(275) = 766$ lbs

$M.S. = \frac{3620}{766} - 1 =$ HIGH

ULT LOADS

TORQUE TO LIMIT LOAD

$T = \frac{P}{2\pi n K}$ n = no of threads per inch (32)
K = 0.244

$T = \frac{766/1.5}{2\pi(32)(.244)} = 10.4$ in-lbs

USE STANDARD CALL OUT FOR 3/16" TENSION FASTENER $T = 20 {}^{+5}_{-0}$ in-lbs

BENDING AT BOLT CUTOUT

766 REF. PG. 2.102

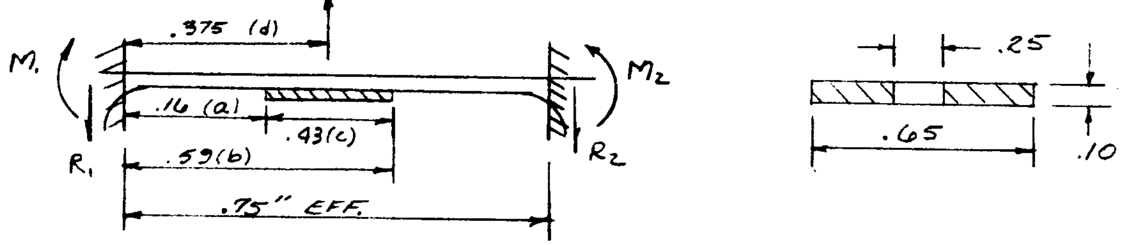

$R_1 = R_2 = 766/2 = 383$ lbs

$M_1 = -M_2 = -\frac{P}{24L}\left(24\frac{d^3}{L} - 6\frac{bc^2}{L} + 3\frac{c^3}{L} + 4c^2 - 24d^2\right)$

REF. L CASE 34 PG. 108

$M_1 = -\frac{766}{24(.75)}\left(24\frac{(.375)^3}{.75} - 6\frac{(.59)(.43)^2}{.75} + 3\frac{(.43)^3}{.75} + 4(.43)^2 - 24(.375)^2\right)$

$M_1 = -42.6(-1.504) = 64$ in-lbs

END MOMENT IS CRITICAL

$f = \frac{6M}{bt^2} = \frac{6(64)}{(.65)(.1)^2} = 59{,}000$ psi

$F_{TU} = 65{,}000$ psi   REF. PG. 2.102

$M.S. = \frac{65{,}000}{59{,}000} - 1 = +0.10$

ULT. LOADS

BUCKLING BETWEEN BOLTS

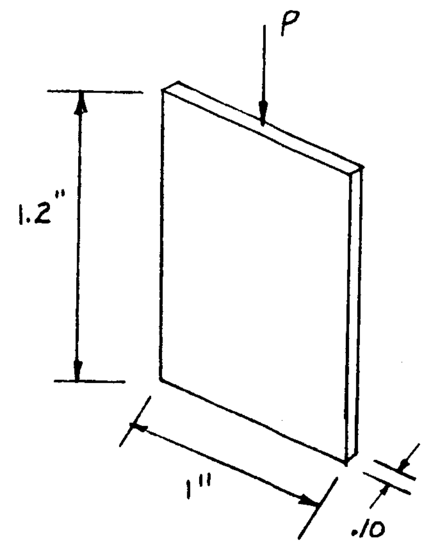

$W_{c_{MAX}} = 368.5$ #/in REF. PG. 4.102

$P = 368.5\left(\frac{3.01}{3.01-1}\right) = 551$ lbs/in net

$P_{CR} = \frac{\pi^2 EI}{L^2}$ REF. M

$P_{CR} = \frac{\pi^2 (10.5)(10^6)(1)(.1)^3}{(1.2)^2 (12)}$

$P_{CR} = 6000$ lbs

$f = P/A \quad P_{CR} = 55{,}000(1)(.1) = 5{,}500$

$M.S. = \frac{5500}{551} - 1 =$ HIGH

MAT'L: 2014-T6 ALUM FORGING

$F_{TU} = 65{,}000$ psi $\quad E = 10.5 \times 10^6$ psi

$F_{TY} = 55{,}000$ psi $\quad G = 4 \times 10^6$ psi

$F_{SU} = 40{,}000$ psi $\quad$ REF. K

RING TORSION

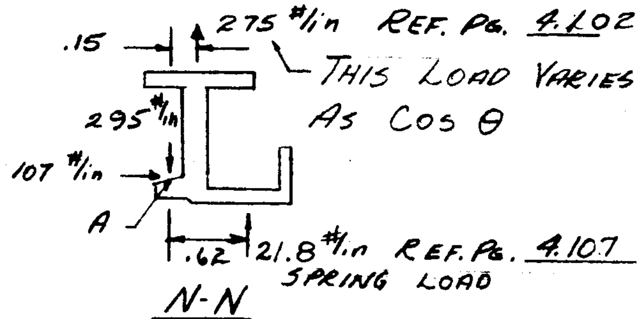

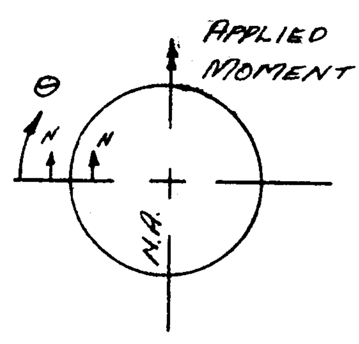

$dM_{t_A} = 275\cos\theta\,(.15) + 21.8(.62) = 0$

ASSUME THERE NO TORQUE INDUCED ON COMPRESSION SIDE

$M_T = \int_0^{\pi/2} dM_t \cos\theta\, R\, d\theta \qquad M_M = \int_0^{\pi/2} dM_t \sin\theta\, R\, d\theta$

TORSION IS CRITICAL

ULT LOADS

$$M_T = \int_0^{\pi/2} (41.2\cos\theta + 13.5)\cos(90-\theta)\, R\, d\theta$$

$$M_T = R\int_0^{\pi/2} (41.2\cos\theta\sin\theta + 13.5\sin\theta)\, d\theta$$

$$M_T = 10.65\left[20.6\sin^2\theta - 13.5\cos\theta\right]_0^{\pi/2}$$

$$M_T = 363 \text{ in-lbs}$$

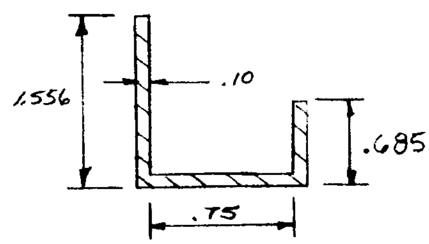

EQUIVALENT SECTION

$b = 1.556 + .75 + .685 = 2.99$

$\tau = \dfrac{3M}{bt^2}$ REF. M

$\tau = \dfrac{3(363)}{2.99(.1)^2} = 36{,}400$ psi

$F_{su} = 40{,}000$ psi REF. PG. 4.104

$$M.S. = \frac{40{,}000}{36{,}400} - 1 = +0.10$$

THE SCOUT CLAMP SHOWN ON PAGE 4.101 IS NOT ANALYZIED HERE BECAUSE IT'S DESIGN LOADS ARE 213% OF THE LOADS SHOWN ON PAGE 4.102, $w_t = 275$ #/in. $w_{t\,SCOUT} = 585$ #/in

PRELOAD THE CLAMP TO LIMIT LOAD

$T = \dfrac{P}{2\pi n K}$ $n = 24$ $K = .171$

3/8" BOLT REF. PG. 4.216

$P = w_t R$

$P = (295)(10.65) = 3140$ $P_{LIMIT} = 3140/1.5 = 2090$ #

REF. PG. 4.104

$$T = \frac{2090}{2\pi(24)(.171)} = 81 \text{ in-lbs}$$

LIMIT LOADS

PRELOAD ROTATION

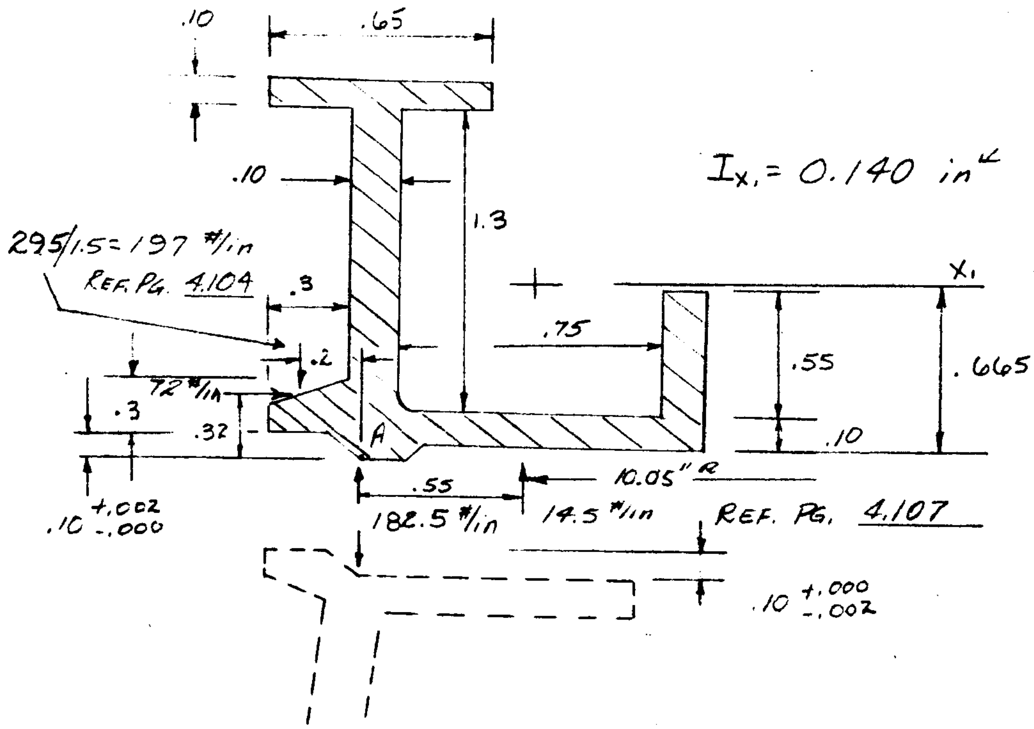

$$\Sigma M_A = M_T = 197(.2) + 14.5(.55) - 72(.32)$$

$$M_T = 24.4 \text{ in-lbs/in}$$

$$\Theta = \frac{MR^2}{EI}$$ REF. L PG. 230

$E = 10.5 \times 10^6$ REF PG. 4.104

$$\Theta = \frac{24.4(10.4)^2}{10.5(10^6)(.140)} = 1830(10^{-6}) \text{ rad}$$

$$\Theta = 0.105°$$

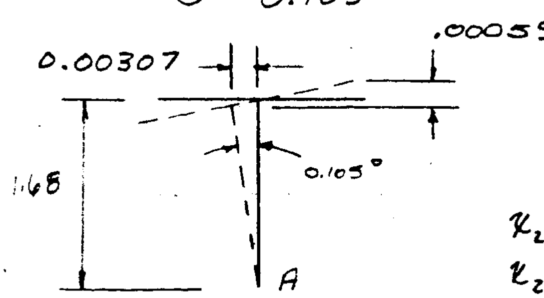

$$x_1 = 1.68 \tan(.105°)$$

$$x_1 = 1.68(.00183) = 0.00307 \text{ in}$$

$$x_2 = \tfrac{1}{2}(.65)\tan(.105°) + x_2 \tan(.105°)$$

$$x_2 = .325(.00183) + (.00307)(.00183)$$

$$x_2 = 0.00059 \text{ in}$$

PAYLOAD SEPARATION VELOCITY

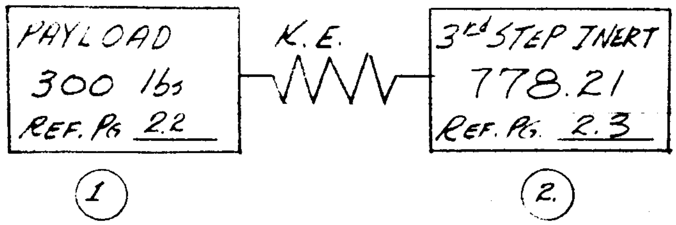

SPRINGS 23-002164

32 REQUIRED

LOAD AT 0.81" = 28.6 lbs

LOAD AT 1.21" = 8.2 lbs

STATIC RUNNING LOAD REF. PG. 4.106

$$\omega_s = \frac{28.6\,(32)}{2\pi\,(10.05)} = 14.5 \ \#/in$$

$$P.E. = \tfrac{1}{2}(.40)(28.6 + 8.2)\left(\frac{32}{12}\right) = 19.6 \ \text{ft-lbs}$$

$$M_1 = \frac{300}{32.2} = 9.31 \qquad M_2 = \frac{778.21}{32.2} = 24.2$$

$$M_1 V_1 = M_2 V_2 \qquad K.E. = \tfrac{1}{2} M_1 V_1^2 + \tfrac{1}{2} M_2 V_2^2$$

$$2K.E. = V_1^2\left(M_1 + \frac{M_1^2}{M_2}\right)$$

$$V_1 = 0.394\sqrt{KE}$$

$$V_2 = V_1 \frac{M_1}{M_2} = .394\sqrt{K.E.}\left(\frac{9.31}{24.2}\right) = 0.152\sqrt{KE}$$

$$V_1 + V_2 = \Delta V = 0.394\sqrt{KE} + 0.152\sqrt{KE} = 0.546\sqrt{KE}$$

$$K.E. = P.E.$$

ASSUME SYSTEM EFFICIENCY $\eta = 80\%$

$$\Delta V = 0.546\sqrt{(.80)(19.6)} = \underline{\underline{2.17 \ fps}}$$

CONFIGURATION II A-2

Introduction

The purpose of this section is to present the structural loads and stress analysis for vehicle structure required to meet the objectives of Configuration II A-2 of the statement of work (Ref. A).

Description

The schematic presented on page 4.210 shows the structure between the payload interface (Sta. 98.25) and the Scout's 23-002109 Ring (Sta. 105). This section of the vehicle consists of a payload support ring, middle "D", the fairing, two Marman type clamps, and other minor items. The payload support ring and Middle "D" are aluminum rolled ring forgings and provide the primary load path between the payload and Scout's Lower Transition "D" Section. A ten ply (0.10 inch thick) phenolic glass laminate fairing completely envelopes the vehicle in that area (Sta. 98.25 - 107) thus protecting the structure and components from aerodynamic heating. The Marman type clamps provide continuity between a). the payload support ring and Middle "D", b). Middle "D" and Scout's 23-002109 ring. At the end of third stage coast, the Marman type clamp at station 103.81 and the fairing jettison as a unit allowing the spin motors to spin-up the payload. At this time the spin bearing provides continuity between Middle "D" and Scout's Lower Transition "D" Section. Because of the low spring rate of the spin bearing which cause the vehicle natural frequency to couple with the Reaction Control system, it was necessary to bypass the spin bearing as a primary load path prior to spin-up. This feat has been accomplished by the "double acting" Marman type clamp at Sta. 103.81, remembering that a clearance between Middle "D" the Scout 23-002109 ring must be maintained to allow payload spin-up after clamp and fairing jettison. After spin-up, the Marman type clamp at station 99.7 jettisons and the payload and Scout Third Step separate at the Middle "D"-payload support ring interface. The payload support ring remains attached to the payload after separation.

Loads

The loads used in this design are consistent with Scout criteria, i.e.

Limit load = anticipated load on structure

Yield load = 1.15 x Limit load

Ultimate load = 1.5 x Limit load

Configuration II A-2 of the statement of work (Ref. A) considers four (4) 12.5 feet conical payloads weighing 300, 400, 500, 600 pounds with their center of gravity at one-half the cone length. The structure was designed to the maximum payload and therefore, only loads of the 600 pound payload are presented.

Three (3) different load conditions were considered, fourth stage design loads, flight loads, and spin-up loads. Fourth stage design loads, as defined in Ref. B, specify a 4.5 g lateral ultimate load at the payload center of gravity varying linearly to zero at Scout Station 131 to be combined with 0 to 15 g longitudinal ultimate load. Fourth stage design loads are critical and are presented on page 4.205. The limit flight loads originate in Section 3 and the maximum ultimate flight loads are reproduced on page 4.206 for convenience of comparison. Maximum flight loads occur at approximately 35 seconds from launch. The limit radial pressure distribution on the fairing originates in Section 5 and the ultimate pressures are reproduced on page 4.207. For this study, it has been conservatively assumed that the loads on the reverse flare are twice the loads on the forward flare. The spin-up loads are an arbitrary condition occurring for two to three seconds between the fairing jettison and payload separation. Payload spin-up occurs during this interval. Theoretically this is a zero g condition; however, small loads may exist from: (1) relieving the preload in the Marman type clamp when the fairing jettisons and/or (2) the "C" Section Reaction Control System. The loads during spin-up were conservatively assumed to be ten (10) percent of the critical ultimate design loads (fourth stage design loads).

Temperatures

The fairing protects all primary structure and components from aerodynamic heating during boost allowing room temperature material properties to be used. Material properties of the fairing are reduced due to temperature. The fairing time-temperature history originated in Section 8 and is reproduced on page 4.208.

Analysis

A stress analysis of the subject structure is presented on pages 4.210 to 4.235 with a summary of the margins of safety on page 4.203. The intent of the analysis is to verify the feasibility of this particular geometrical configuration. In many cases conservative assumptions were made for simplicity and expediency. When detail drawings are released, a more refined analysis will probably result in a slight weight savings. Material for each part has been selected and is noted in the analysis. In most cases, the material was chosen from an economic standpoint. Generally, the material selected also had the highest strength to weight ratio of those considered. The fairing has high margins of safety because stiffness, rather than strength, was the designing criterion. The separation velocity of the payload and the Scout Third Step is presented on pages 4.218 through 4.219 for a varying number of Scout fourth stage separation spring assemblies (23-002164). System efficiency was assumed to be 80% and 100%. The Marman type clamp and fairing jettison system is composed of helical compression springs. Presently there is not an energy requirement to jettison the fairing and Marman type clamp at Sta. 103.8; therefore, this report does not contain a specific spring design. Because of a similar jettison system on

Scout's 34 inch Heat Shield, the fairing jettison system is considered to be routine and an analysis is not presented in this study. As noted on page 4.210 the payload is required to provide two (2) shear lips, one to transfer the shear load between the payload and the payload support ring and one to support the forward end of the fairing.

Qualification Testing

To be consistent with Scout criteria (reference b), the subject structure shall have a static failing load test.

SUMMARY OF RESULTS

Item	Margin of Safety	With Respect To	Ref. Page
			4.200
Payload Support Ring	+ 0.98	Bolt tension	.211
	+ 0.12	Bolt Cutout bending	.212
	HIGH	Panel Buckling	.212
	+ 0.09	Ring torsion	.213
Marmon Type Clamp Sta. 99.7	+ 0.24	V-Segment bending	.215
	+ 0.12	Strap tension	.215
	+ 0.43	Bolt tension	.216
	+ 0.21	Fitting bending	.217
	+ 0.41	Fitting fasteners	.217
Payload Separation Velocity	-	-	.218
			.219
Middle "D"	HIGH	Panel Buckling	.220
	+ 0.01	Ring torsion (Sta. 99.7)	.222
	HIGH	Spring shelf	.222
	+ 0.07	Ring torsion (Sta. 103.81)	.224
Marmon Type Clamp Sta. 103.81	+ 0.64	Bolt tension	.226
	+ 0.05	Strap tension	.226
	+ 0.21	V-Segment bending	.227
	+ 0.35	Fitting bending	.228
	+ 0.07	Fitting fasteners	.228
Middle "D" at Spin-Up	Positive	Deflection	.230
	HIGH	Ring bending	.231
	+ 0.20	Ring bending	.231
Fairing	HIGH	Fasteners shear	.233
	HIGH	Fairing bending	.235

Subject	Ref. Page
Torque Bolt at Sta. 98.25 to 25 in-lbs.	4.211
Torque Marmon Clamp Bolt at Sta. 99.7 to 145 in-lbs.	.216
Torque Marmon Clamp Bolt at Sta. 103.81 to 636 in-lbs.	.226

ULTIMATE LOADS

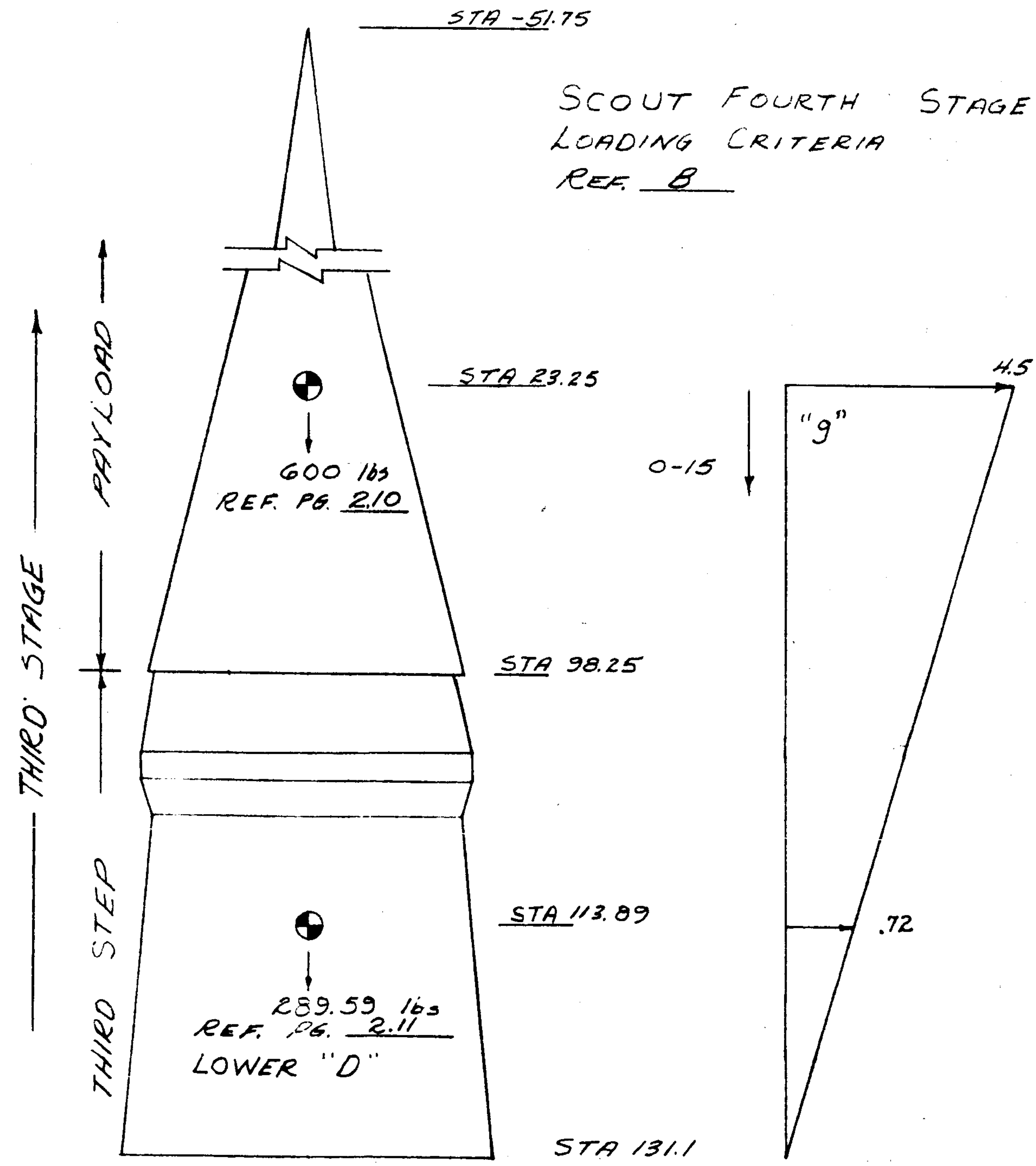

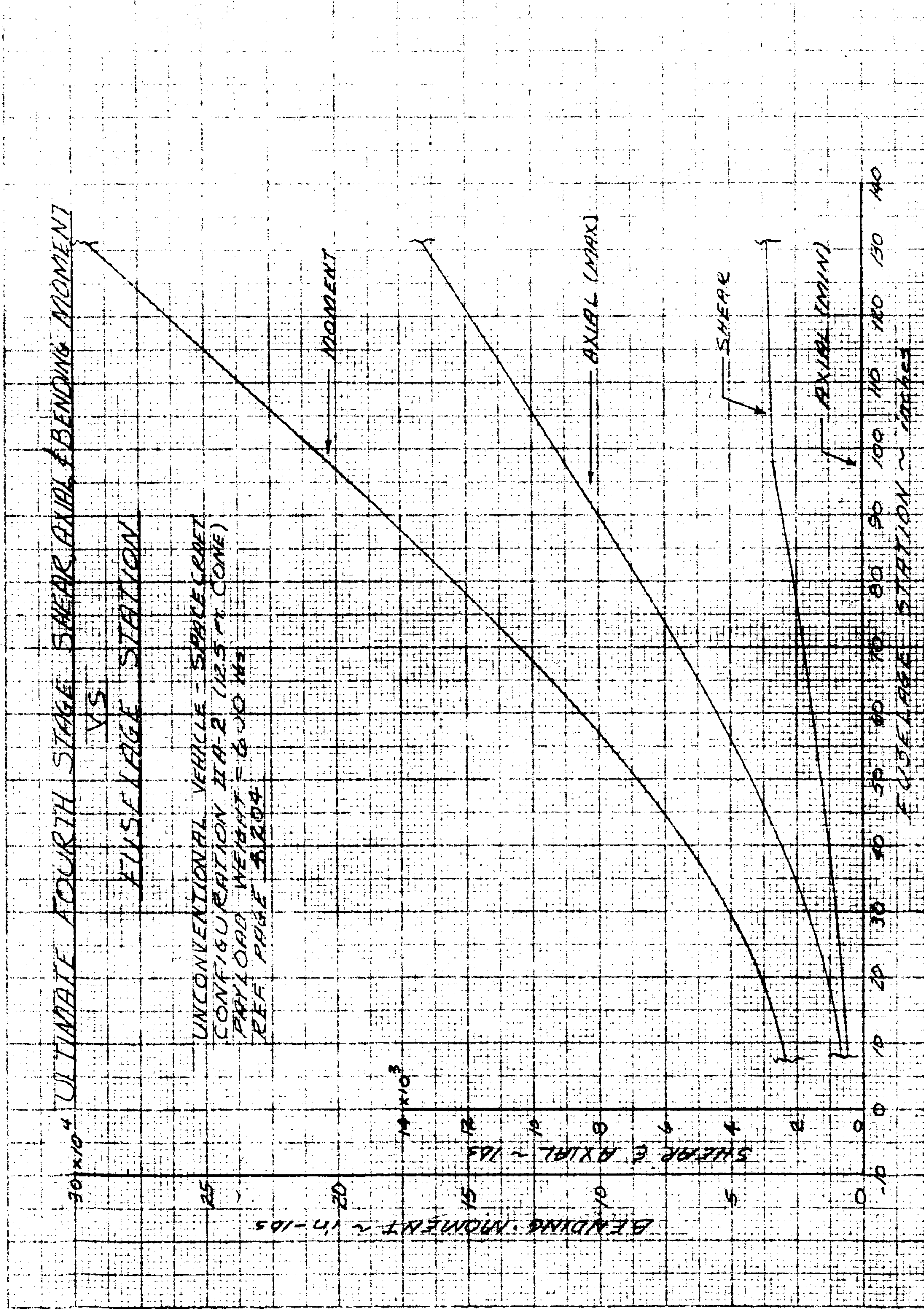
ULTIMATE FOURTH STAGE SHEAR, AXIAL & BENDING MOMENT
VS
FUSELAGE STATION
UNCONVENTIONAL VEHICLE - SPACECRAFT
CONFIGURATION IIA-2 (12.5 FT. CONE)
PAYLOAD WEIGHT = 600 lbs
REF PAGE 4.204
MOMENT
AXIAL (MAX)
SHEAR
AXIAL (MIN)
FUSELAGE STATION ~ inches
SHEAR & AXIAL ~ lbs
BENDING MOMENT ~ in-lbs
30×10^4
14×10^3

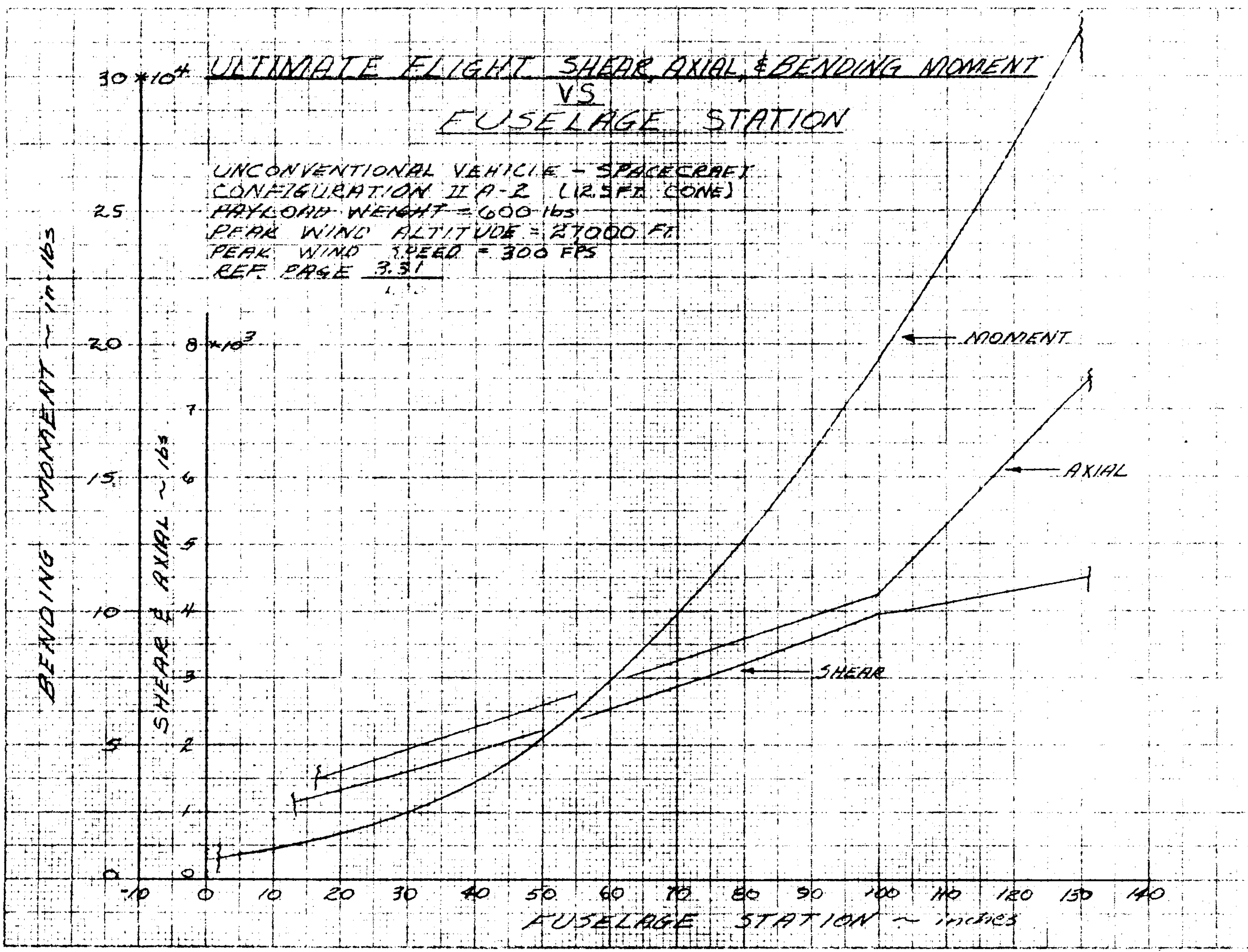
ULTIMATE FLIGHT SHEAR, AXIAL, & BENDING MOMENT
VS
FUSELAGE STATION
UNCONVENTIONAL VEHICLE - SPACECRAFT
CONFIGURATION II A-2 (12.5 FT. CONE)
PAYLOAD WEIGHT = 600 lbs
PEAK WIND ALTITUDE = 27000 FT.
PEAK WIND SPEED = 300 FPS
REF. PAGE 3.31
MOMENT
AXIAL
SHEAR
BENDING MOMENT ~ in-lbs
SHEAR & AXIAL ~ lbs
FUSELAGE STATION ~ inches

ULTIMATE RADIAL PRESSURE DISTRIBUTION ON FIBERGLASS FAIRING

UNCONVENTIONAL VEHICLE - SPACECRAFT
CONFIGURATION IIA-2 (12.5 FT. CONE)

M = 2.02
q = 2209.8 LBS/FT²
α = 5.40 DEGREES
REF. PG. 5.20

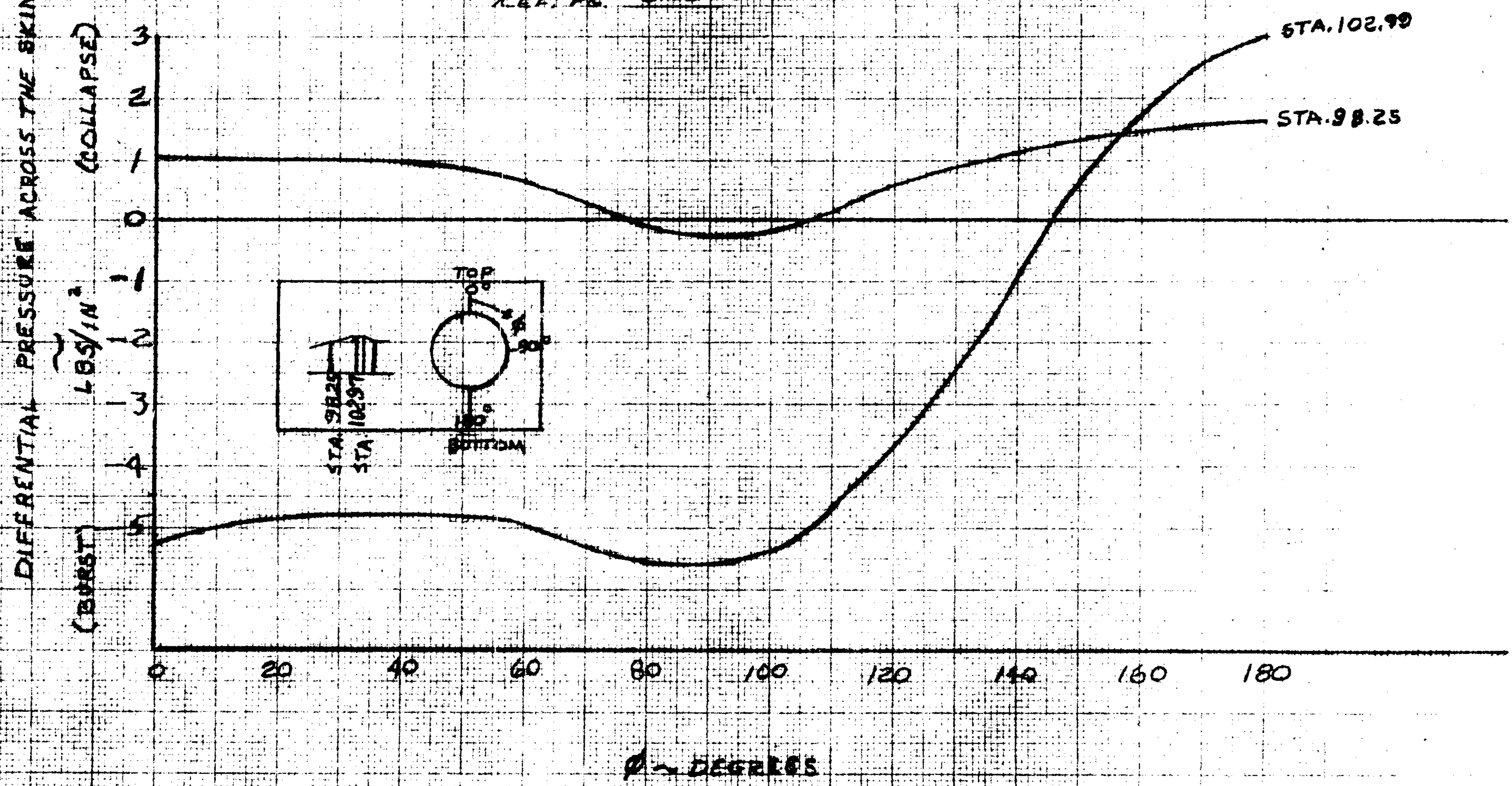

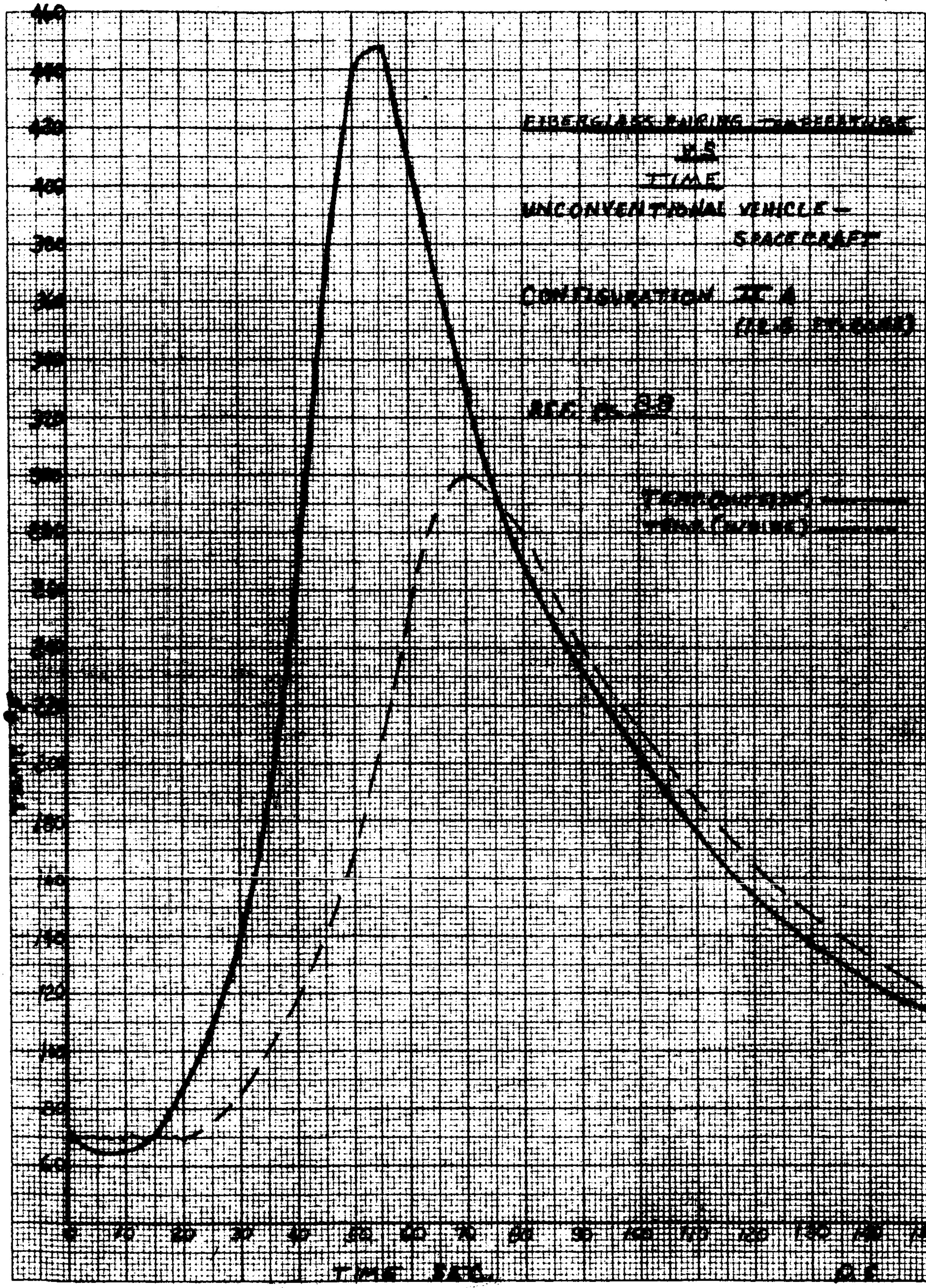
FIBERGLASS FAIRING
V.S
TIME
UNCONVENTIONAL VEHICLE —
SPACECRAFT
CONFIGURATION IIA
0 10 20 30 40 50 60 70 80 90 100 110 120 130 140 150
TIME SEC.

ULTIMATE RUNNING LOADS

STA	r in	M (1) in-lbs	P (1) lbs	ω_m (2) #/in	ω_p (2) #/in	$\omega_{t_{MAX}}$ (3) #/in	$\omega_{c\,MAX}$ #/in
98.25	11.5	203,000	9,000	± 608	- 176	+608	-784
99.70	11.5	207,500	9,200	± 622	- 179	+ 622	-801
103.81	12.3	220,000	9,800	± 705	- 174	+ 705	-879

(+) tension (−) compression

(1) REF. PG. 4.205

(2) THERE ARE FOUR (4) 5.20 in. SPIN MOTOR CUTOUTS BETWEEN STA 99.7 AND 103.81.

$$f = \frac{Mc}{I}$$

$$c = R$$

$$I = \pi r^3 t - 2Ad^2$$

$$I = r^2 t(\pi r - 2(5.2))$$

$$I = (11.92)^2 t(\pi(11.92) - 10.4)$$

$$I = 3840\,t$$

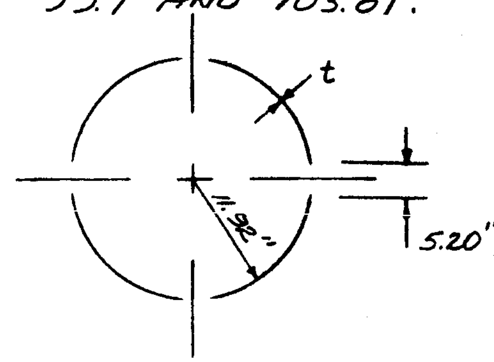

$$ft = \frac{MR}{3840} = \omega_M$$

$$f = P/A = P/(2\pi r t - 4(5.2)t)$$

$$ft = P/(2\pi R - 20.8) = \omega_P$$

(3) MIN. AXIAL LOAD = 0 REF. PG. 4.205

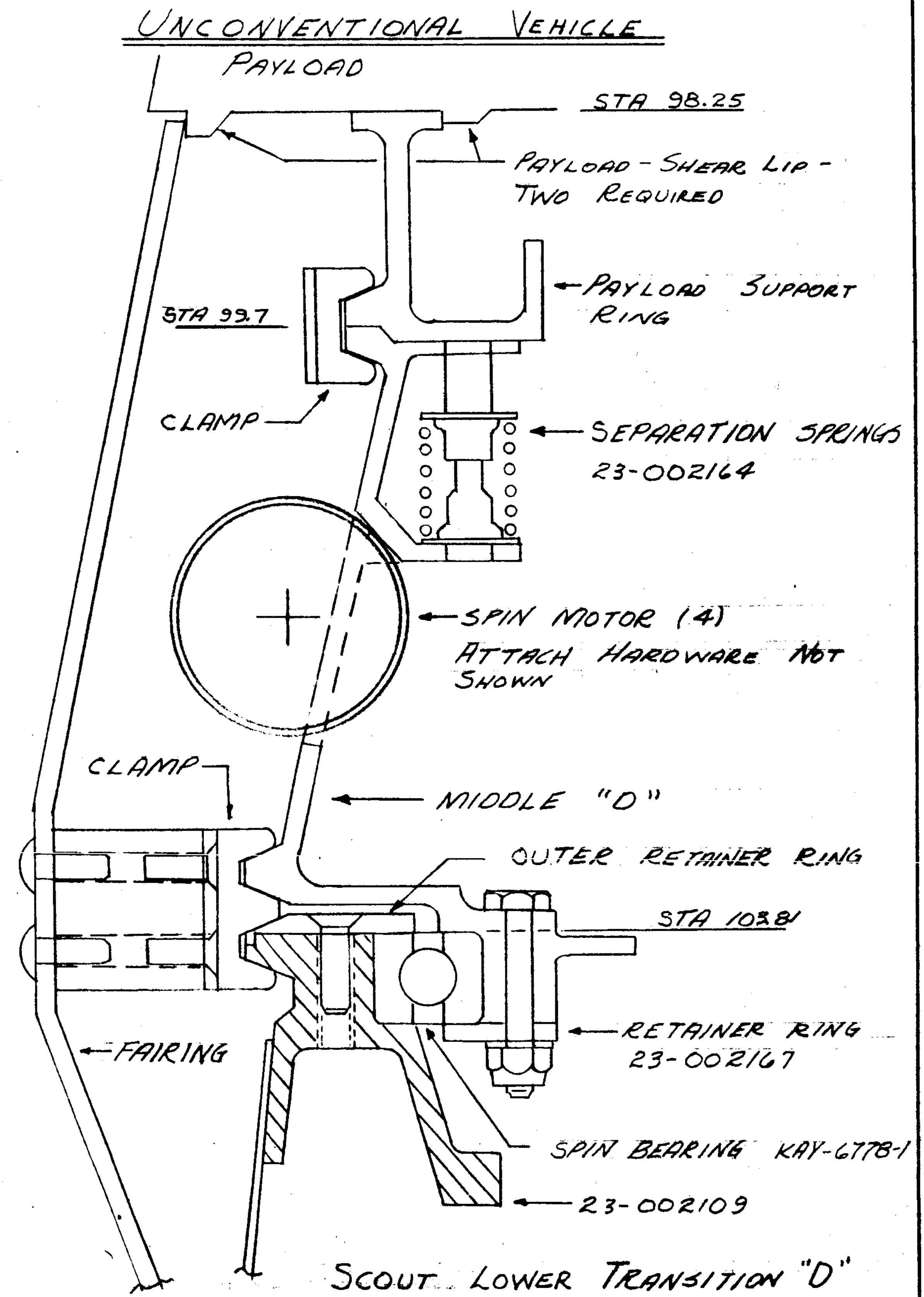

SCOUT LOWER TRANSITION "D"

ULT. LOADS

PAYLOAD SUPPORT RING

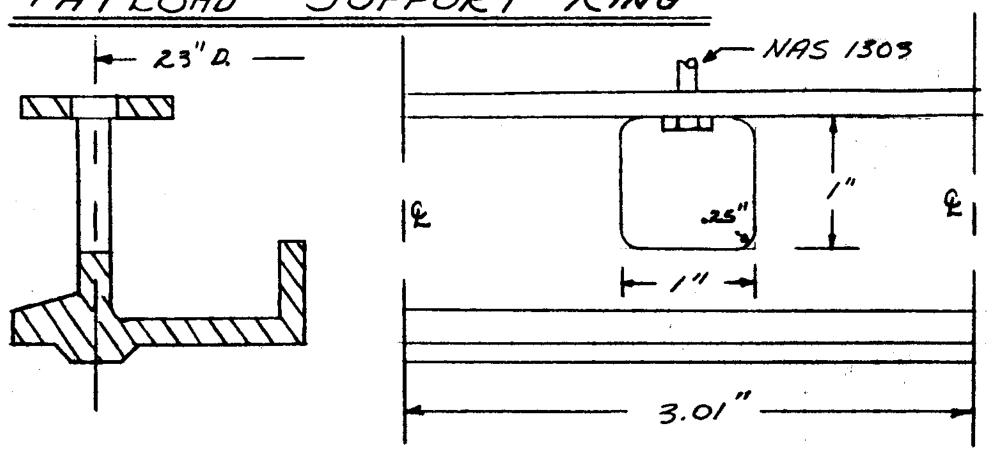

MAT'L: 2014-T6 ALUM FORGING

$F_{TU} = 65{,}000$ psi $E = 10.5 \times 10^6$

$F_{TY} = 55{,}000$ psi $G = 4.0 \times 10^6$

$F_{SU} = 40{,}000$ psi REF. K

BOLTS

24 REQ'D. $\text{SPACE} = \frac{\pi(23)}{24} = 3.01''$

$\omega_{t\,MAX} = 608$ #/in REF. PG. 4.209

BOLT LOAD = (3.01)(608) = 1830 #

NAS 1303 TENSION ALL = 3620 lbs.
REF. NATIONAL STANDARD ASSOCIATION

$$M.S. = \frac{3620}{1830} - 1 = +0.98$$

TORQUE TO LIMIT LOAD

$$T = \frac{P}{2\pi n K}$$

n = no. of threads per inch (32)
K = 0.244

$$T = \frac{1830/1.5}{2\pi(32)(.244)} = 24.9 = 25 \text{ in-lbs}$$

ULT LOADS

BENDING AT BOLT CUTOUT

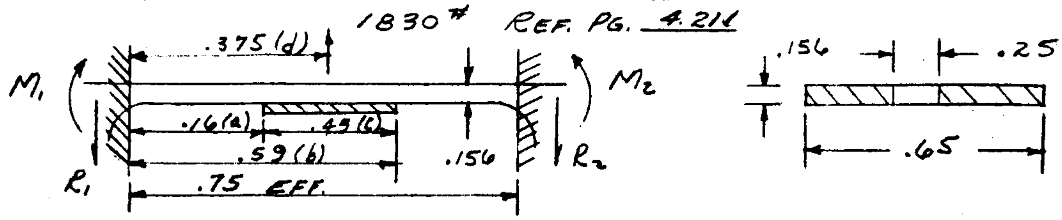

$$R_1 = R_2 = \frac{1830}{2} = 915\,\#$$

$$M_1 = -M_2 = -\frac{P}{24L}\left(24\frac{d^3}{L} - 6\frac{bc^2}{L} + 3\frac{c^3}{L} + 4c^2 - 24d^2\right)$$

REF. L CASE 34 PG. 108

END MOMENT IS CRITICAL

$$M_1 = -\frac{1830}{24(.75)}\left[24\left(\frac{.375^3}{.75}\right) - 6\left(\frac{.59(.43)^2}{.75}\right) + 3\frac{(.43)^3}{.75} + 4(.43)^2 - 24(.375)^2\right]$$

$$M_1 = 102(-1.504) = 153 \text{ in-lbs}$$

$$f = \frac{6M}{bt^2} = \frac{6(153)}{(.65)(.156)^2} = 58{,}000 \text{ psi}$$

$$M.S. = \frac{65{,}000}{58{,}000} - 1 = \underline{+0.12}$$

BUCKLING BETWEEN BOLTS

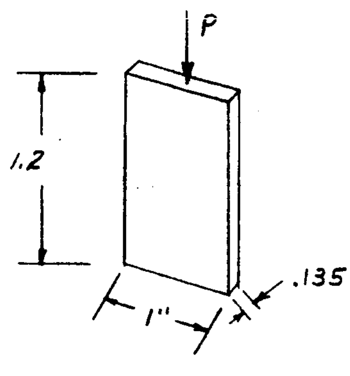

$$w_{c\,MAX} = 784\ \#/in \qquad \text{REF. PG. } 4.209$$

$$P = 784\left(\frac{3.01}{3.01-1}\right) = 1175 \text{ lbs}$$

$$P_{CR} = \frac{\pi^2 EI}{L^2} \qquad \text{REF. } M$$

$$P_{CR} = \frac{\pi^2(10.5)(10^6)(1)(.135)^3}{1.2^2(12)}$$

$$P_{CR} = 14{,}700 \text{ lbs}$$

$$f = P/A \qquad P_{CR} = 55{,}000(.135) = 7{,}425 \text{ lbs}$$

$$F_{cy} = 55{,}000 \text{ psi} \qquad \text{REF. PG. } 4.211$$

$$M.S. = \frac{7425}{1145} - 1 = \underline{HIGH}$$

ULT. LOADS

RING TORSION

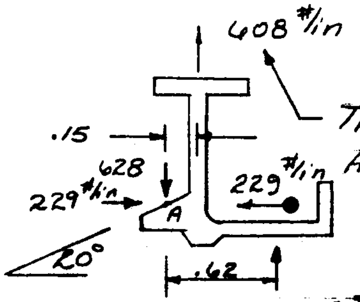

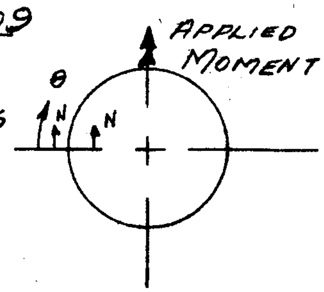

REF. PG. 4.214

N-N

$dM_{t_A} = (.15)608\cos\Theta + .62(19.8) = 0$

$\cos\Theta = -0.135$

$\Theta = 98°$

ASSUME NO TORQUE ON COMPRESSION SIDE ∴ $\Theta = 90°$

$M_T = \int dM_t \cos\Theta\, R\, d\Theta \qquad M_M = \int dM_t \sin\Theta\, R\, d\Theta$

TORSION IS CRITICAL

$$M_T = \int_0^{\pi/2} (91.2\cos\Theta + 12.3)(\cos(90-\Theta))\, R\, d\Theta$$

$$M_T = 11.5\int_0^{\pi/2} (91.2\cos\Theta\sin\Theta + 12.3\sin\Theta)\, d\Theta$$

$$M_T = 11.5\left[45.6\sin^2\Theta - 12.3\cos\Theta\right]\Big|_0^{\pi/2}$$

$M_T = 665$ in-lbs

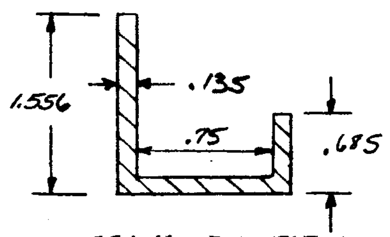

EQUIV. SECTION

$b = 1.556 + .75 + .685 = 2.99$

$\tau = \dfrac{3M}{bt^2}$ REF. M

$\tau = \dfrac{3(665)}{(2.99)(.135)^2}$

$\tau = 36{,}600$ psi

$F_{su} = 40{,}000$ psi REF. PG. ____

$$M.S. = \frac{40{,}000}{36{,}600} - 1 = +0.09$$

3-51324

LIMIT LOADS

PRELOAD ROTATION

$I_{xx} = 0.182\ in^4$

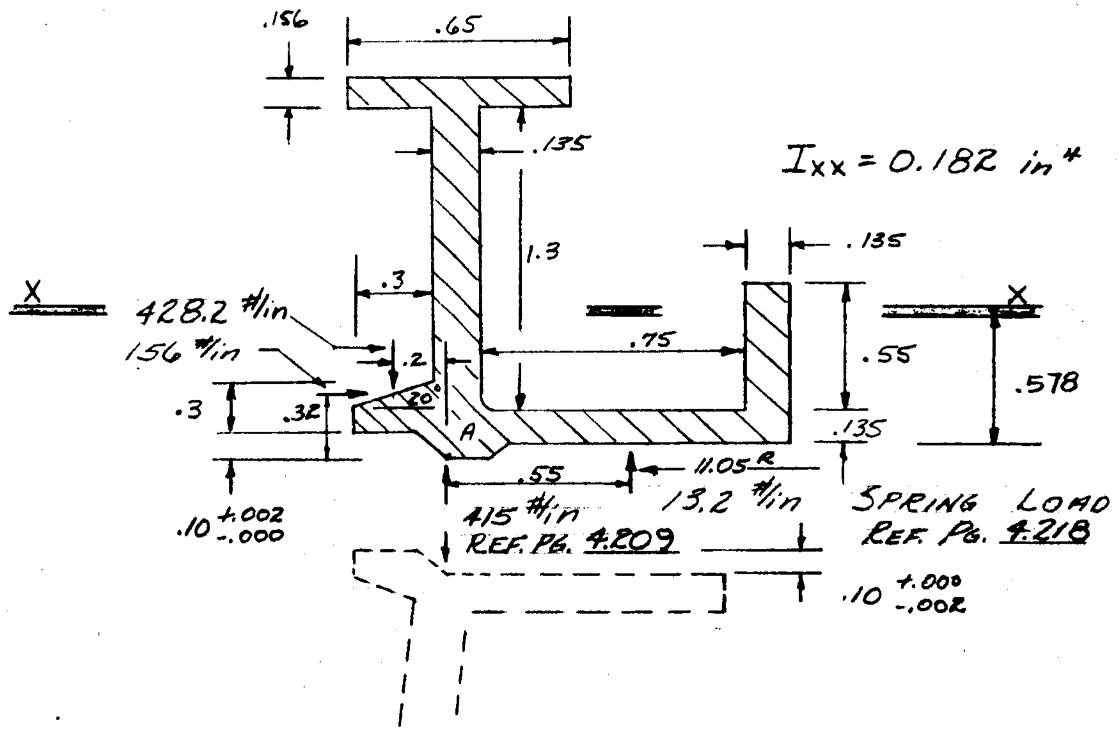

$\Sigma M_A = M_T = 428.2(.2) + 13.2(.55) - 156(.32)$

$M_T = 42.75$ in-lbs/in

$\Theta = \dfrac{MR^2}{EI}$ REF. L   PG. 230

$E = 10.5 \times 10^6$ $R = 11.5$ REF. PG. 4.211

$\Theta = \dfrac{42.75(11.5)^2}{10.5(10^6)(.182)} = 2960 \times 10^{-6}$ rad

$\Theta = 0.17°$

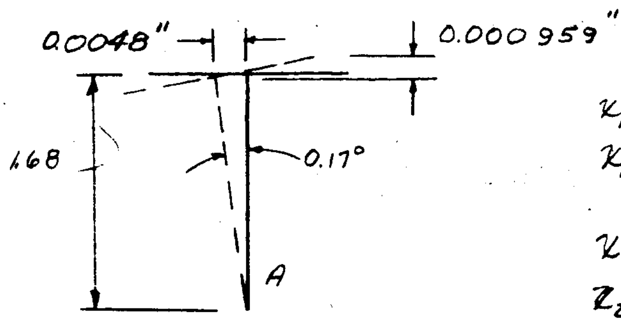

$x_1 = 1.68 \tan(.17°)$

$x_1 = 1.68(.00291) = .0048$ in

$x_2 = \tfrac{1}{2}(.65)\tan(.17)° + x_2 \tan(.17°)$

$x_2 = .325(.00291) + (.0048)(.00291)$

$x_2 = .000959$ in

ULT LOADS

CLAMP STA 99.7

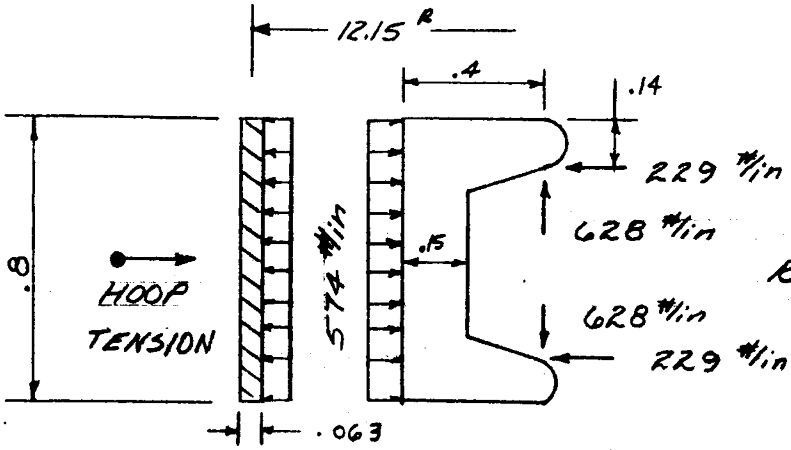

V- SEGMENT

MAT'L: 7075-T6 ALUM

F_{TU} = 77,000 psi REF. K

$f = P/A + 6M/bt^2$ $M = 628(.4 - .15/2) + 229(.8/2 - .14) - 574(.4^2/2) = 217.6$ in-lbs

$f = 628/(1)(.15) + 6(217.6)/(1)(.15)^2$

$f = 4190 + 58{,}000 = 62{,}190$ psi

$M.S. = \frac{77{,}000}{62{,}190} - 1 = +0.24$

STRAP

MAT'L: 4130 STEEL 180,000 psi H.T.

LOAD $= P = pR = (.8)(574)(12.15) = 5{,}580$ lbs

$f = P/A$ REMOVE 1/4" RIVET HOLE

$f = 5{,}580/(1.8 - .25)(.063) = 161{,}000$ psi

$M.S. = \frac{180{,}000}{161{,}000} - 1 = +0.12$

ULT LOADS

EXPLOSIVE BOLT

USE (3/8)" HOLEX BOLT DWG 322-00131

TENSION ALL. = 8000 lbs

LOAD = 5,580 lbs REF. PG. 4.215

$$M.S. = \frac{8000}{5580} - 1 = +0.43$$

PRELOAD TORQUE TO LIMIT LOAD

$$T = \frac{P}{2\pi n K} \qquad P_{LIMIT} = 5{,}580/1.5 = 3720 \text{ lbs}$$

$$n = 24 \qquad K = .171$$

$$T = \frac{3720}{2\pi(24)(.171)} = 145 \text{ in-lbs}$$

FITTING

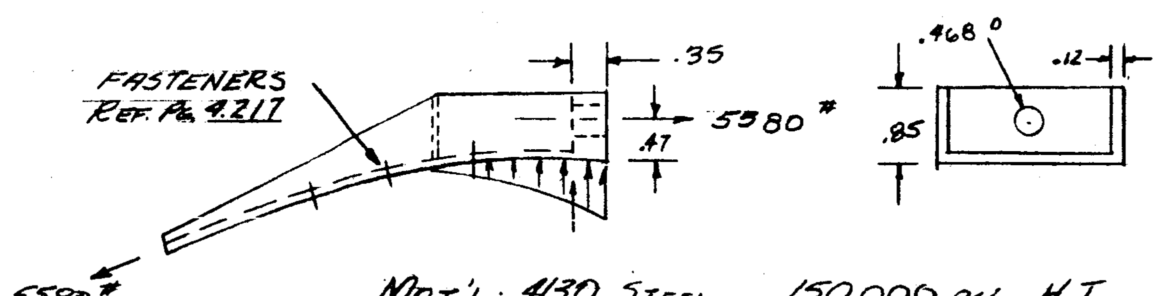

MAT'L: 4130 STEEL 150,000 psi H.T.

LOCAL WALL BENDING IS CRITICAL. LET THE WORKING STRESS LEVEL IN THE WALL AND ℄ OF END PAD BE EQUAL.

$$f_e = \frac{6 M_e}{b_e t_e^2} \qquad f_w = \frac{6 M_w}{b_w t_w^2} = \frac{6 M_e}{b_e t_e^2} \qquad \text{EQ. 1}$$

$b_e = .85 - .468 = .382$; $t_e = .35$; $b_w = .85$; $t_w = .12$

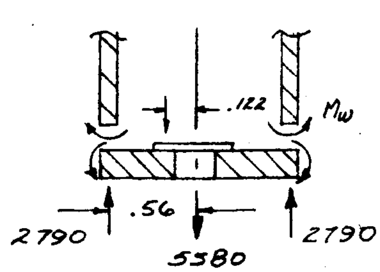

$$M_e = -M_w + 2790(.56 - .122)$$

$$M_e = 943 - M_w \qquad \text{EQ. 2}$$

ULT LOADS

$$\frac{6(943-M_w)}{(.382)(.35)^2} = \frac{6M_w}{(.85)(.12)^2}$$

$$M_w = \frac{6(943)}{28.9} = 196 \text{ in-lbs}$$

$$f = P/A + 6M/bt^2 = \frac{2790}{(.85)(.12)} + \frac{6(196)}{(.85)(.12)^2}$$

$$f = 27{,}400 + 96{,}000 = 123{,}400 \text{ psi}$$

$F_{TU} = 150{,}000$ psi REF. PG. 4.216

$$M.S. = \frac{150{,}000}{123{,}400} - 1 = +0.21$$

FASTENERS REF. PG. 4.216

USE 3/16" HKM-ACT 509H-T6 HUCK BOLT

SHEAR ALL = 2620 lbs 3 REQ'D REF. N

$$M.S. = \frac{3(2620)}{5580} - 1 = +0.41$$

PAYLOAD SEPARATION VELOCITY

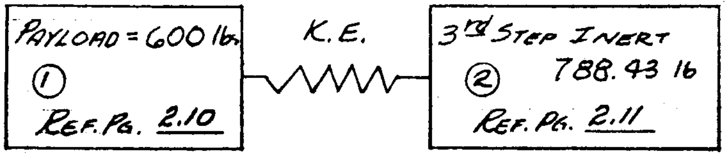

FAIRING AND CLAMP - STA 103.81 JETTISON PRIOR TO PAYLOAD SEPARATION. ASSUME THEY WEIGH 25 lbs, THEREFORE 3rd STEP INERT WEIGHS 788.43 - 25 = 763.43 lbs.

$$M_1 = \frac{600}{32.2} = 18.65 \qquad M_2 = \frac{763.43}{32.2} = 23.7$$

$$M_1 V_1 = M_2 V_2 \qquad K.E. = \tfrac{1}{2} M_1 V_1^2 + \tfrac{1}{2} M_2 V_2^2$$

$$2K.E. = V_1^2 \left(M_1 + \frac{M_1^2}{M_2} \right)$$

$$V_1 = 0.245 \sqrt{K.E.}$$

$$V_2 = \frac{M_1}{M_2} V_1 = \frac{18.65}{23.7} (.245 \sqrt{KE}) = 0.193 \sqrt{KE}$$

$$\Delta V = V_1 + V_2 = 0.438 \sqrt{KE}$$

KE = PE

SPRINGS 23-002164

LOAD AT 0.81" = 28.6 lbs

LOAD AT 1.21" = 8.2 lbs

$$PE = \eta \left(\frac{N}{12}\right)\left(\frac{1}{2}\right)(.40)(28.6 + 8.2) = 0.613\, \eta N \text{ ft-lbs}$$

WHERE η = SYSTEM EFF. N = No. of SPRINGS

$$\Delta V = 0.438 \sqrt{0.613\, \eta N} = \underline{0.343 \sqrt{\eta N}}$$ ~~REF. PG.~~ 4.219

STATIC RUNNING LOAD REF. PG. 4.214
FOR 32 SPRINGS

$$\omega_s = \frac{28.6\,(32)}{2\pi\,(11.05)} = \underline{13.2 \text{ \#/in LIMIT}}$$

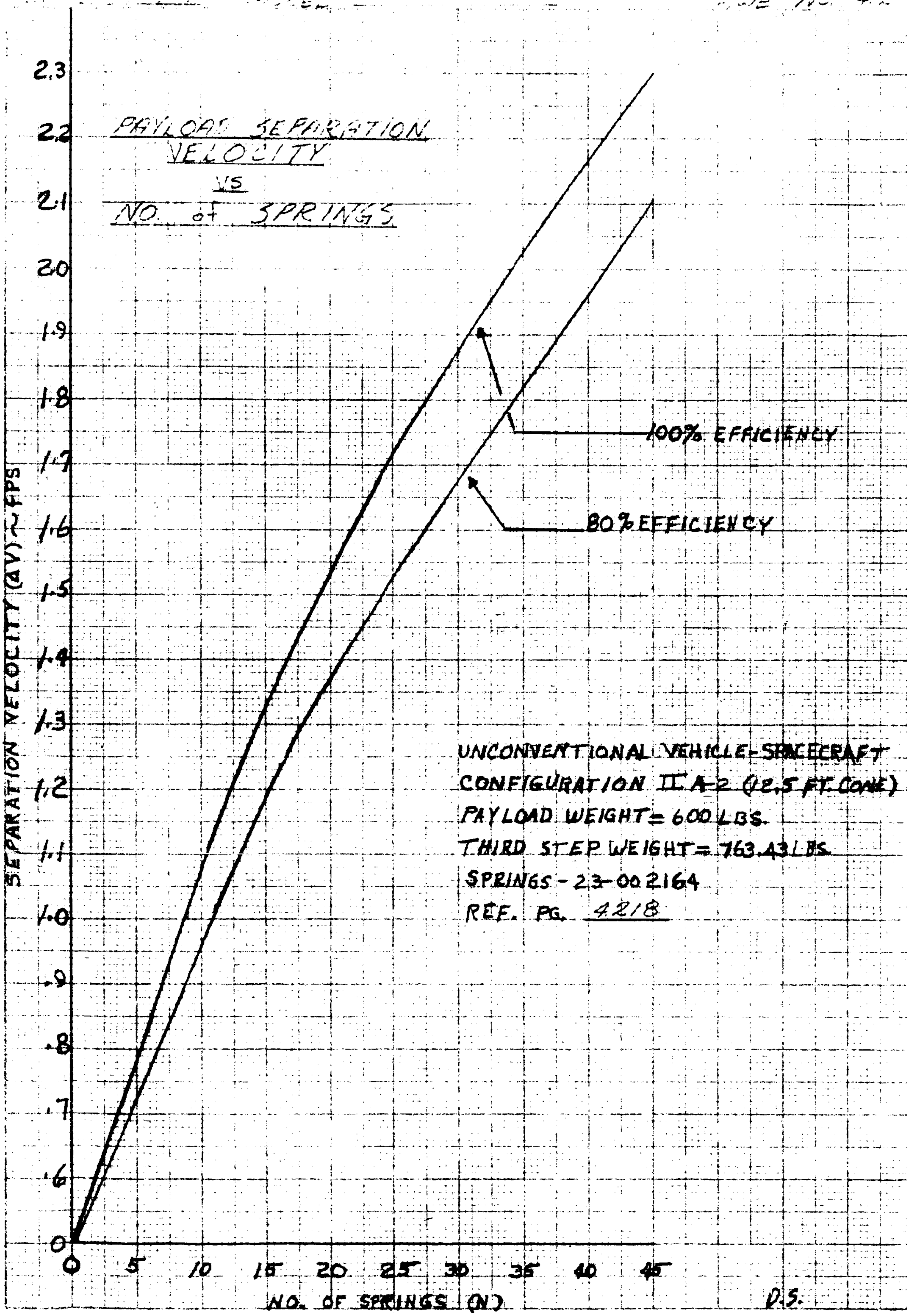
PAYLOAD SEPARATION VELOCITY VS NO. of SPRINGS
SEPARATION VELOCITY (ΔV) ~ FPS
2.3
2.2
2.1
2.0
1.9
1.8
1.7
1.6
1.5
1.4
1.3
1.2
1.1
1.0
.9
.8
.7
.6
0
0
5
10
15
20
25
30
35
40
45
NO. OF SPRINGS (N)
100% EFFICIENCY
80% EFFICIENCY
UNCONVENTIONAL VEHICLE-SPACECRAFT
CONFIGURATION II A-2 (12.5 FT. CONE)
PAYLOAD WEIGHT = 600 LBS.
THIRD STEP WEIGHT = 763.43 LBS.
SPRINGS - 23-002164
REF. PG. 4218
D.S.

ULT LOADS

MIDDLE "D"

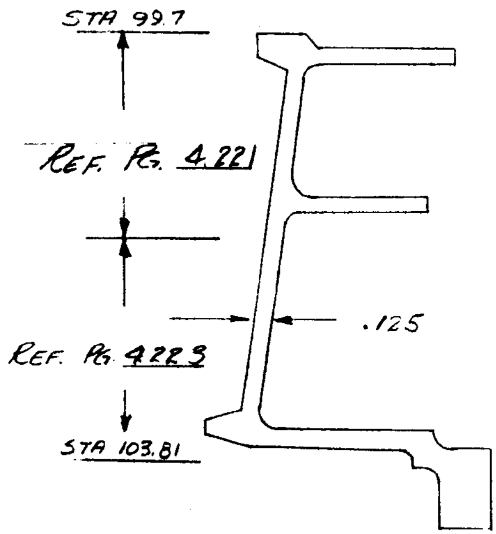

MAT'L: 2014-T6 ALUM FORGING
$F_{TU} = 65{,}000$ psi
$F_{TY} = 55{,}000$ psi
$F_{SU} = 40{,}000$ psi
$E = 10.5 \times 10^6$ psi $\mu = .3$
$G = 4.0 \times 10^6$ psi
REF. K

PANEL BUCKLING

REF. L CASE K PG. 315

TREAT AREA BETWEEN CUTOUTS AS A PANEL
CUTOUTS = 5.2 in $R = 11.92$ REF. PG. 4.209

PANEL WIDTH $(b) = \frac{2\pi(11.92) - 4(5.2)}{4} = 13.55$

$$f' = \frac{E}{6(1-\mu^2)}\left[\sqrt{12(1-\mu^2)\left(\frac{t}{R}\right)^2 + \left(\frac{\pi t}{b}\right)^4} + \left(\frac{\pi t}{b}\right)^2\right]$$

$$f' = \frac{10.5(10^6)}{6(1-.09)}\left[\sqrt{12(1-.09)\left(\frac{.125}{11.92}\right)^2 + \left(\frac{\pi(.125)}{13.55}\right)^4} + \left(\frac{\pi(.125)}{13.55}\right)^2\right]$$

$$f' = 1.925 \times 10^6 (35{,}550 \times 10^{-6}) = 68{,}300 \text{ psi}$$

$F_{CY} = 55{,}000$ psi

$f = W_{cmax}/t = 879/0.10 = 8{,}790$ psi REF. PG. 4.209

$$M.S. = \frac{55{,}000}{8{,}790} - 1 = \text{HIGH}$$

ULT LOADS

RING TORSION REF. PG. 4.220

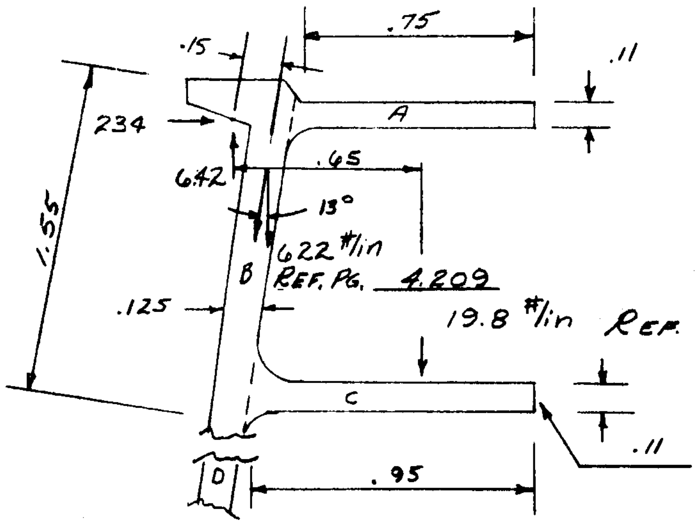

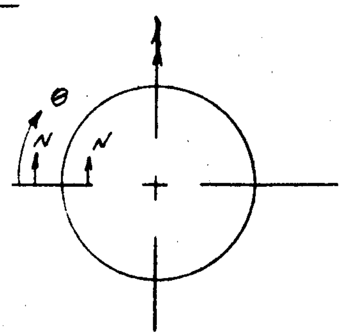

N-N

$dM_t = 637\cos\theta(.15) + 19.8(.65)$

As on page 4.213, assume torque on compression side = zero.

$$M_T = \int_0^{\pi/2} (95.5\cos\theta + 12.9)\cos(90-\theta)\,R\,d\theta$$

$$M_T = \int_0^{\pi/2} (95.5\sin\theta\cos\theta + 12.9\sin\theta)\,R\,d\theta$$

$$M_T = 11.5\left[47.75\sin^2\theta - 12.9\cos\theta\right]\Big|_0^{\pi/2} = 697 \text{ in-lbs}$$

STIFFNESS

			REF.
$(M/\theta)_A = G\frac{bt^3}{3} = \frac{4(10^6)(.75)(.11)^3}{3}$		$= 1330$	M
$(M/\theta)_B = G\frac{bt^3}{3} = \frac{4(10^6)(1.55)(.125)^3}{3}$		$= 4030$	M
$(M/\theta)_C = G\frac{bt^3}{3} = \frac{4(10^6)(.95)(.11)^3}{3}$		$= 1685$	M

$(M/\theta)_D = \lambda D$

$$\lambda = \sqrt[4]{\frac{3(1-\mu^2)}{R^2t^2}} = \sqrt[4]{\frac{3(1-.3^2)}{(11.5)^2(.125)^2}} = 1.072$$

$$D = \frac{Et^3}{12(1-\mu^2)} = \frac{10.5(10^6)(.125)^3}{12(1-.3^2)} = 1875$$

$\lambda D = 1.072(1875) \quad = 2010 \quad$ L

$$\Sigma(M/\theta) = 9055 \ \frac{\text{in-lbs}}{\text{rad}}$$

ULT LOADS

$M_{TA} = \frac{1330}{9055}(687) = 102.5$ in-lbs

$M_{TB} = \frac{4030}{9055}(687) = 310$ in-lbs

$M_{TC} = \frac{1685}{9055}(687) = 130$ in-lbs

$M_{TD} = \frac{2010}{9055}(687) = 154$ in-lbs

$\tau = \frac{3M}{bt^2}$

REF. M

$\tau_A = \frac{3M}{bt^2} = \frac{3(102.5)}{(.75)(.11)^2} = 33{,}900$ $\quad$ $M.S. = \frac{40{,}000}{33{,}900} - 1 = +0.18$

$\tau_B = \frac{3M}{bt^2} = \frac{3(310)}{(1.55)(.125)^2} = 38{,}400$ $\quad$ $M.S. = \frac{40{,}000}{38{,}400} - 1 = +0.04$

$\tau_C = \frac{3M}{bt^2} = \frac{3(130)}{(.95)(.11)^2} = 33{,}900$ $\quad$ $M.S. = \frac{40{,}000}{33{,}900} - 1 = +0.18$

$f_D = P/A + \frac{6M}{bt^2} = \frac{687}{(.125)(1)} + \frac{6(154)}{(1)(.125)^2} = 64{,}100$ $\quad$ $M.S. = \frac{65{,}000}{64{,}100} - 1 = +0.01$

SPRING SHELF REF. PG. 4.221

SPRING LOAD = 28.6(1.5) = 42.9 lbs REF. PG. 4.218

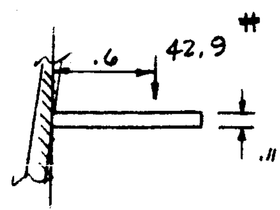

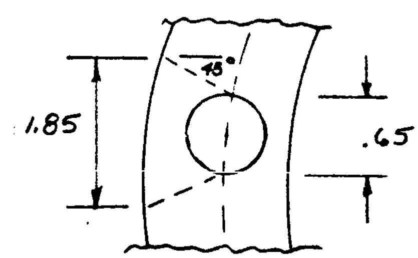

$f = \frac{6M}{bt^2} = \frac{6(.6)(42.9)}{(1.85)(.11)^2} = 6{,}900$ psi

$M.S. = \frac{65{,}000}{6{,}900} - 1 = \text{HIGH}$

DEFLECTION AT SPRING ℄ (LIMIT LOAD)

$\Delta = \frac{PL^3}{3EI}$ $\quad$ REF. L

$\Delta = \frac{(28.6)(.6)^3(12)}{3(10.5)(10^6)(1.85)(.11)^3} = 955 \times 10^{-6} = 0.000955$ in

ULT. LOADS

RING TORSION   REF. PG. 4.220

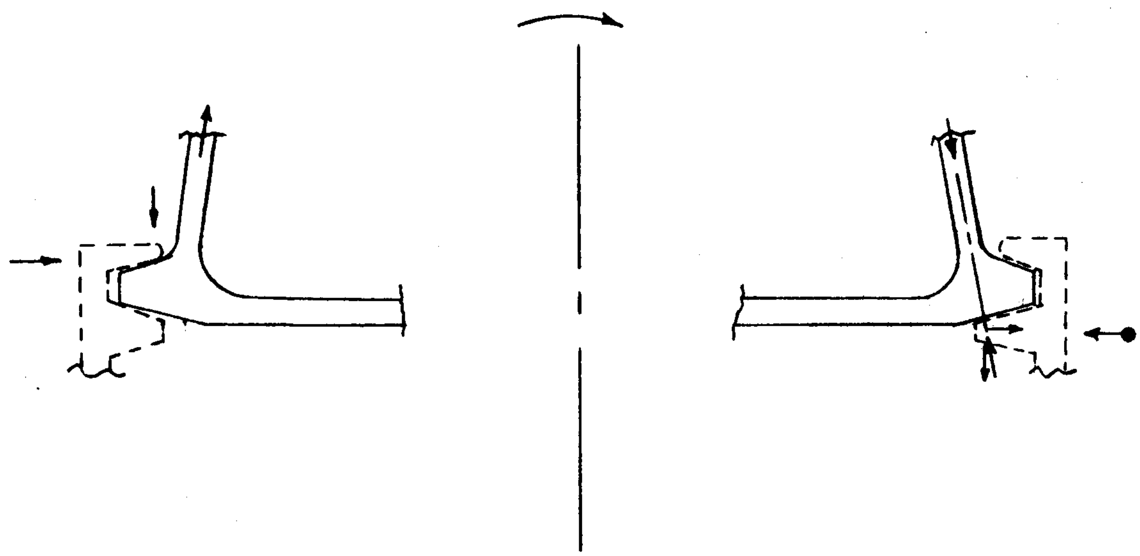

COMPRESSION SIDE

NO TORSION

TENSION SIDE   705 #/in   REF. PG. 4.209

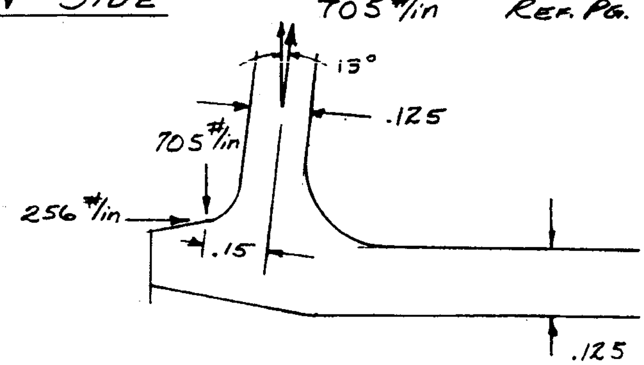

$$dM_t = 724\cos\theta(.15)$$

$$M_T = \int_0^{\pi/2} (108.5\cos\theta)\cos(90-\theta)\, R\, d\theta$$

$$M_T = 12.5\int_0^{\pi/2} 108.5\sin\theta\cos\theta\, d\theta$$

$$M_T = 12.5\left[54.25\sin^2\theta\right]\Big|_0^{\pi/2} = 677 \text{ in-lbs}$$

ULT. LOADS

STIFFNESS

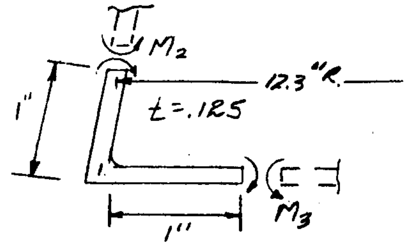

$M_1/\theta = \frac{Gbt^3}{3}$ REF. M

$M_1/\theta = \frac{4(10^6)(2)(.125)^3}{3} = 5200$

$M_2/\theta = \lambda D$ REF. L

$D = \frac{Et^3}{12(1-\mu^2)} = \frac{10.5(10^6)(.125)^3}{12(1-.3^2)} = 1880$

$\lambda = \sqrt[4]{\frac{3(1-\mu^2)}{R^2t^2}} = \sqrt[4]{\frac{3(1-.3^2)}{(12.3)^2(.125)^2}} = 1.0345$

$\lambda D = (1.0345)(1880) = 1950$

$M_3/\theta = \frac{Et^3}{12(1-\mu^2)} = 1880$ REF. L

$\Sigma M/\theta = 9030 \ \frac{in\text{-}lbs}{rad}$

$M_{T_1} = \frac{677}{9030}(5200) = 390$ in-lbs

$M_{T_2} = \frac{677}{9030}(1950) = 146$ in-lbs

$M_{T_3} = \frac{677}{9030}(1880) = 141$ in-lbs

$\tau_1 = \frac{3M_T}{bt^2} = \frac{3(390)}{(2)(.125)^2} = 37{,}400$ psi REF. M

$F_{SU} = 40{,}000$ psi REF. PG. 4.220

$M.S. = \frac{40{,}000}{37{,}400} - 1 = +0.07$

$\sigma_2 = \frac{6M}{bt^2} = \frac{6(146)}{(1)(.125)^2} = 56{,}000$ psi

$F_{TU} = 65{,}000$ psi REF. PG. 4.220

$M.S. = \frac{65{,}000}{56{,}000} - 1 = +0.16$

ULT LOADS

CLAMP - STA 103.81

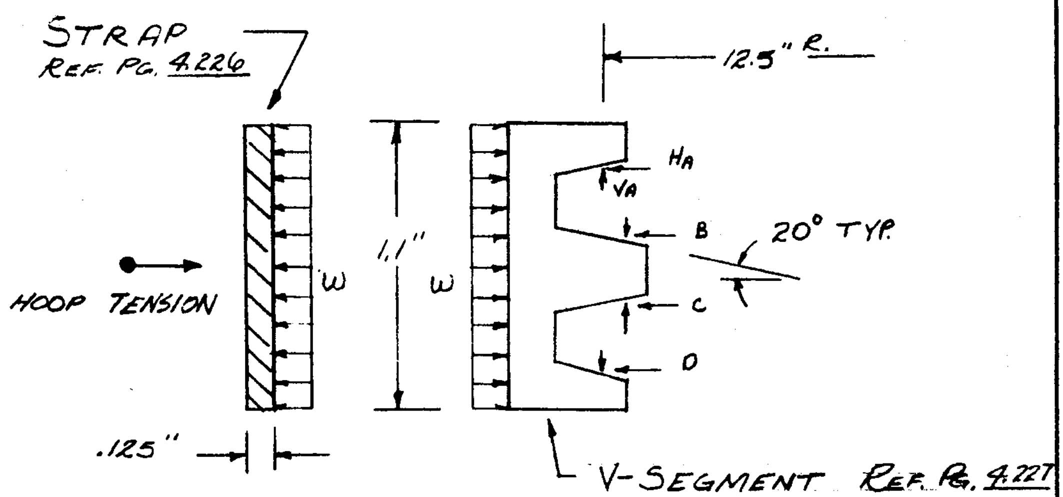

THE JOINT WILL BE PRELOADED TO LIMIT LOAD OF THE MAXIMUM TENSION LOADING CONDITION.

$\omega_{L\,MAX} = 705$ #/in $= V_{A,B,C,D}$ REF. PG. 4.209

$\sum_{i=A}^{D} H_i = 4(705 \tan 20°)/1.5 = 684$ #/in LIMIT

$\omega = 684/1.1 = 622$ #/in-in

$P = 684(12.5) = 8{,}550$ lbs LIMIT

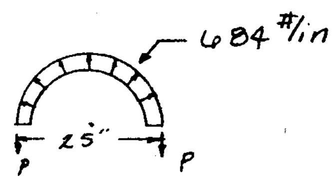

USE BOLT NO. 2549 OR EQUIVALENT
EXPLOSIVE ORDNANCE TECHNICAL DATA BOOK
McCORMICK SELPH, HOLLISTER AIRPORT
HOLLISTER, CALIF.

1/2" - 20 200,000 psi H.T. MAX.
TENSION ALL. = 21,000 lbs REF. DATA BOOK

ULT LOADS

PRELOAD

$$T = \frac{P}{2\pi n K}$$

n = 20 K = 0.107
P = 8,550 lbs REF. PG. 4.225

$$T = \frac{8550}{2\pi(20)(.107)} = \underline{\underline{636 \text{ in-lbs TORQUE}}}$$

BECAUSE OF THE CHARACTERISTICS OF THE CLAMP (SEE SKETCH) THE PRELOAD LOAD IS CRITICAL FOR THE BOLT AND STRAP.

LOADS - REF. PG. 4.209

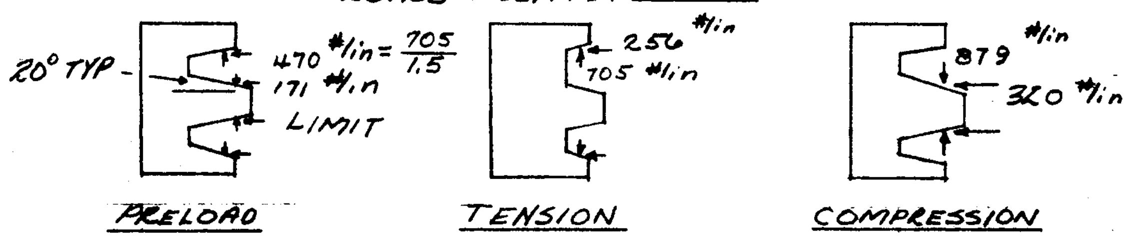

$$4(171)(1.5) > 2(256) \; ; > (2)(320)$$
$$1025 > 512 \; ; > 640$$

BOLT REF. PG. 4.225

BOLT LOAD = 4(171)(1.5)(12.5) = 12,840 lbs
TENSION ALL = 21,000 lbs REF. PG. 4.225

$$M.S. = \frac{21,000}{12,840} - 1 = \underline{\underline{+0.64}}$$

STRAP REF. PG. 4.225

$f = P/A$ $A = tb$ $b = 1.1 - 2(.25) = 0.6$
$f = 12,840/(.125)(.6)$ REMOVE 2 1/4" HOLES
$f = 171,000$ psi

MAT'L: 4130 STEEL 180,000 psi H.T.

$$M.S. = \frac{180,000}{171,000} - 1 = \underline{\underline{+0.05}}$$

ULT LOADS

V-SEGMENT REF. PG. 4.225

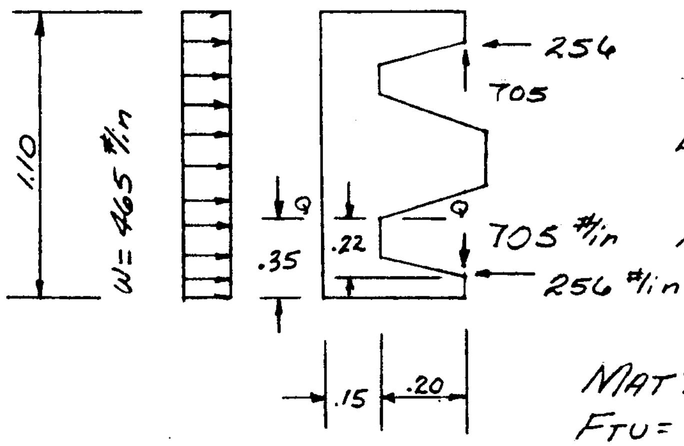

ULT TENSION LOADING IS CRITICAL.

REF. PG. 4.223

MAT'L: 7075-T6 ALUM
F_{TU} = 77,000 psi
REF. K

SECTION Q-Q

$$M_{Q-Q} = 256(.22) + 705(.20 + .15/2) - 465\left(\frac{.35^2}{2}\right) = 221.8 \text{ in-lb}$$

$$f = P/A + \frac{6M}{bt^2} = 705/(1)(.15) + \frac{6(221.8)}{(1)(.15^2)}$$

$$f = 4700 + 59{,}000 = 63{,}700 \text{ psi}$$

$$M.S. = \frac{77{,}000}{63{,}700} - 1 = \underline{\underline{+0.21}}$$

FITTING

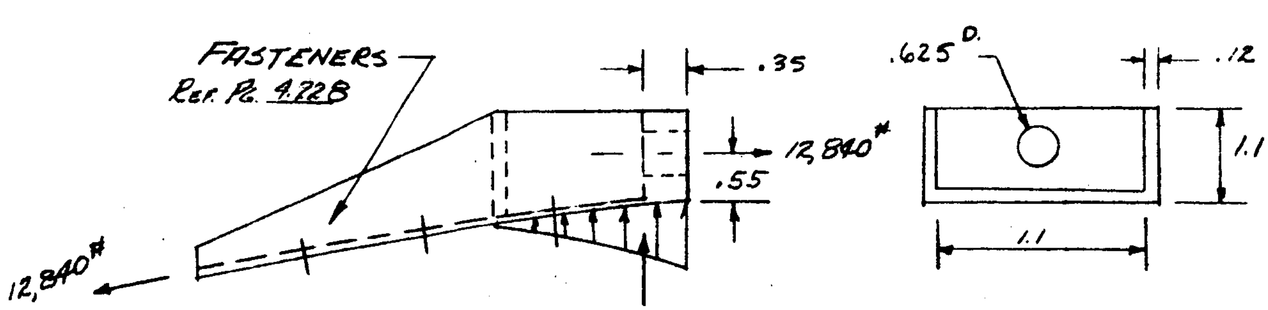

MAT'L: 4130 STEEL 150,000 psi H.T.
F_{BU} = 225,000 psi BEND. MOD. K=1.5 REF. O

ULT. LOADS

LOCAL WALL BENDING IS CRITICAL. LET THE WORKING STRESS LEVEL IN THE WALL AND ℄ OF END PAD BE EQUAL.

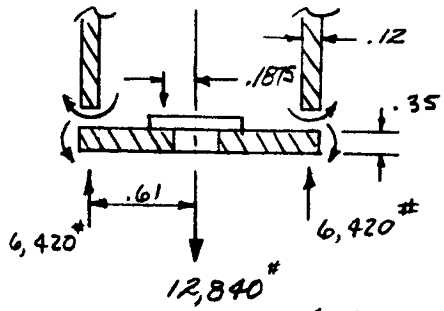

REF. PG. 4.226

$f_e = \frac{6 M_e}{b_e t_e^2}$

$b_e = 1.1 - .625 = .475 \quad t_e = .35$

$f_w = \frac{6 M_w}{b_w t_w^2}$

$b_w = 1.1 \quad t_w = .12$

$M_e = -M_w + 6420(.61 - .1875) = -M_w + 2070 \quad (1)$

$\frac{6 M_e}{b_e t_e^2} = \frac{6 M_w}{b_w t_w^2} \quad (2)$

$\frac{6(-M_w + 2070)}{(.475)(.35)^2} = \frac{6 M_w}{(1.1)(.12)^2}$

$M_w = 437$ in-lbs

ASSUME 70% OF THE LOAD IS CARRIED BY THE WALLS AND 30% BY THE BOTTOM.

$f = (.7) P/A + (.7) \frac{6M}{bt^2}$

$f = (.7)(6420)/(1.1)(.12) + (.7) \frac{6(437)}{(1.1)(.12)^2}$

$f = 34000 + 116{,}000$

$M.S. = \frac{1}{\frac{34{,}000}{150{,}000} + \frac{116{,}000}{225{,}000}} - 1 \quad \underline{+0.35}$

FASTENERS REF. PG. 4.227

USE (3) 1/4" HKM-ACT 509 HUCK BOLT
SHEAR ALL. = 4560 lbs REF. N
JOINT ALL. = (3)(4560) = 13,700 lbs
JOINT LOAD = 12,840 lbs

$M.S. = \frac{13{,}700}{12{,}840} - 1 = \underline{+0.07}$

LOADS DURING SPIN-UP

DEFLECTION ANALYSIS

Just prior to fourth stage spin-up, the spin bearing becomes the primary load path; however, the situation at this time is a "zero" g condition. A deflection analysis is presented to show that Middle "D" does not deflect and "drag" on the 23-002109 ring during spin-up. Ten (10) per cent of the ultimate fourth stage design load has been conservatively assumed for this condition. Loads of lesser magnitude could occur from (1) the fairing separation (relieving the preload) and/or (2) the 'C' Section Reaction Control System.

$w = (.10)(879) \approx 88$ #/in REF. PG. 4.209

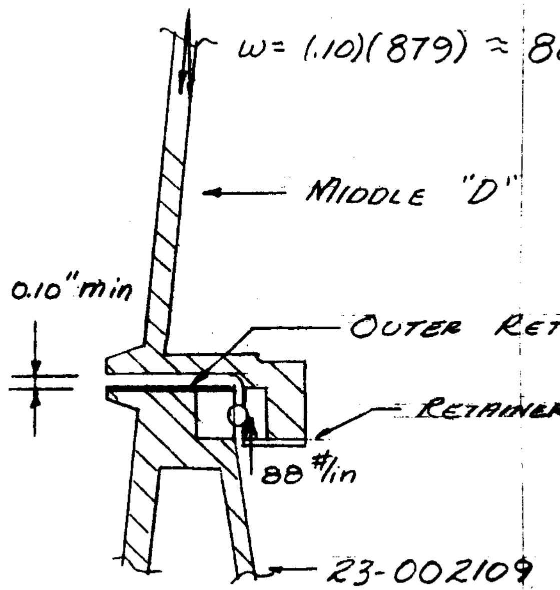

BY SUPERPOSITION, ADD THE EFFECTS OF
1. BEARING TOLERANCE
2. DEFLECTION
3. ROTATION

1. BEARING TOLERANCE

DIAMETRICAL BALL CLEARANE = 0.002"
REF. DWG. KAYDON A-6778-1

$\delta_1 = 0.0022$ in REF. J PG. 4.40

LOADS DURING SPIN-UP

2. DEFLECTION

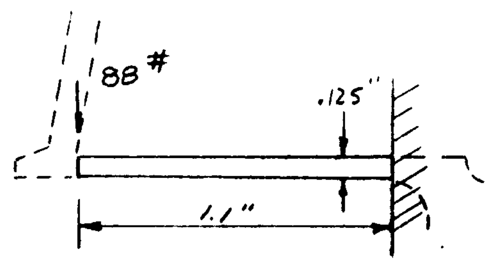

MAT'L : ALUM
$E = 10.5 \times 10^6$
$G = 4 \times 10^6$
REF. PG. 4.220

$$\delta_2 = \frac{PL^3}{3EI} = \frac{88(1.1)^3(12)}{3(10.5)(10^6)(1)(.125)^3} = \underline{0.0228 \text{ in}}$$

3. ROTATION

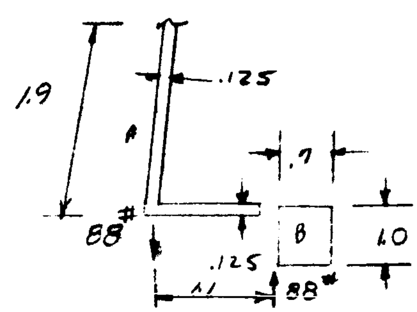

EQUIVALENT SECTION

BY ANALYSIS SIMILAR TO PAGE 4.225

$$dM_t = 88 \cos\theta (1.1)$$

$$M_T = \int_0^{\pi/2} 97 \cos\theta (\cos(90-\theta)) R d\theta$$

$$M_T = 655 \text{ in-lbs}$$

$$(M/\theta)_A = \frac{Gbt^3}{3} = \frac{4 \times 10^6 (1.9 + 1.1)(.125)^3}{3} = 7800$$

$$(M/\theta)_B = \frac{GA^4}{40(I_p)} = \frac{4(10^6)(.7)^4}{40(.0869)} = 277{,}000$$

REF. M

$$M/\theta = 284{,}800 \ \frac{\text{in-lbs}}{\text{rad.}}$$

$$\theta_L = \frac{M}{284{,}800}(R\theta) = \frac{655(13.5)(\pi/2)}{284{,}800}(57.3) = 2.88^\circ$$

$$\delta_3 = 1.1 \sin 2.88^\circ = 1.1(.0503) = \underline{0.05533 \text{ in}}$$

TOTAL DEFLECTION

$\delta_1 + \delta_2 + \delta_3 < 0.10$ $\quad \delta_{MIN} = 0.10$ REF. PG. 4.219

$0.0022 + 0.0228 + 0.05533 = \underline{0.08033 < 0.10}$

LOADS DURING SPIN-UP

RETAINER RING 23-002167 REF. PG. 4.229

CRITICAL FOR TENSION LOADS

$W_{t\,MAX} = 705(0.10) = 70.5$ #/in REF. PGS. 4.209

THIS RING IS ANALYZED FOR $W_{t\,MAX} = 840$ #/in IN REF. J PG. 430-31 WITH M.S. = +0.23

∴ M.S. = HIGH

OUTER RETAINER RING REF. PG. ______

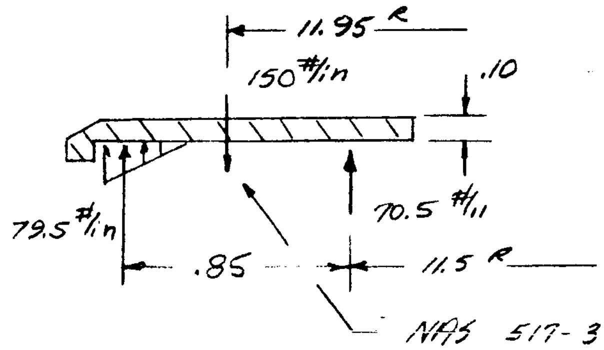

MAT'L 2024-T4
$F_{TY} = 42{,}000$ psi
REF. K

PLATE TENSION ALL = 1287 lbs REF. O

BOLT SPACE $= \frac{2\pi(11.95)}{30} = 2.5$ in.

BOLT LOAD = 2.5 (150) = 375 lbs

$M.S. = \frac{1287}{375} - 1$ HIGH

BENDING

$f = \frac{6M}{bt^2}$ $b = \frac{1}{2}(2.5) - .201 = 1.049$

$f = \frac{6(70.5)(2.5)(.45)}{(1.049)(.1)^2(1.3)} = 35{,}000$ psi YIELD

$M.S. = \frac{42{,}000}{35{,}000} - 1 = +0.20$ YIELD

ULT LOADS

FAIRING

REF. PG. 4.200 FOR DISCUSSION

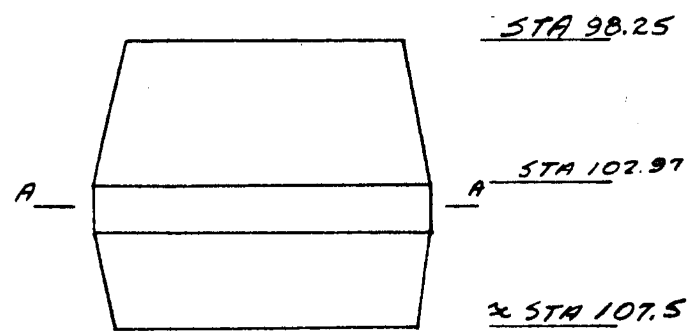

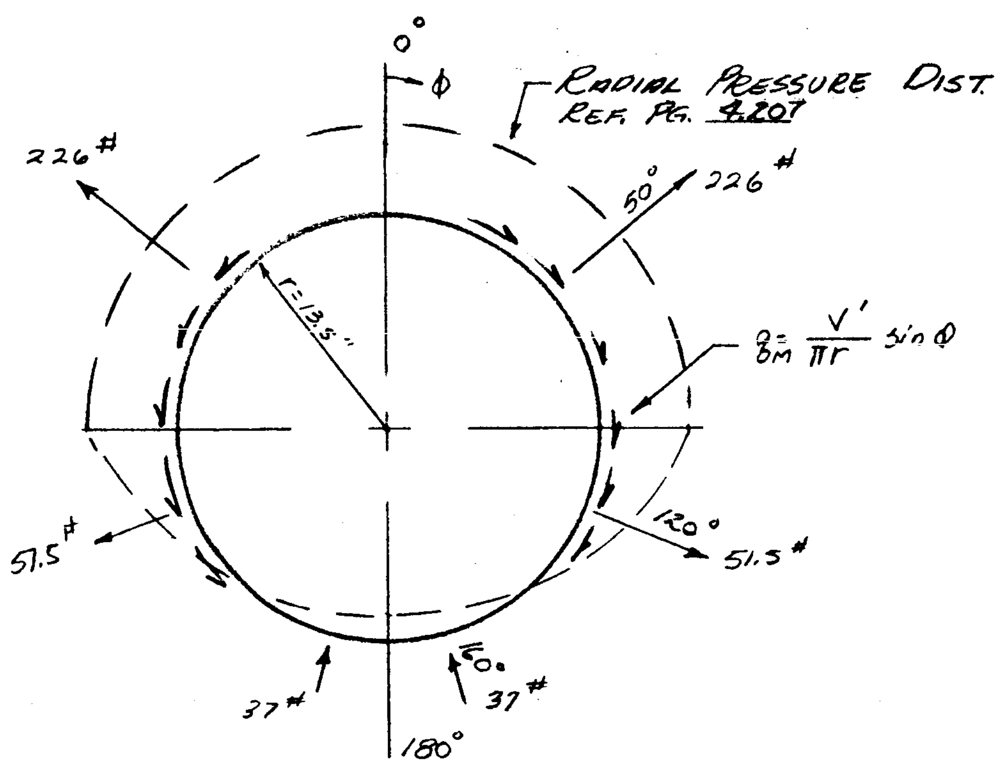

$$\Sigma F_H = V' = 2(226)\cos 50^\circ - 2(51.5)\cos 60^\circ + 2(37)\cos 20^\circ$$

$$V' = 308\ \#$$

$$q_{MAX} = \frac{308}{\pi(13.5)} \sin 90 = 7.25\ \#/in$$

ULT LOADS

THE LOADS SHOWN ON PAGE 4.207 ARE PRELIMINARY. IT HAS BEEN CONSERVATIVELY ASSUMED THAT THE LOAD ON THE REVERSE FLARE (STA 102.97-107) ARE TWICE THE LOADS ON THE FORWARD FLARE (STA 98.25-102.97).

$V' = 308 + 2(308) = 924$ #

$q_{max} = 7.25 + 2(7.25) = 21.75$ #/in

FASTENERS REF. PG. 4.234

SPACING = 7.0 in

$P = 7(21.75) = 152$ lbs

NAS 623 (3/16) OR EQUIVALENT

SHEAR ALL. = 2690 lbs REF. O

BRG. IN FIBERGLASS = 1090 lbs

REF. P FOR NAS 517 SCREW - OUTSIDE TEMP = 640°F

$M.S. = \frac{1090}{152} - 1 =$ HIGH

THIS SHEAR LOAD IS NOT CRITICAL AND THEREFORE ONLY A LOAD PATH IS PRESENTED.

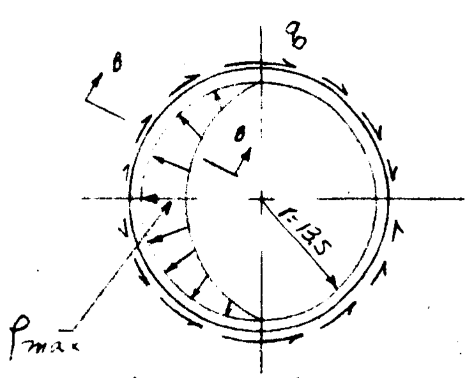

q HAS BEEN ROTATED 90° FOR CLARITY

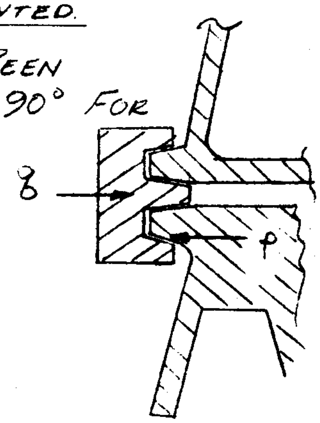

B-B

$V' = 924$ #

$V' = 2\int_0^{\pi/2} P_m R \sin^2\theta \, d\theta$

$P_{max} = 87.2$ lbs

ULT LOADS

LOCAL DEFLECTION AND BENDING

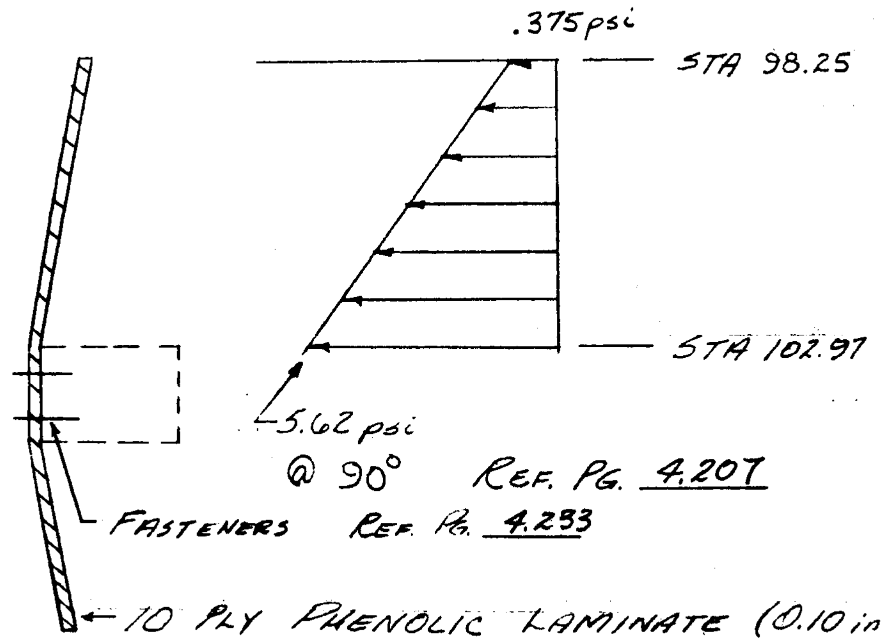

@ 90° REF. PG. 4.207

F_{BR_U} = 34,750 psi
F_{CU} = 37,500 psi REF. D
E = 3.5×10⁶ μ = .28
T_{SAVE} = 145°F REF. PG. 4.208
@ 35 sec.

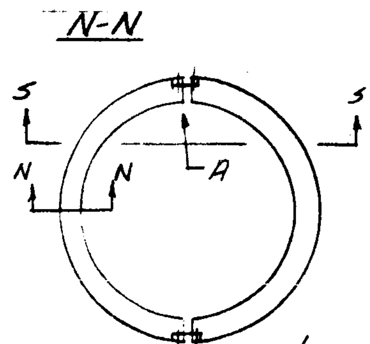

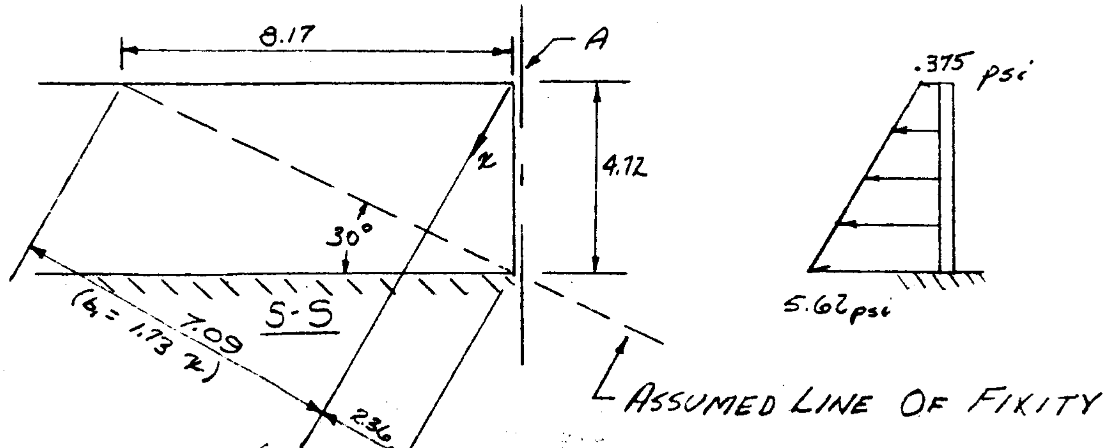

x = 0 → 4.08"

ULT LOADS

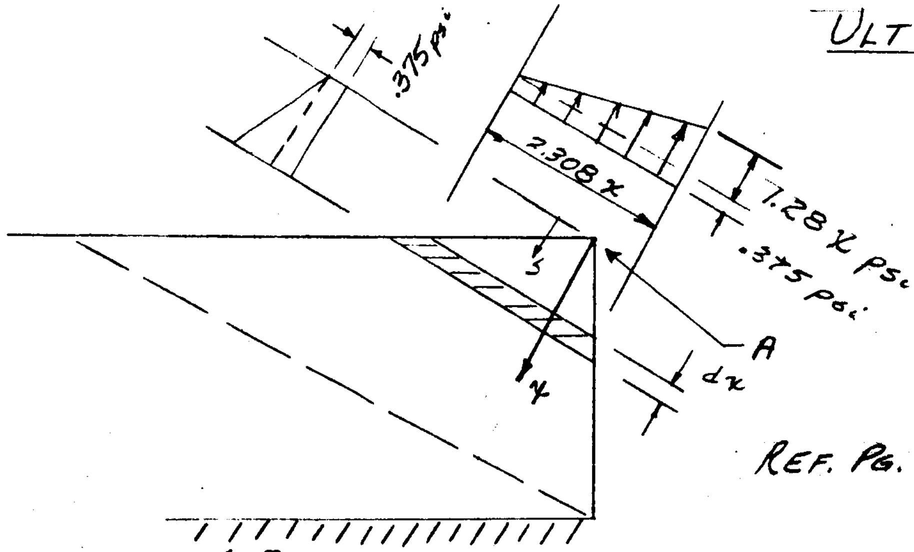

REF. PG. 4.234

$$\Delta_A = \int_0^{4.08} \frac{M m}{EI} dx \qquad \text{WHERE} \quad m = 1^{\#}(x)$$

$$I = \frac{bt^3}{12} = \frac{(.1)^3(2.308x)}{12}$$

$$M = \int_{s=0}^{s=x} \tfrac{1}{2}(2.308s)(1.28s)(s/3)ds + \tfrac{1}{2}(2.308x)(x)(x/3)(.375)$$

$$M = \int_{s=0}^{s=x} 0.493 s^3 ds + 0.144 x^3$$

$$M = (0.123 x^4 + 0.144 x^3) \text{ in-lbs}$$

$$M = (0.082 x^4 + 0.096 x^3) \text{ in-lbs} \quad \underline{\text{LIMIT}}$$

USE LIMIT LOAD FOR DEFLECTION

$$\Delta_A = \int_0^{4.08} \frac{(.082x^4 + .096x^3)(x)}{E\left(\frac{(.1)^3(2.308x)}{12}\right)} dx = \frac{1}{192(10^{-6})E} \int_0^{4.08} (.082x^4 + .096x^3) dx$$

$$\Delta_A = \frac{1}{192(3.5)} \left[\frac{.082}{5}x^5 + \frac{.096}{4}x^4\right]_0^{4.08}$$

$$\Delta_A = \frac{1}{672}(18.7 + 6.61) = \underline{\underline{0.0377 \text{ in @ LIMIT LOAD}}}$$

BENDING

$$M_{x=4.08} = 0.123(4.08)^4 + 0.144(4.08)^3 = 44 \text{ in-lbs}$$

$$I_{x=4.08} = 0.785 \times 10^{-3}$$

$$f = \frac{Mc}{I} = \frac{44(.05)}{.785(10^{-3})} = 2{,}800 \text{ psi}$$

$$M.S. = \frac{37{,}500}{2800} - 1 = \underline{\text{HIGH}}$$

STUDY

"UNCONVENTIONAL VEHICLE - SPACECRAFT CONFIGURATION"

STABILITY AND CONTROL

Prepared by

T. C. Walker

Reviewed by

J. E. Melugin

5.0 Stability and Control

5.1 Aerodynamic Analysis

5.1.1 Introduction

As part of Ling-Temco-Vought Astronautics study for the determination of requirements for modification of the NASA Scout research vehicle to accommodate the Unconventional Vehicle - Spacecraft configurations, aerodynamic data must be presented for use in trajectory, stability and control, and structural analyses. It is the purpose of this section to discuss and present aerodynamic coefficients and load and pressure distributions necessary for these analyses.

5.1.2 Summary

Two configurations are to be studied, Case I-A and Case II-A-2. Cast I-A is a conventional Scout vehicle with a standard 34 inch diameter heat shield and a nose station at -25 inches which covers the payload. Complete aerodynamic data for this configuration is presented in reference (d) and will not be presented within the text of this report. Case II-A-2 has the payload exposed with no heat shield. This payload is a 12.5 foot sharp nosed cone with a five degree cone half-angle. The aerodynamics for this configuration are discussed in the following section.

5.1.3 Discussion of Case II-A-2 Aerodynamics

5.1.3.1 Normal Force Derivative and Center of Pressure

The normal force derivative and center of pressure were predicted using as a base the aerodynamic data for the Scout vehicle with a 20 inch diameter heat shield and nose station at -10 inches which are presented in Addendum A of reference (d). Case II-A-2 payload nose cone predictions were taken from reference (e). Increments between the two nose shapes were taken and the normal force derivative and center of pressure were thus obtained for the first, second, third, and reentry stages of configuration Case II-A-2. Figures 5.1 through 5.5 present these aerodynamic predictions as a function of Mach number.

5.1.3.2 Zero Lift Drag Coefficient

The zero lift drag coefficient was predicted from the same base Scout vehicle configuration as were the normal force derivative and center of pressure mentioned in Section 5.1.3.1, with the exception that the nose station was at -30 inches. The cone zero lift drag coefficient predictions were made from unpublished aerodynamic drag curves. Increments between the two nose shapes were taken and the zero lift drag coefficient was thus obtained for the first, second, and reentry stages of configuration Case II-A-2. Figures 5.6 through 5.8 present the zero lift drag coefficient as a function of Mach number. In Figure 5.6, the first stage zero lift drag coefficient as a function of Mach number is presented for both boosting and coasting. Because the vehicle will be in essentially a zero dynamic pressure atmosphere after second stage burn out, base drag has not been included in the second stage predictions presented in Figure 5.7 and third stage drag predictions have been omitted. However, base drag was included in the reentry stage predictions presented in Figure 5.8.

5.1.3.3 Running Load Distributions

The supersonic running load distribution was predicted using Newtonian Impact Theory, reference (e), and reference (f). The loads on the small transition flare between the cone and the "D" section flare were neglected in this running load distribution prediction. The transition flare is reversed, making this region extremely difficult to predict without test data. However, the loads will be small.

This transition flare configuration was later revised. This revision in configuration is not reflected in the running load distribution predictions. However, the load on this revised transition flare section represents only about ten percent of the total load and occurs in the local area where the payload is attached to the vehicle. This supersonic running load distribution is presented in Figure 5.9.

5.1.3.4 Radial Pressure Distributions

Radial pressure distributions have been predicted for the revised transition flare between the payload and the "D" section flare. The total load on the forward face of this flare was predicted from unpublished design curves. No information was available for predicting the loads on the reverse aft face of this flare. The running load distribution for a Mach number of 1.90, near where the maximum product of dynamic pressure and angle of attack occurs, was predicted using data from the Scout vehicle second stage flare presented in reference (d). Using the radial pressure distributions of the Scout vehicle second stage flare as shaping factors and correlating these factors with the predicted running load distribution at the respective station locations, two radial pressure distributions were obtained for the forward face of the revised transition flare. These distributions, differential pressure across the skin as a function of radial angle, are presented in Figure 5.10.

5.2 Stability and Control Analysis

5.2.1 Introduction

Modification of the NASA Scout research vehicle is being considered to accommodate two Unconventional Vehicle - Spacecraft configurations. Under this consideration, a detailed stability and control analysis had to be conducted to ensure that changes in weight, inertia, and geometry will not adversely affect the stability or control of any stage of the vehicle for either configuration.

5.2.2 Summary

The two configurations to be studied are Case I-A and Case II-A-2. Case I-A is a conventional Scout vehicle with a standard 34 inch diameter heat shield and a nose station at -25 inches which covers the payload. Case II-A-2 has the payload exposed with no heat shield. This payload is a 12.5 foot sharp nose cone with a five degree cone half-angle.

In these analyses, the reentry control system evaluated in reference (g) was used. Standard Scout criteria was used in all considerations, however, a parametric study concerning second stage booster thrust misalignment criterion is presented. In the second stage capture maneuver analysis, an ignition thrust level of 62,500 pound was used, higher than that currently being predicted for the Castor II motor. However, the propulsion group indicated that these predictions may increase.

Both configurations of the Unconventional Vehicle-Spacecraft have acceptable stability and control characteristics for all stages. Case II-A-2 is a more promising configuration because of the less severe destabilizing aerodynamics resulting from the sharp cone.

Extended second stage coast times ranging from 420 to 630 seconds, depending upon the desired reentry angle, was required of both configurations in order to meet the mission requirements. The above mentioned second stage reentry control system is not adequate to operate over such long coast times because of the hydrogen peroxide consumption. Several control system modifications were considered in order to reduce the second stage coast hydrogen peroxide consumption. These modifications consisted of reduction in reaction control motor thrust, reduction in nitrogen pressure, and increased control system deadbands during second stage coast. The first two considerations were either major system changes or were inadequate to gain the required coast time. A study of the increased deadband concept during second stage coast revealed that it was feasible to maintain control through out these extended second stage coast times and not deplete the hydrogen peroxide on either of the two configurations studied. Configuration II-A-2 is capable of slightly longer second stage coast times than Configuration I-A because the less destabilizing aerodynamics makes the hydrogen peroxide consumed during capture at second stage ignition less. The required modifications to the control system hardware have been determined and only minor wiring changes will be required to obtain increased second stage deadbands.

5.2.3 Discussion of Case I-A Stability and Control

5.2.3.1 First Stage Stability

The first stage of this vehicle exhibits satisfactory longitudinal static stability. A maximum allowable unstable flexible static margin of 76 inches for a Scout vehicle with the 34 inch diameter -25 inch nose station heat shield was determined from Addendum D of reference (h). This was based on a dynamic pressure of 3,000 pounds per square foot. For Configuration I-A, the ignition and burnout centers of gravity from Section 2.0 were compared to the first stage flexible center of pressure at a dynamic pressure of 3,000 pounds per square foot taken from Addendum E of reference (d). The unstable flexible static margin was 36 inches, well within the allowable range. The control moment remained essentially unchanged because the centers of gravity in this comparison were about the same location.

5.2.3.2 Second Stage Control System

The second stage reentry control system used in this study was that determined from the Castor II evaluation study in reference (g) and the second stage filter was that determined in reference (i). Table 5.1 presents this control system.

TABLE 5.1

Second Stage Control System

Control Parameter	Pitch & Yaw	Roll
Deadband Halfwidth (Radians)	.025 ± 10%	.025 ± 10%
Gain Ratio (K_R/K_D) (Seconds)	.62 ± 10%	.45 ± 10%
Capture Delay Time On (Seconds)	.154	.053
Capture Delay Time Off (Seconds)	.100	.032
Coast Delay Time On (Seconds)	.1025	.053
Coast Delay Time Off (Seconds)	.0625	.032
Hysteresis (Percent)	5.0	5.0
Control Motor Thrust (Pounds)	510 ± 30	46 ± 6

The tolerances on these control system parameters were chosen to give the most conservative results in capture and in coast. The second stage second bending mode frequency from Section 3.0 for this configuration with a 300 pound payload is slightly greater than that for a conventional Scout vehicle because of the absence of the fourth stage motor. Therefore, the above mentioned second stage filter is suitable for this application. This filter is switched out during second stage coast operation. This is reflected in the delay times given in Table 5.1.

To obtain extended second stage coast times, increased second stage coast deadbands were considered ranging from .025 to .100 radians. At various points in this analysis, the term deadband or increased deadband will be discussed. This term is here defined as deadband halfwidth, that is to say, the control system contains a positive and a negative value for positive and negative error signals. This increased second stage coast deadband consideration will be discussed later in the text.

5.2.3.3 Second Stage Ignition Capture Maneuver

With the ignition of the second stage, a diaphragm is bursted and the inert first stage motor case is separated. The bursting of this diaphragm can generate a lateral impulse which puts the second stage in a large angular excursion. In addition, angular initial conditions in rate and displacement can exist at the time of this excursion. This transient excursion has to be reduced or "captured" down to normal operation by the second stage control system. The reduction of this transient motion, sometimes referred to as "capture maneuver", is studied on a phase plane of angular rate as a function of angular displacement. Phase plane analysis techniques including thrust misalignment and aerodynamic accelerations were used to analyze the capture maneuver.

The maximum second stage ignition dynamic pressure was 35 pounds per square foot. This criterion is currently acceptable for the Scout/Castor I second stage configuration. The destabilizing aerodynamics taken from Addendum B of reference (d) were Normal Force Derivative (C_{N_α} S) = .37 Ft^2/Deg and Center of Pressure (CP) = Sta. 75.0 Inches. A Castor II second stage motor ignition thrust spike of 62,500 pounds was used at the recommendation of the propulsion group in conjunction with a thrust misalignment angle of .25 degrees. This thrust spike was considered constant over the time the capture maneuver was being negotiated. The specified weight for the payload of Configuration I-A was 300 pounds. The initial conditions of angular rate and displacement for the capture maneuver were -3 degrees per second and -3 degrees, respectively. The specific impulse of the second stage control motors is 130 pound-seconds per pound.

The second stage control system negotiated the second stage capture maneuver in .118 radians of overshoot angle. The phase plane analysis of this capture maneuver is presented in Figure 5.11. The capture maneuver is considered complete at point 4 in Figure 5.11. The total capture time was 5.6 seconds and the capture motor-on time was 5.3 seconds. The hydrogen peroxide required for this capture maneuver was 19.4 pounds.

5.2.3.4 Second Stage Boost Hydrogen Peroxide Consumption

The roll channel hydrogen peroxide consumption during second stage boost was evaluated from flight test results presented in reference (g). The required hydrogen peroxide for the roll channel during second stage boost is 3.5 pounds.

The pitch and yaw channel hydrogen peroxide consumption during second stage boost was based on the concept that all disturbance impulse put in by the second stage booster would be taken out by the second stage control system. The control system impulse can be expressed as follows:

$$I_{MPULSE} = \sqrt{2}\, T_{\epsilon_T} \frac{\ell_T}{\ell_c} t_{BOOST}$$

were T = booster thrust, ϵ_t = thrust misalignment angle, l_t = thrust component moment arm, l_c = control moment arm, and t_{boost} = time the stage is boosting after capture. In this calculation, T_{tboost} is the booster impulse after second stage capture has been negotiated. The required hydrogen peroxide for the pitch plus yaw channels is 95.7 pounds.

A total rate change of 4.0 degrees per second was considered for the second stage pitch program which required .60 pounds of hydrogen peroxide.

The total hydrogen peroxide required for capture, boost, and pitch program operation is then 119.2 pounds. The second stage usable hydrogen peroxide is considered to be 170 pounds. Therefore, there is 50.8 pounds of hydrogen peroxide remaining for coasting and deadband reduction which will be discussed in the following section.

5.2.3.5 Second Stage Deadband Reduction Capture Maneuver

The consideration of increased deadbands during second stage coast requires a study of second stage deadband reduction prior to third stage ignition. This deadband reduction is necessary for dispersion accuracy of the third stage. Increased deadbands in pitch and yaw up to .10 radians were considered.

The deadband reduction capture maneuver was evaluated based on an increased deadband in pitch and yaw of .10 radians. The remaining control system parameters did not change. The initial conditions for initiation of the deadband reduction capture maneuver were obtained by computing the angular rate and displacement at which the control motor comes on when the phase plane trajectory breaks out of the deadband at the increased deadband limit cycle velocity. At the instant the control motor comes on, the increased deadband is assumed to be switched back to .025 radians. The phase plane trajectory is then computed down to a point in time where limit cycle velocity is obtained for the .025 radian deadband.

This deadband reduction capture maneuver occurs at a zero dynamic pressure and in a second stage coasting condition so that the only existing angular acceleration is that from the control motors. This phase plane analysis is presented in Figure 5.12. The time required to go from point 1 to point 10 in Figure 5.12 is 4.3 second and the motor on time .76 seconds. The variation in these times with the amount of increased deadband is assumed to be linear. Only the time from point 1 to point 6 is affected by the amount of deadband increase. The time from point 6 to point 10 is assumed constant for any deadband increase. Under these considerations, the variation in deadband reduction time and motor-on time with increased deadband is presented in Figures 5.13 and 5.14, respectively. The hydrogen peroxide required for the deadband reduction as a function of increased deadband is presented in Figure 5.15.

5.2.3.6 Second Stage Coast Hydrogen Peroxide Flow Rate

The second stage coast hydrogen peroxide flow rate was based on the control system presented in Table 5.1 of Section 5.2.3.2. However, variations in deadband were considered up to .10 radians. Duty cycle was computed in pitch, yaw, and roll for each deadband considered. Figure 5.16 and 5.17 present the duty cycle as a function of increased deadband for the pitch or yaw and roll channels, respectively. The tolerances on the control system parameters were selected to obtain the largest possible duty cycle. The total flow rates for pitch plus yaw channels were computed based on the above mentioned duty cycles and are presented for .025 and .0698 radian roll deadbands in Figures 5.18 and 5.19, respectively.

5.2.3.7 Second Stage Coast Time Evaluation

The major variation in second stage coast time with increased deadband is in the pitch and yaw channels rather than in the roll channel. For this reason, only two roll deadbands have been considered, the first being a standard reentry roll deadband of .025 radians and the second being an arbitrary roll deadband of .0698 radians (4 degrees). The second roll deadband was chosen simply to show the coast time variation for a change in roll deadband.

The hydrogen peroxide requirements for second stage ignition capture, boost, pitch program, and deadband reduction as a function of increased deadband was combined and subtracted from the total usable second stage hydrogen peroxide capacity of 170 pounds. This hydrogen peroxide difference was divided by flow rate to obtain second stage coast time as a function of increased pitch and yaw deadbands for the two roll deadbands considered. Trajectory analysis supplied the variation of reentry angle with second stage coast time. The variation of pitch and yaw deadbands and reentry angle with second stage coast time as a function of the two roll deadbands considered is presented in Figure 5.20. By the elimination of time as a variable, the pitch and yaw deadbands as a function of reentry angle for the two roll deadbands is presented in Figure 5.21.

The thrust misalignment angle for the Castor II second stage motor was assumed to be .25 degrees which was taken from the Castor I motor evaluation. To study effects of thrust misalignment on second stage coast time, angles ranging from .25 to .15 degrees were considered. It was assumed that the thrust misalignment angle would affect only the pitch and yaw channel hydrogen peroxide consumption during second stage boost and that all other factors would remain constant. Figure 5.22 presents the incremental second stage coast time per .025 degrees of thrust misalignment angle as a function of pitch and yaw deadbands for the two roll deadbands considered. From the equation presented in Section 5.2.3.4, the second stage coast time is seen to be a linear function of thrust misalignment angle. The data in Figure 5.22 was applied to the data in Figure 5.21 to obtain the variation in pitch and yaw deadbands and reentry angle with second stage coast time as a function of thrust misalignment angle for a roll deadband of .025 radians which is presented in Figure 5.23. Figure 5.24 presents the variation of pitch and yaw deadbands with reentry angle as a function of thrust misalignment angle for a roll deadband of .025 radians. This variation was obtained by eliminating time as a variable from Figure 5.23. Figures 5.25 and 5.26 presents this same information for a roll deadband of .0698 radians.

5.2.3.8 Third Stage Considerations

The third stage does not present any stability and control problems with the existing control system. The mission requirement of long second stage coast time places the third stage capture maneuver in a zero dynamic pressure atmosphere. A short third stage coast time is required prior to the spin-up and separation of the payload. Therefore, third stage hydrogen peroxide consumption is no problem.

5.2.4 Discussion of Case II-A-2 Stability and Control

5.2.4.1 First Stage Stability

The first stage of this vehicle exhibits satisfactory longitudinal static stability. A maximum allowable unstable flexible static margin of 76 inches was discussed in Section 5.2.3.1. For Configuration II-A-2, the minimum flexible stable static margin is 25 inches, assuming Scout flexibility at a dynamic pressure of 3,000 pounds per square foot. This stable static margin is based on the lightest payload weight, 300 pounds, giving the most aft center of gravity and is seen in Figure 5.2.

5.2.4.2 Second Stage Control System

The second stage control system for Configuration II-A-2 has been discussed under Section 5.2.3.2. The second stage second bending mode frequency from Section 3.0 for Configuration II-A-2 with a 600 pound payload is slightly greater than that for a conventional Scout vehicle because of the absence of the fourth stage motor and the structural stiffening of the spin bearing juncture with a Marmon clamp. Therefore, the filter mentioned in Section 5.2.3.2 is suitable for this application.

5.2.4.3 Second Stage Ignition Capture Maneuver

The second stage capture maneuver has been discussed in detail under Section 5.2.3.3. However, Configuration II-A-2 has a payload weight range of from 300 to 600 pounds which requires additional discussion. The destabilizing aerodynamics were taken from Figure 5.3. The maximum second stage ignition dynamic pressure used in the capture maneuver calculation was 40 pounds per square foot. Figure 5.27 presents the second stage negotiated capture angle as function of payload weight.

Complete capture maneuver phase planes were computed for the 400 and 600 pound payload weights and are presented in Figures 5.28 and 5.29, respectively. From these phase planes, total capture time and motor-on time was evaluated. These respective times were assumed to be linear with payload weight and are presented in Figure 5.30. The motor-on time was used to compute the hydrogen peroxide consumption required for the second stage ignition capture maneuver as a function of payload weight and is presented in Figure 5.31.

5.2.4.4 Second Stage Boost Hydrogen Peroxide Consumption

The second stage boost and pitch program hydrogen peroxide consumption is discussed in Section 5.2.3.4. The average hydrogen peroxide consumption for these two maneuvers was 110 pounds with very little variation with payload weight.

5.2.4.5 Second Stage Deadband Reduction Capture Maneuver

The second stage deadband reduction capture maneuver has been discussed in Section 5.2.3.5. Complete deadband reduction capture maneuver phase planes were computed for payload weights of 300 and 600 pounds and are presented in Figures 5.32 and 5.33, respectively. The time variation of this maneuver was assumed linear with payload weight and increased deadband. Figures 5.34 and 5.35 present the variation of deadband reduction time and motor-on time with payload weight as a function of increased deadband. The hydrogen peroxide required for the deadband reduction maneuver as a function of payload weight and increased deadband is presented in Figure 5.36.

5.2.4.6 Second Stage Coast Hydrogen Peroxide Flow Rate

The second stage coast hydrogen peroxide flow rate has been discussed in Section 5.2.3.6. Figures 5.37 and 5.38 present the pitch or yaw and roll channel duty cycles as a function of increased deadband and payload weight for Configuration II-A-2. The total flow rates for pitch plus yaw channels for a .025 and .0698 radian roll deadband are presented in Figures 5.39 and 5.40, respectively.

5.2.4.7 Second Stage Coast Time Evaluation

The second stage coast time evaluation was discussed in Section 5.2.3.7. The variables considered in this section were second stage coast time, pitch, yaw, and roll deadbands, reentry engle, payload weight, and thrust misalignment angle. The first comparisons made are the variations with payload weight. Figures 5.41 and 5.42 presents the variation in pitch and yaw deadbands and reentry angle with second stage coast time as a function of payload weight for roll deadbands of .025 and .0698 radians, respectively. In order to see the direct variation in pitch and yaw deadbands with reentry angle, Figures 5.43 and 5.44 are given. These figures differ from Figures 5.41 and 5.42 only in that the second stage coast time variable has been eliminated.

To evaluate the effects of thrust misalignment angle on second stage coast time, a second set of comparisons are made showing parametric variations with thrust misalignment angle for a given payload weight and a given roll deadband. Figure 5.45 presents the variation in incremental second stage coast time per .025 degrees of thrust misalignment angle with pitch and yaw deadbands for the standard roll deadband of .025 radians as a function of payload weight. This data combined with the data in Figure 5.41 was used to obtain the variations in pitch and yaw deadbands and reentry angle with second stage coast time as a function of thrust misalignment angle for a standard roll deadband of .025 radians. Figures 5.46 through 5.49 presents this parametric data for payload weights of 300, 400, 500, and 600 pounds, respectively. By eliminating second stage coast time as a variable from each of these figures, a direct variation of pitch and yaw deadbands with reentry angle is obtained and is presented in Figures 5.50 through 5.53.

The secønd part of the second comparison are these same variations associated with the .0698 radian (4 degrees) roll deadband. Figure 5.54 presents the variation in incremental second stage coast time per .025 degrees of thrust misalignment angle with pitch and yaw deadbands for a roll deadband of .0698 radians (4 degrees) as function of payload weight. This data combined with the data in Figure 5.42 was used to obtain the variations in pitch and yaw deadbands and reentry angle with second stage coast time as a function of thrust misalignment angle for a roll deadband of .0698 radians. Figures 5.55 through 5.58 presents this parametric data for payload weights of 300, 400, 500, and 600 pounds, respectively. By eliminating second stage coast time as a variable from each of these figures, a direct variation of pitch and yaw deadbands with reentry angle is obtained and is presented in Figures 5.59 through 5.62.

5.2.4.8 Third Stage Considerations

The third stage considerations hav been discussed in Section 5.2.3.8. Configuration II-A-2 has much less destabilizing aerodynamics than does Configuration I-A because of the sharp cone payload geometry.

5.2.4.9 Reentry Stage Stability

The aerodynamic center of pressure for the 12.5 foot cone payload of Configuration II-A-2 is presented in Figure 5.5. The center of gravity presented in Figure 5.5 is actually that for any of the payload weights by definition of the statement of work. Thus, the reentry stage has a stable static margin of 25 inches.

5.2.5 Second Stage Minimum Nitrogen Supply

A NASA request was made to study the effects of second stage minimum nitrogen supply on second stage coast time. The basic concept of this consideration will be discussed later in Section 5.3.

The consideration has been applied to Configuration II-A-2. The configuration was selected at second stage burnout with a 300 pound payload and 110 pounds of hydrogen peroxide already consumed for capture, boost, and pitch program maneuver requirements. The light payload was chosen as it would be the critical case.

The control system used in this analysis is defined in Table 5.1 of Section 5.2.3.2 with the coast delay times. The control system tolerances were chosen in such a manner as to give conservative results. Pitch or yaw and roll duty cycles were computed as a function of control motor thrust for the above mentioned configuration and are presented in Figures 5.63 and 5.64, respectively. The roll duty cycle was computed for a two-motor angular roll acceleration and plotted as a function of a single roll motor thrust.

The pitch, yaw, and roll control motor thrust variation with nitrogen pressure was taken from Figures 5.68 and 5.69 in Section 5.3. The maximum allowable thrust line was used from each of these figures. The summations of the products of control motor thrust and duty cycle for the pitch, yaw, and roll motors divided by the control motor specific impulse produced the total hydrogen peroxide flow rate as a function of nitrogen pressure. The variation in hydrogen peroxide remaining with nitrogen pressure was taken from Figure 5.67 in Section 5.3.

Incremental second stage coast times were obtained by taking the incremental hydrogen peroxide consumed for a change in nitrogen pressure and dividing by the total hydrogen peroxide flow rate occurring half-way between the change in nitrogen pressure. The nitrogen pressure increments were taken at 10 psia intervals starting with 500 psia and decaying down to 345 psia. An accumulative summation of second stage coast time as a function of nitrogen pressure was thus obtained and is presented in Figure 5.65.

The maximum second stage coast time for the minimum nitrogen supply consideration is 251 seconds, nowhere near that coast time required by the Unconventional Vehicle - Spacecraft mission requirements. However, to evaluate the second stage coast time gain from this consideration, the second stage coast time was computed using a constant regulated 500 psia nitrogen pressure which resulted in 178 seconds of coast time. A 73 second coast time gain is realized out of this minimum nitrogen supply consideration based on 75 pounds of hydrogen peroxide available for second stage coast.

5.3 Reaction Control System Analysis

5.3.1 Introduction

The following study has been made to determine reaction control system motor thrusts and fuel supply as functions of decaying regulated nitrogen pressure for the "B" transition section. This information was necessary for the Stability and Control Section to evaluate the effect of the minimum nitrogen supply (described below) on vehicle coast time.

5.3.2 Summary

Based on the initial conditions described in paragraph 5.3.3.2, the nitrogen pressure may be expected to drop according to Figure 5.67, reaching 340 psia when the fuel supply is exhausted; and, correspondingly, the thrusts of the pitch-yaw motors and roll motors may be expected to decay according to Figures 5.68 and 5.69.

5.3.3 Discussion

5.3.3.1 Minimum Nitrogen Supply

If a smaller-than-normal amount of nitrogen were used to pressurize the reaction control system. such that, before all the hydrogen peroxide was expelled, the unregulated nitrogen pressure dropped to the regulated nitrogen pressure level, the two would then begin to drop together. As a result of the falling regulated nitrogen pressure, the motor thrusts would begin to decay and the rate of fuel consumption would decrease. The net result would be a longer available coast time, so long as the reduced thrusts provided sufficient control forces.

5.3.3.2 Initial Conditions

The following conditions had to be met to satisfy stability and control requirements:

(a) During the burn phase, 110 lbs. of hydrogen peroxide are consumed.

(b) The amount of nitrogen originally charged into the system is sufficient to maintain regulated nitrogen pressure (hence, rated thrust) throughout the burn phase.

5.3.3.3 Assumptions

The following assumptions were made:

(a) At second stage burn-out, the unregulated nitrogen pressure exactly equals the regulated nitrogen pressure so that the two start dropping together immediately at burn-out. If the two pressures became equal any earlier in the flight, the requirement that rated thrust exist throughout burn phase would be violated. If the equality first occurred any later in the flight, unnecessary fuel consumption would occur, reducing the coast time.

(b) Regulated nitrogen pressure is 500 psia (485 psig). This is based on an average of all Scout vehicle "B" section regulator settings used thus far in the program.

(c) Based on prior analysis and in-flight data, the nitrogen temperature does not exceed 120°F.

(d) Below 500 psia and 120°F nitrogen behaves as a perfect gas. The compressibility factor for nitrogen at 500 psia is 1.0 for all temperatures below 180°F.

(e) The usable amount of hydrogen peroxide on board "B" section is 185 lb. such that 75 lb. is available for the coast phase. This is approximately the maximum amount which can be charged into the present system.

(f) The nitrogen temperature is constant. Actually, temperature during a flight would increase, which would have a tendency to increase the nitrogen pressure. The effect of this would be an increase in fuel consumption and a corresponding decrease in coast time.

(g) The hydrogen peroxide temperature is a constant 70°F. While it is true that the increasing temperatures encountered during a flight will decrease fuel consumption, experience with previous flights shows that the change in system performance is negligible. The value of 70°F is based on previous in-flight data.

(h) The specific impulse of the motors is approximately constant. The reason for this assumption is that for both the pitch-yaw and the roll motors, the fuel flow required for rated thrust is greater than the most efficient flow based on the catalyst bed areas, such that the motors will actually operate with greater efficiency at the lower flow rate. As further justification of the assumption, the fourteen lb. motors in "C" transition section are throttled down to three lb. with no degradation in the specific impulse.

5.3.3.4 Analysis

The volume of the nitrogen system is found as follows:

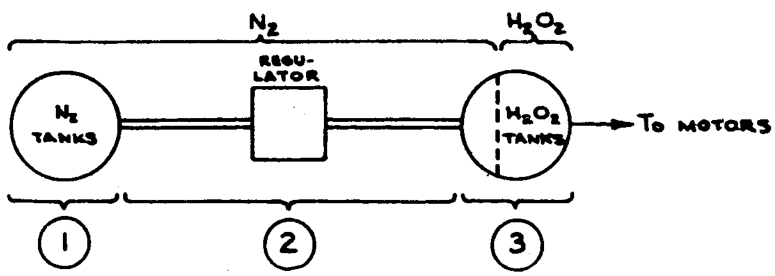

Volumes

$$\text{(1)}\quad 2\text{ TANKS}\cdot\frac{386\text{ IN.}^3}{\text{TANK}} = 772\text{ IN.}^3$$

$$\text{(2)}\quad \text{LINES, FITTINGS, AND REGULATOR} = 10\text{ IN.}^3$$

$$\text{(3)}\quad 10\text{ TANKS}\cdot\frac{384\text{ IN.}^3}{\text{TANK}} = 3840\text{ IN.}^3$$

$$V_{N_2} = \text{(1)} + \text{(2)} + \text{(3)} - V_{H_2O_2}$$

$$= 772\text{ IN.}^3 + 10\text{ IN.}^3 + 3840\text{ IN.}^3 - V_{H_2O_2}$$

$$= 4622\text{ IN.}^3 - V_{H_2O_2}$$

Applying the perfect gas equation of state to the nitrogen system results in

$$(pV)_{N_2} = (mRT)_{N_2}$$

But m, R, and T are constant; therefore,

$$(pV)_{N_2} = \text{CONSTANT}$$

or

$$p_{N_2}(4622\text{ IN.}^3 - V_{H_2O_2}) = \text{CONSTANT}$$

The constant may be evaluated at burn-out, where $p_{N_2} = p_{REG.\,N_2}$; thus

$$p_{N_2}(4622\text{ IN.}^3 - V_{H_2O_2}) = p_{REG.\,N_2}(4622\text{ IN.}^3 - V_{H_2O_2\,@\,\text{BURN-OUT}}) \qquad \text{Eq. (1)}$$

The volume occupied by the hydrogen peroxide may be found by noting that

$$V_{H_2O_2} = \frac{m_{H_2O_2}}{\rho_{H_2O_2}}$$

Where m is mass and ρ is density. Using a density vs. temperature curve for 90% (by weight) hydrogen peroxide, the density may be found as

$$\rho_{H_2O_2} = \frac{0.0517\text{ LB}_m}{\text{IN.}^3} - \frac{0.0002\text{ LB}_m}{\text{IN.}^3\,°\text{F}}\,T_{H_2O_2}$$

Thus,

$$V_{H_2O_2} = \frac{m_{H_2O_2}}{\frac{0.0517\text{ LB}_m}{\text{IN.}^3} - \frac{0.0002\text{ LB}_m}{\text{IN.}^3\,°\text{F}}\,T_{H_2O_2}}$$

Substituting this into Eq. (1) results in

$$p_{N_2}\left(4622\ \text{in.}^3 - \frac{m_{H_2O_2}}{\frac{0.0517\ \text{lb}_m}{\text{in.}^3} - \frac{0.0002\ \text{lb}_m}{\text{in.}^3\ {}^\circ F}\,T_{H_2O_2}}\right)$$

$$= p_{REG.\,N_2}\left(4622\ \text{in.}^3 - \frac{m_{H_2O_2\ @\ \text{BURN-OUT}}}{\frac{0.0517\ \text{lb}_m}{\text{in.}^3} - \frac{0.0002\ \text{lb}_m}{\text{in.}^3\ {}^\circ F}\,T_{H_2O_2}}\right)$$

$$p_{N_2}\left(239\ \text{lb}_m - \frac{0.1\ \text{lb}_m}{{}^\circ F}T_{H_2O_2} - m_{H_2O_2}\right) = p_{REG.\,N_2}\left(239\ \text{lb}_m - \frac{0.1\ \text{lb}_m}{{}^\circ F}T_{H_2O_2} - m_{H_2O_2\ @\ \text{BURN-OUT}}\right)$$

Or

$$p_{N_2} = p_{REG.\,N_2}\left(\frac{239\ \text{lb}_m - \frac{0.1\ \text{lb}_m}{{}^\circ F}T_{H_2O_2} - m_{H_2O_2\ @\ \text{BURN-OUT}}}{239\ \text{lb}_m - \frac{0.1\ \text{lb}_m}{{}^\circ F}T_{H_2O_2} - m_{H_2O_2}}\right)$$

For a regulated nitrogen pressure of 500 psia, a peroxide temperature of 70°F, and fuel mass at burn-out of 75 lb_m, the preceding equation becomes

$$p_{N_2} = 500\ \text{psia}\left(\frac{239\ \text{lb}_m - 7\ \text{lb}_m - 75\ \text{lb}_m}{239\ \text{lb}_m - 7\ \text{lb}_m - m_{H_2O_2}}\right)$$

$$= 500\ \text{psia}\left(\frac{157\ \text{lb}_m}{232\ \text{lb}_m - m_{H_2O_2}}\right)$$

This relation is plotted as Figure 5.67.

From Figure 5.67 it is seen that when the fuel supply is exhausted the nitrogen pressure is 340 psia. With data from an actual experimental test, curves showing thrust vs. nitrogen pressure are drawn for the pitch-yaw motors and the roll motors as Figures 5.68 and 5.69, respectively. These curves are extrapolated to tail-off at 340 psia (fuel exhaustion). Finally, lines parallel to the experimental curves are presented to allow for the permissible ranges of rated thrust.

5.4.0 Guidance System Modifications

5.4.1 Introduction

The necessity of providing a wider reaction control system deadband during second stage coast has been discussed elsewhere in this report. The following discussion describes the changes in the guidance system circuitry required to provide the wider deadbands for second stage coast.

5.4.2 Summary

The guidance system was reviewed to determine whether or not the system could be modified to provide a wider reaction control system deadband to be used during second stage coast. The results of the review has determined that the system can be modified to provide the necessary gain switching and deadbands.

The modifications required are fairly simple and involve the rearrangement of the contacts of relay K4 located on the Gain Control Board which is a part of the Inertial Reference Unit. The relay contacts are rearranged such that resistors are switched in the pitch and yaw control channels thereby providing the wider deadband. The modifications necessary to provide a wider roll channel deadband were also determined.

The only changes required in the vehicle wiring involve the interconnections of two Intervalometer Channels with the IRP. No changes are required in the GSE.

5.4.3 Discussion

The most direct means of providing the wider deadbands, i.e., lower gains, is to modify the Gain Control Board (GCB) which is a part of the Inertial Reference Package (IRP). The GCB contains the relays and resistors which are used for the normal Scout gain changes.

5.4.3.1 Gain Control Board

The IRP for the 140 and subsequent series vehicles is part number DGG122 C3, and contains a GCB which is a revision of the GCB in the earlier model IRP, part number DGG122 C1. The revision provided a yaw torquing capability. The mission of the vehicle studied in this report does not require yaw torquing, therefore, the relay on the GCB which provides this capability is not needed. It is this relay (K4) which is to be used to provide the necessary switching to obtain the wider deadband.

The GCB for the C1 model IRP is more suitable for modification than that of the C3 model IRP since relay K4 is already partially connected into the gain changing circuitry and resistor terminals are available. The use of a C1 GCB from the 62 procurement spares program will provide a use for this component which otherwise would not be used due to the model change for the 140 series vehicles. Figure 5.70 is a partial schematic of the C1 GCB, part number AD932461, as it is supplied in the IRP and shown on schematic C8649. This board is physically interchangeable with the GCB in the C3 model IRP.

5.4.3.1.1 Pitch and Yaw Deadband

Figure 5.71 is a partial schematic of the C1 GCB as modified to provide a wider deadband for pitch and yaw for second stage coast. The gain changing or widening of the deadbands is to be accomplished by the switching of gain resistors by relay K4 and is described as follows:

(a) Relay K2 actuates at second stage ignition providing the gains for the second stage burn deadbands. The second stage pitch deadband is set by resistors R1, R3 and R4 in parallel with R24 in series, with the voltage developed across R24 going to the Poppet Valve Electronics Unit (PVE). The second stage yaw deadband is set by resistors R6, and R8 in parallel with R25 in series, with the voltage developed across R25 going to the PVE. The roll deadband circuitry remains unchanged in this figure.

(b) Relay K4 is actuated by the application of 28 volts DC at P3-19 by a channel of the Intervalometer after second stage burnout. When K4 is actuated resistors R4 and R8 are disconnected from their respective parallel combinations. The removal of R4 causes the pitch deadband to change to a value set by the parallel combination of R1 and R3 while the new yaw deadband, with the removal of R8, is set by the value of R6. The roll deadband in this circuit arrangement remains the same as the deadband set for second stage burn. A jumper is added from K4 relay terminal 16 to 15 to prevent disruption of the roll channel circuitry when K4 is actuated. The ratio of displacement gyro gain to rate gyro gain during second stage coast remains the same as set for second stage burn.

(c) Just prior to third stage ignition relya K4 is again actuated by the application of 28 VDC to terminal P3-17, and the removal of 28 VDC from terminal P3-19. The 28 VDC is controlled by a second channel in the Intervalometer. This actuation of K4 returns the gain circuitry to the condition for second stage burn and hence the same deadbands which existed prior to the initial actuation of K4.

5.4.3.1.2 Roll Deadband

Figure 5.72 is a partial schematic of the C1 GCB with additional modifications to add the capability of widening the roll deadbands during second stage coast. This modification would not be made should it be determined that a wider roll deadband is not needed. The circuitry is identical to that of Figure 5.71 except for the modifications to add the roll deadband gain change. The roll deadband is set for second stage burn by the parallel combinations of resistors R12 - R13 and R11 - R20. The second stage coast deadband is obtained by the actuation of relay K4 which removes resistors R12 and R20 from their respective parallel combinations. The second stage coast deadband is then determined by the values of resistors R11 and R12. The ratio of displacement gyro gain to rate gyro gain remains the same as set for second stage burn gains.

5.4.3.1.3 Additional Modifications

One additional modification is required on the C1 GCB to enable the C3 IRP to function properly with the C1 GCB installed. A jumper is connected between terminal P3-31 and terminal P3-37. This connection completes the circuit to the pitch gyro torquer. There are no other modifications required of the Guidance components.

5.4.3.2 Vehicle and GSE

The vehicle wiring requires modification to connect the proper Intervalometer channels to the IRP. The required circuitry is shown in Figure 5.73 which shows that Intervalometer channel T-28 is used to command second stage coast gain and channel T-25 is used to remove the second stage coast gain and to reapply the second stage burn gain and deadbands. Channel T-28 was previously used to command yaw torquing and channel T-25 is a spare. It will be noted that due to the arrangement of the Intervalometer channel relay contacts power is applied continuously to one of the relay coils dependent upon the switching sequence. No change to the GSE is required as a result of these modifications.

FIGURE 5.1
UNCONVENTIONAL VEHICLE-SPACECRAFT
THE VARIATION OF FIRST STAGE NORMAL FORCE DERIVATIVE WITH MACH NUMBER

CONFIGURATION II-A-2

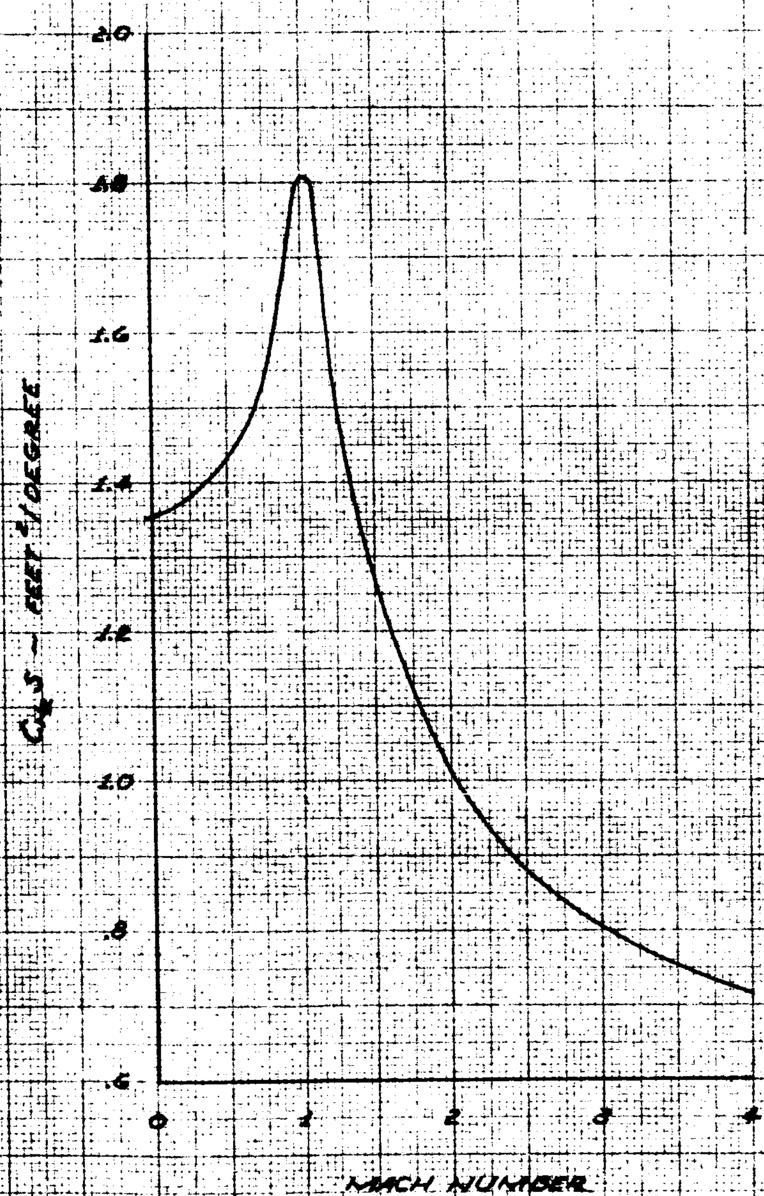

FIGURE 5.2
UNCONVENTIONAL VEHICLE - SPACECRAFT
THE VARIATION OF FIRST STAGE CENTER
OF PRESSURE WITH MACH NUMBER

CONFIGURATION II-A-2
PAYLOAD WEIGHT = 300 POUNDS

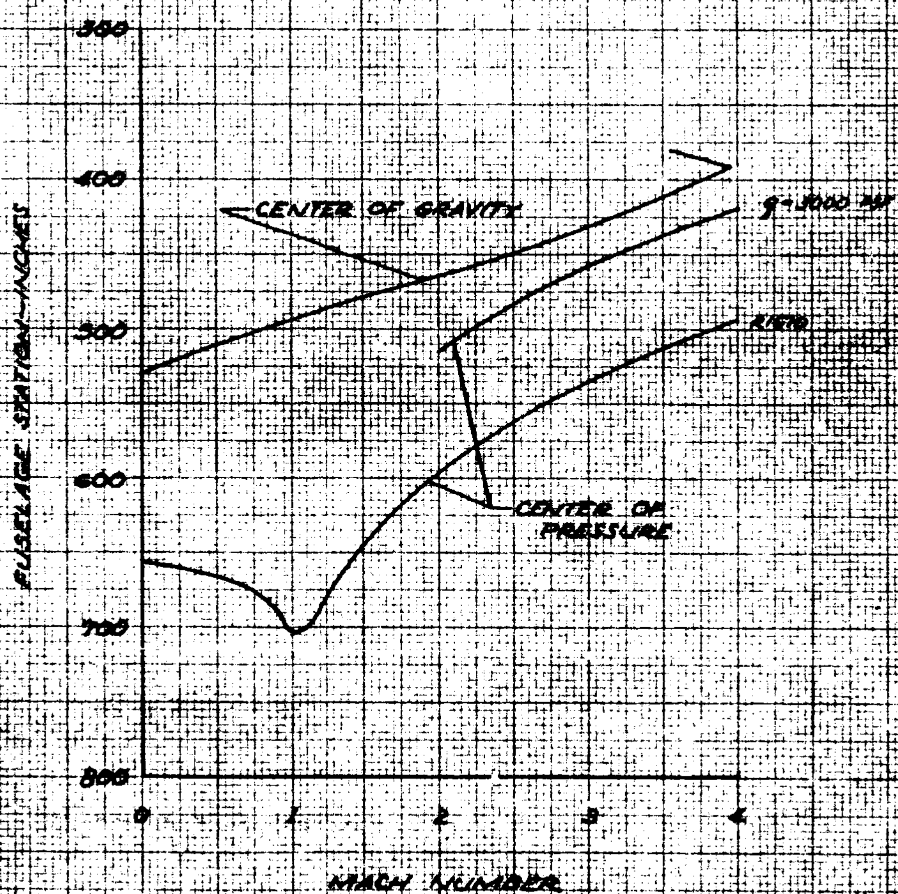

FIGURE 5.3
UNCONVENTIONAL VEHICLE ~ SPACECRAFT
THE VARIATION OF SECOND STAGE NORMAL FORCE
DERIVATIVE AND CENTER OF PRESSURE WITH
MACH NUMBER

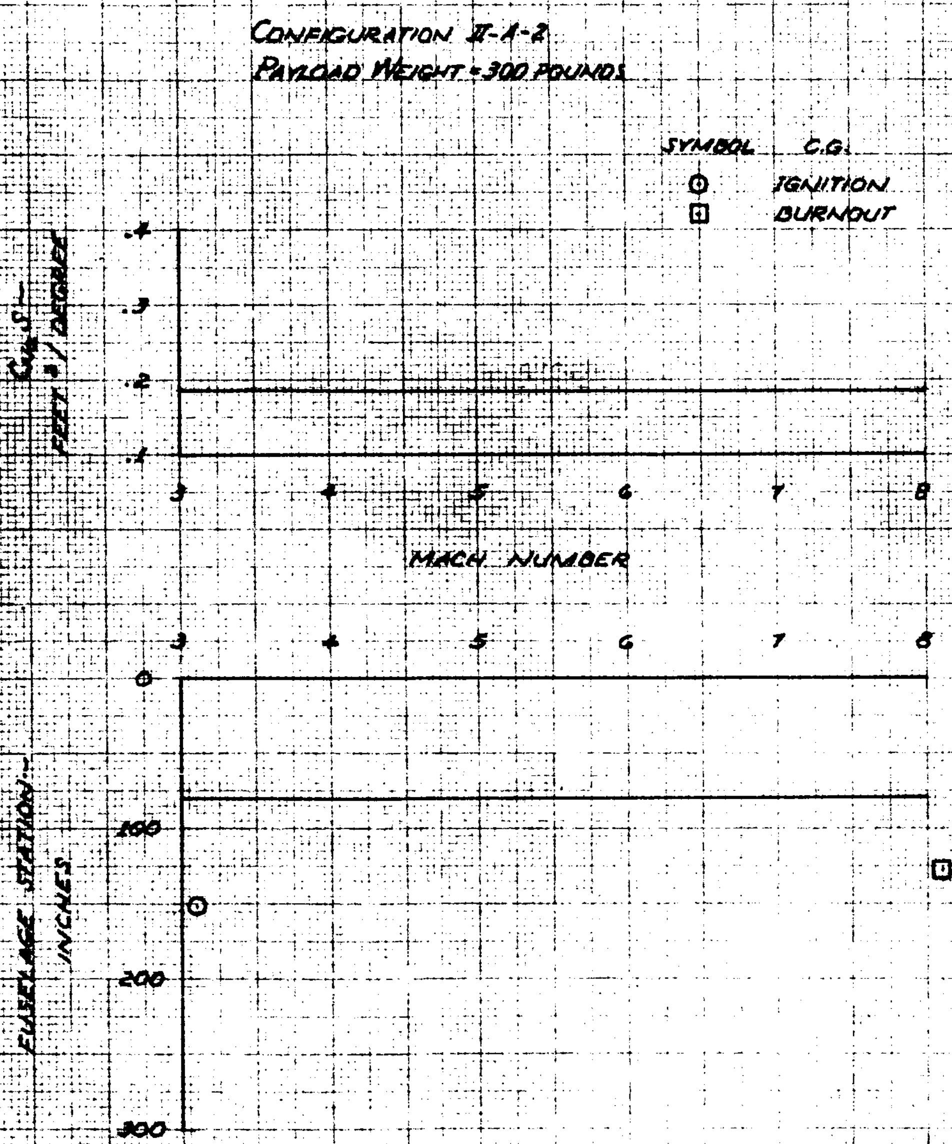

FIGURE 5.4
UNCONVENTIONAL VEHICLE - SPACECRAFT
THE VARIATION OF THIRD STAGE NORMAL FORCE DERIVATIVE AND CENTER OF PRESSURE WITH MACH NUMBER

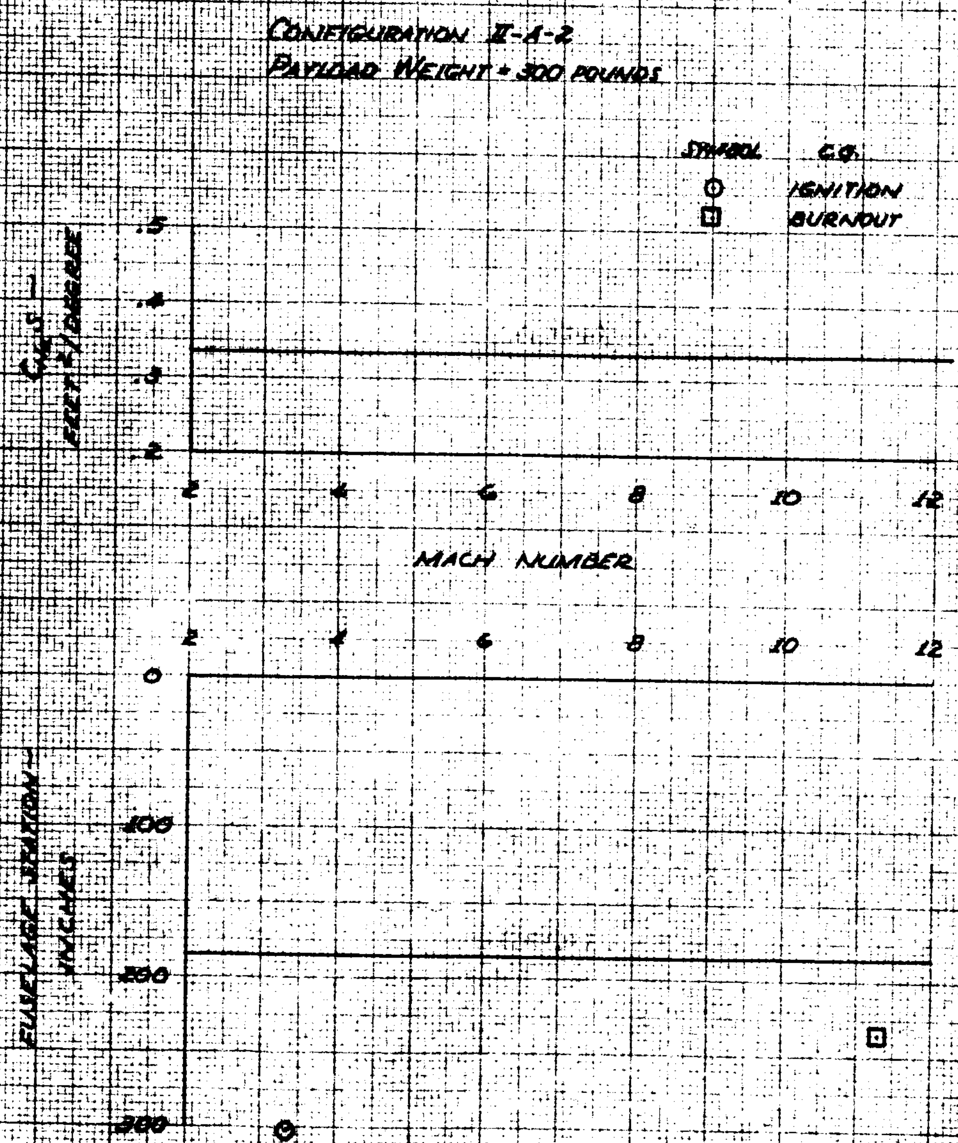

FIGURE 5.5
UNCONVENTIONAL VEHICLE - SPACECRAFT
THE VARIATION OF REENTRY STAGE NORMAL FORCE
DERIVATIVE AND CENTER OF PRESSURE WITH
MACH NUMBER

CONFIGURATION II-A-2
PAYLOAD WEIGHT = 300 POUNDS

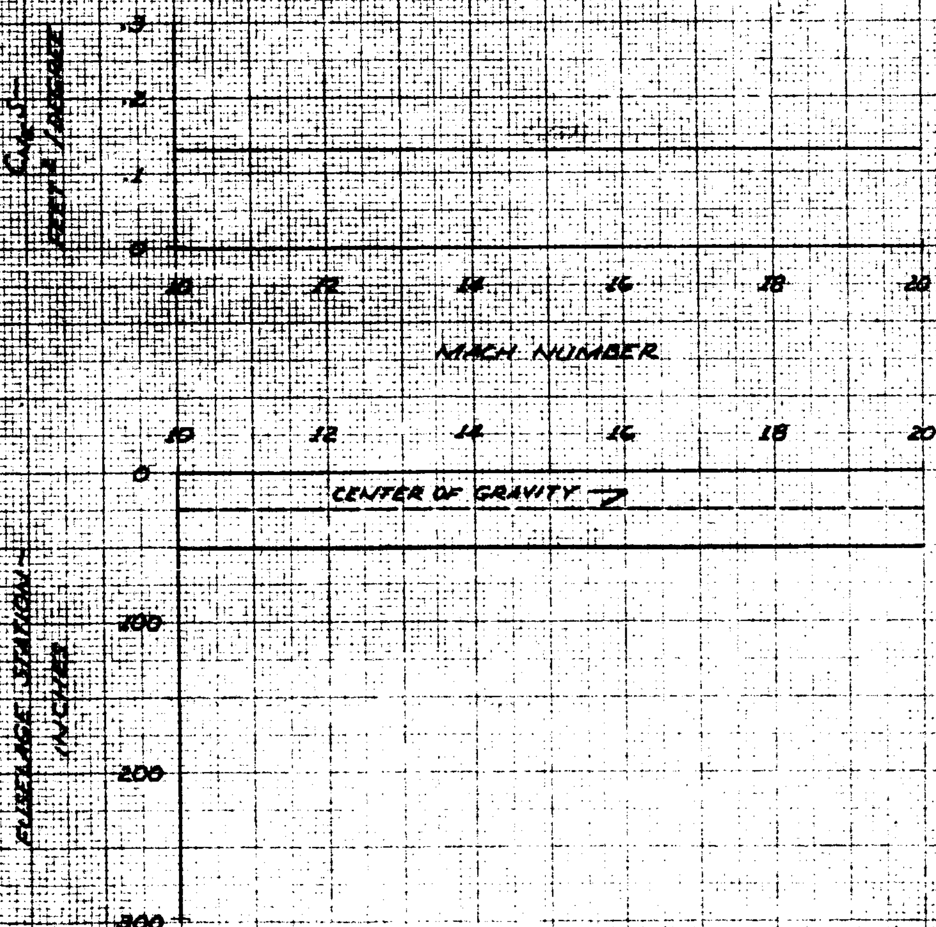

FIGURE 5.6
UNCONVENTIONAL VEHICLE - SPACECRAFT
THE VARIATION OF FIRST STAGE ZERO LIFT DRAG COEFFICIENT WITH MACH NUMBER

CONFIGURATION II-A-2

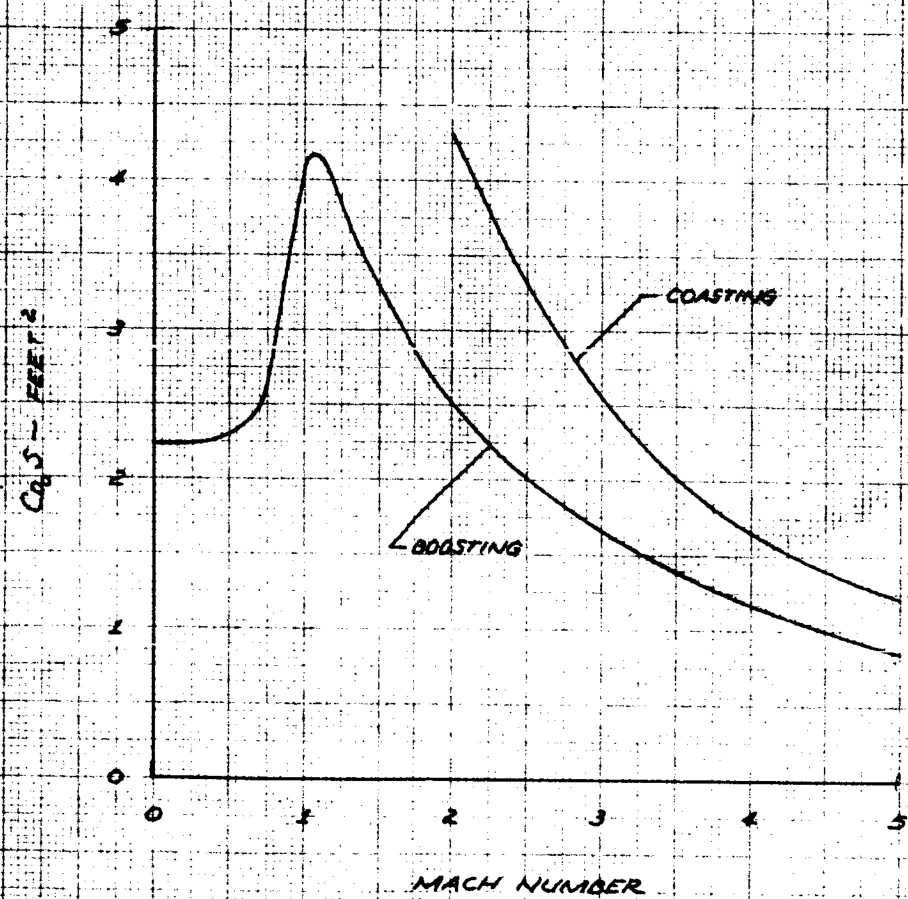

FIGURE 5.7
UNCONVENTIONAL VEHICLE - SPACECRAFT
THE VARIATION OF SECOND STAGE ZERO LIFT DRAG COEFFICIENT WITH MACH NUMBER

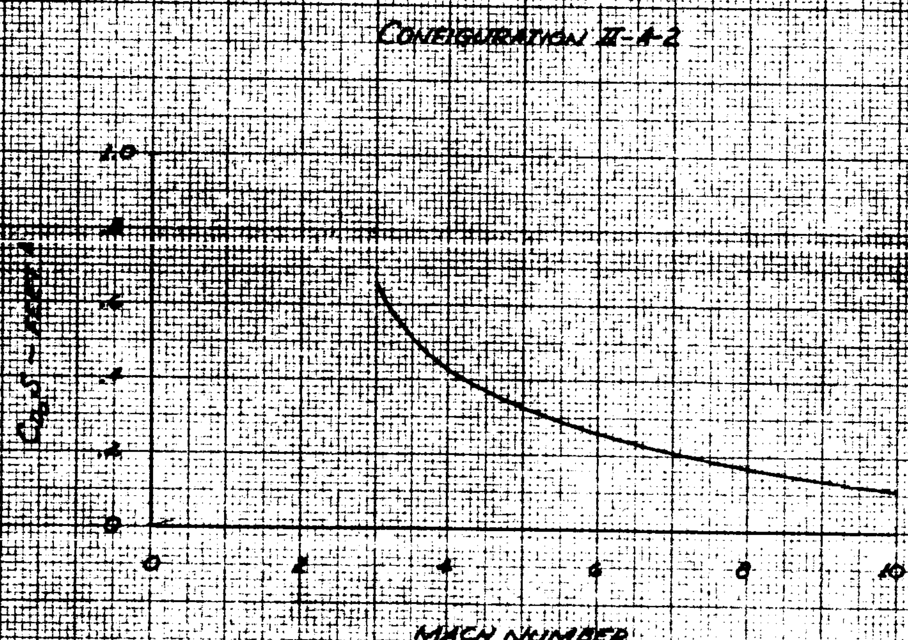

FIGURE 5.8
UNCONVENTIONAL VEHICLE - SPACECRAFT
THE VARIATION OF REENTRY STAGE ZERO LIFT
DRAG COEFFICIENT WITH MACH NUMBER

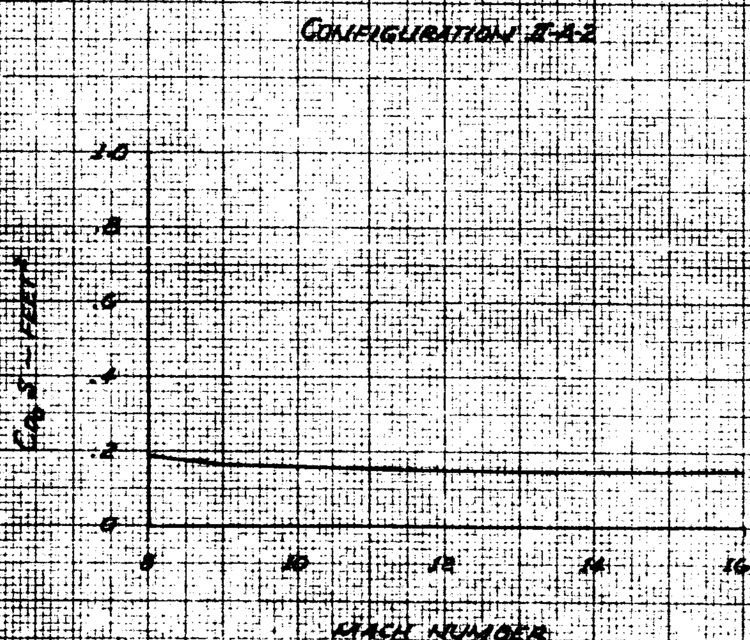

Figure 5.9
Unconventional Vehicle – Spacecraft
Supersonic Running Load Distribution

Configuration II-A-2

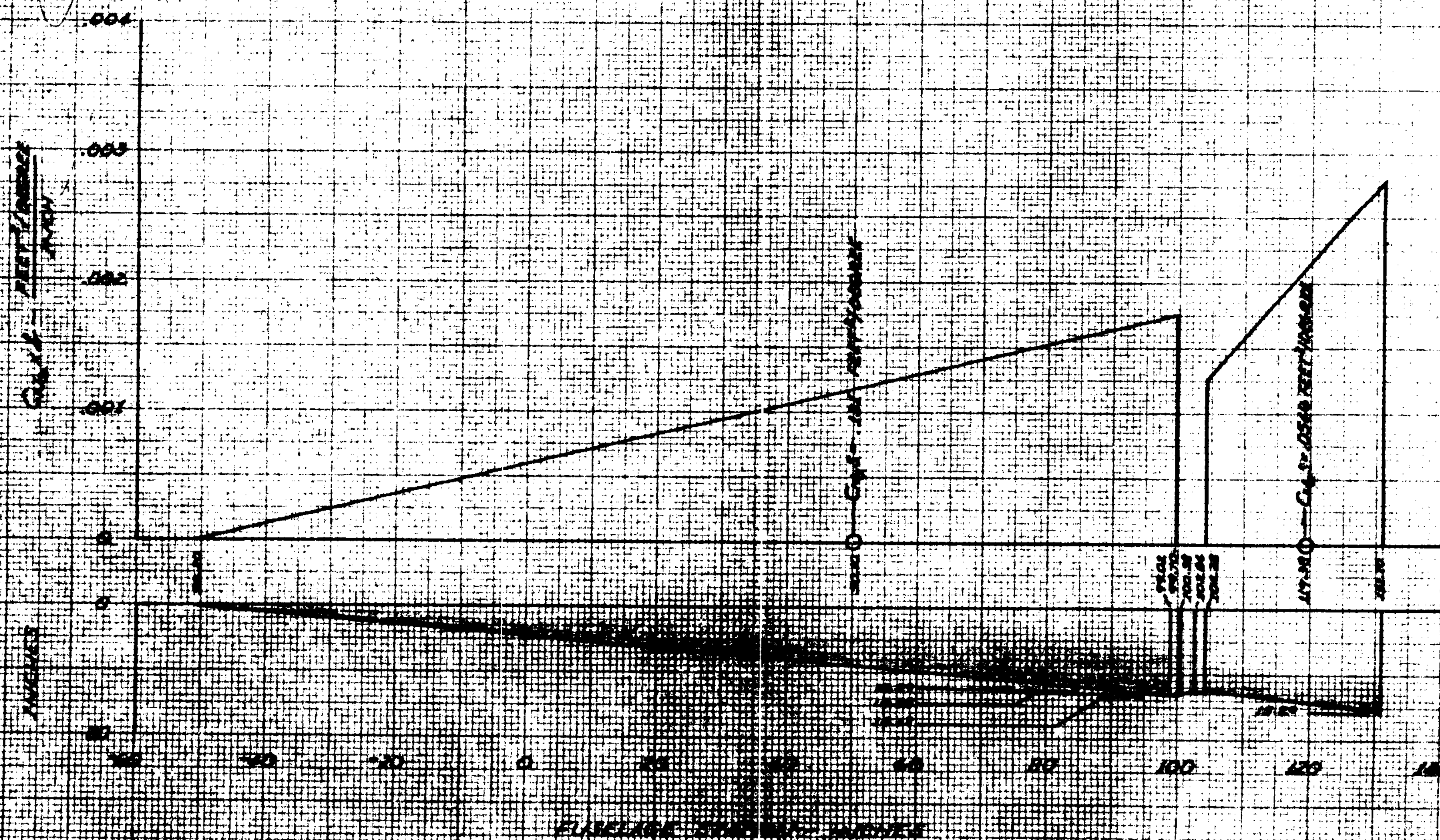

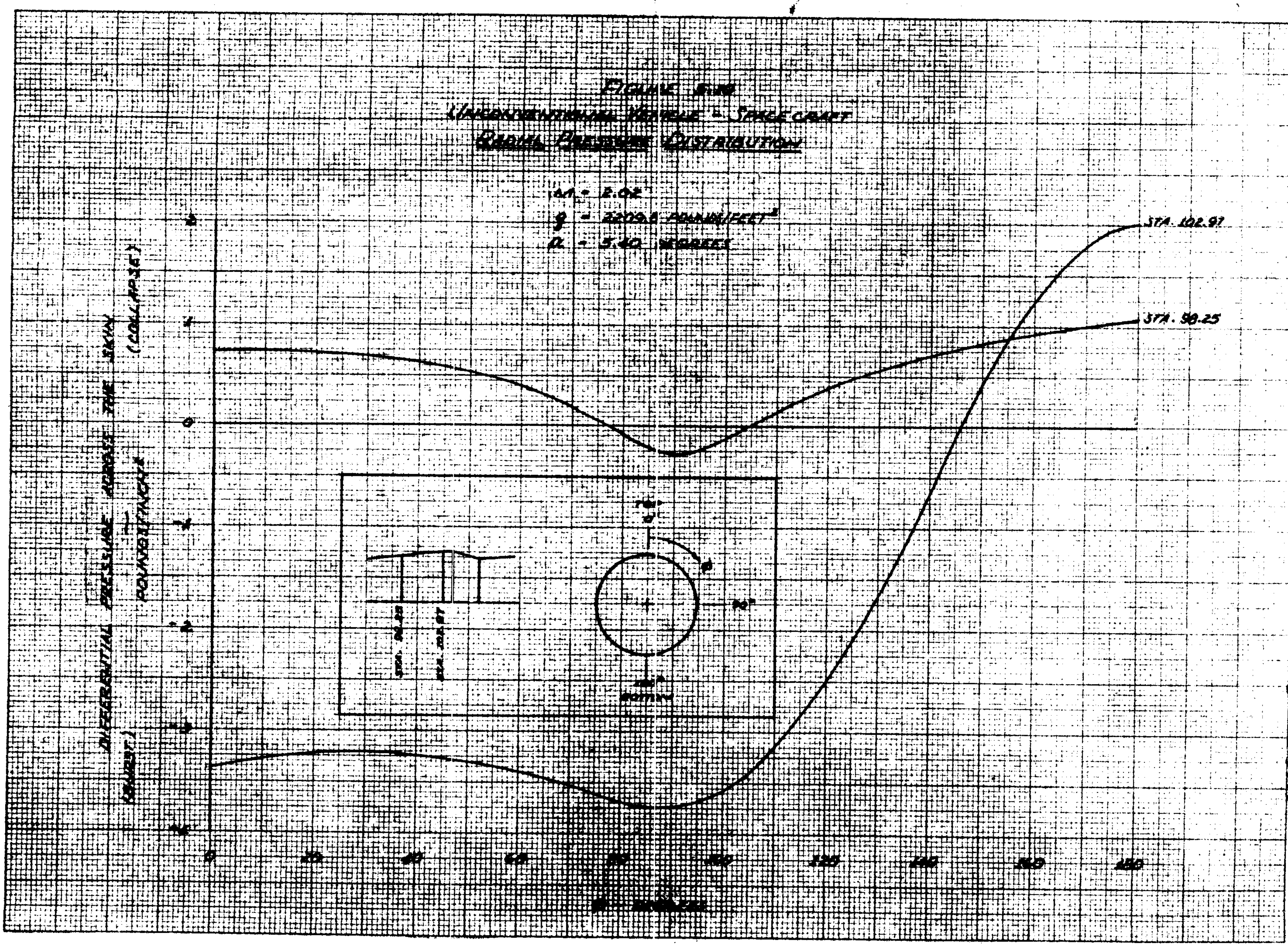
Spacecraft
Radial Pressure Distribution
STA. 102.97
STA. 98.25

FIGURE 5.11
UNCONVENTIONAL VEHICLE - SPACECRAFT
SECOND STAGE IGNITION CAPTURE MANEUVER

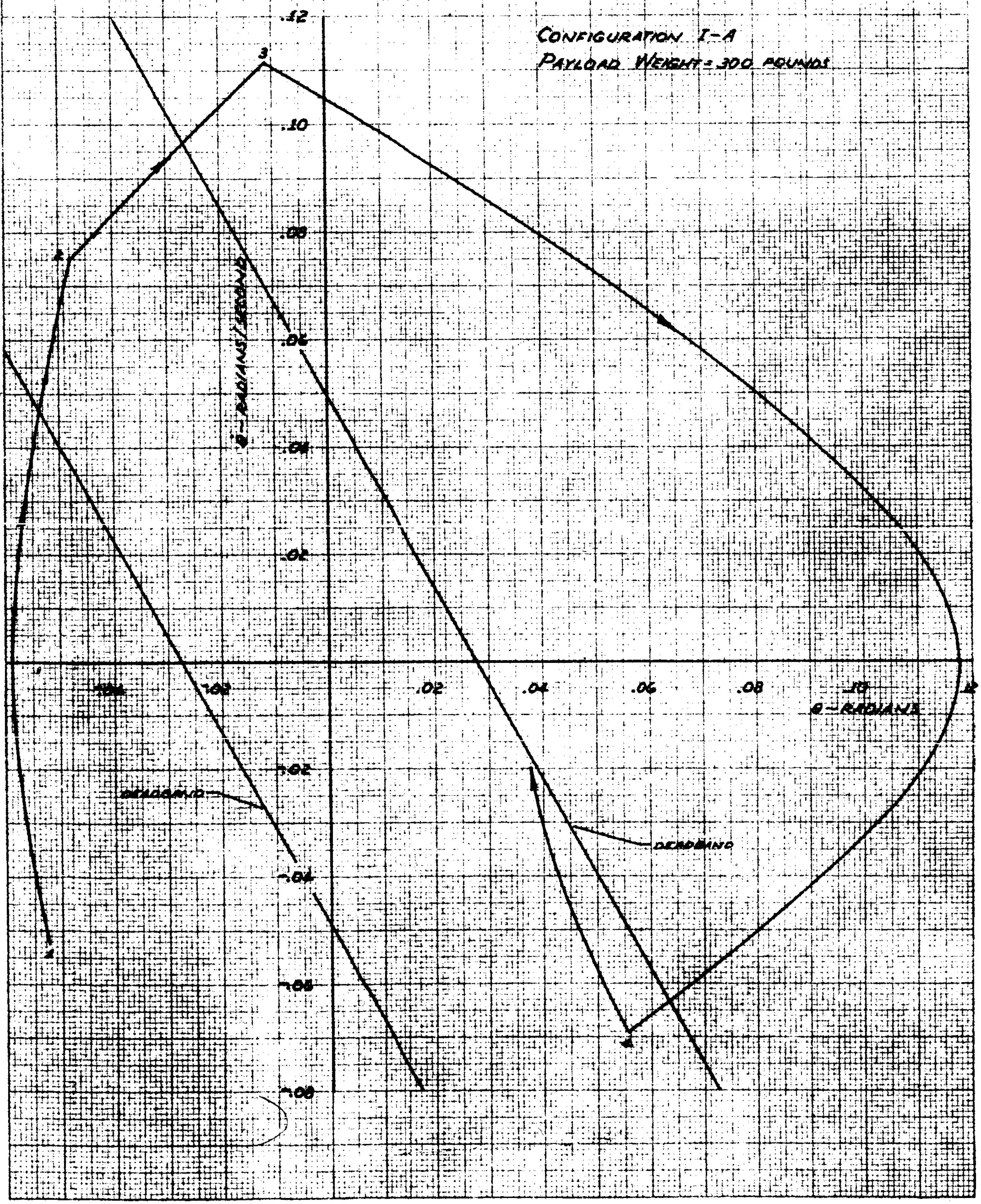

FIGURE 5.12
UNCONVENTIONAL VEHICLE - SPACECRAFT
SECOND STAGE COAST DEADBAND REDUCTION CAPTURE MANEUVER

CONFIGURATION I-A
SECOND STAGE COAST
PAYLOAD WEIGHT = 300 POUNDS

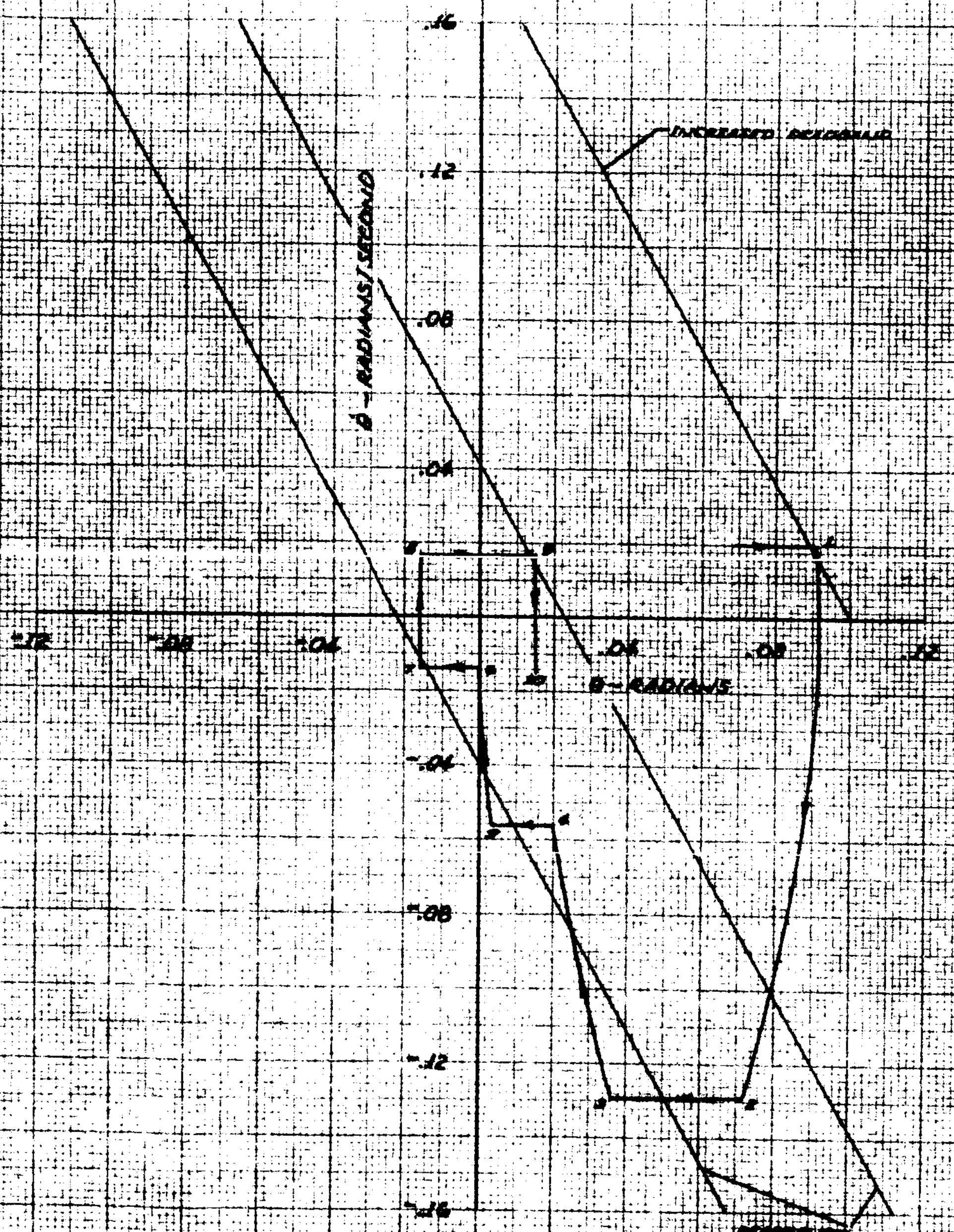

FIGURE 5.13
UNCONVENTIONAL VEHICLE - SPACECRAFT
THE VARIATION OF DEADBAND REDUCTION TIME
WITH INCREASED DEADBAND

CONFIGURATION I-A
SECOND STAGE COAST
PAYLOAD WEIGHT = 300 POUNDS

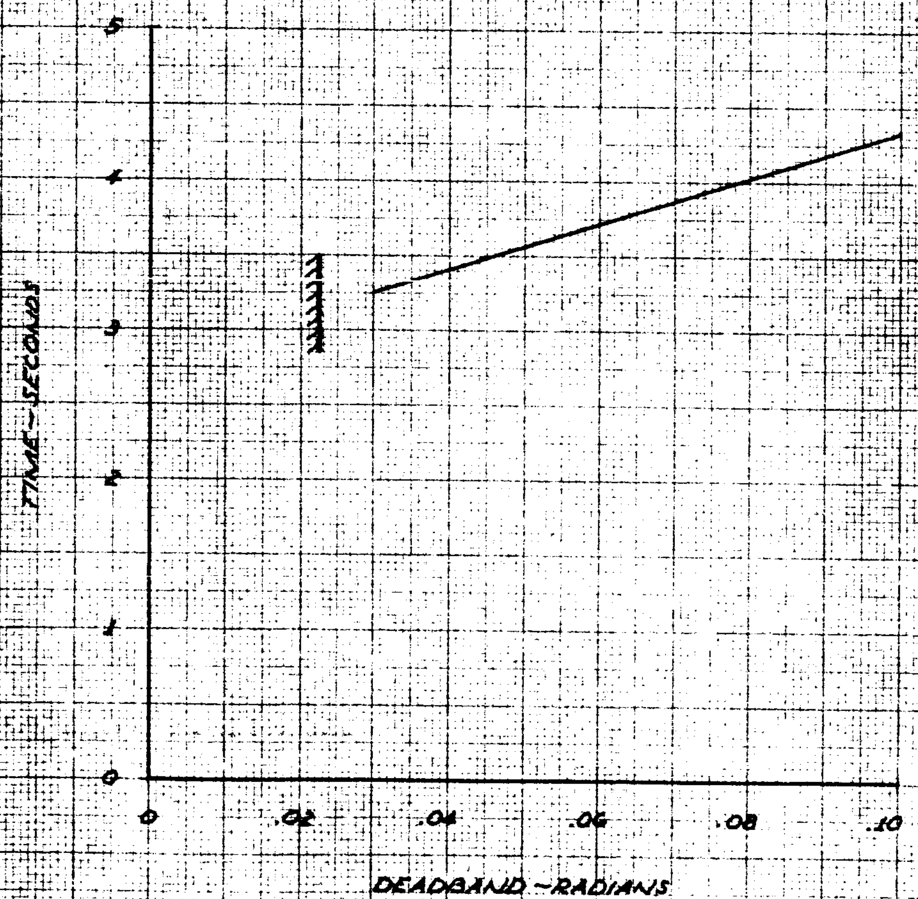

FIGURE 5.14

UNCONVENTIONAL VEHICLE - SPACECRAFT

THE VARIATION OF DEADBAND REDUCTION MOTOR-ON TIME WITH INCREASED DEADBAND

CONFIGURATION I-A
SECOND STAGE COAST
PAYLOAD WEIGHT = 300 POUNDS

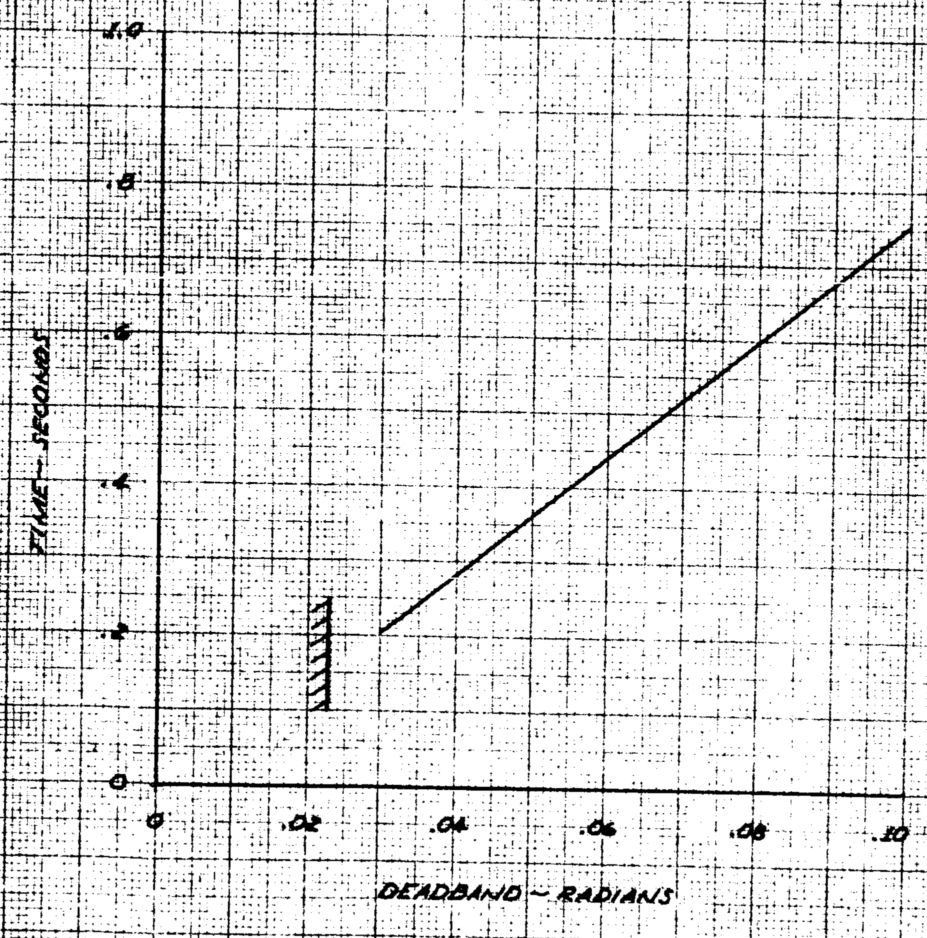

FIGURE 5.15
UNCONVENTIONAL VEHICLE - SPACECRAFT
THE VARIATION OF DEADBAND REDUCTION
HYDROGEN PEROXIDE CONSUMPTION WITH
INCREASED DEADBAND

CONFIGURATION I-A
SECOND STAGE COAST
PAYLOAD WEIGHT = 300 POUNDS

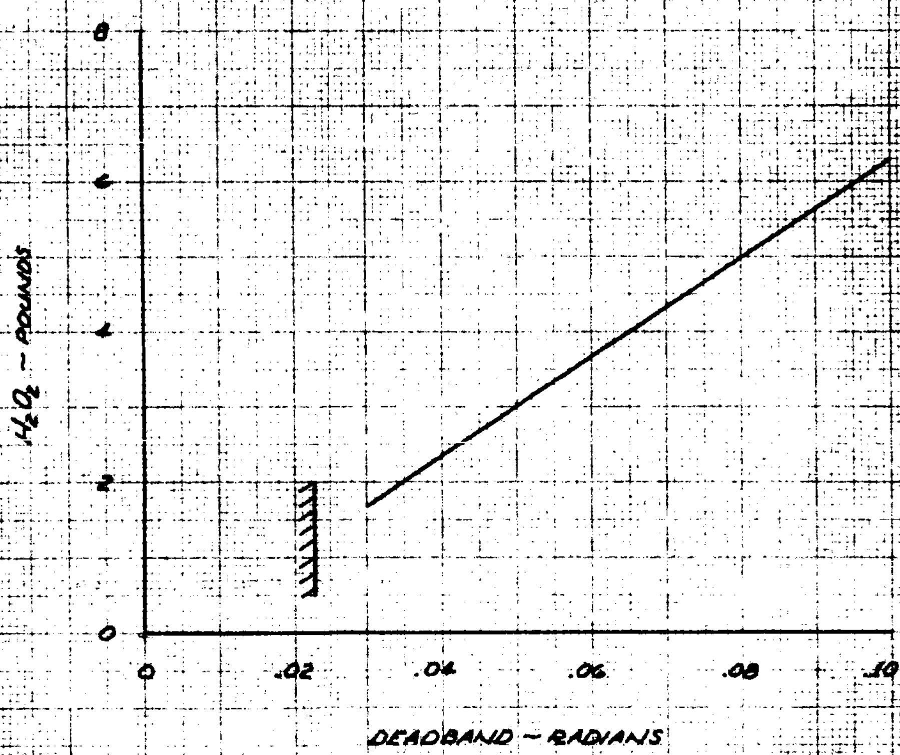

FIGURE 5.16
UNCONVENTIONAL VEHICLE - SPACECRAFT
THE VARIATION OF PITCH AND YAW DUTY
CYCLE WITH INCREASED DEADBAND

CONFIGURATION I-A
SECOND STAGE COAST
PAYLOAD WEIGHT = 300 POUNDS

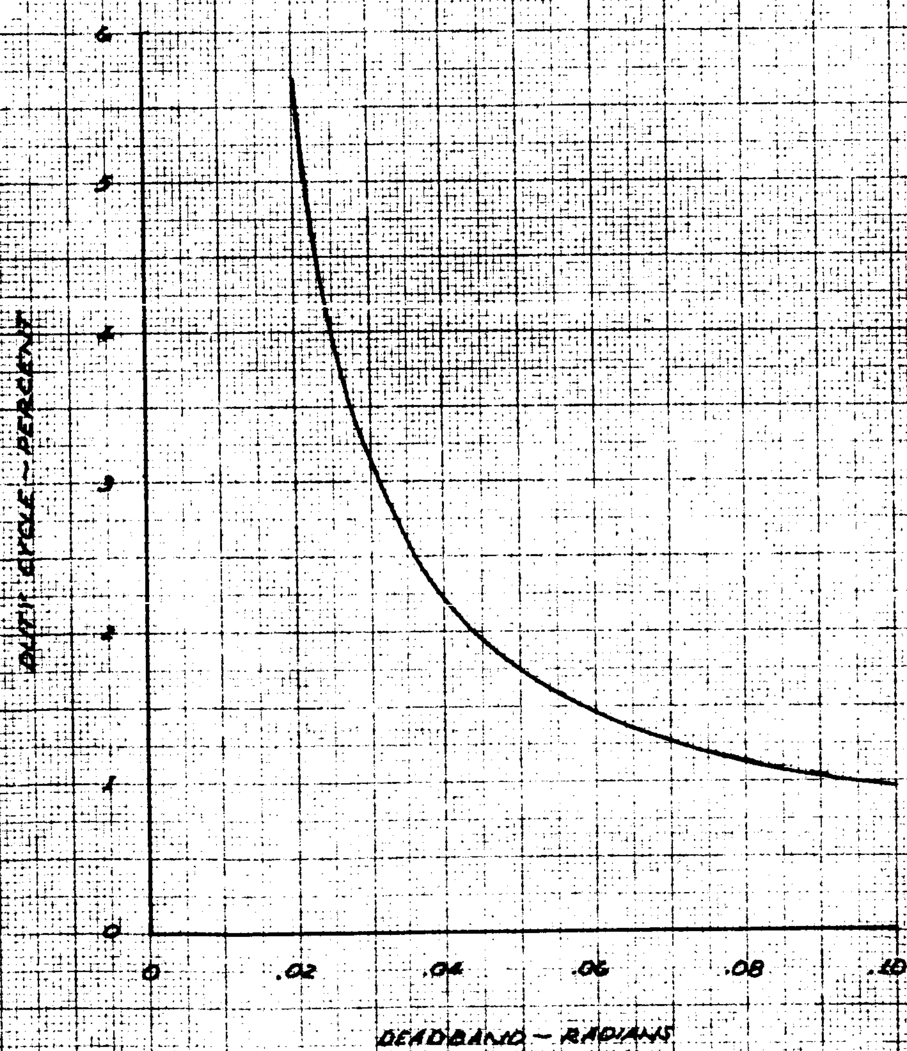

FIGURE 5.17
UNCONVENTIONAL VEHICLE - SPACECRAFT
THE VARIATION OF ROLL DUTY CYCLE
WITH INCREASED DEADBAND

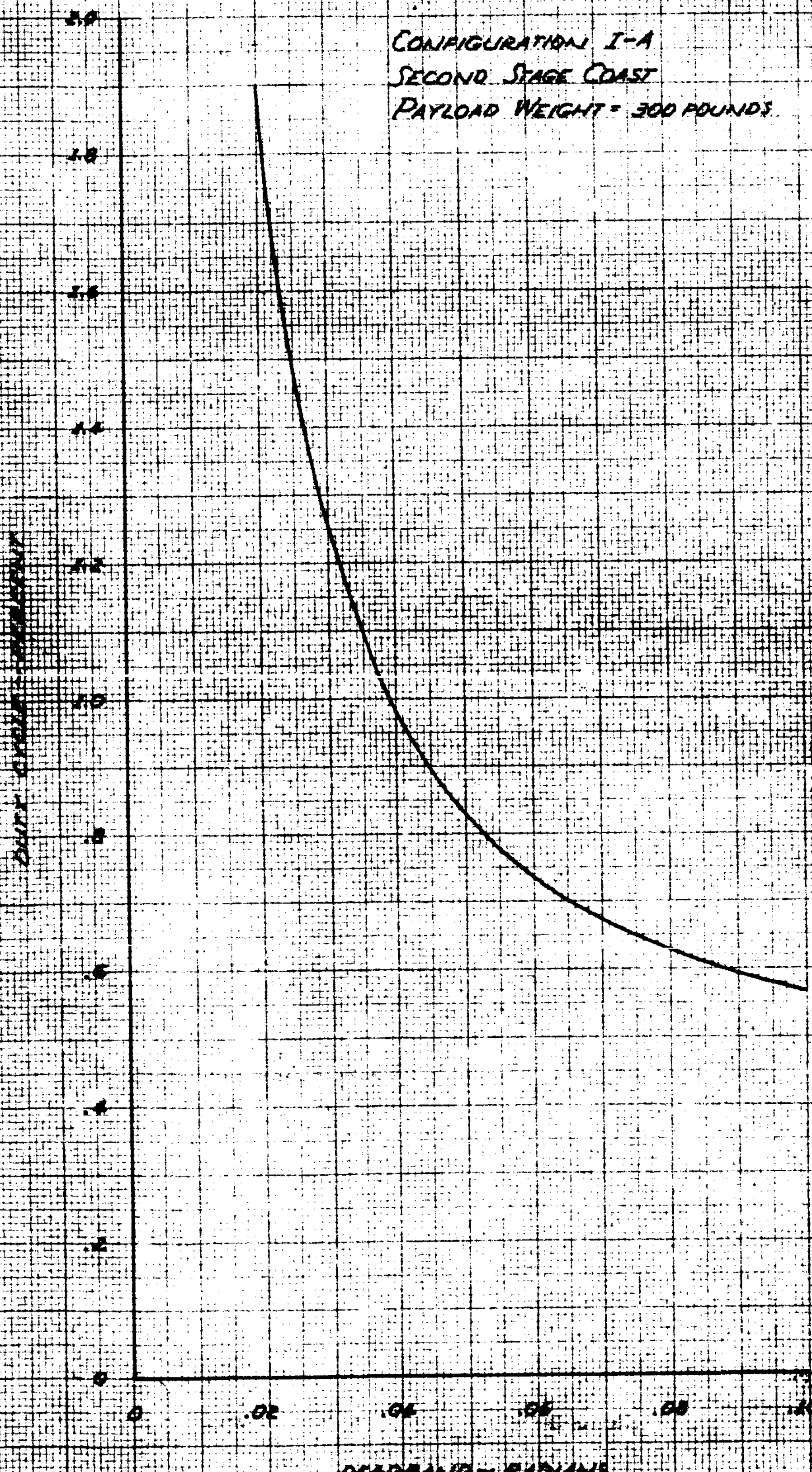

FIGURE 5.18

UNCONVENTIONAL VEHICLE — SPACECRAFT

THE VARIATION OF TOTAL HYDROGEN PEROXIDE FLOW RATE WITH INCREASED DEADBANDS

CONFIGURATION I-A
SECOND STAGE COAST
PAYLOAD WEIGHT = 300 POUNDS
α_{max} = .025 - 10% RADIANS

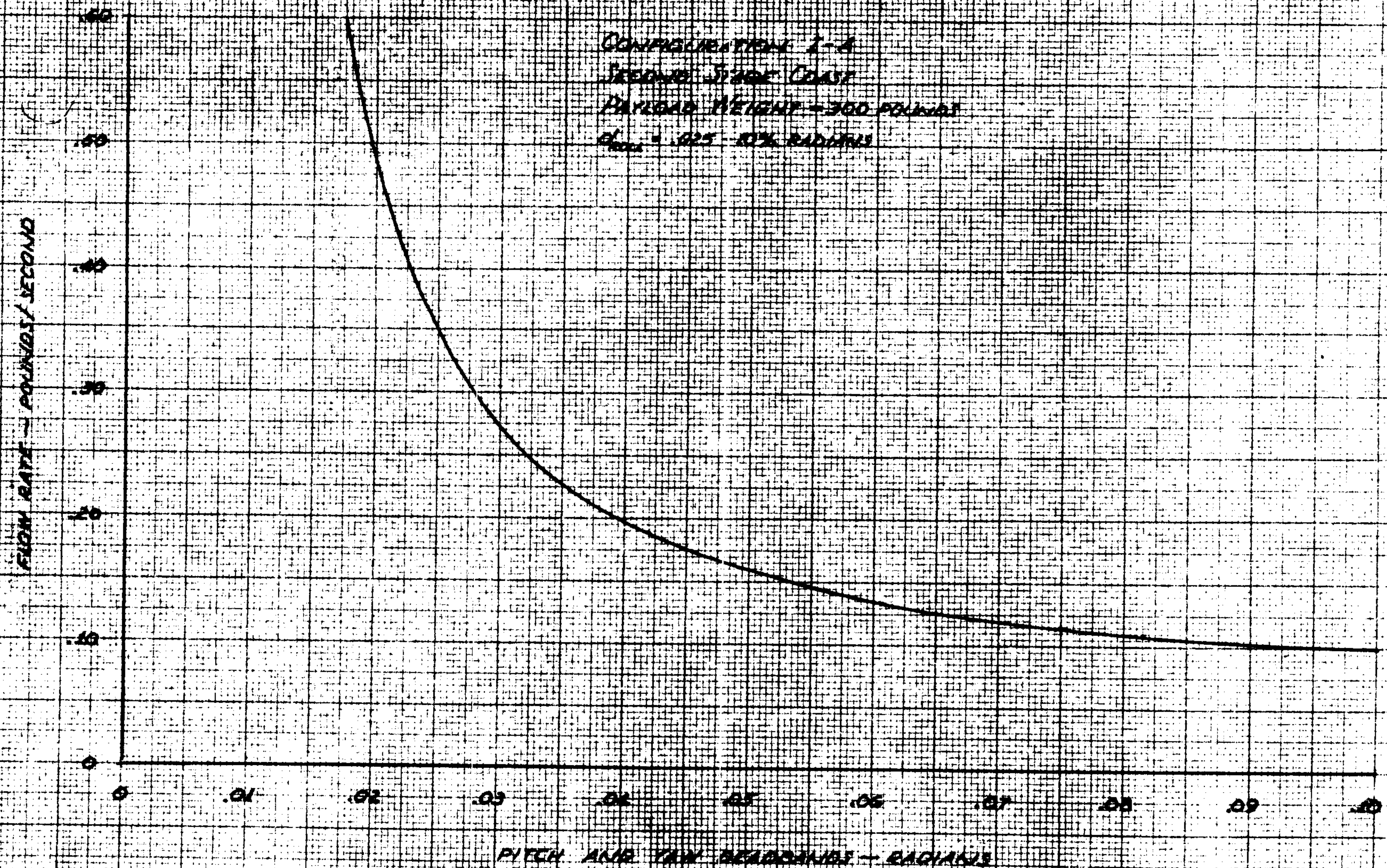

FIGURE 5.19

UNCONVENTIONAL VEHICLE - SPACECRAFT

THE VARIATION OF TOTAL HYDROGEN PEROXIDE FLOW RATE WITH INCREASED DEADBAND

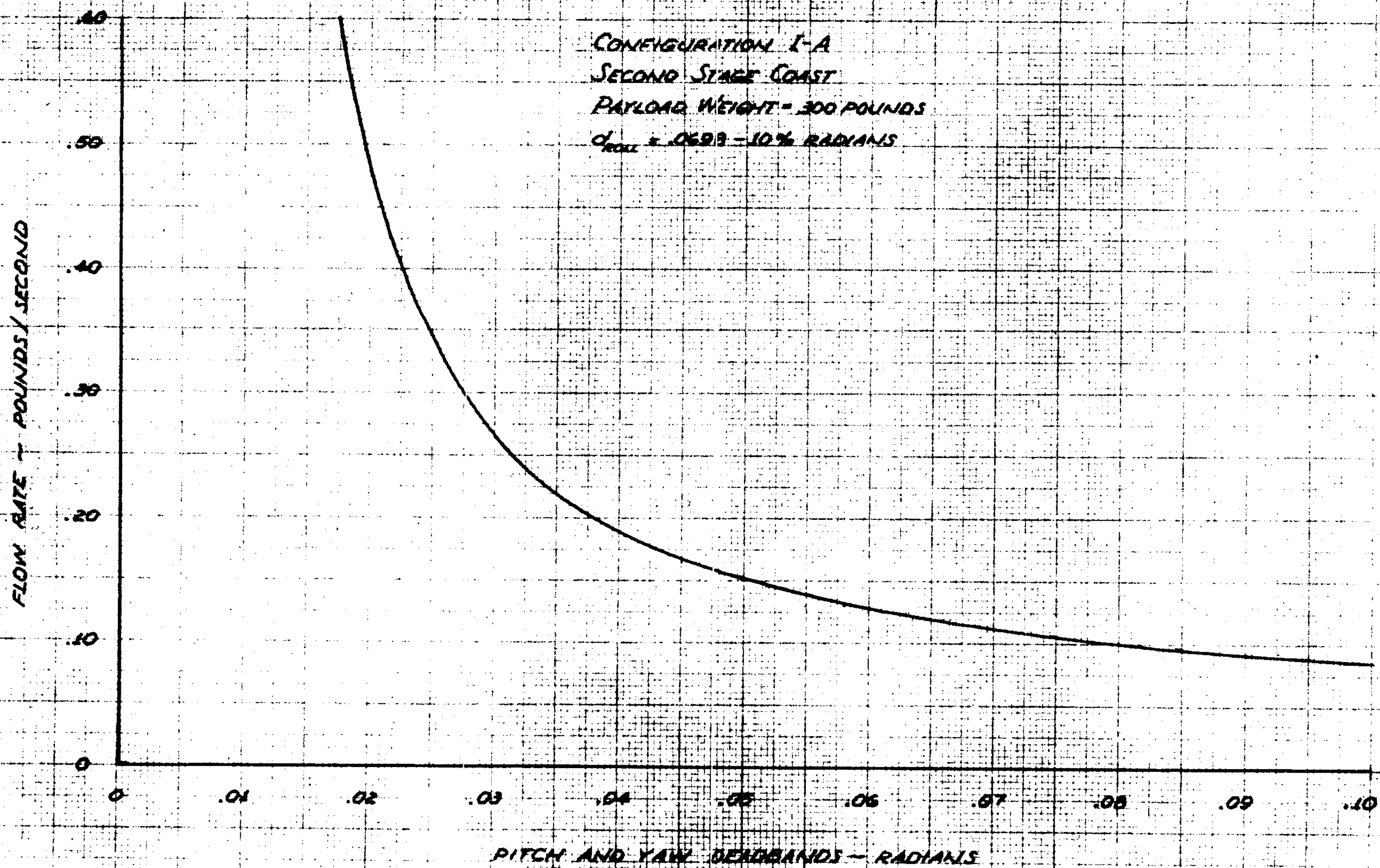

FIGURE 5.20

UNCONVENTIONAL VEHICLE – SPACECRAFT

THE VARIATION OF PITCH AND YAW DEADBANDS AND REENTRY ANGLE WITH SECOND STAGE COAST TIME AS A FUNCTION OF THE ROLL DEADBANDS

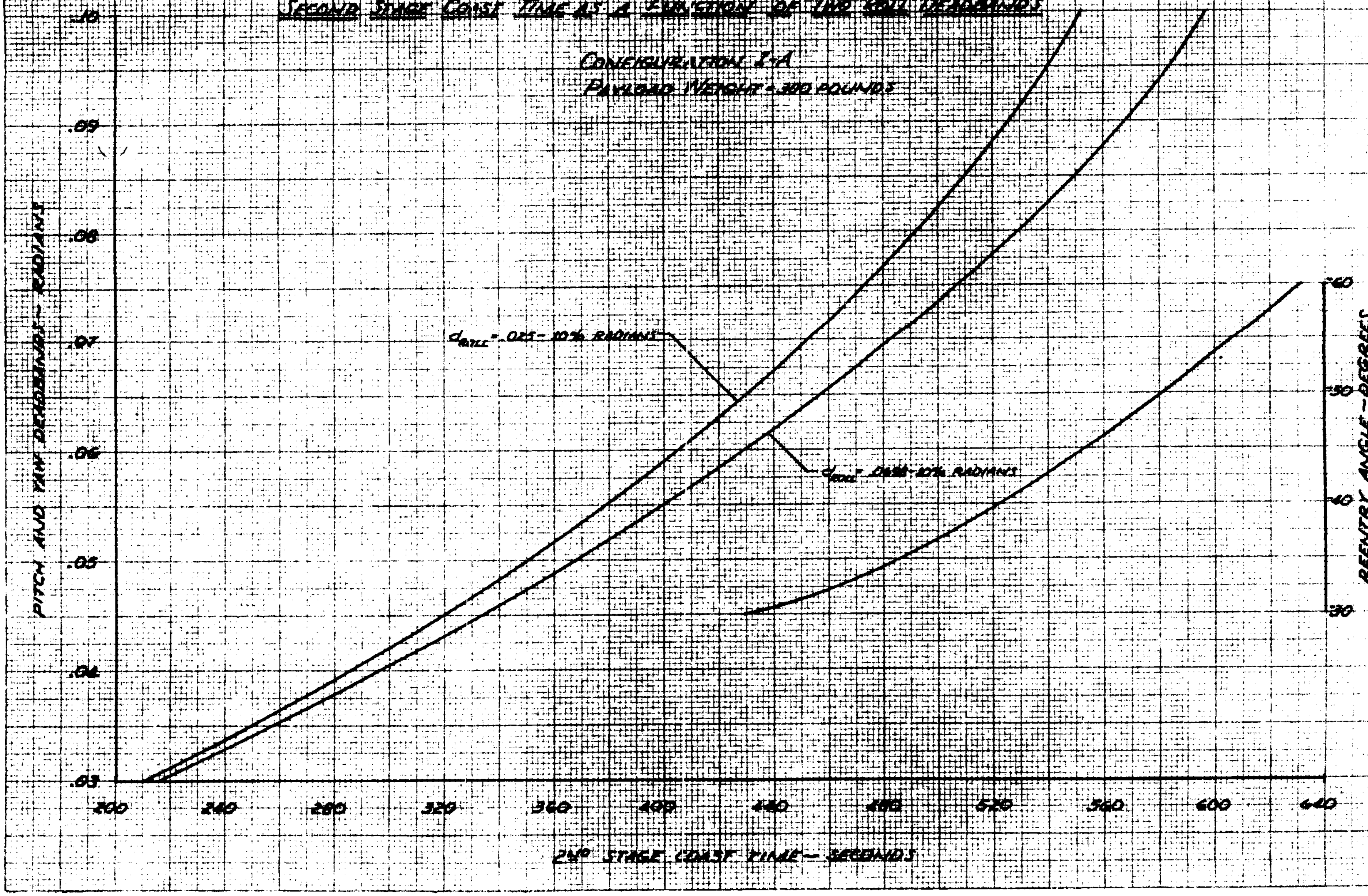

FIGURE 5.21
UNCONVENTIONAL VEHICLE - SPACECRAFT
THE VARIATION OF PITCH AND YAW DEADBANDS WITH REENTRY ANGLE AS A FUNCTION OF TWO ROLL DEADBANDS

CONFIGURATION I-A
SECOND STAGE COAST
PAYLOAD WEIGHT = 300 POUNDS

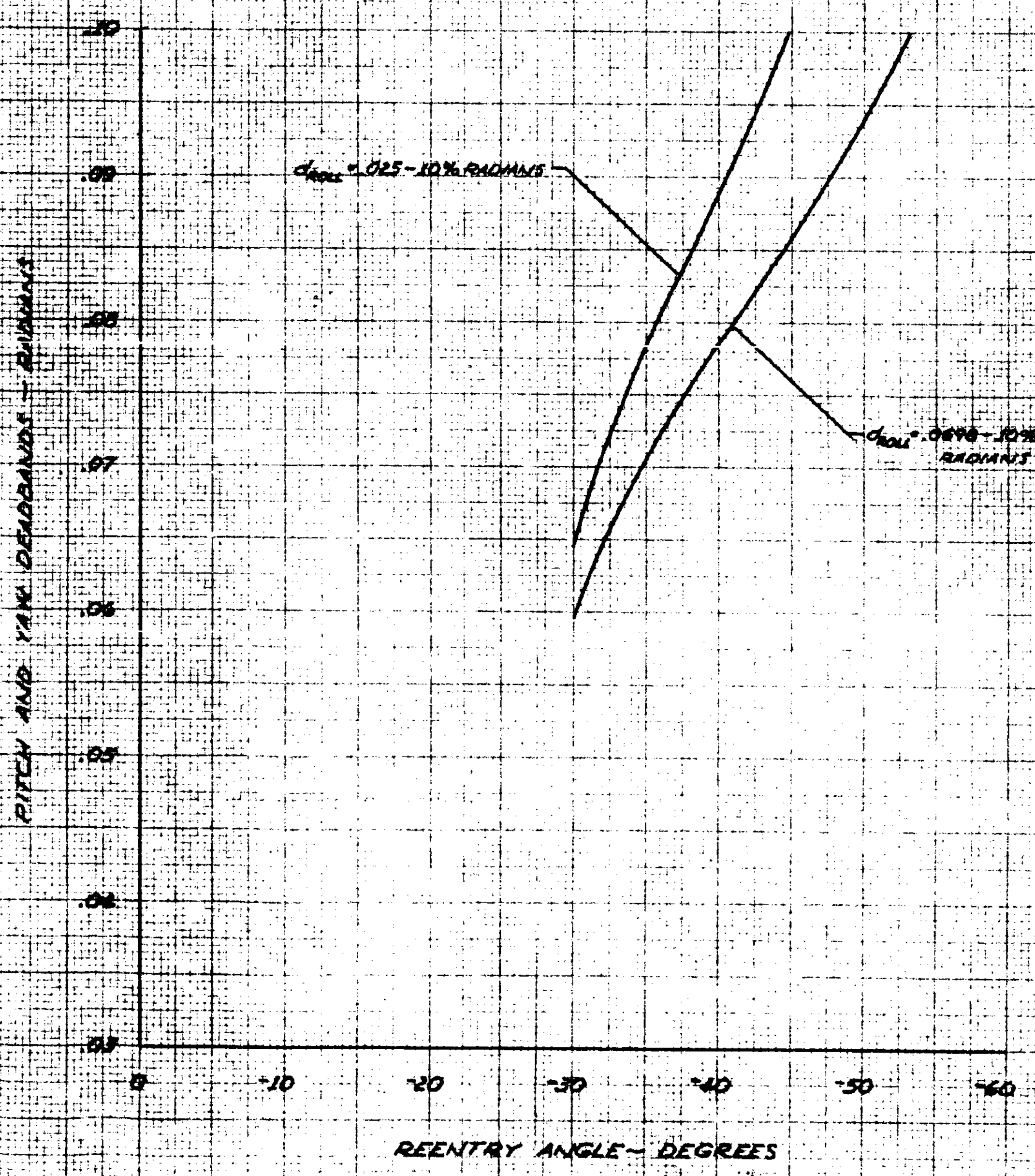

FIGURE 5.22

UNCONVENTIONAL VEHICLE - SPACECRAFT

THE VARIATION OF INCREMENTAL SECOND STAGE COAST TIME PER .025 DEGREES OF THRUST MISALIGNMENT ANGLE WITH PITCH AND YAW DEADBANDS AS A FUNCTION OF TWO ROLL DEADBANDS

CONFIGURATION I-A

PAYLOAD WEIGHT = 300 POUNDS

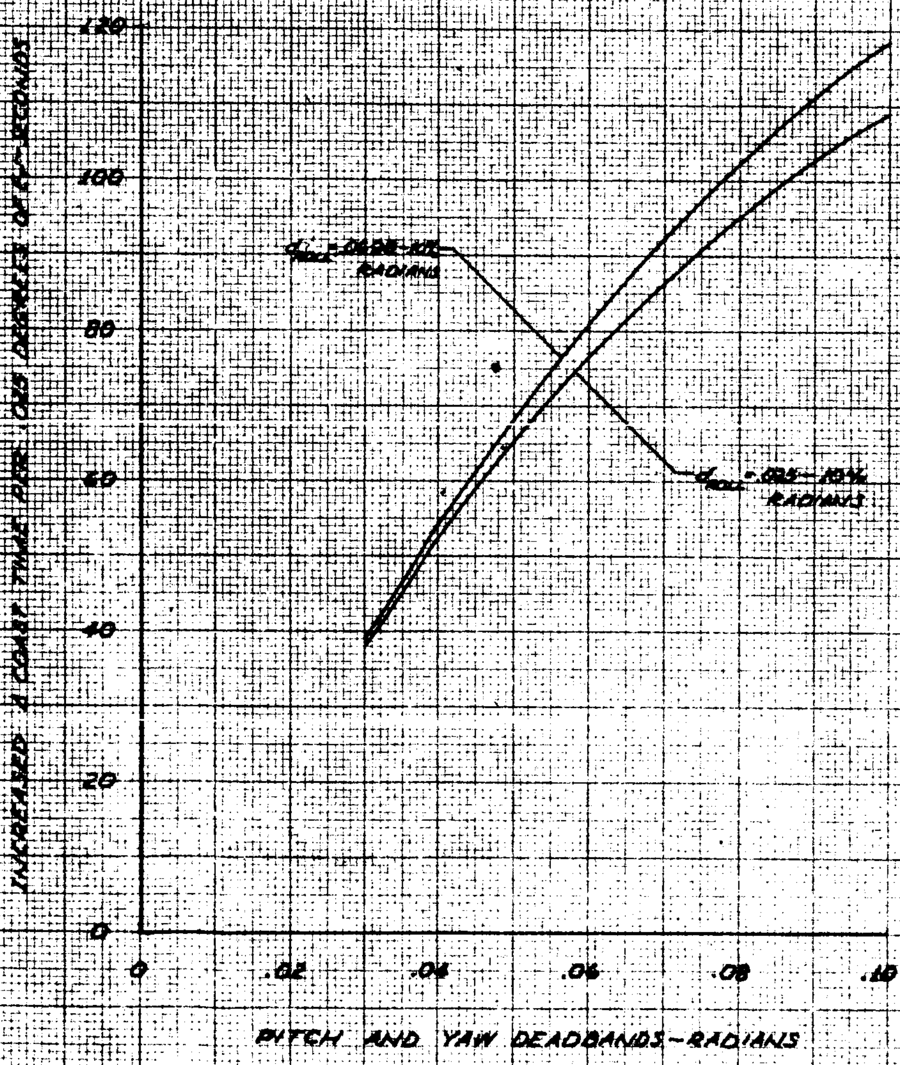

FIGURE 5.23

UNCONVENTIONAL VEHICLE – SPACECRAFT

THE VARIATION OF PITCH AND YAW DEADBANDS AND REENTRY ANGLE WITH SECOND STAGE COAST TIME AS A FUNCTION OF THRUST MISALIGNMENT ANGLE

CONFIGURATION I-A
PAYLOAD WEIGHT = 300 POUNDS
σ_{ROLL} = .025 – 10% RADIANS

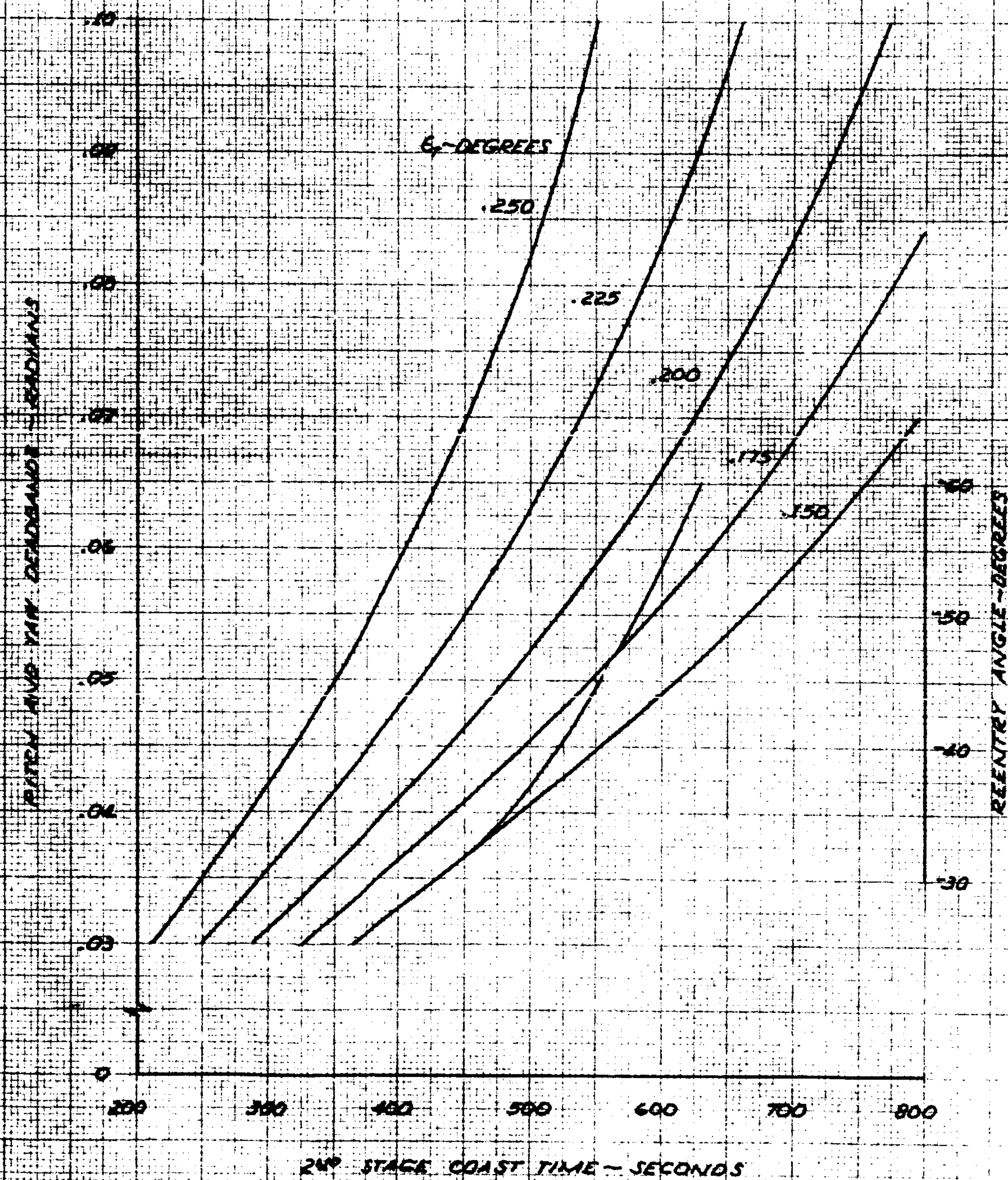

FIGURE 5.24
UNCONVENTIONAL VEHICLE - SPACECRAFT
THE VARIATION OF PITCH AND YAW DEADBANDS WITH REENTRY ANGLE AS A FUNCTION OF THRUST MISALIGNMENT ANGLE

CONFIGURATION I-A
SECOND STAGE COAST
PAYLOAD WEIGHT = 300 POUNDS
d_{ROLL} = .025 - 10% RADIANS

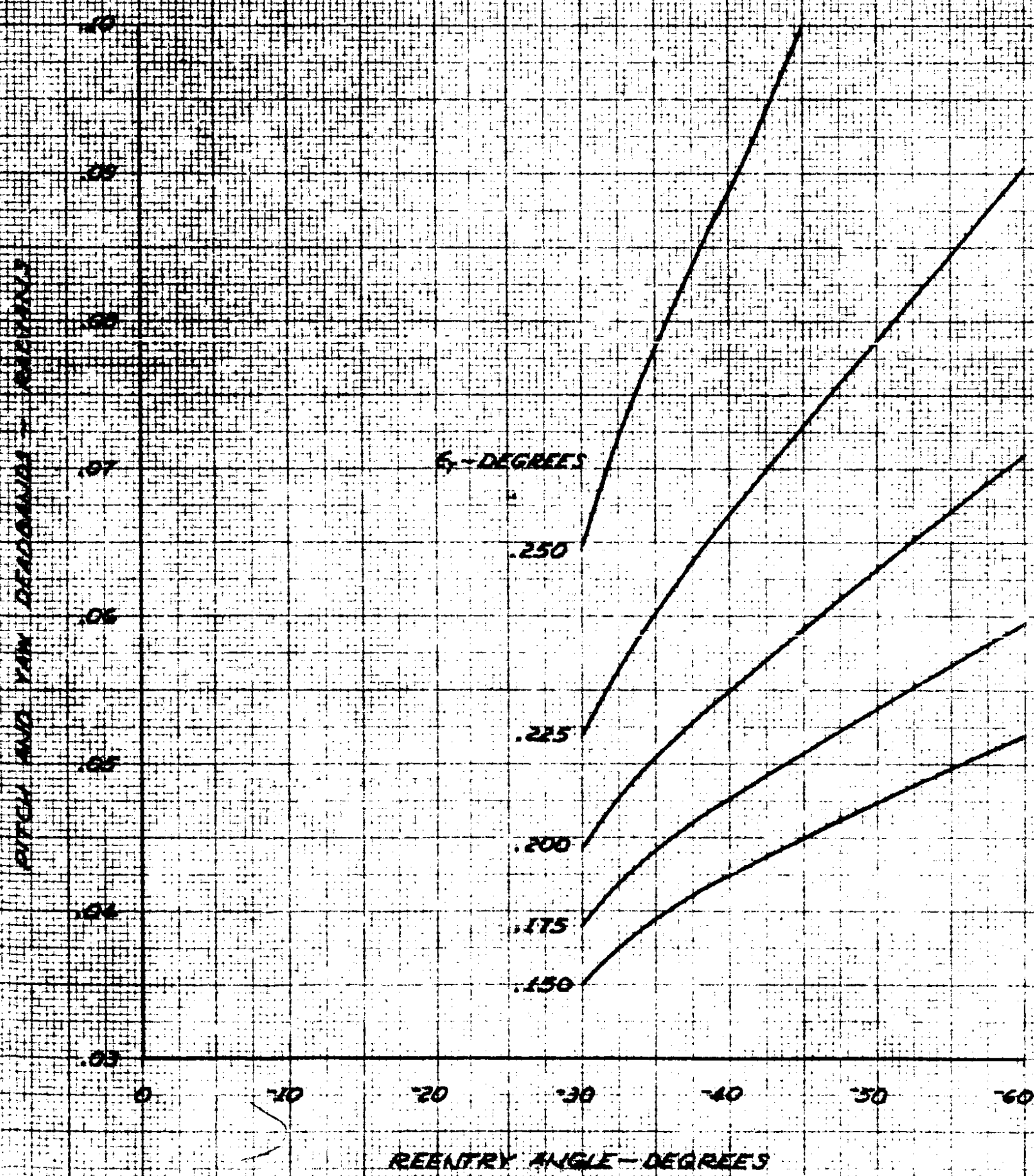

FIGURE 5.25

UNCONVENTIONAL VEHICLE - SPACECRAFT

THE VARIATION OF PITCH AND YAW DEADBANDS AND REENTRY ANGLE WITH SECOND STAGE COAST TIME AS A FUNCTION OF THRUST MISALIGNMENT ANGLE

CONFIGURATION I-A

PAYLOAD WEIGHT = 300 POUNDS

σ_{ROLL} = .0698 - 10% RADIANS

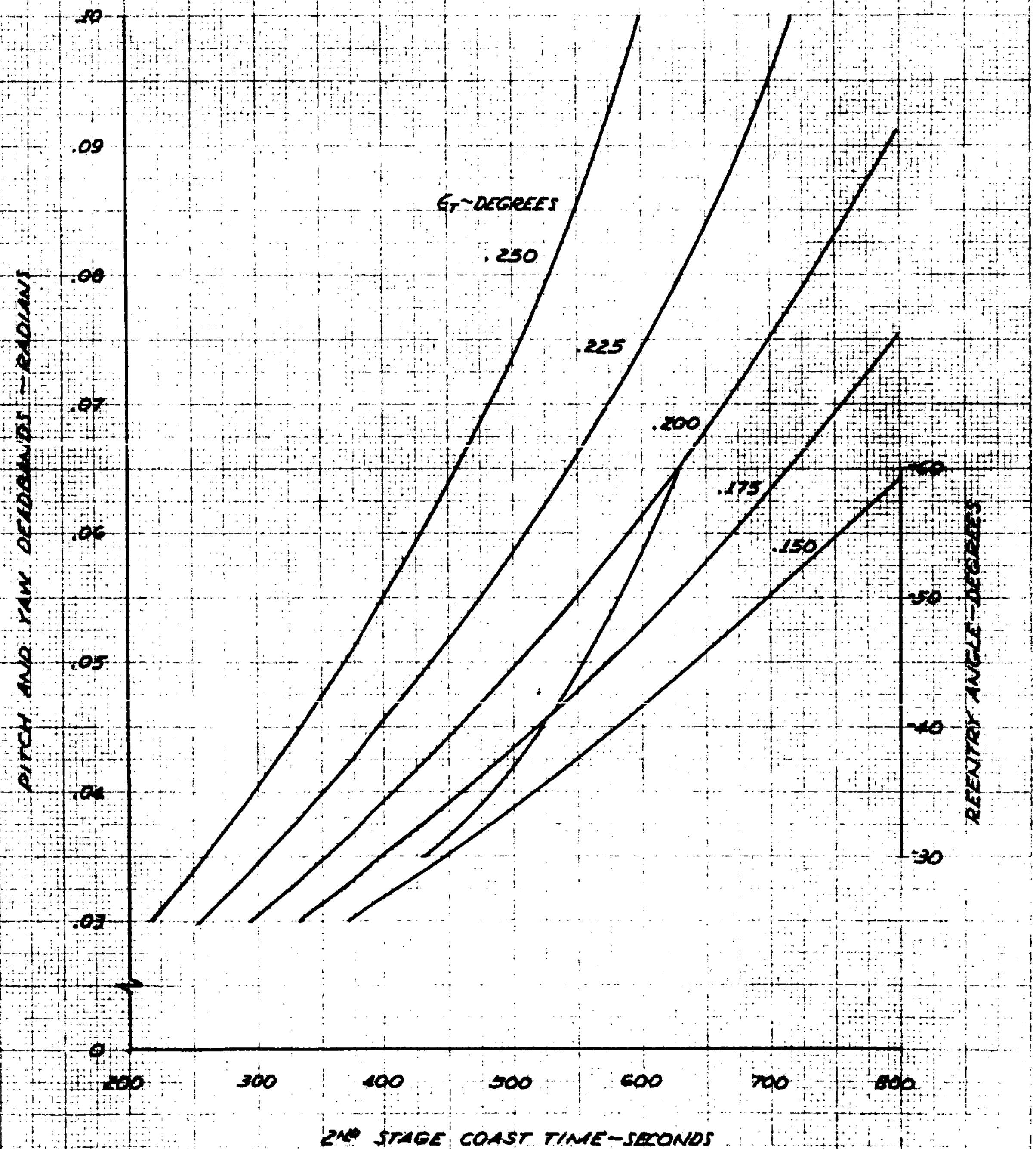

FIGURE 5.26
UNCONVENTIONAL VEHICLE- SPACECRAFT
THE VARIATION OF PITCH AND YAW DEADBANDS
WITH REENTRY ANGLE AS A FUNCTION OF
THRUST MISALIGNMENT ANGLE

CONFIGURATION I-A
SECOND STAGE COAST
PAYLOAD WEIGHT = 300 POUNDS
σ_{ROLL} = .0698 - 10% RADIANS

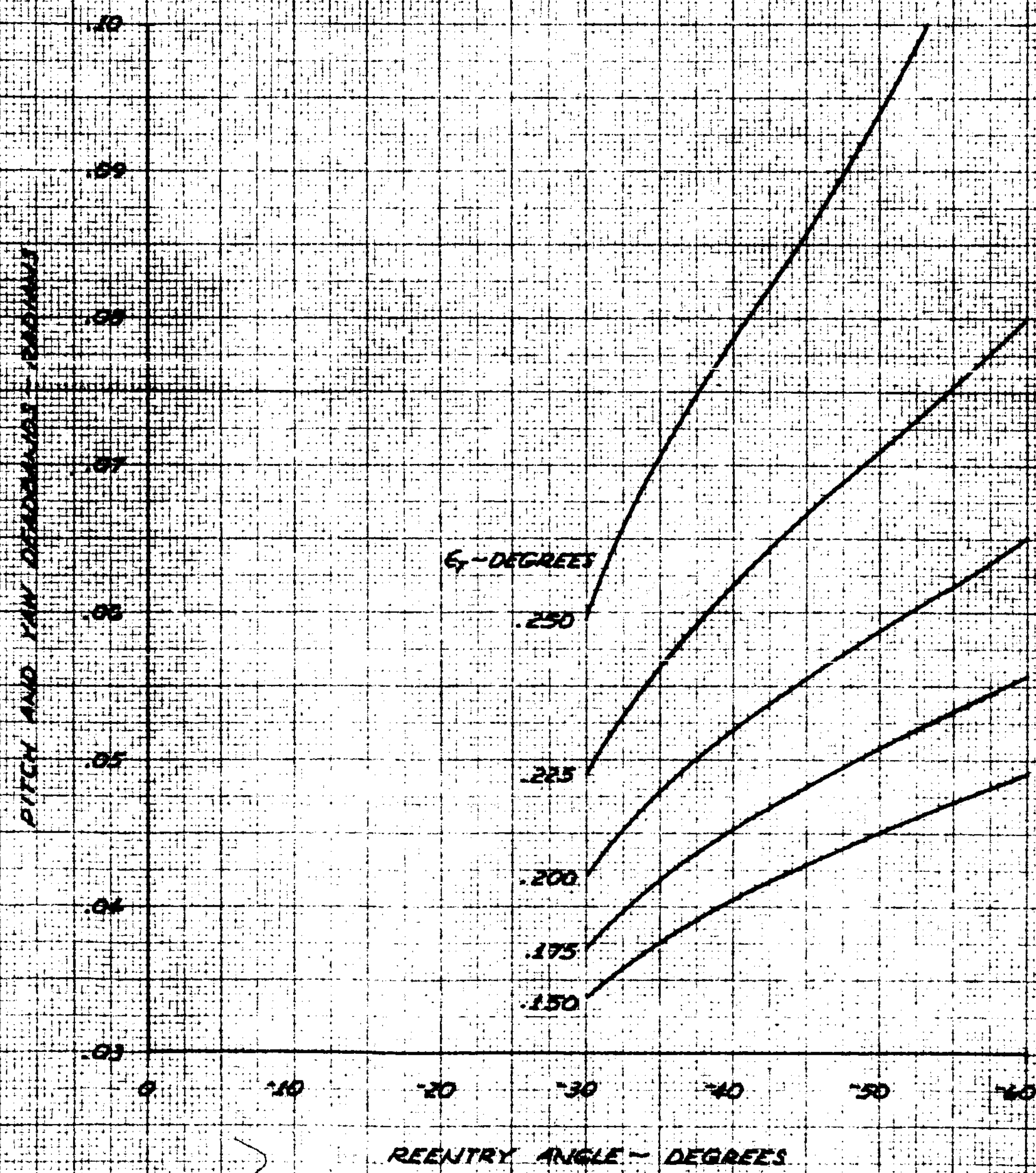

FIGURE 5.27
UNCONVENTIONAL VEHICLE - SPACECRAFT
THE VARIATION OF CAPTURE ANGLE WITH
PAYLOAD WEIGHT AT SECOND STAGE IGNITION

CONFIGURATION II-A-2

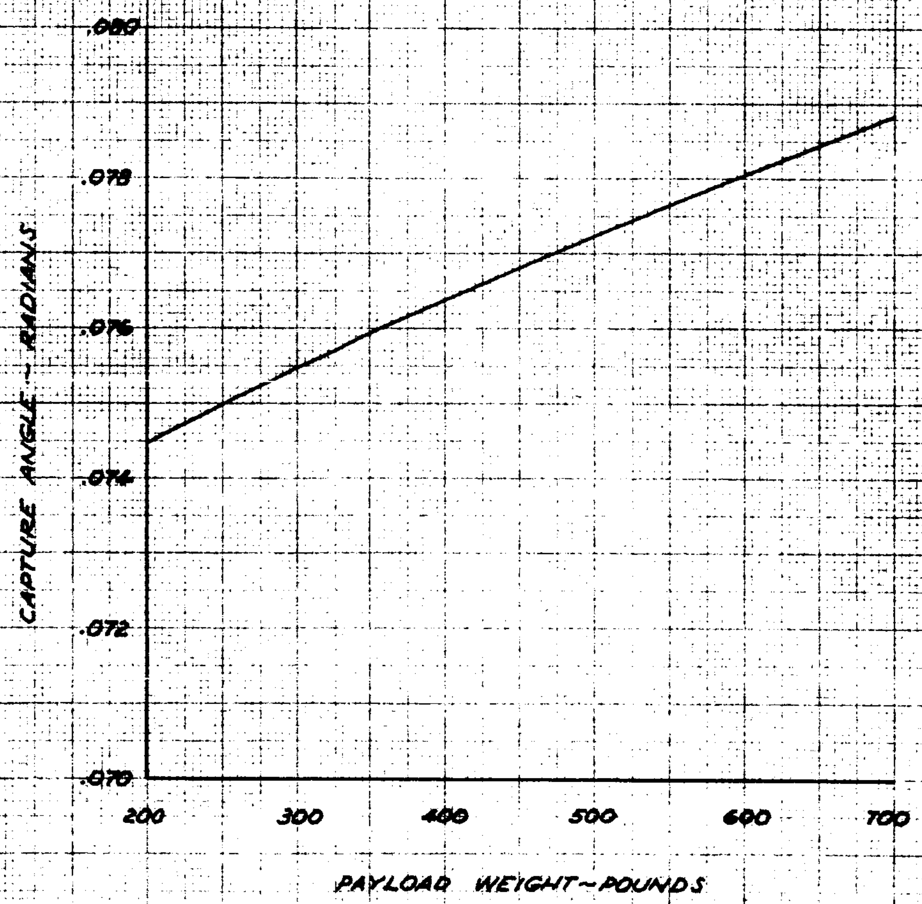

FIGURE 5.28
UNCONVENTIONAL VEHICLE - SPACECRAFT
SECOND STAGE IGNITION CAPTURE MANEUVER

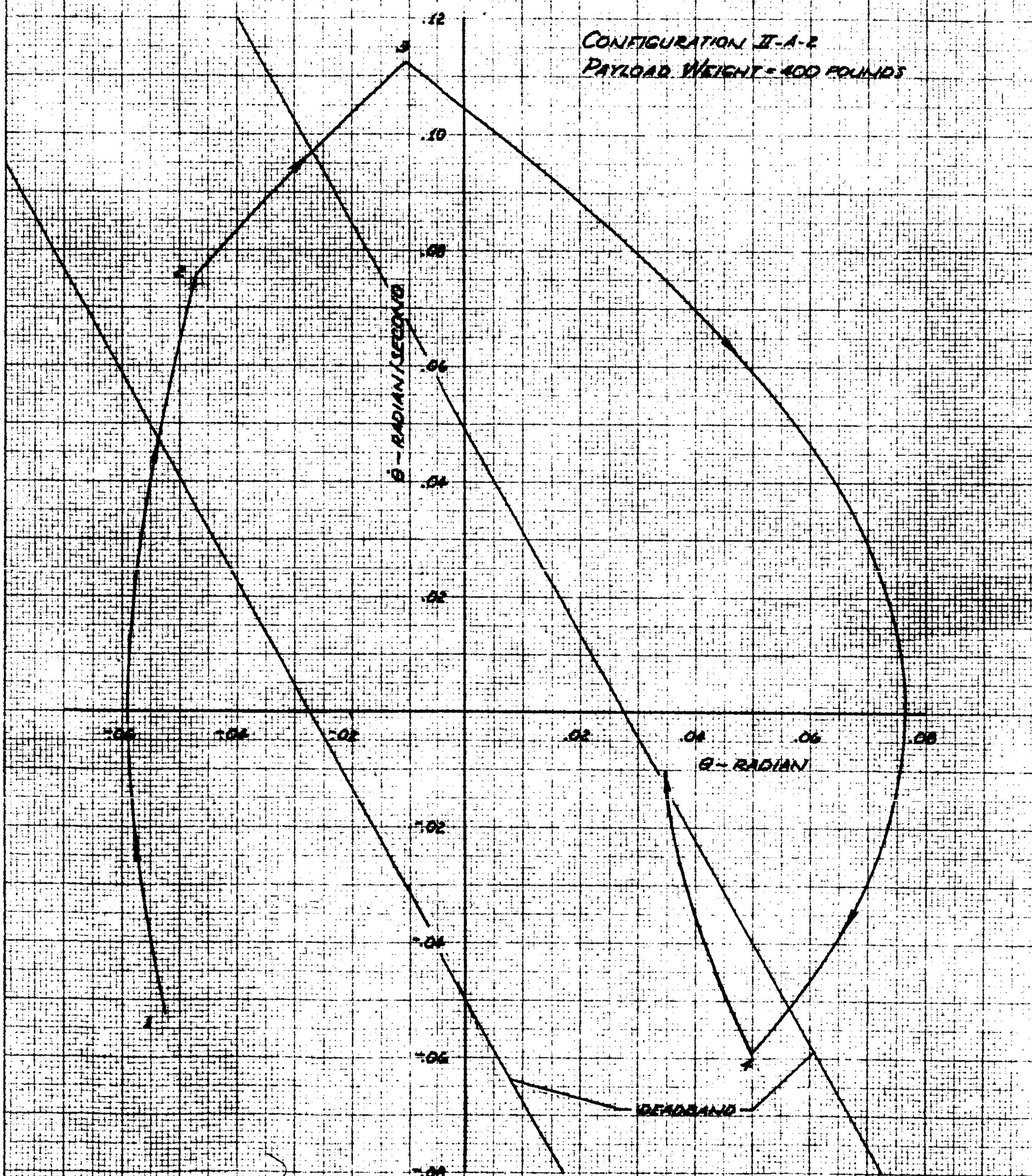

FIGURE 5.29
UNCONVENTIONAL VEHICLE - SPACECRAFT
SECOND STAGE IGNITION CAPTURE MANEUVER

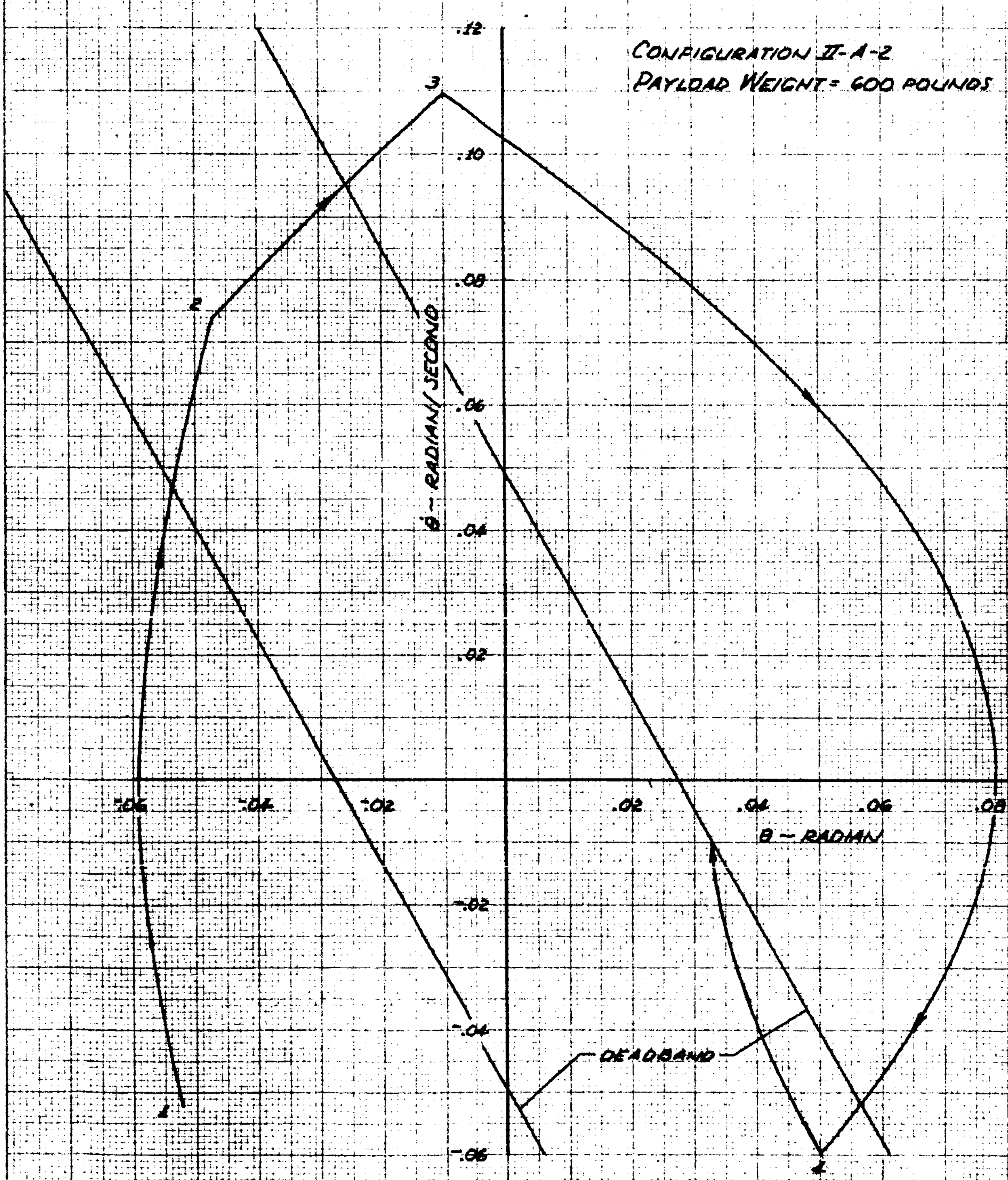

FIGURE 5.30
UNCONVENTIONAL VEHICLE - SPACECRAFT
THE VARIATION OF SECOND STAGE IGNITION CAPTURE
AND MOTOR-ON TIME WITH PAYLOAD WEIGHT

CONFIGURATION II-A-2

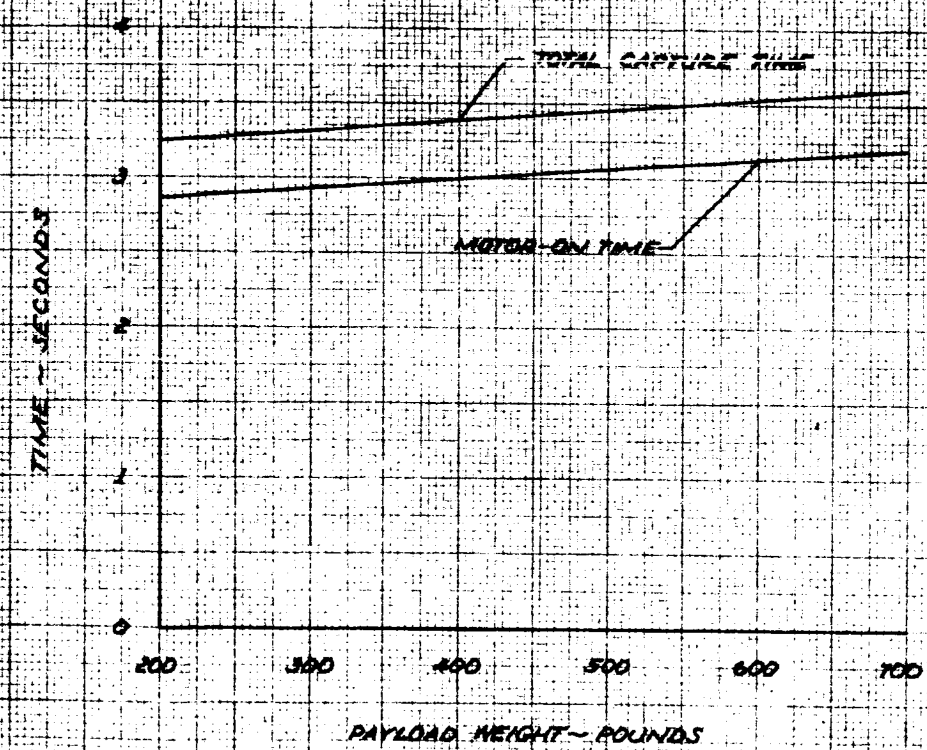

FIGURE 5.31
UNCONVENTIONAL VEHICLE - SPACECRAFT
THE VARIATION OF SECOND STAGE IGNITION
CAPTURE MANEUVER HYDROGEN PEROXIDE
CONSUMPTION WITH PAYLOAD WEIGHT

CONFIGURATION II-A-2

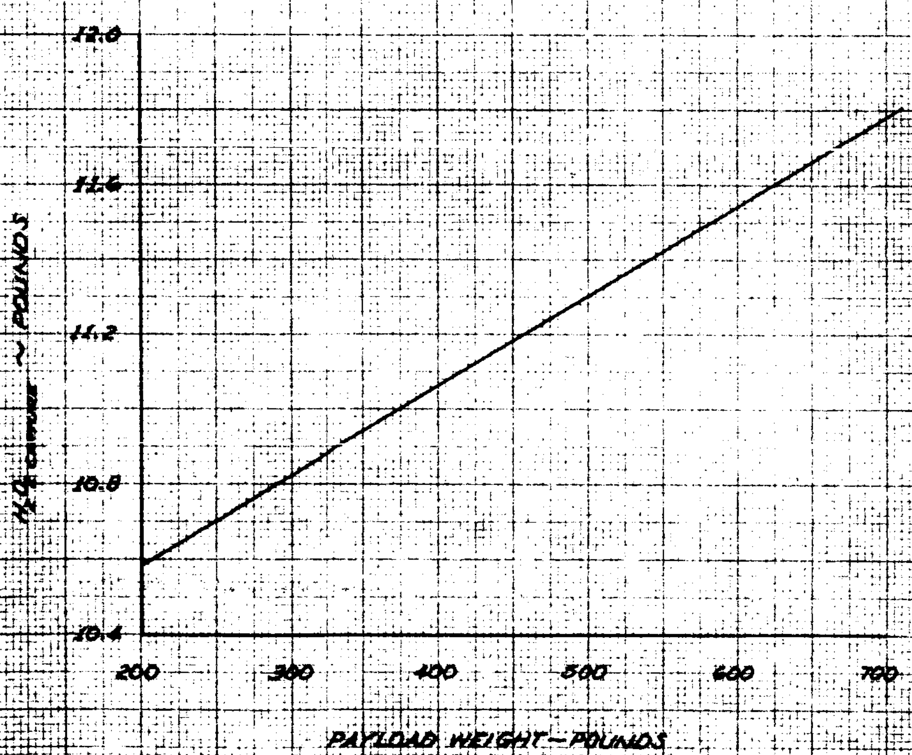

FIGURE 5.32
UNCONVENTIONAL VEHICLE - SPACECRAFT
SECOND STAGE COAST DEADBAND REDUCTION CAPTURE MANEUVER

CONFIGURATION II-A-2
SECOND STAGE COAST
PAYLOAD WEIGHT = 300 POUNDS

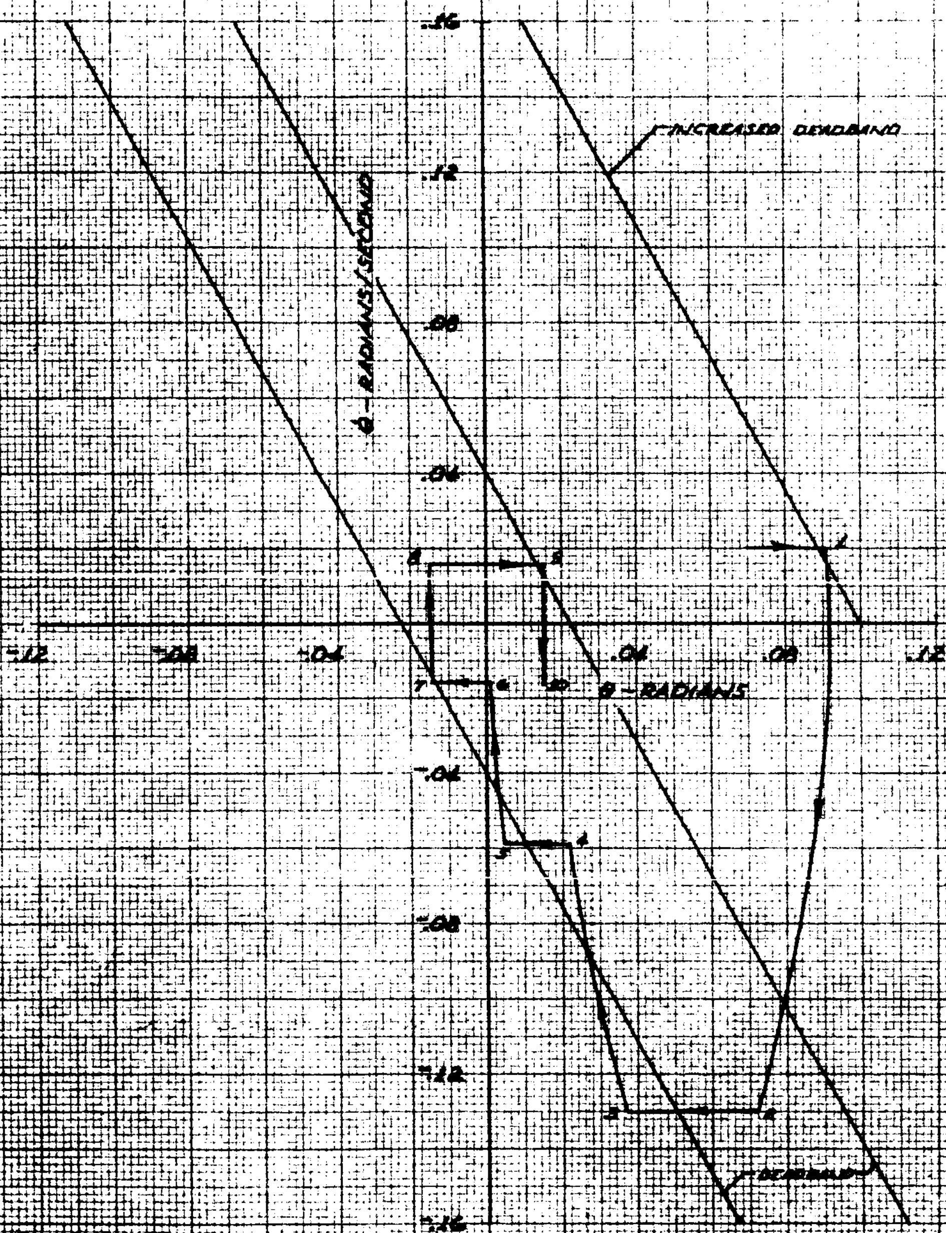

FIGURE 5.33
UNCONVENTIONAL VEHICLE - SPACECRAFT
SECOND STAGE COAST DEADBAND REDUCTION CAPTURE MANEUVER

CONFIGURATION II-A-2
SECOND STAGE COAST
PAYLOAD WEIGHT = 600 POUNDS

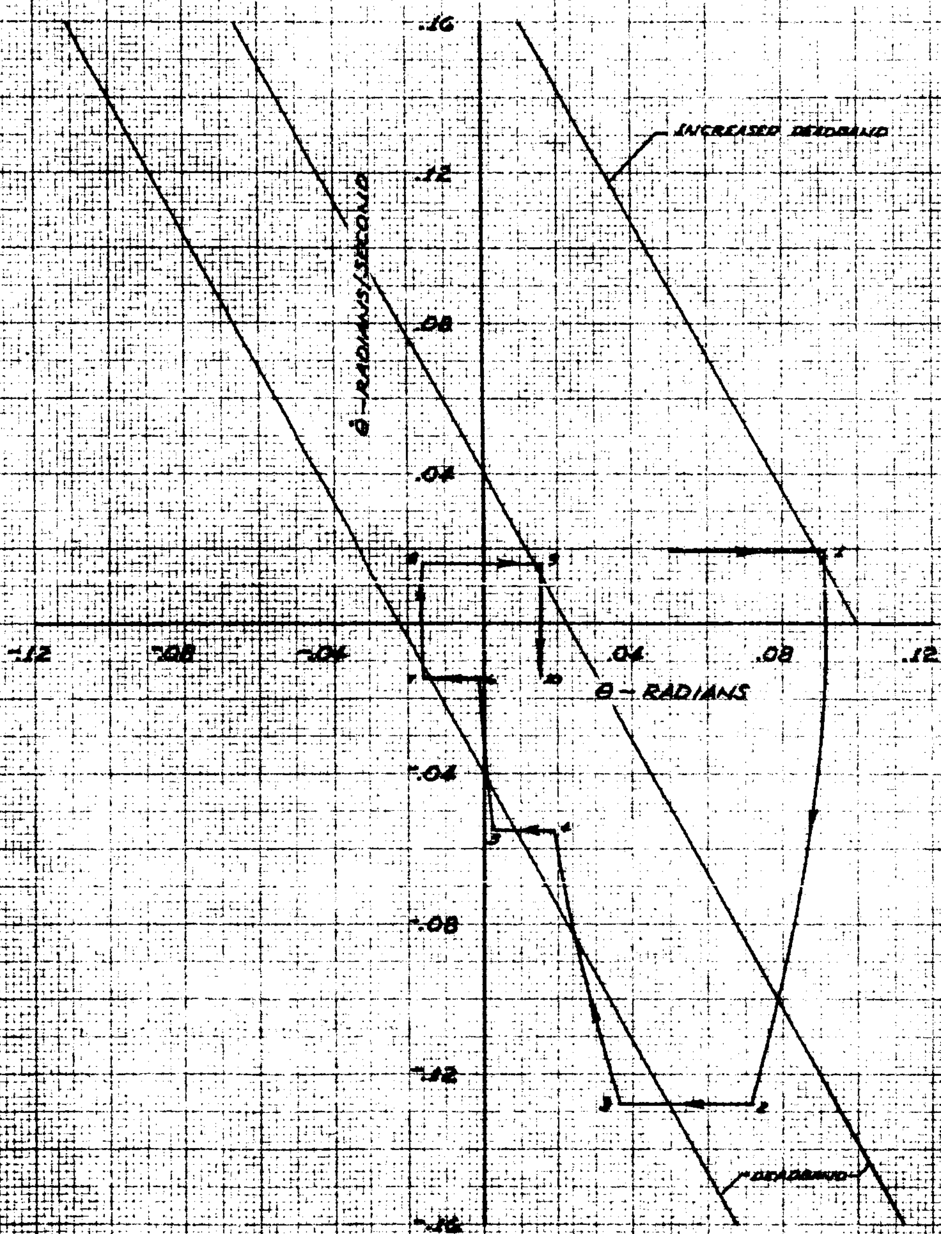

FIGURE 5.34
UNCONVENTIONAL VEHICLE - SPACECRAFT
THE VARIATION OF DEADBAND REDUCTION TIME WITH PAYLOAD WEIGHT AND INCREASED DEADBAND

CONFIGURATION II-A-2
SECOND STAGE COAST

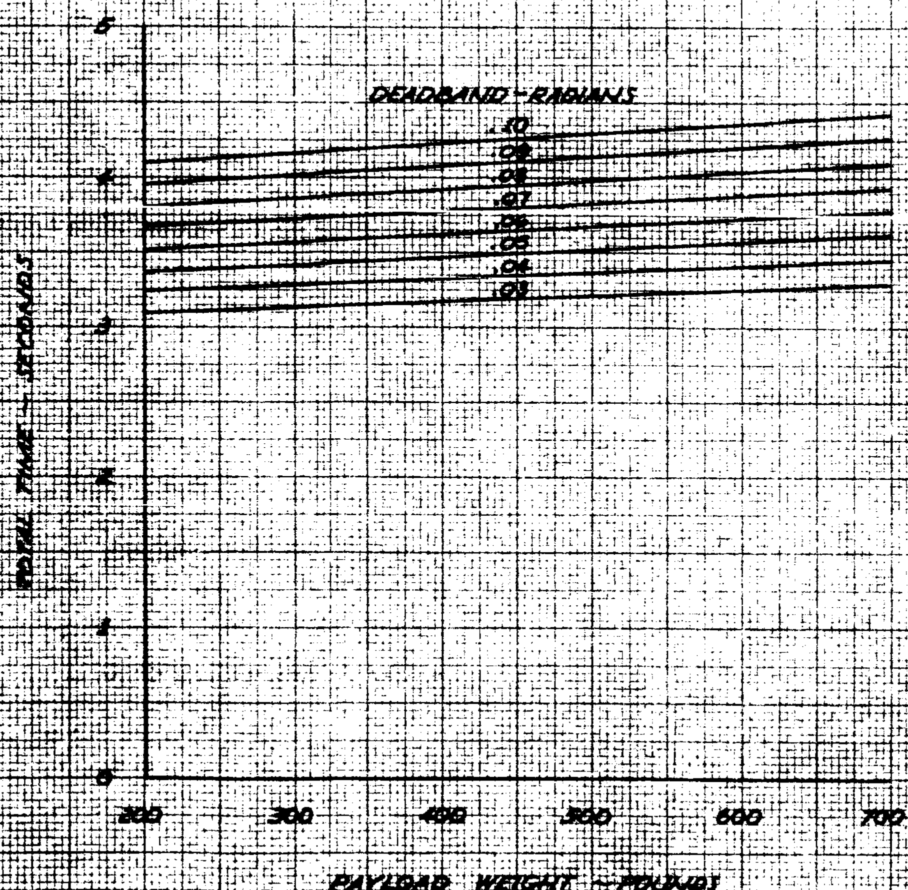

FIGURE 5.35
UNCONVENTIONAL VEHICLE - SPACECRAFT
THE VARIATION OF DEADBAND REDUCTION MOTOR-ON TIME WITH PAYLOAD WEIGHT AND INCREASED DEADBAND

CONFIGURATION II-A-2
SECOND STAGE COAST

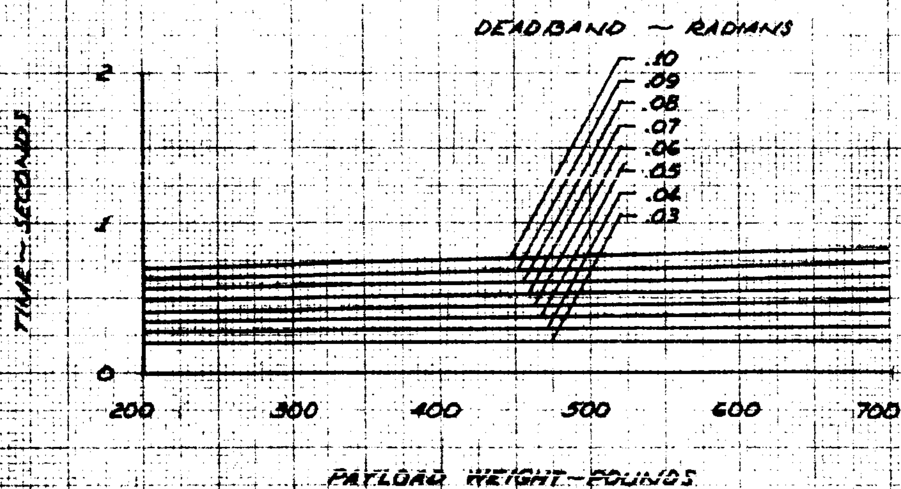

FIGURE 5.36

UNCONVENTIONAL VEHICLE - SPACECRAFT

THE VARIATION OF DEADBAND REDUCTION HYDROGEN PEROXIDE CONSUMPTION WITH PAYLOAD WEIGHT AND INCREASED DEADBAND

CONFIGURATION II-A-2

SECOND STAGE COAST

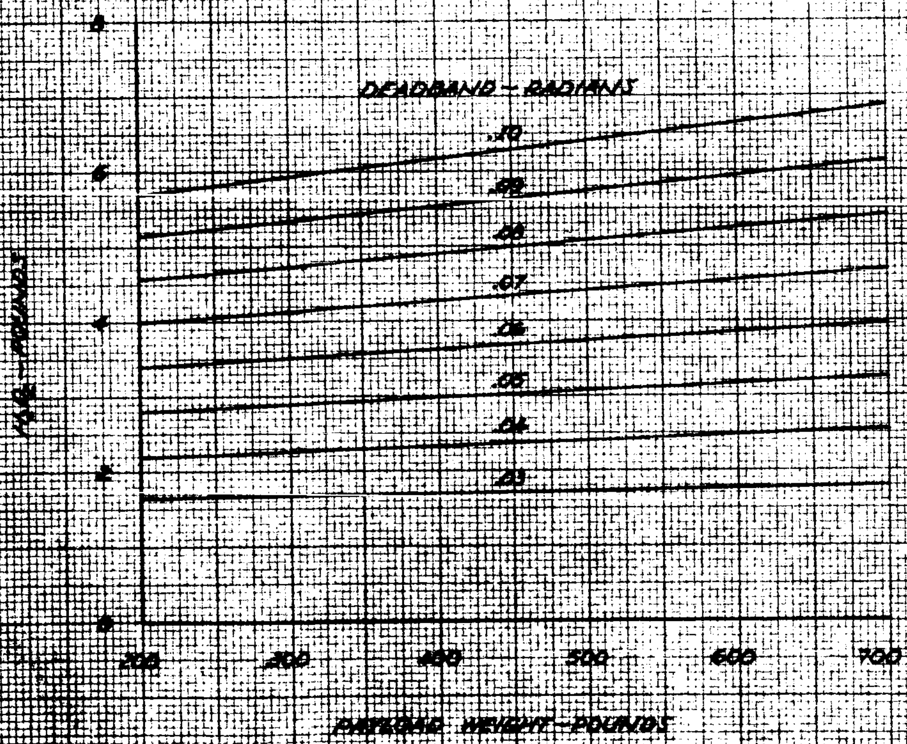

FIGURE 5.37
UNCONVENTIONAL VEHICLE - SPACECRAFT
THE VARIATION OF PITCH AND YAW DUTY CYCLE WITH
INCREASED DEADBAND AS A FUNCTION OF PAYLOAD WEIGHT

CONFIGURATION II-A-2
SECOND STAGE COAST

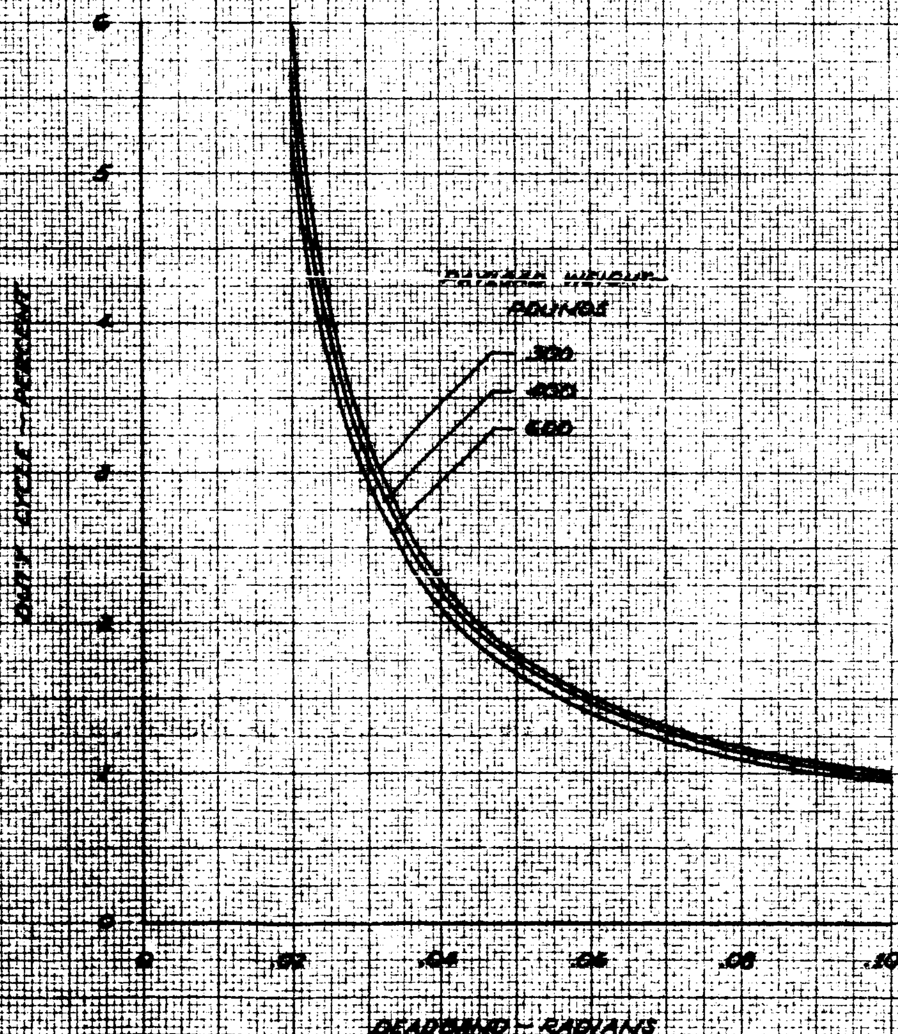

FIGURE 5.38
UNCONVENTIONAL VEHICLE - SPACECRAFT
THE VARIATION OF ROLL DUTY CYCLE WITH INCREASED DEADBAND AS A FUNCTION OF PAYLOAD WEIGHT

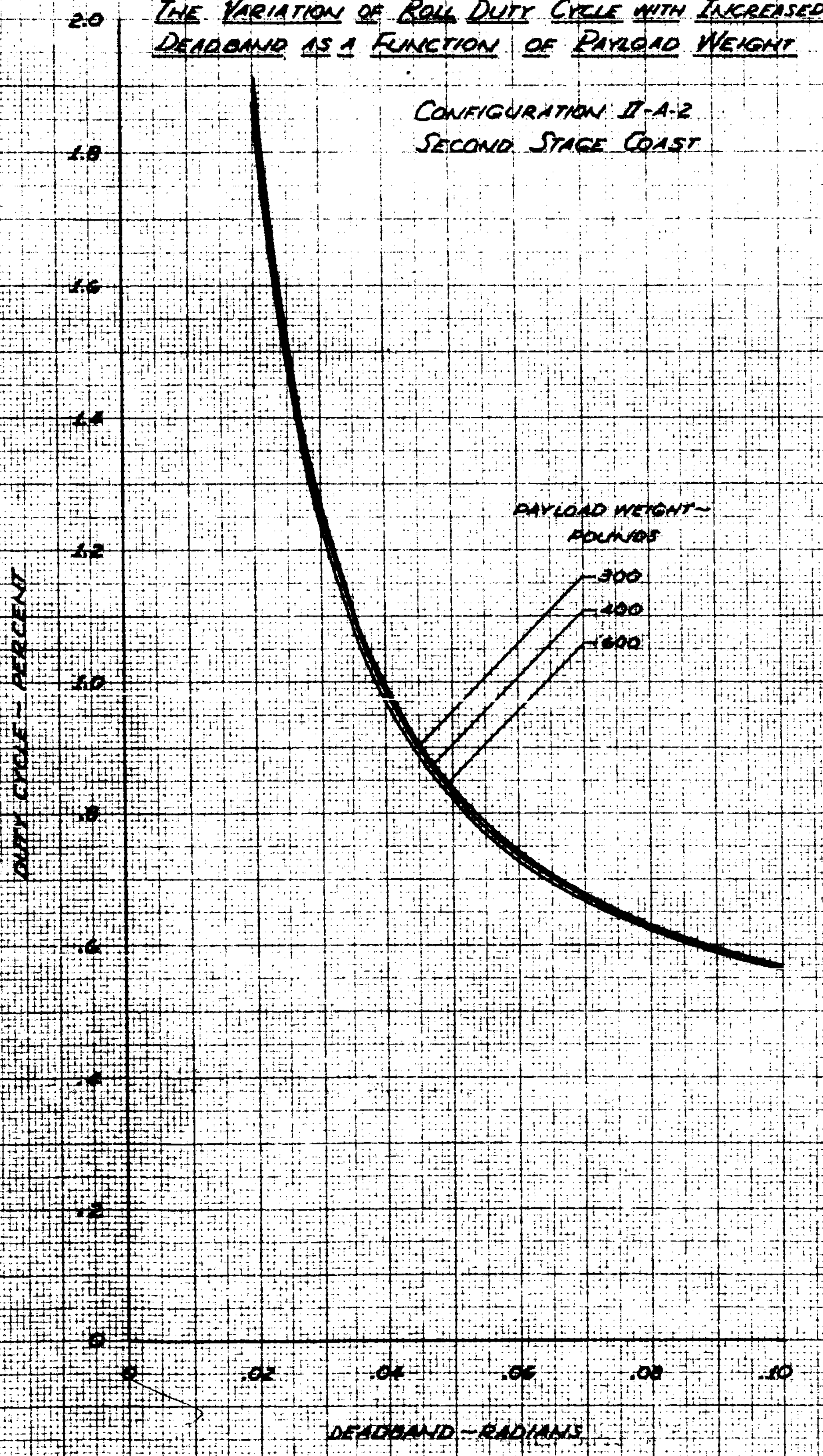

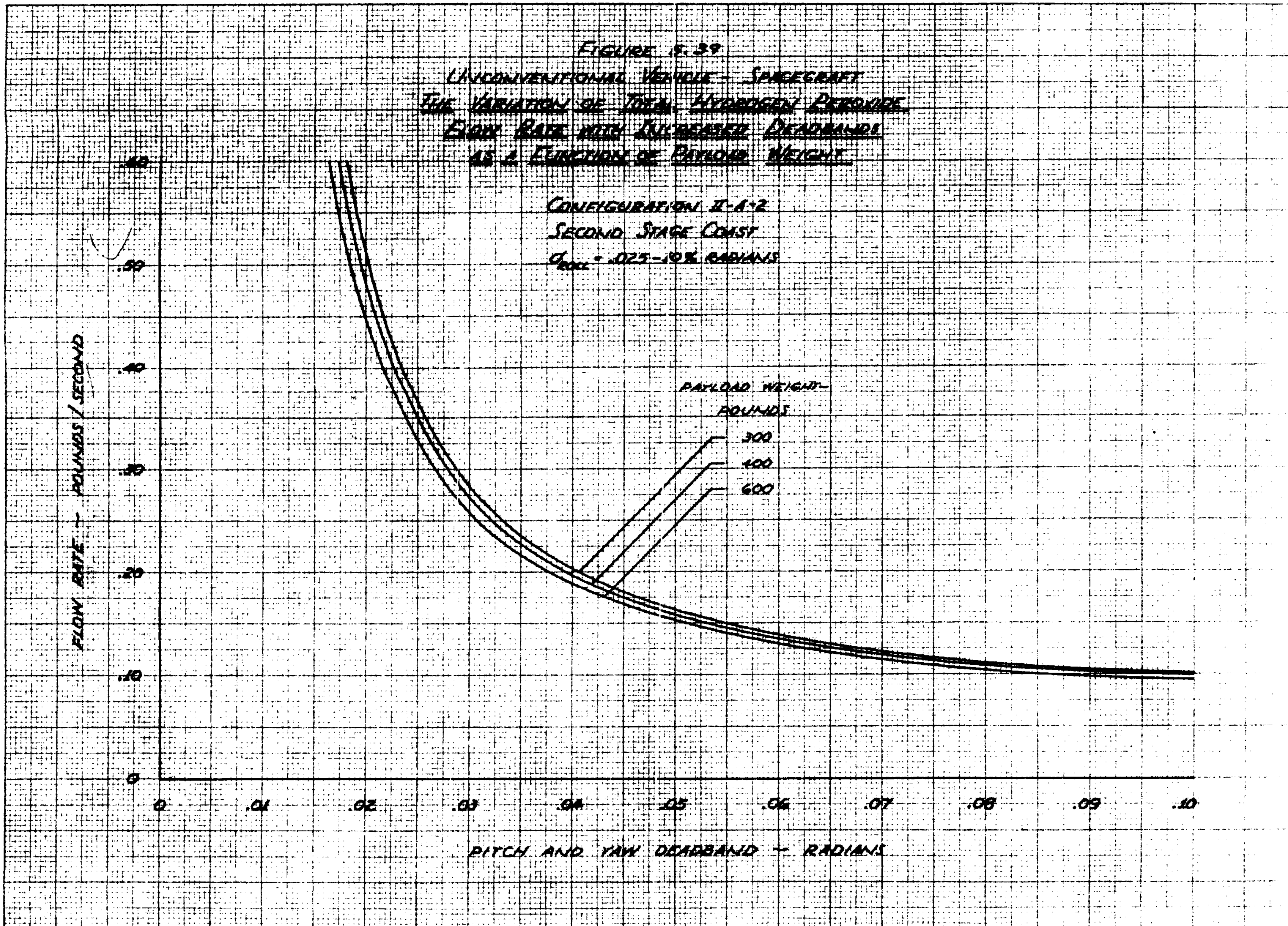

Figure 5.39
Unconventional Vehicle — Spacecraft
The Variation of Total Hydrogen Peroxide
Flow Rate with Increased Deadbands
As a Function of Payload Weight

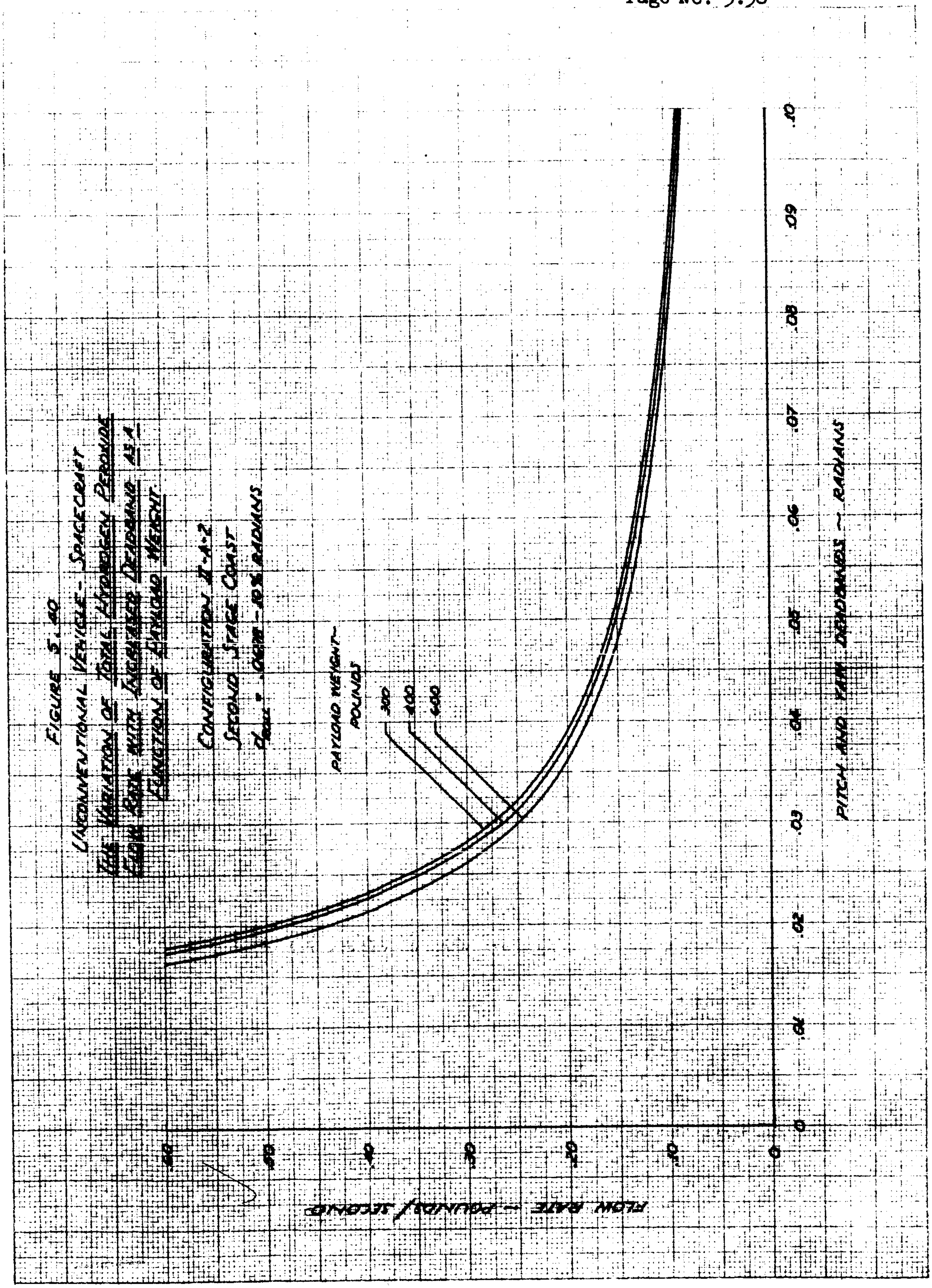
FIGURE 5.40
UNCONVENTIONAL VEHICLE - SPACECRAFT
THE VARIATION OF TOTAL HYDROGEN PEROXIDE
FLOW RATE WITH INCREASED DEADBAND AS A
FUNCTION OF PAYLOAD WEIGHT
CONFIGURATION II-A-2
SECOND STAGE COAST
ROLL = .0698-.105 RADIANS
PAYLOAD WEIGHT ~
POUNDS
300
400
600
0
.01
.02
.03
.04
.05
.06
.07
.08
.09
.10
PITCH AND YAW DEADBANDS ~ RADIANS
0
.10
.20
.30
.40
.50
.60
FLOW RATE — POUNDS/SECOND

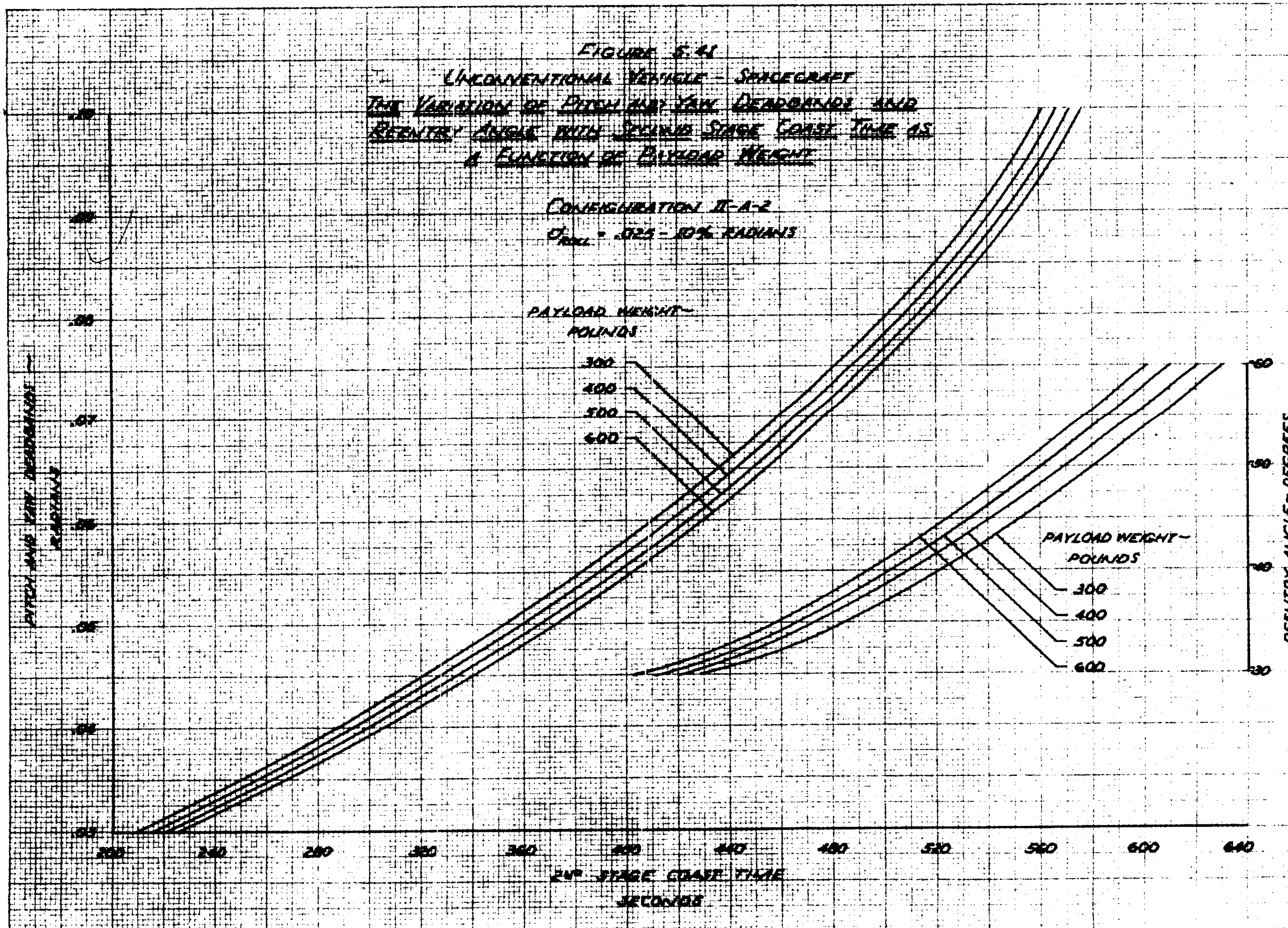

FIGURE 5.41
UNCONVENTIONAL VEHICLE - SPACECRAFT
THE VARIATION OF PITCH AND YAW DEADBANDS AND
REENTRY ANGLE WITH SECOND STAGE COAST TIME AS
A FUNCTION OF PAYLOAD WEIGHT

CONFIGURATION II-A-2
σ_{ROLL} = .025 - 10% RADIANS

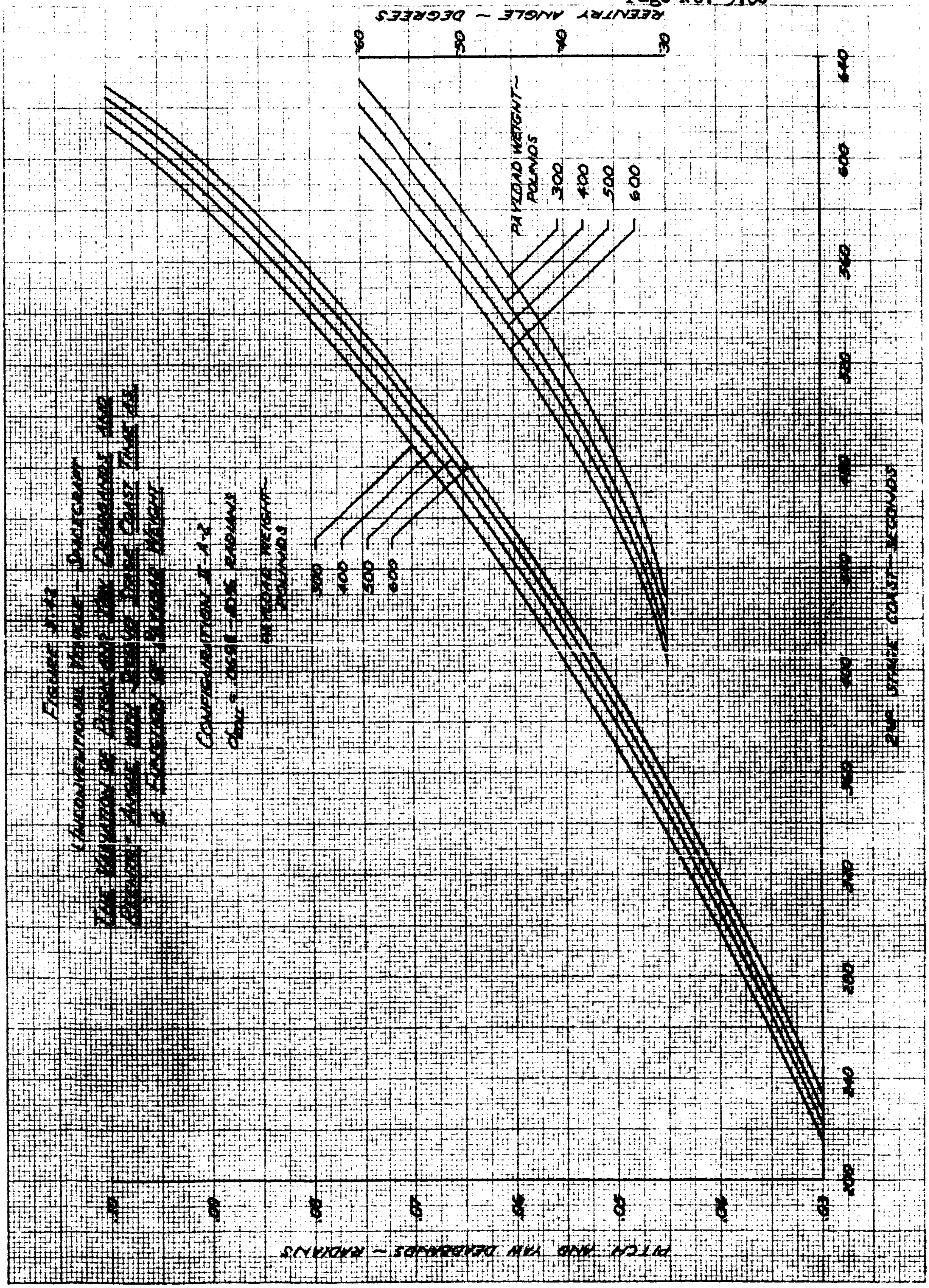
CONFIGURATION II-A-2
PAYLOAD WEIGHT ~ POUNDS
300
400
500
600
REENTRY ANGLE ~ DEGREES
30
40
50
60
PITCH AND YAW DEADBANDS ~ RADIANS
.03
.04
.05
.06
.07
.08
.09
.10
2ND STAGE COAST—SECONDS
200
240
280
320
360
400
440
480
520
560
600
640

FIGURE 5.43
UNCONVENTIONAL VEHICLE - SPACECRAFT
THE VARIATION OF PITCH AND YAW DEADBANDS
WITH REENTRY ANGLE AS A FUNCTION OF
PAYLOAD WEIGHT

CONFIGURATION II-A-2
SECOND STAGE COAST
σ_{ROLL} = .025 - 10% RADIANS

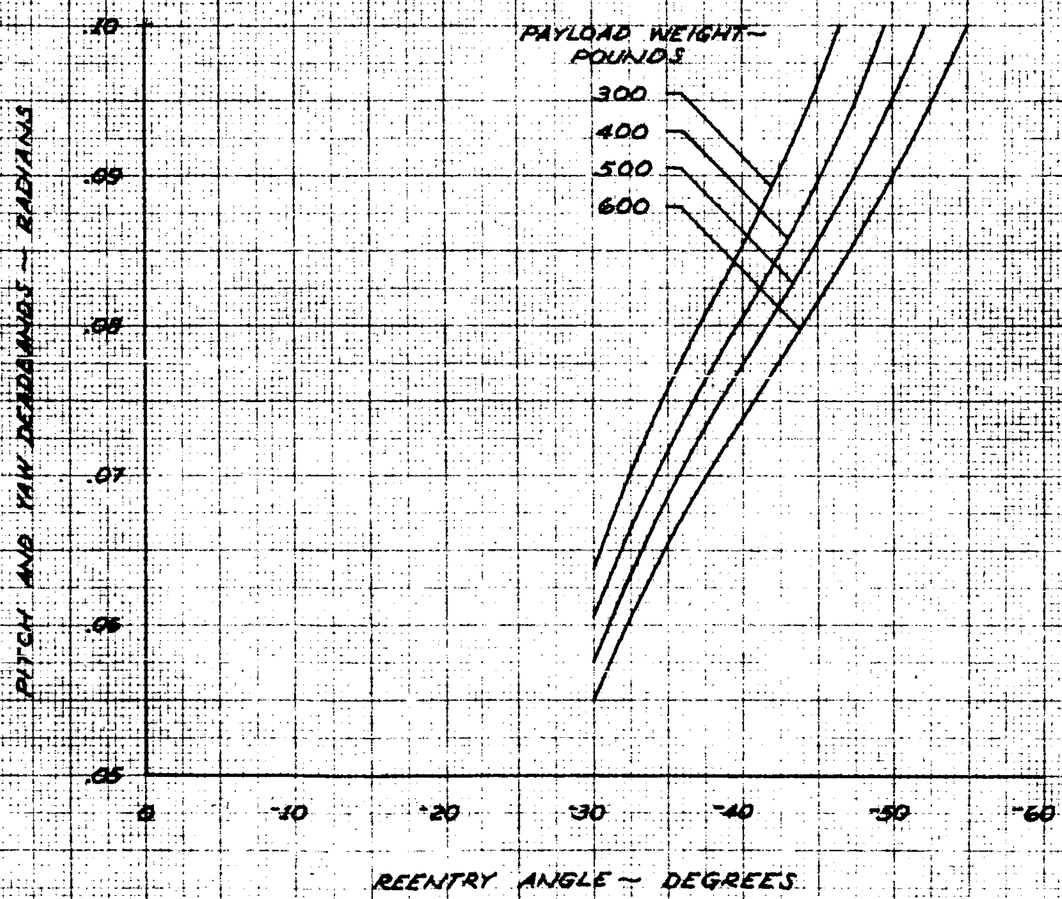

FIGURE 5.44

UNCONVENTIONAL VEHICLE - SPACECRAFT
THE VARIATION OF PITCH AND YAW DEADBANDS
WITH REENTRY ANGLE AS A FUNCTION OF
PAYLOAD WEIGHT

CONFIGURATION II-A-2
SECOND STAGE COAST
σ_{ROLL} = .0698 - 10% RADIANS

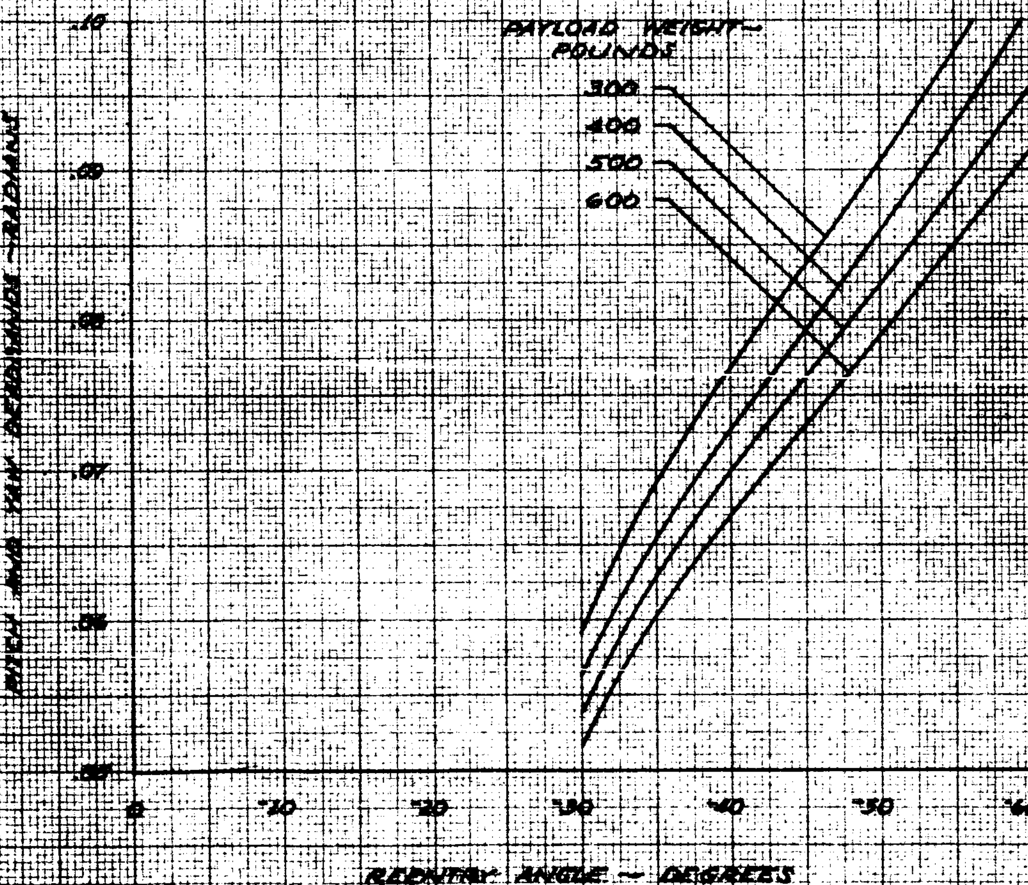

FIGURE 5.45

UNCONVENTIONAL VEHICLE – SPACECRAFT

THE VARIATION OF INCREMENTAL SECOND STAGE COAST TIME PER .025 DEGREES OF THRUST MISALIGNMENT ANGLE WITH PITCH AND YAW DEADBANDS AS A FUNCTION OF PAYLOAD WEIGHT

CONFIGURATION II-A-2

α_{ROLL} = .025 – 10% RADIANS

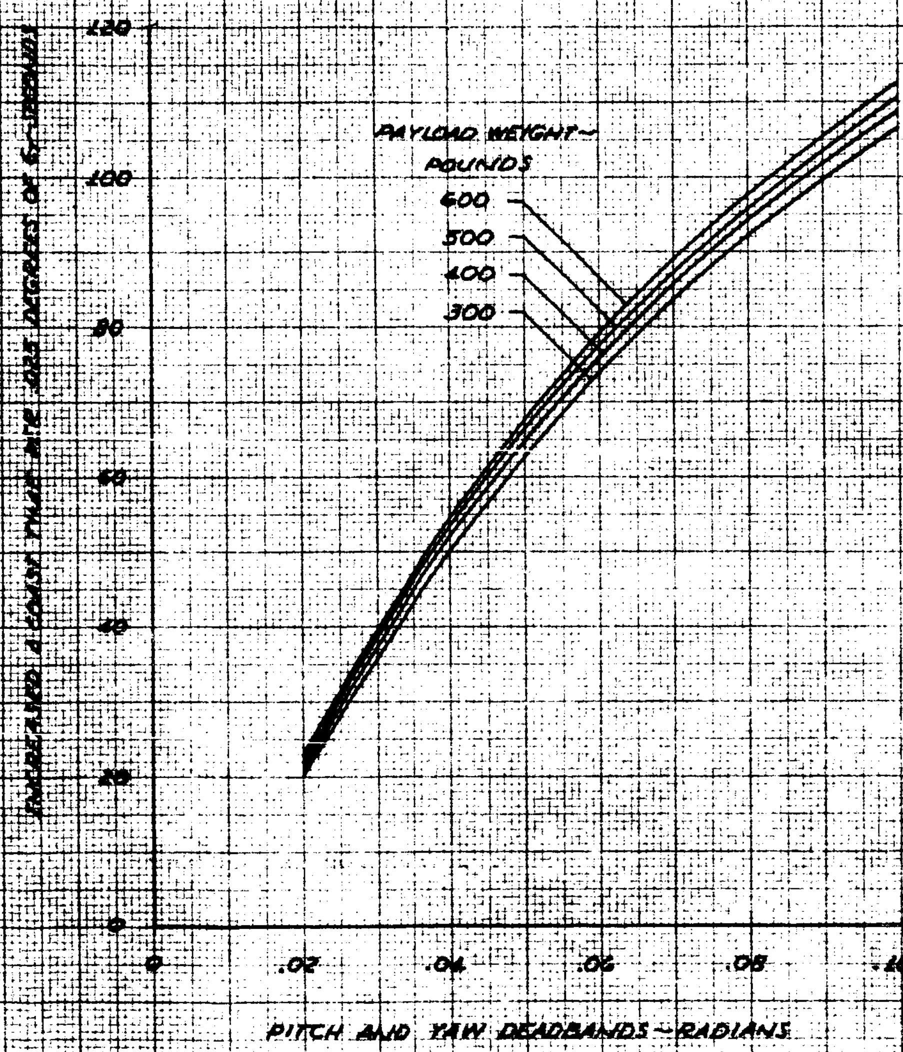

FIGURE 5.46

UNCONVENTIONAL VEHICLE - SPACECRAFT

THE VARIATION OF PITCH AND YAW DEADBANDS AND REENTRY ANGLE WITH SECOND STAGE COAST TIME AS A FUNCTION OF THRUST MISALIGNMENT ANGLE

CONFIGURATION II-A-2

PAYLOAD WEIGHT = 300 POUNDS

α_{ROLL} = .025 - 10% RADIANS

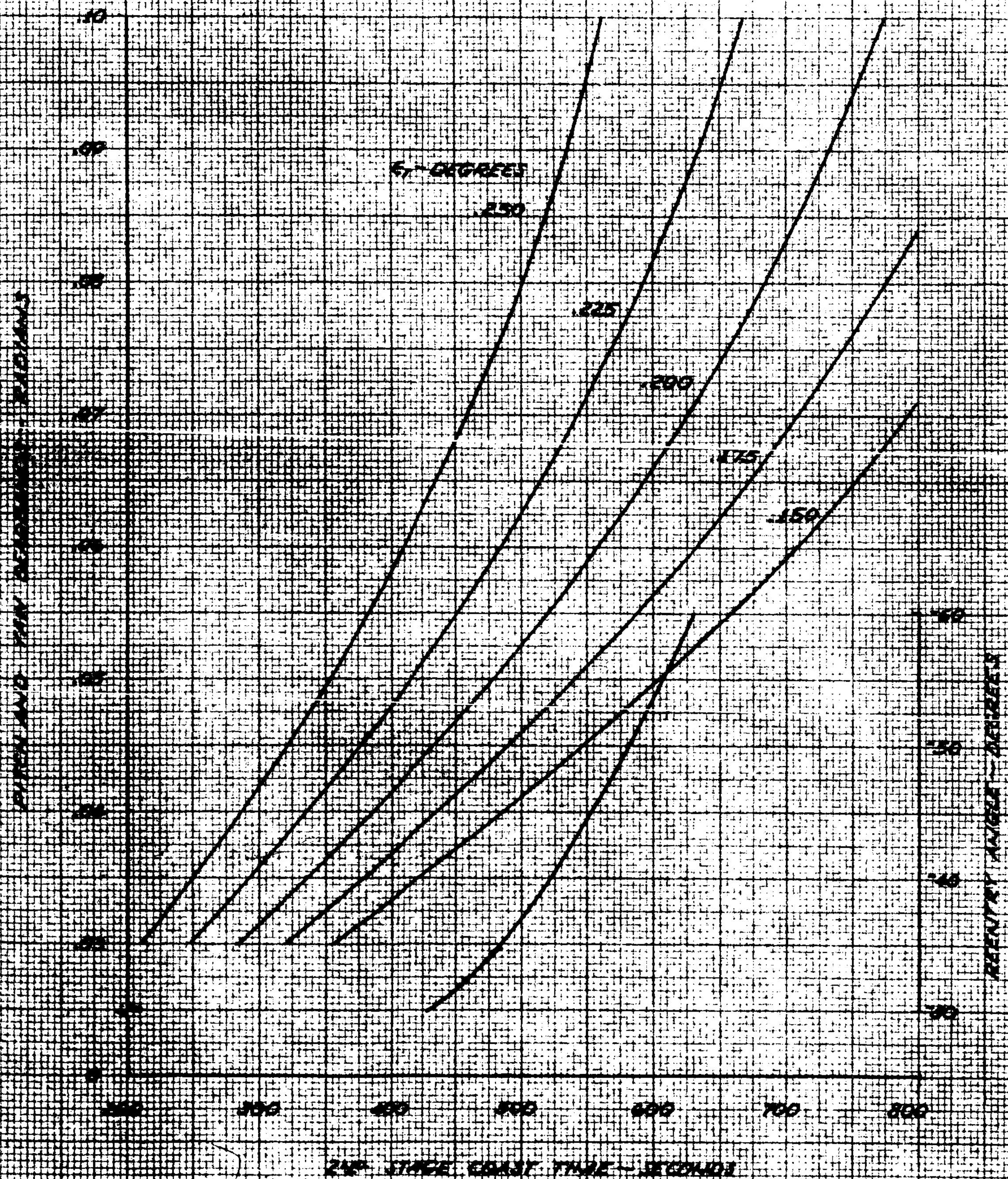

FIGURE 5.47
UNCONVENTIONAL VEHICLE - SPACECRAFT
THE VARIATION OF PITCH AND YAW DEADBANDS AND REENTRY ANGLE WITH SECOND STAGE COAST TIME AS A FUNCTION OF THRUST MISALIGNMENT ANGLE

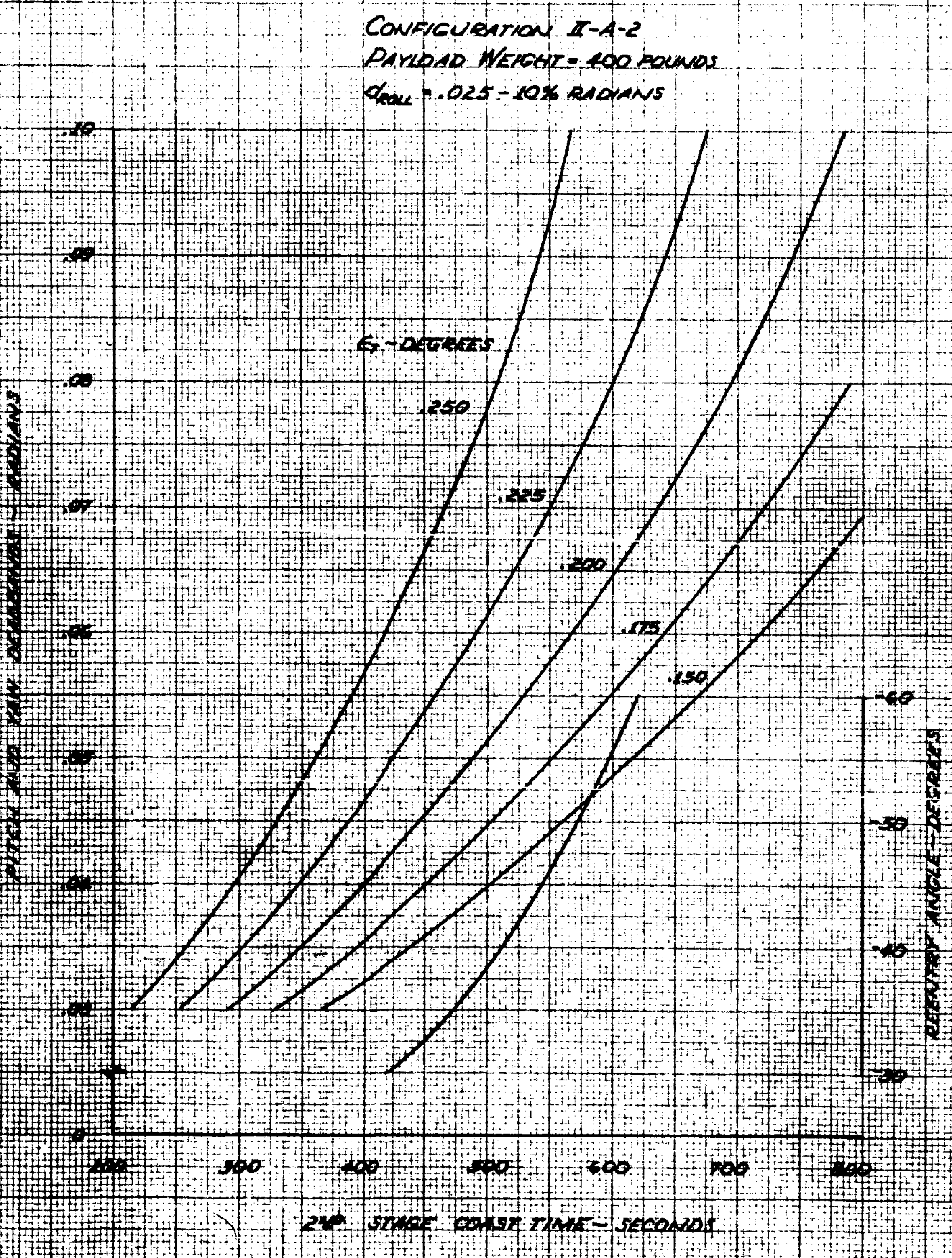

FIGURE 5.48
UNCONVENTIONAL VEHICLE - SPACECRAFT
THE VARIATION OF PITCH AND YAW DEADBANDS AND REENTRY ANGLE WITH SECOND STAGE COAST TIME AS A FUNCTION OF THRUST MISALIGNMENT ANGLE

CONFIGURATION II-A-2
PAYLOAD WEIGHT = 500 POUNDS
σ_{ROLL} = .025 - 10% RADIANS

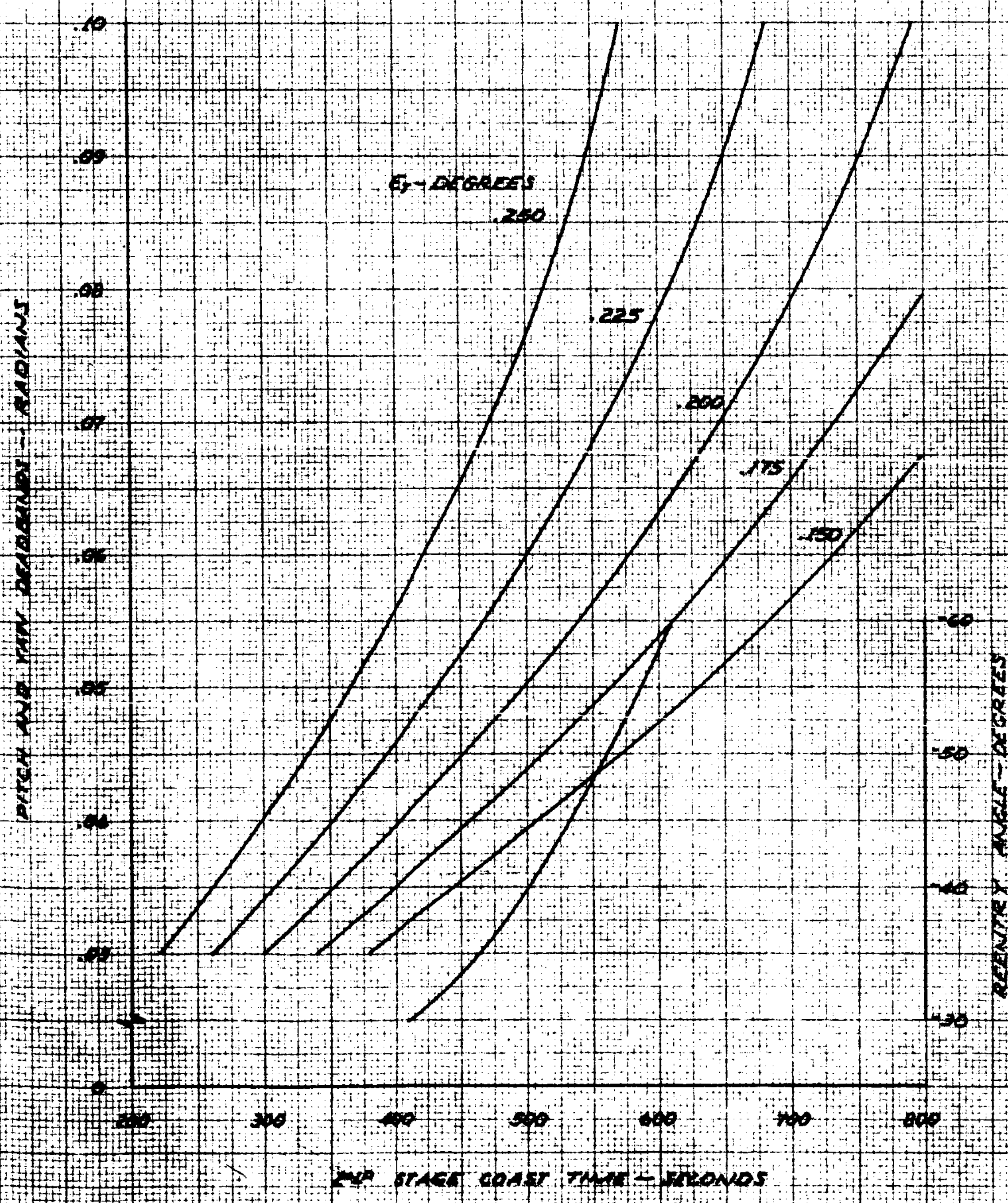

FIGURE 5.49

UNCONVENTIONAL VEHICLE - SPACECRAFT

THE VARIATION OF PITCH AND YAW DEADBANDS AND REENTRY ANGLE WITH SECOND STAGE COAST TIME AS A FUNCTION OF THRUST MISALIGNMENT ANGLE

CONFIGURATION II-A-2

PAYLOAD WEIGHT = 600 POUNDS

d_{ROLL} = .025-10% RADIANS

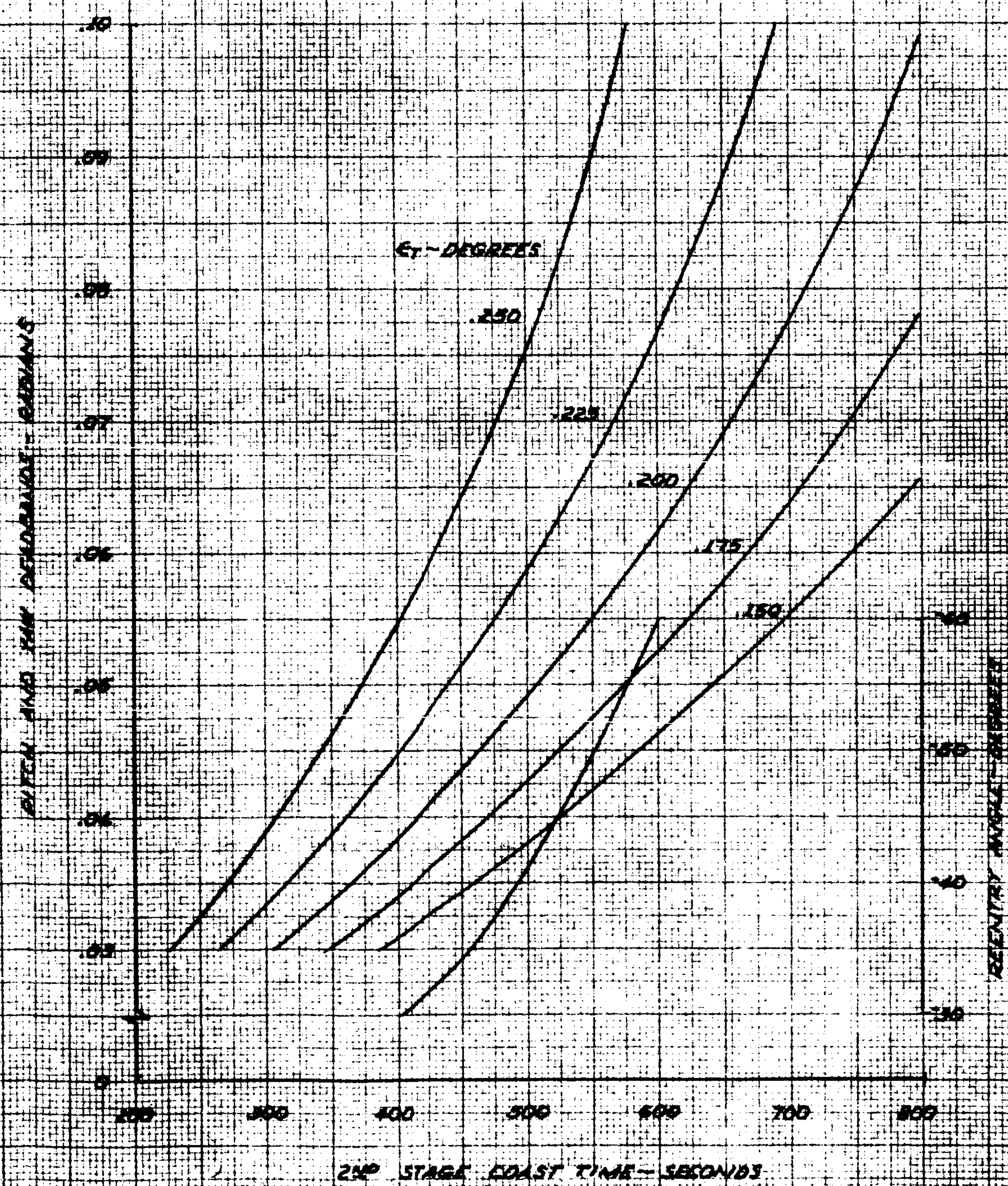

FIGURE 5.50
UNCONVENTIONAL VEHICLE - SPACECRAFT
THE VARIATION OF PITCH AND YAW DEADBANDS
WITH REENTRY ANGLE AS A FUNCTION OF
THRUST MISALIGNMENT ANGLE

CONFIGURATION II-A-2
SECOND STAGE COAST
PAYLOAD WEIGHT = 300 POUNDS
α_{ROLL} = .025-10% RADIANS

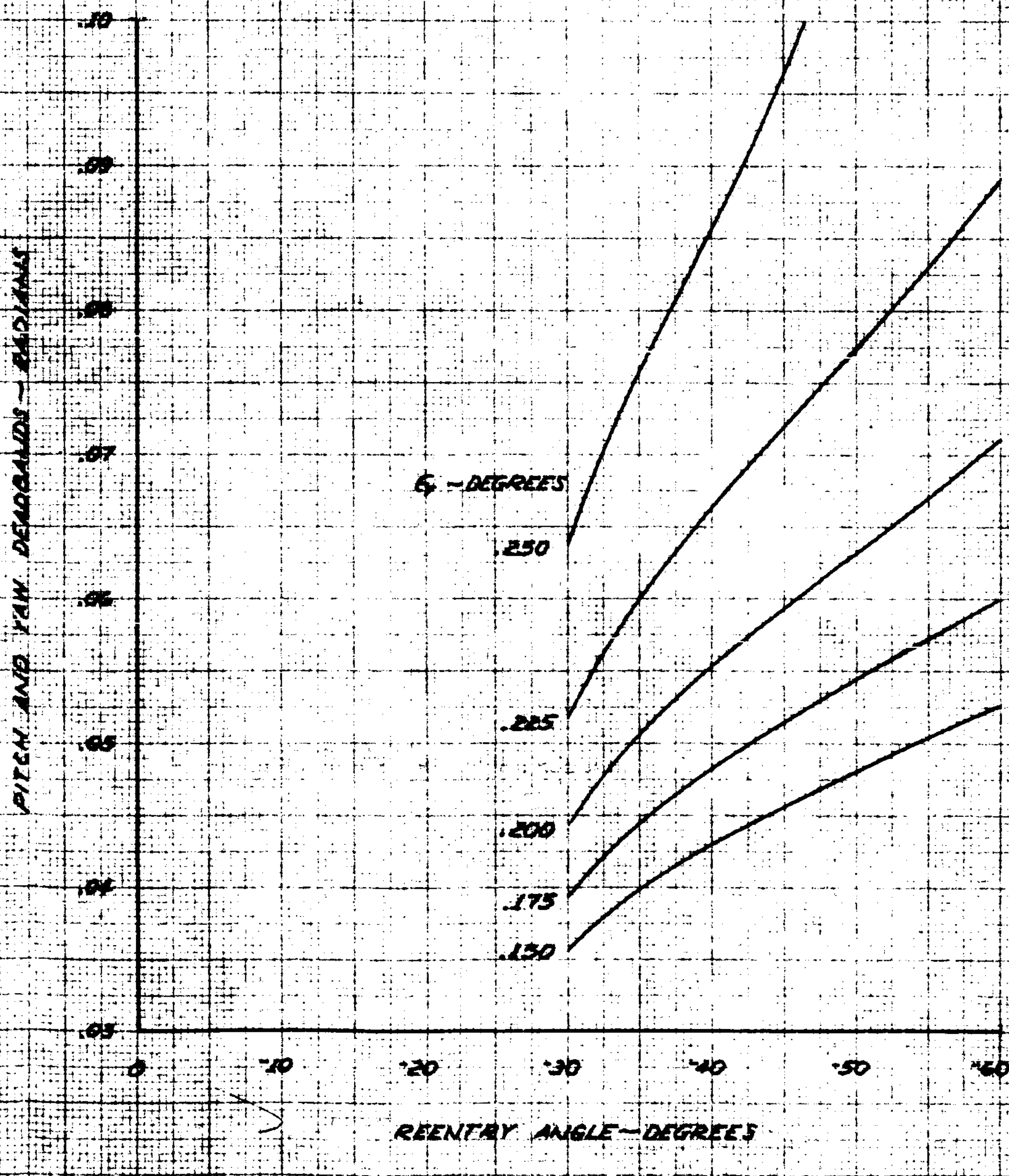

FIGURE 5.51
UNCONVENTIONAL VEHICLE - SPACECRAFT
THE VARIATION OF PITCH AND YAW DEADBANDS WITH REENTRY ANGLE AS A FUNCTION OF THRUST MISALIGNMENT ANGLE

CONFIGURATION II-A-2
SECOND STAGE COAST
PAYLOAD WEIGHT = 400 POUNDS
ϕ_{ROLL} = .025 ± 10% RADIANS

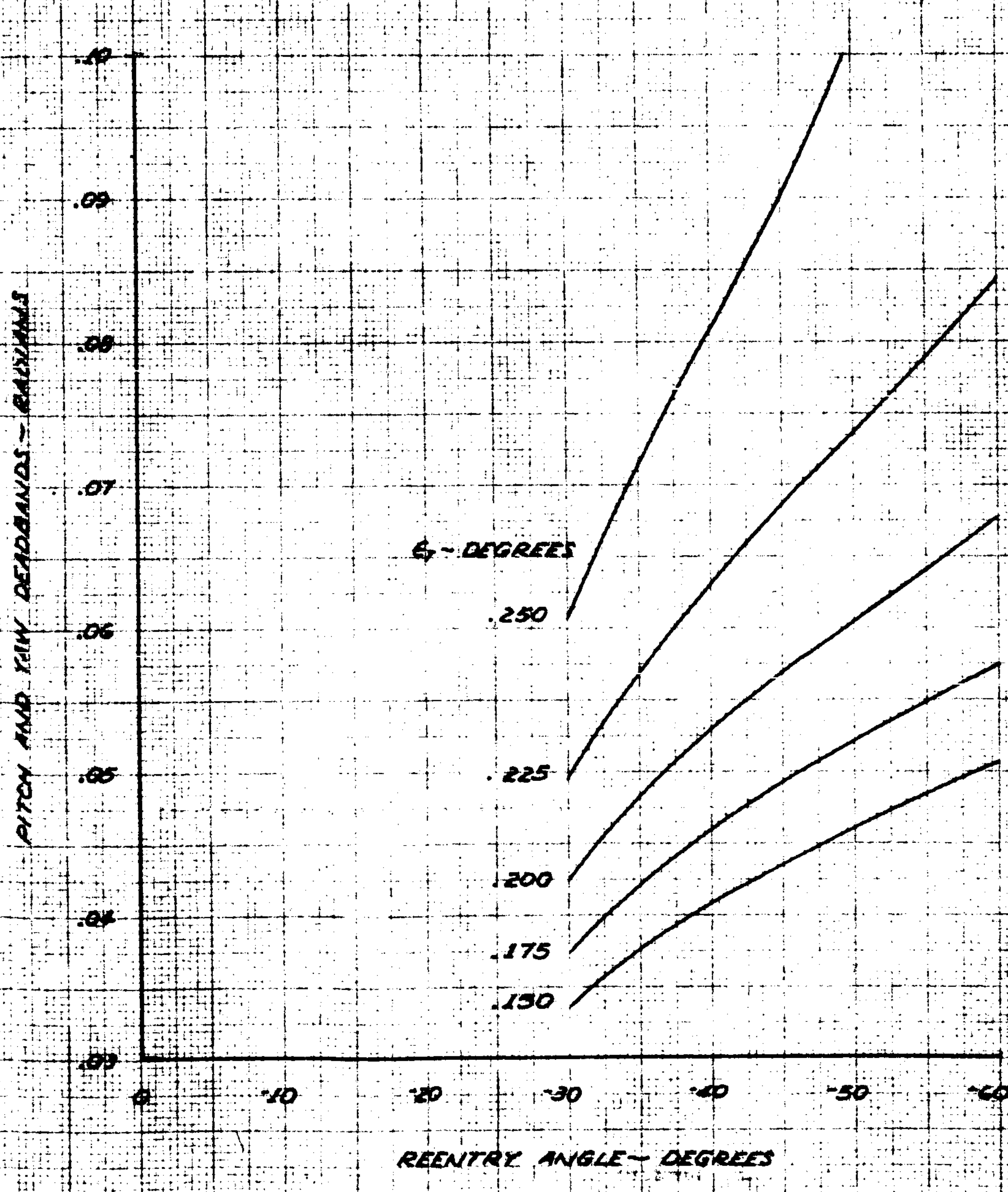

FIGURE 5.52
UNCONVENTIONAL VEHICLE - SPACECRAFT
THE VARIATION OF PITCH AND YAW DEADBANDS WITH REENTRY ANGLE AS A FUNCTION OF THRUST MISALIGNMENT ANGLE

CONFIGURATION II-A-2
SECOND STAGE COAST
PAYLOAD WEIGHT = 500 POUNDS
α_{ROLL} = .025 - 10% RADIANS

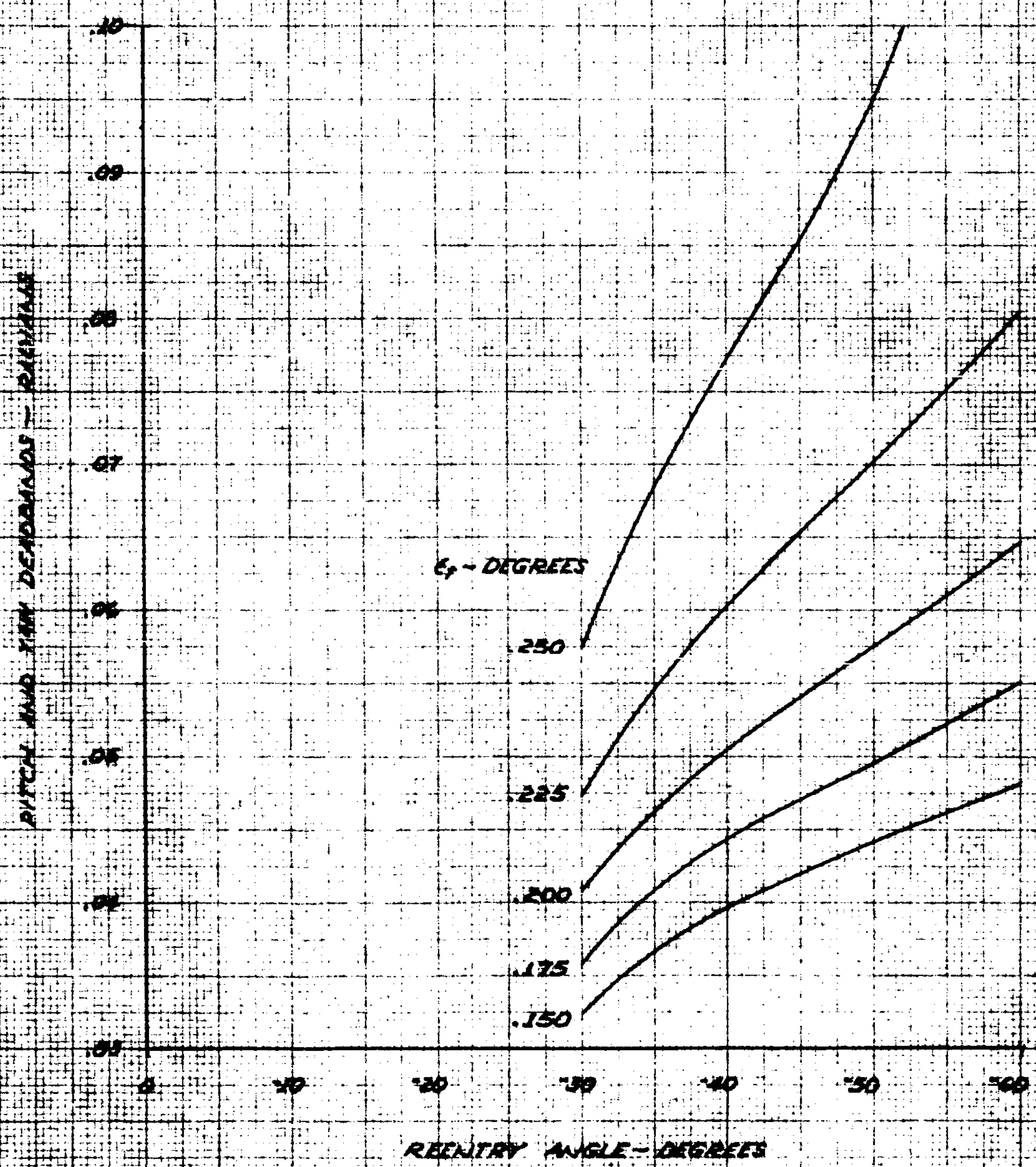

FIGURE 5.53
UNCONVENTIONAL VEHICLE- SPACECRAFT
THE VARIATION OF PITCH AND YAW DEADBANDS
WITH REENTRY ANGLE AS A FUNCTION OF
THRUST MISALIGNMENT ANGLE

CONFIGURATION II-A-2
SECOND STAGE COAST
PAYLOAD WEIGHT = 600 POUNDS
σ_{ROLL} = .025-10% RADIANS

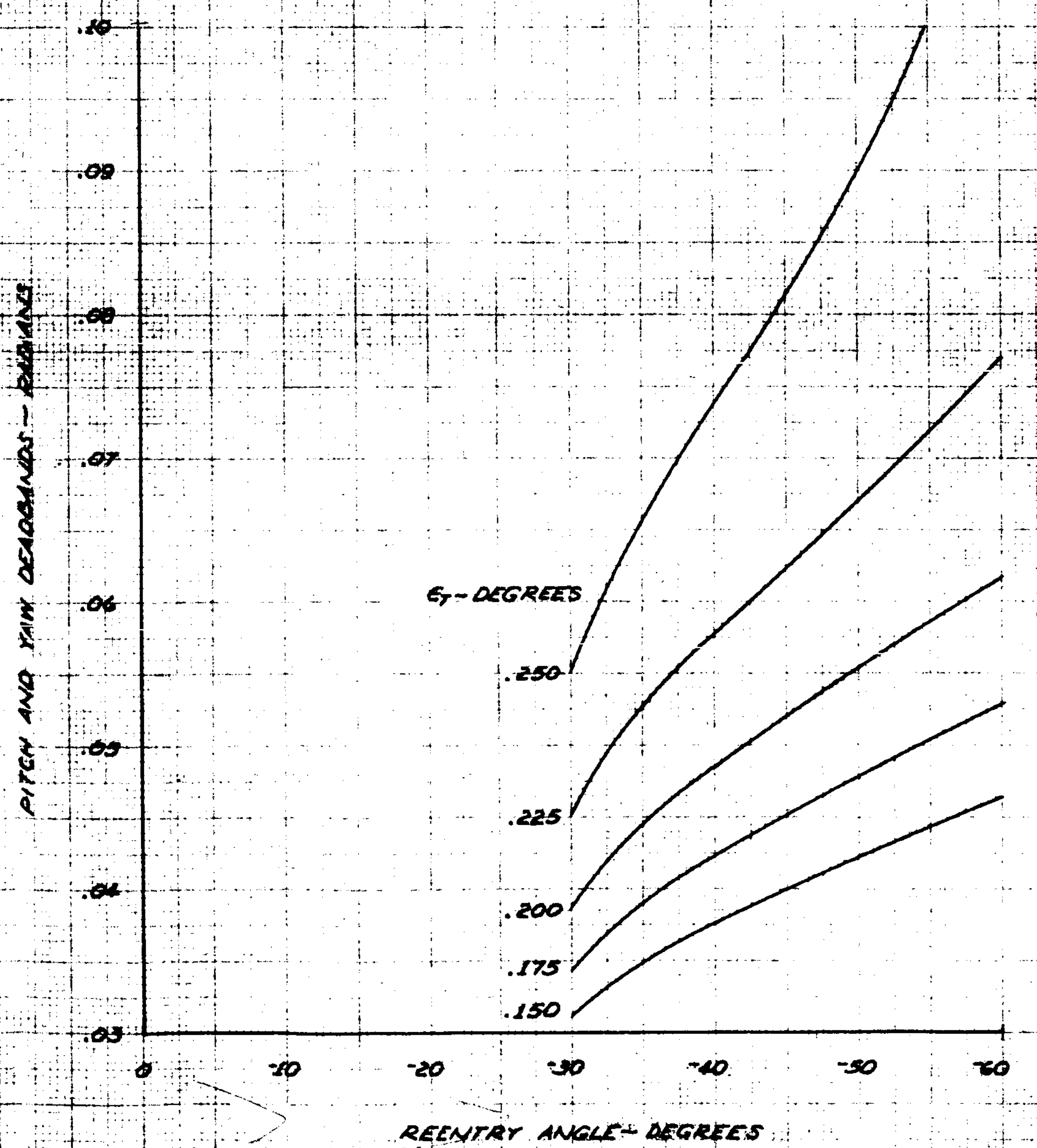

FIGURE 5.54

UNCONVENTIONAL VEHICLE - SPACECRAFT

THE VARIATION OF INCREMENTAL SECOND STAGE COAST TIME PER .025 DEGREES OF THRUST MISALIGNMENT ANGLE WITH PITCH AND YAW DEADBANDS AS A FUNCTION OF PAYLOAD WEIGHT

CONFIGURATION II-A-2

α_{ROLL} = .0698 -10% RADIANS

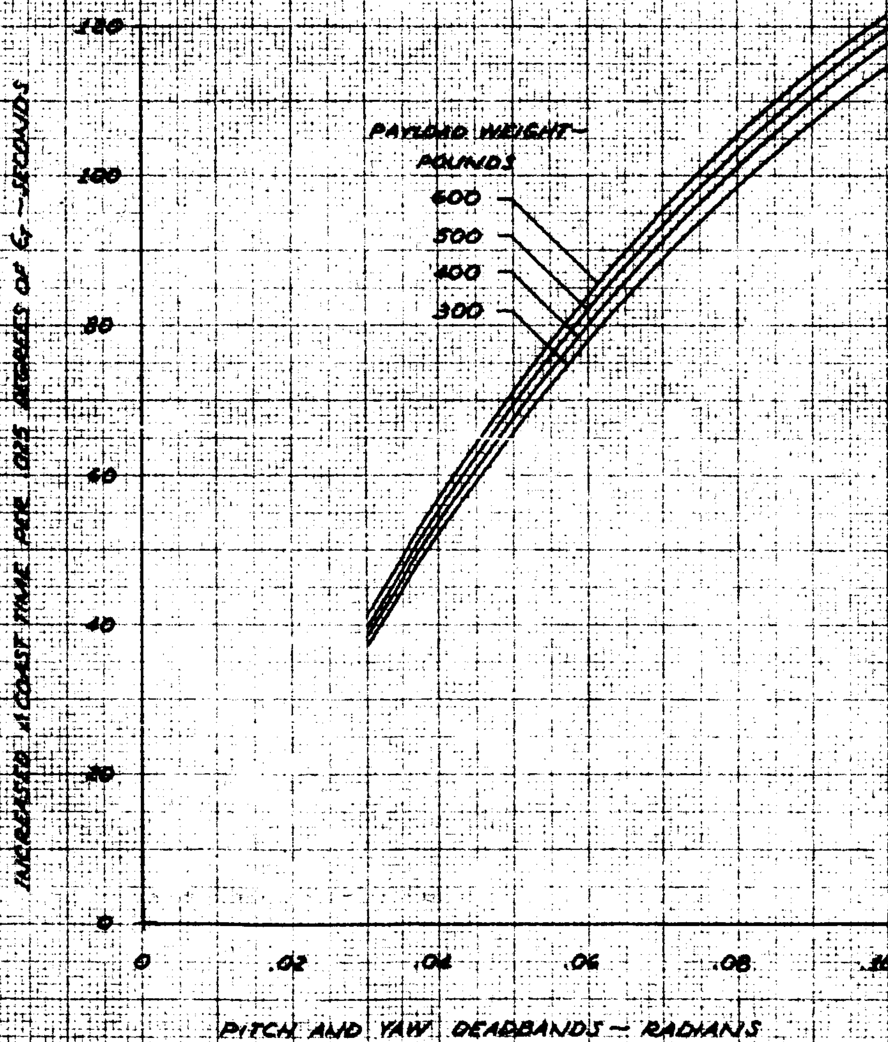

FIGURE 5.55
UNCONVENTIONAL VEHICLE-SPACECRAFT
THE VARIATION OF PITCH AND YAW DEADBANDS AND
REENTRY ANGLE WITH SECOND STAGE COAST TIME
AS A FUNCTION OF THRUST MISALIGNMENT ANGLE

CONFIGURATION II-A-2
PAYLOAD WEIGHT = 300 POUNDS
σ_{ROLL} = .0698-10% RADIANS

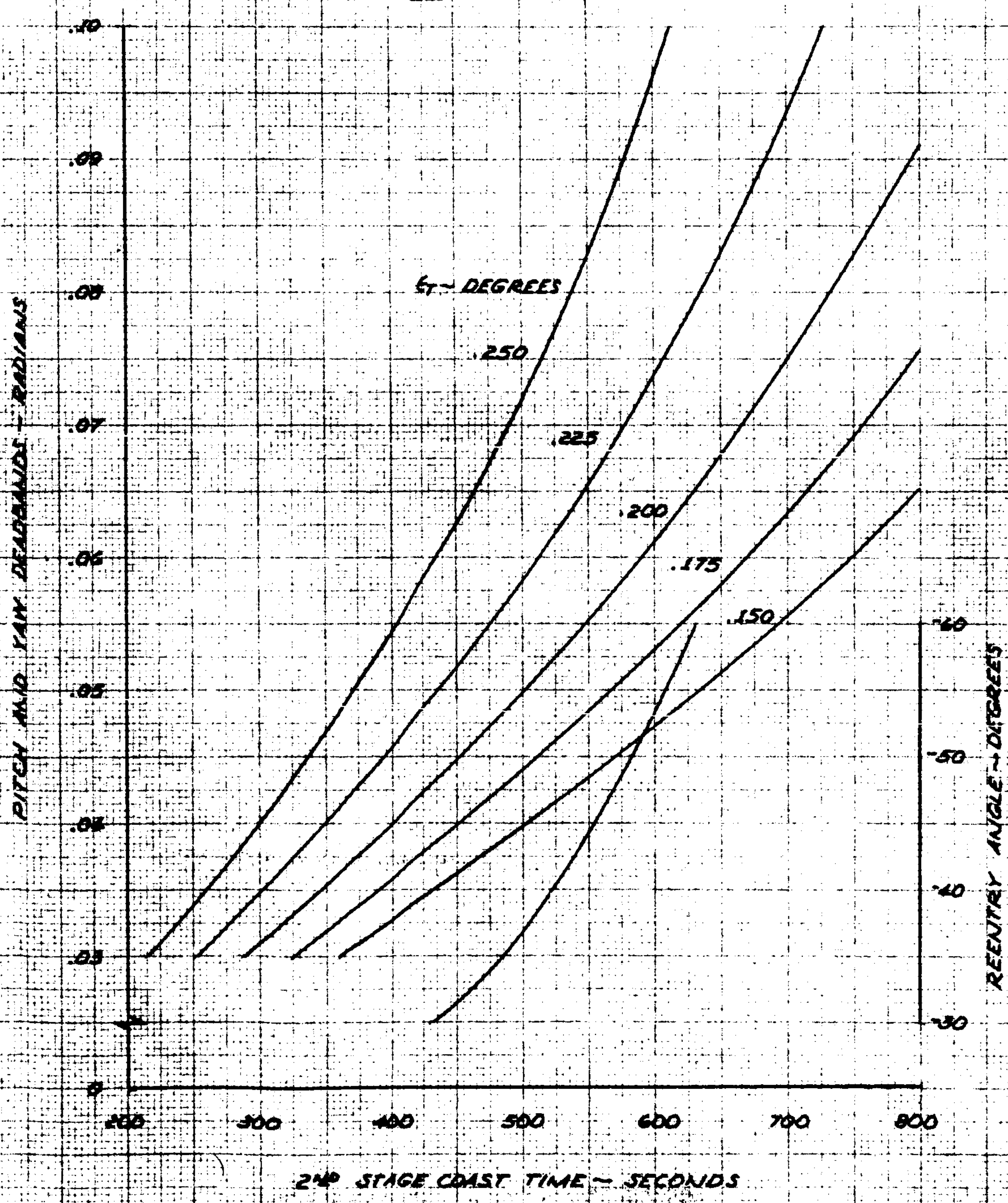

FIGURE 5.56

UNCONVENTIONAL VEHICLE - SPACECRAFT

THE VARIATION OF PITCH AND YAW DEADBANDS AND REENTRY ANGLE WITH SECOND STAGE COAST TIME AS A FUNCTION OF THRUST MISALIGNMENT ANGLE

CONFIGURATION II-A-2
PAYLOAD WEIGHT = 400 POUNDS
σ_{ROLL} = .0698-10% RADIANS

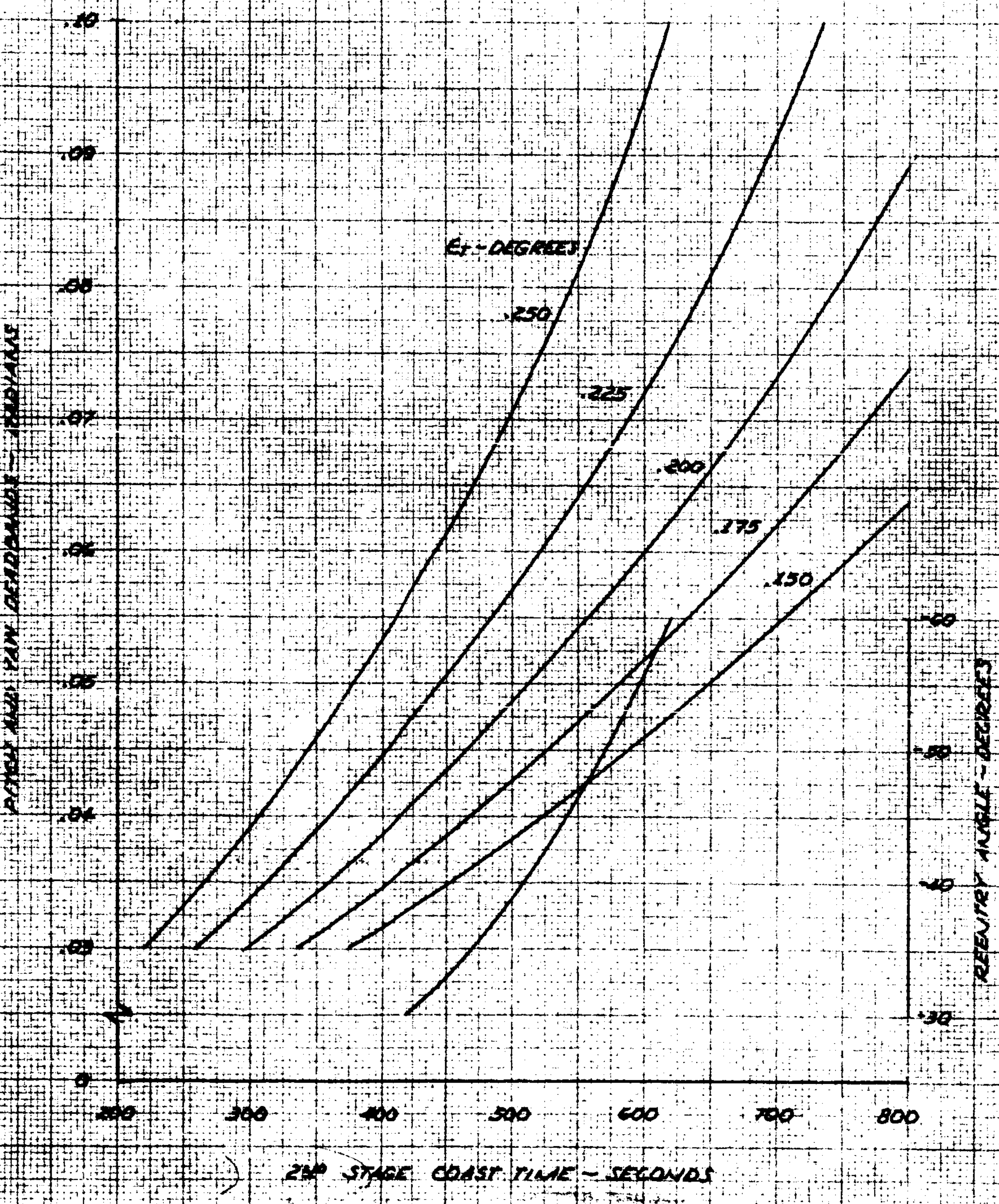

FIGURE 5.57

UNCONVENTIONAL VEHICLE - SPACECRAFT

THE VARIATION OF PITCH AND YAW DEADBANDS AND REENTRY ANGLE WITH SECOND STAGE COAST TIME AS A FUNCTION OF THRUST MISALIGNMENT ANGLE

CONFIGURATION II-A-2
PAYLOAD WEIGHT = 500 POUNDS
α_{ROLL} = .0698 - 10% RADIANS

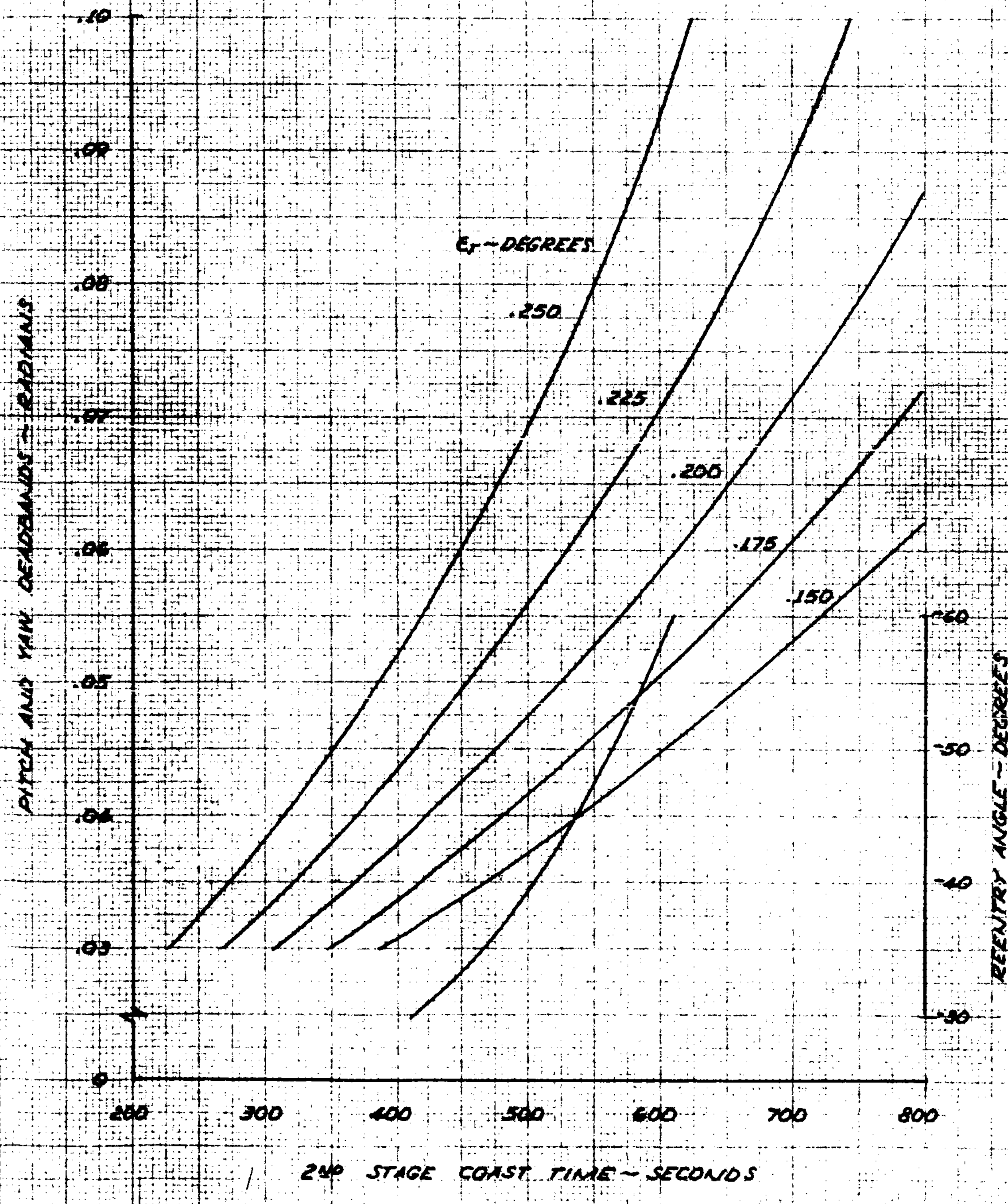

FIGURE 5.58

UNCONVENTIONAL VEHICLE - SPACECRAFT

THE VARIATION OF PITCH AND YAW DEADBANDS AND REENTRY ANGLE WITH SECOND STAGE COAST TIME AS A FUNCTION OF THRUST MISALIGNMENT ANGLE

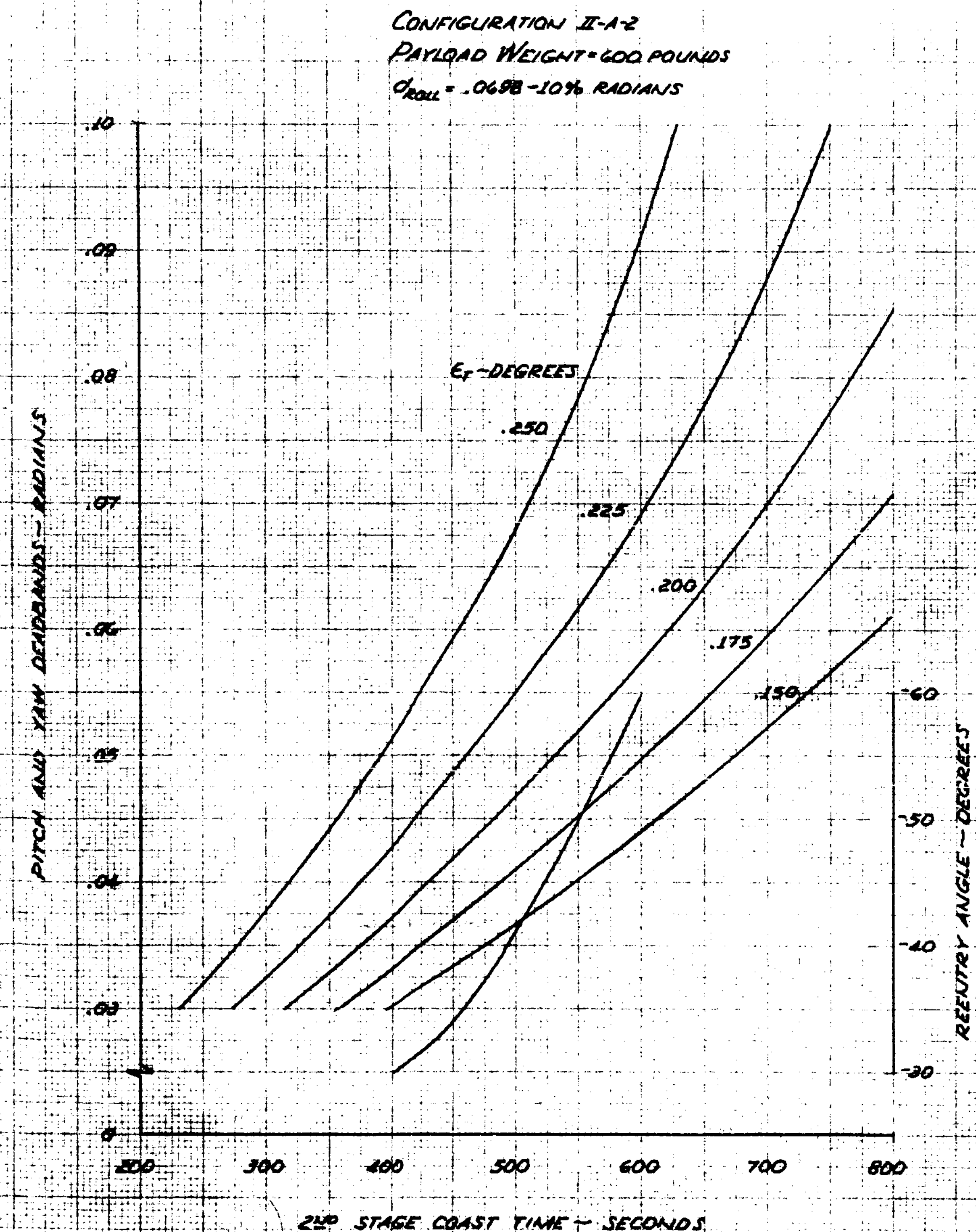

FIGURE 5.59
UNCONVENTIONAL VEHICLE – SPACECRAFT
THE VARIATION OF PITCH AND YAW DEADBANDS
WITH REENTRY ANGLE AS A FUNCTION OF
THRUST MISALIGNMENT ANGLE

CONFIGURATION II-A-2
SECOND STAGE COAST
PAYLOAD WEIGHT = 300 POUNDS
α_{BKL} = .0698 - 10% RADIANS

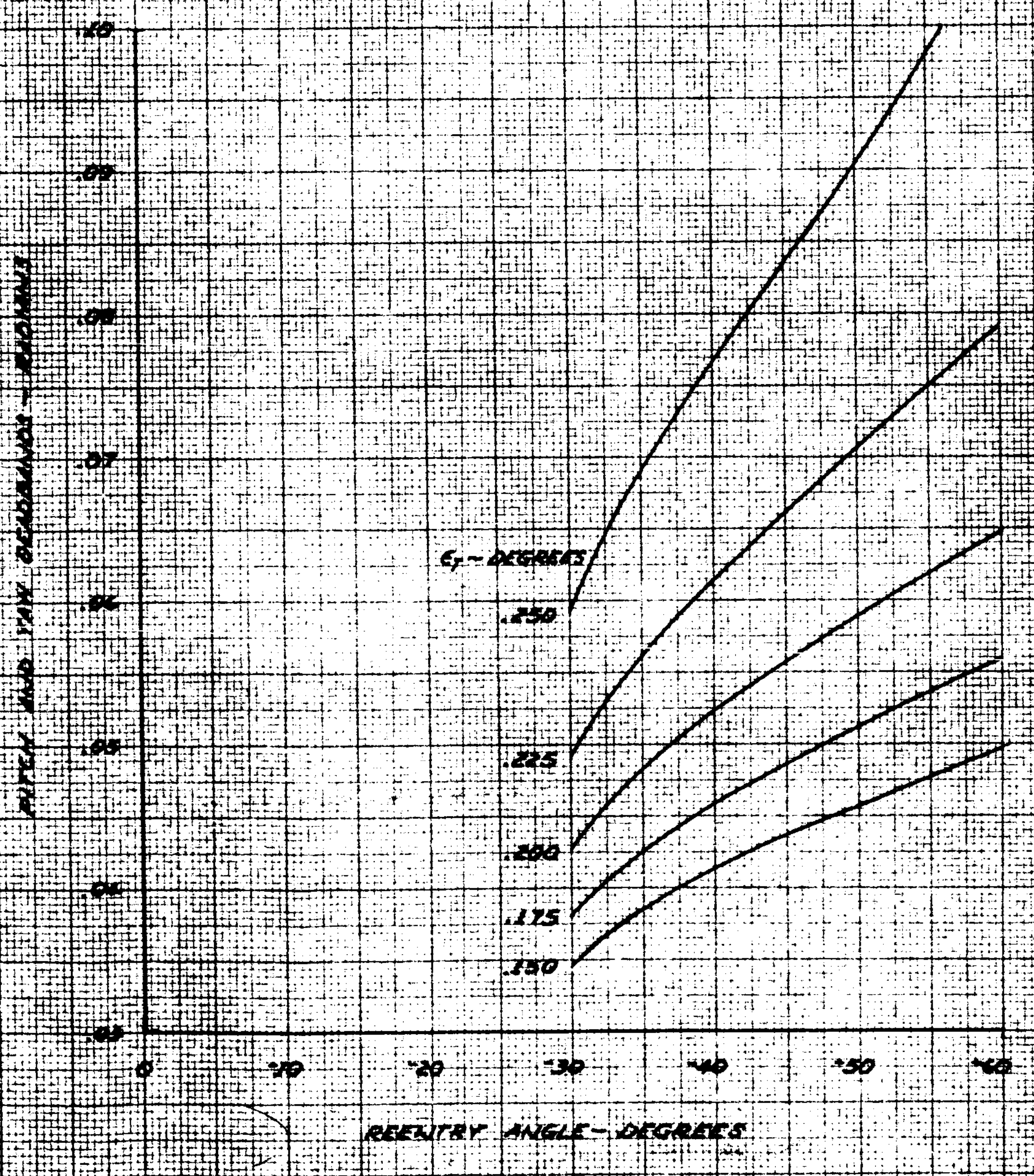

FIGURE 5.60
UNCONVENTIONAL VEHICLE- SPACECRAFT
THE VARIATION OF PITCH AND YAW DEADBANDS WITH REENTRY ANGLE AS A FUNCTION OF THRUST MISALIGNMENT ANGLE

CONFIGURATION II-A-2
SECOND STAGE COAST
PAYLOAD WEIGHT = 400 POUNDS
α_{ROLL} = .0698 - 10% RADIANS

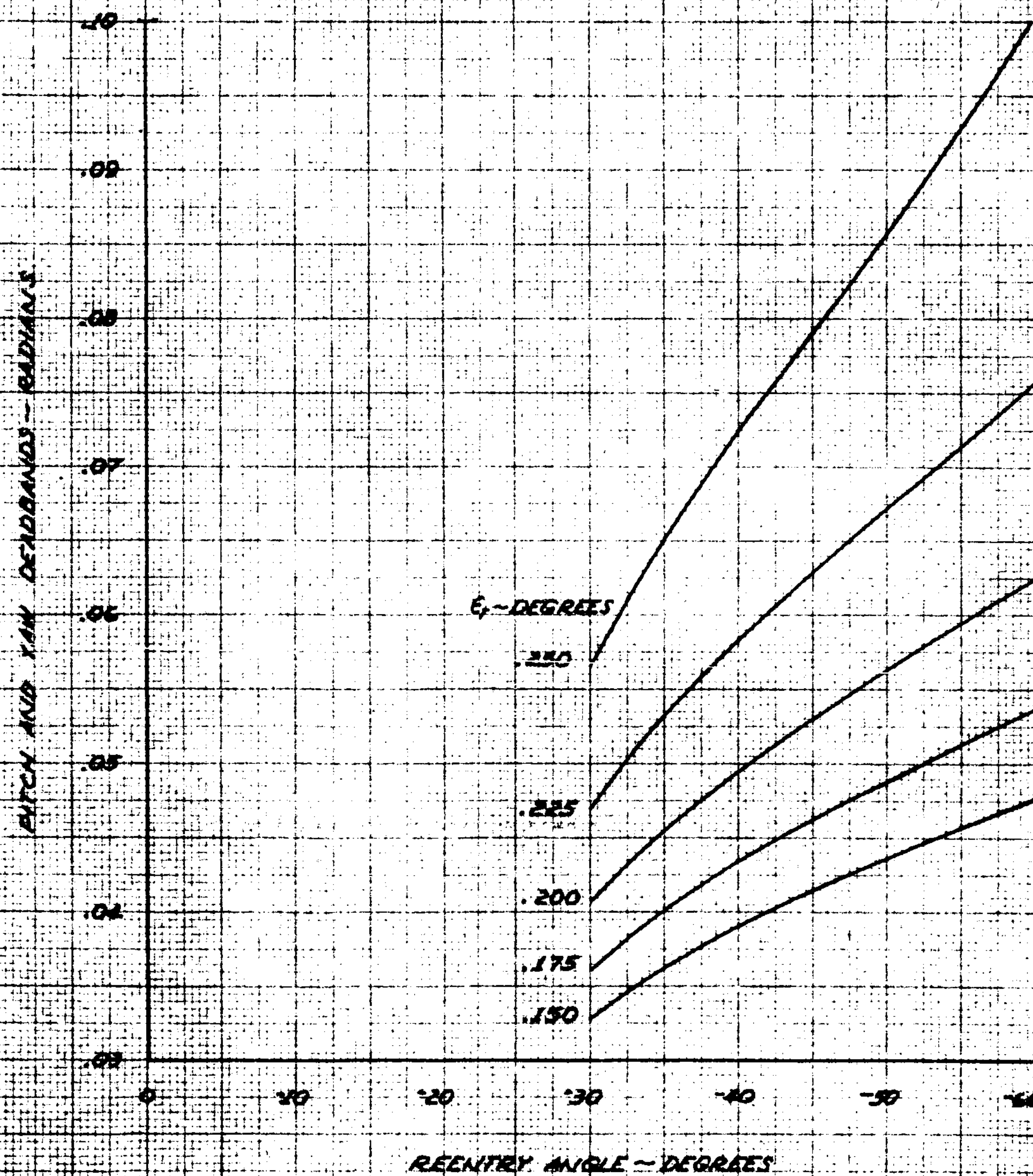

FIGURE 5.61
UNCONVENTIONAL VEHICLE - SPACECRAFT
THE VARIATION OF PITCH AND YAW DEADBANDS WITH REENTRY ANGLE AS A FUNCTION OF THRUST MISALIGNMENT ANGLE

CONFIGURATION II-A-2
SECOND STAGE COAST
PAYLOAD WEIGHT = 500 POUNDS
α_{ROLL} = .0698 - 10% RADIANS

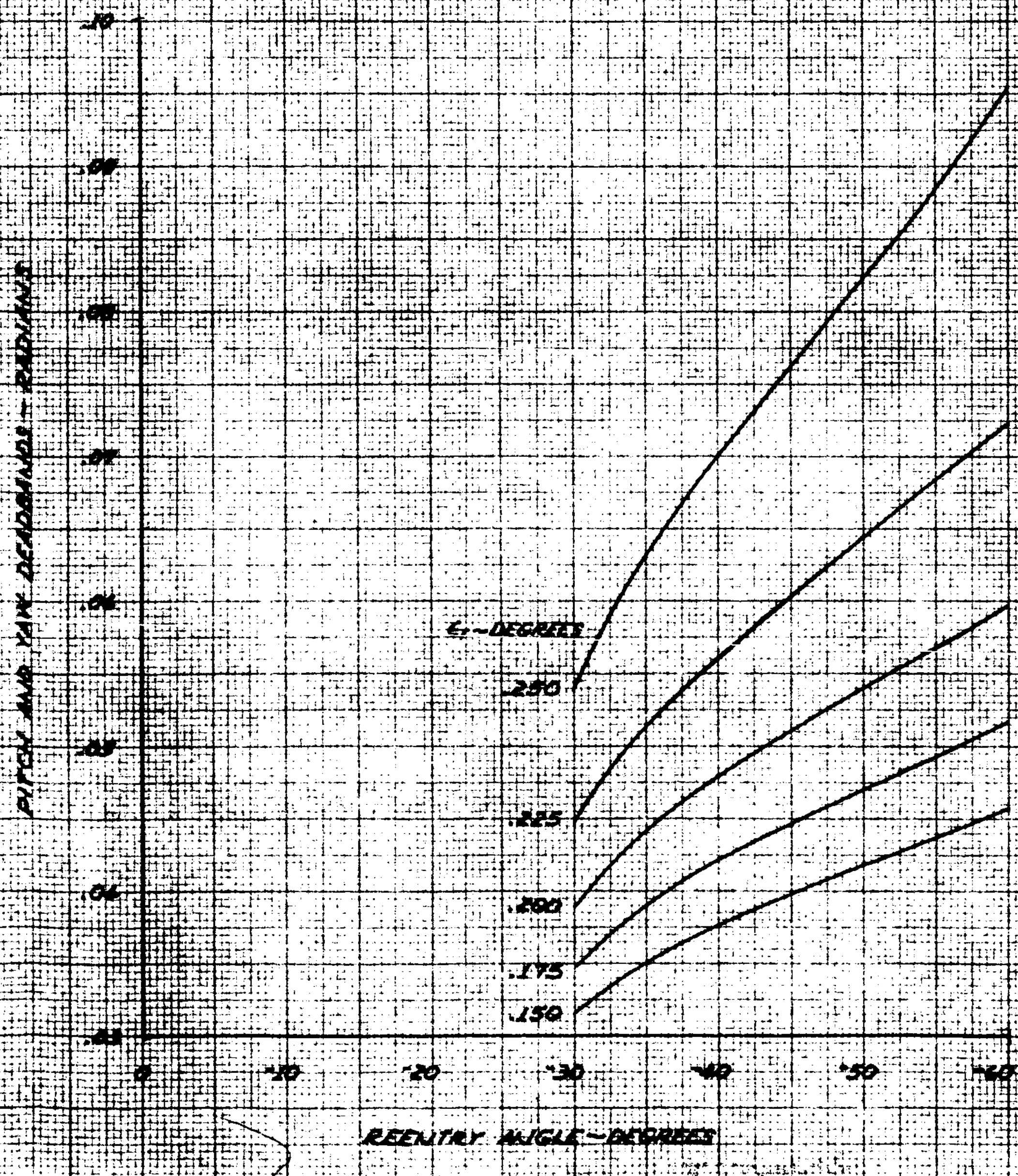

FIGURE 5.62
UNCONVENTIONAL VEHICLE - SPACECRAFT
THE VARIATION OF PITCH AND YAW DEADBANDS WITH REENTRY ANGLE AS A FUNCTION OF THRUST MISALIGNMENT ANGLE

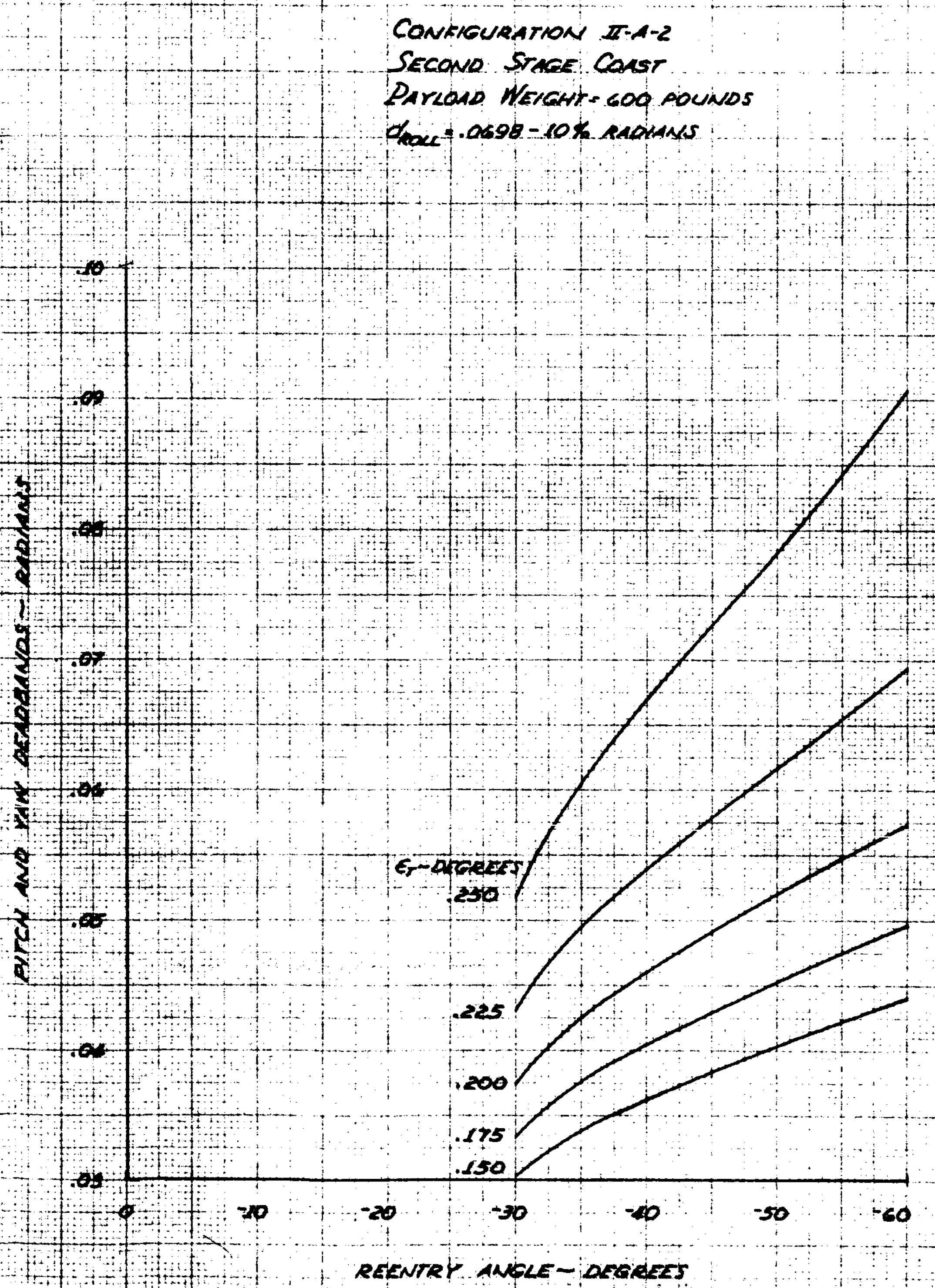

FIGURE 5.63
UNCONVENTIONAL VEHICLE - SPACECRAFT
THE VARIATION OF PITCH AND YAW DUTY CYCLE WITH CONTROL MOTOR THRUST

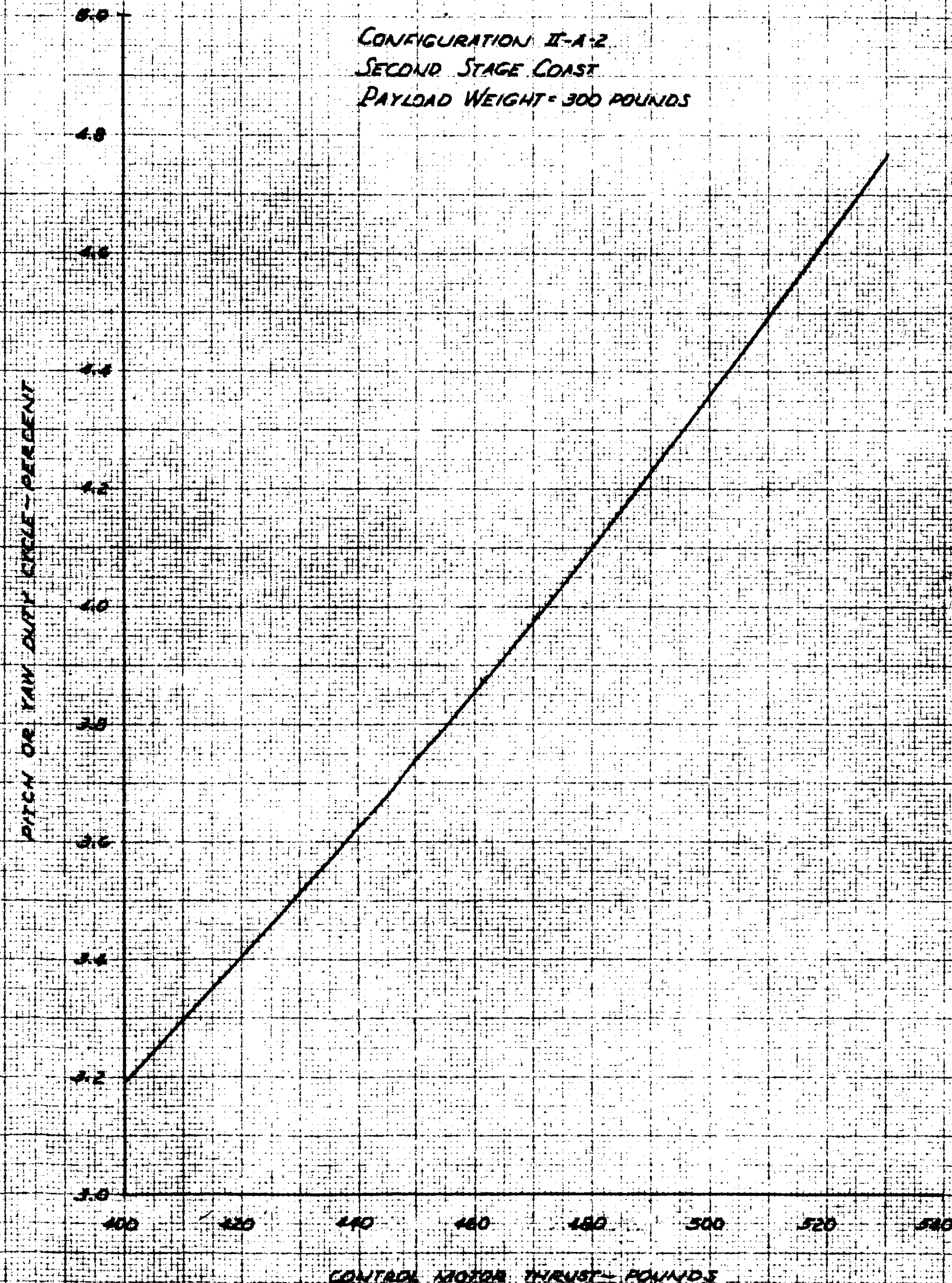

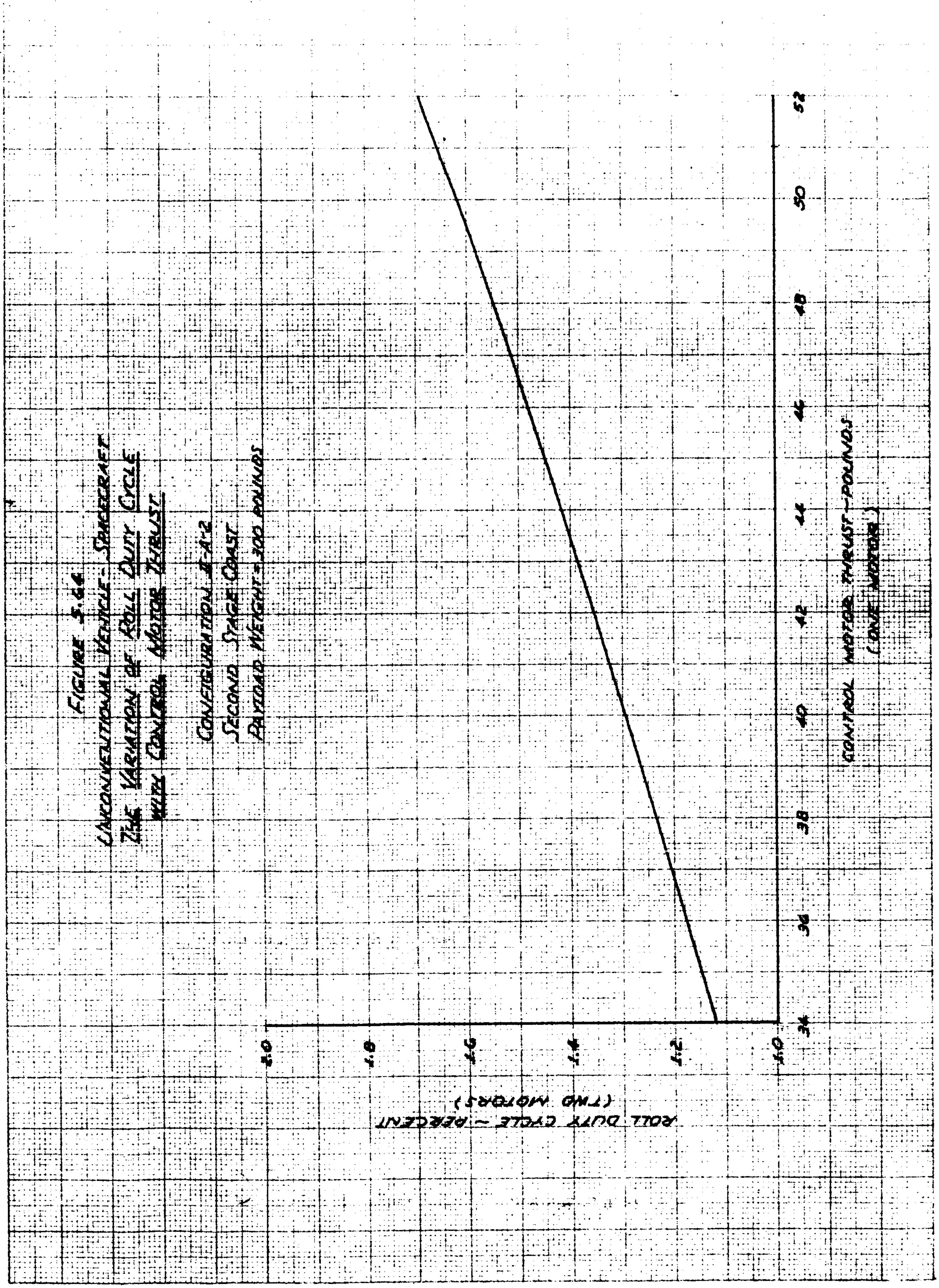
FIGURE 5.64
UNCONVENTIONAL VEHICLE - SPACECRAFT
THE VARIATION OF ROLL DUTY CYCLE WITH CONTROL MOTOR THRUST
CONFIGURATION I-A-2
SECOND STAGE COAST
PAYLOAD WEIGHT = 300 POUNDS
ROLL DUTY CYCLE ~ PERCENT
(TWO MOTORS)
1.0
1.2
1.4
1.6
1.8
2.0
34
36
38
40
42
44
46
48
50
52
CONTROL MOTOR THRUST - POUNDS
(ONE MOTOR)

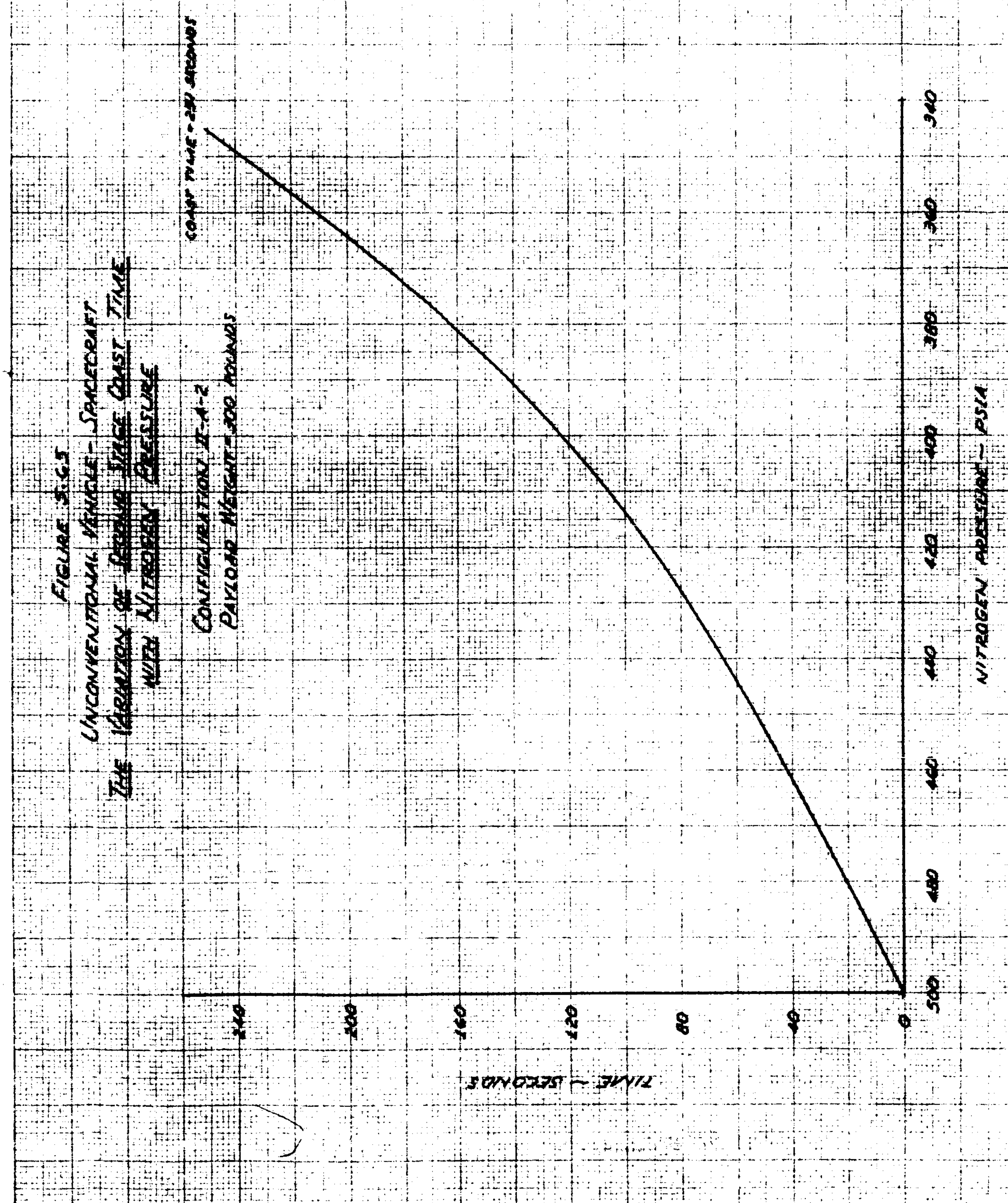
FIGURE 5.6.5
UNCONVENTIONAL VEHICLE - SPACECRAFT
THE VARIATION OF SECOND STAGE COAST TIME
WITH NITROGEN PRESSURE
CONFIGURATION II-A-2
PAYLOAD WEIGHT = 300 POUNDS
COAST TIME = 251 SECONDS
TIME ~ SECONDS
0
40
80
120
160
200
240
500
480
460
440
420
400
380
360
340
NITROGEN PRESSURE ~ PSIA

FIGURE 5.66

FIGURE PURPOSELY OMITTED

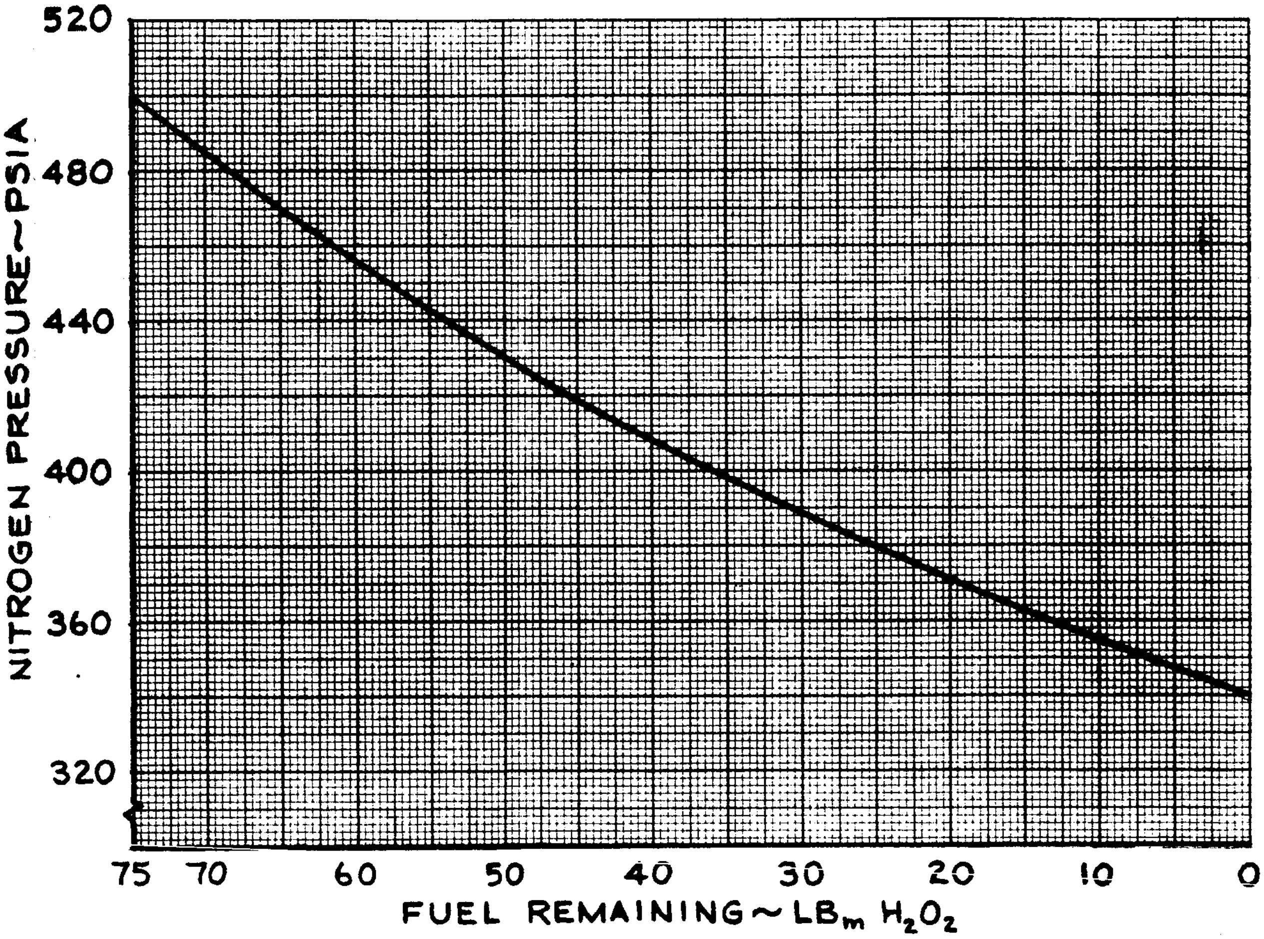

FIGURE 5.67. NITROGEN PRESSURE VS. FUEL REMAINING FOR "B" SECTION REACTION CONTROL SYSTEM.

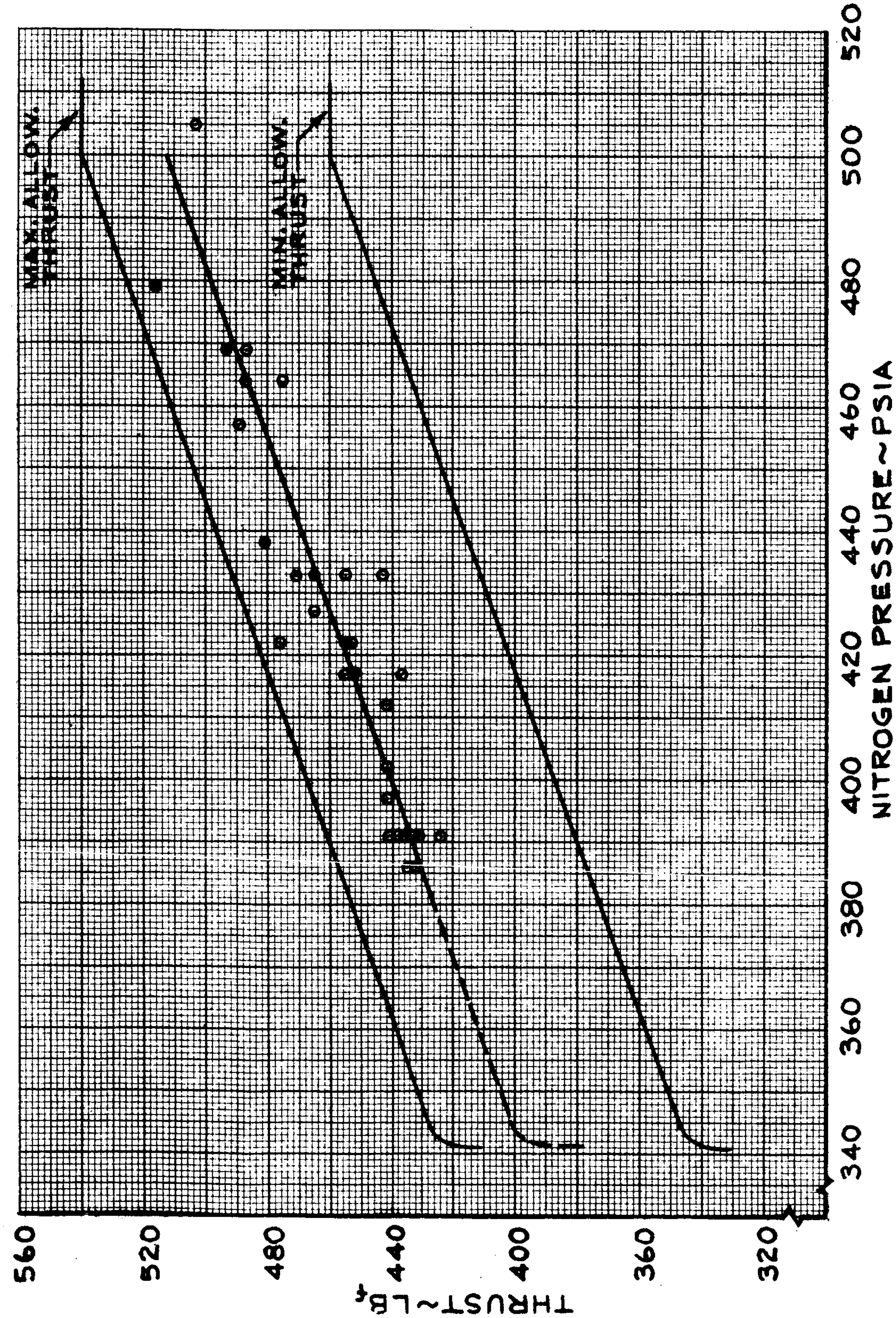

FIGURE 5.63. PITCH-YAW MOTOR THRUST VS. NITROGEN PRESSURE FOR "B" SECTION REACTION CONTROL SYSTEM.

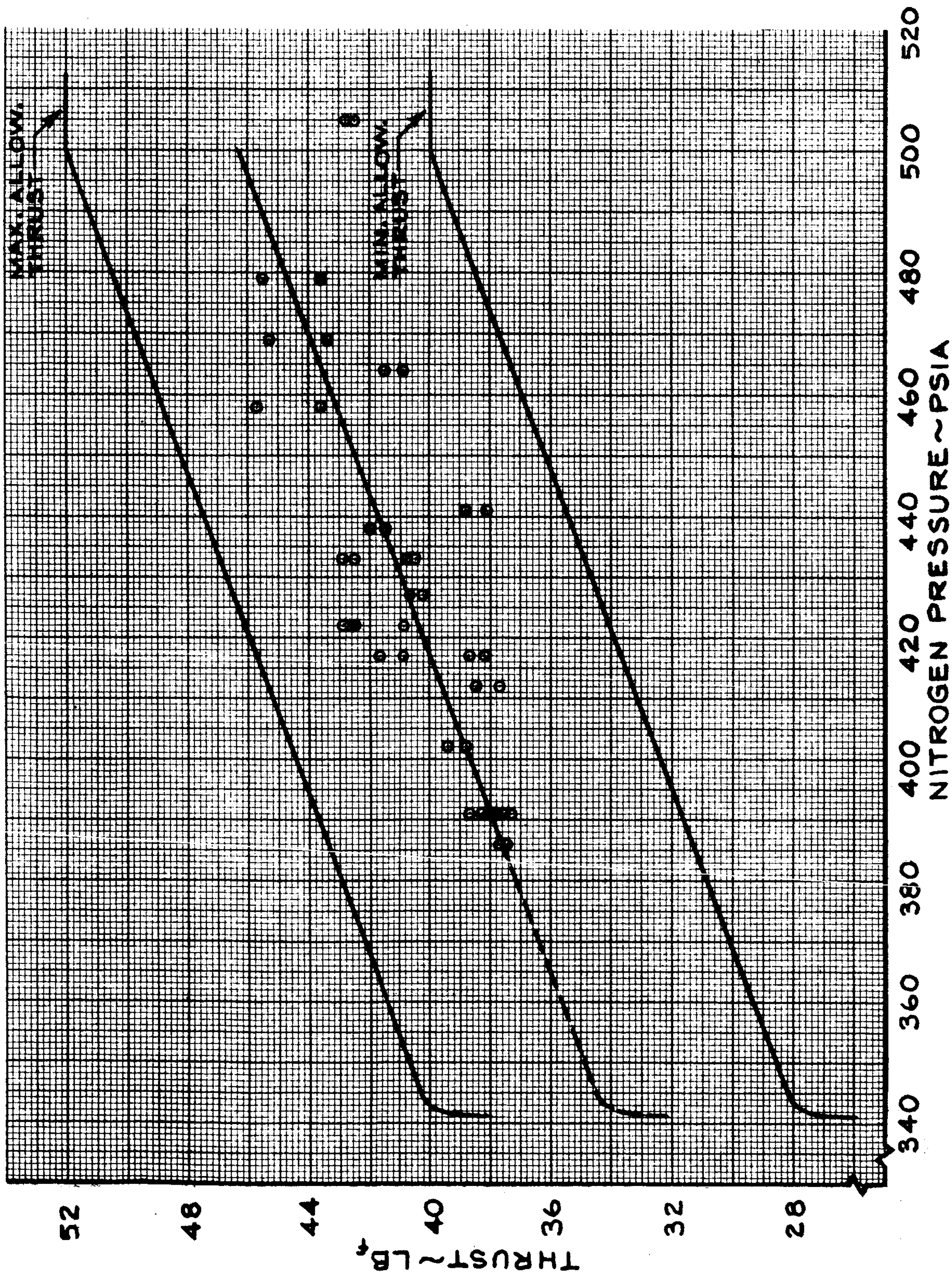

FIGURE 5.69 ROLL MOTOR THRUST VS. NITROGEN PRESSURE FOR "B" SECTION REACTION CONTROL SYSTEM.

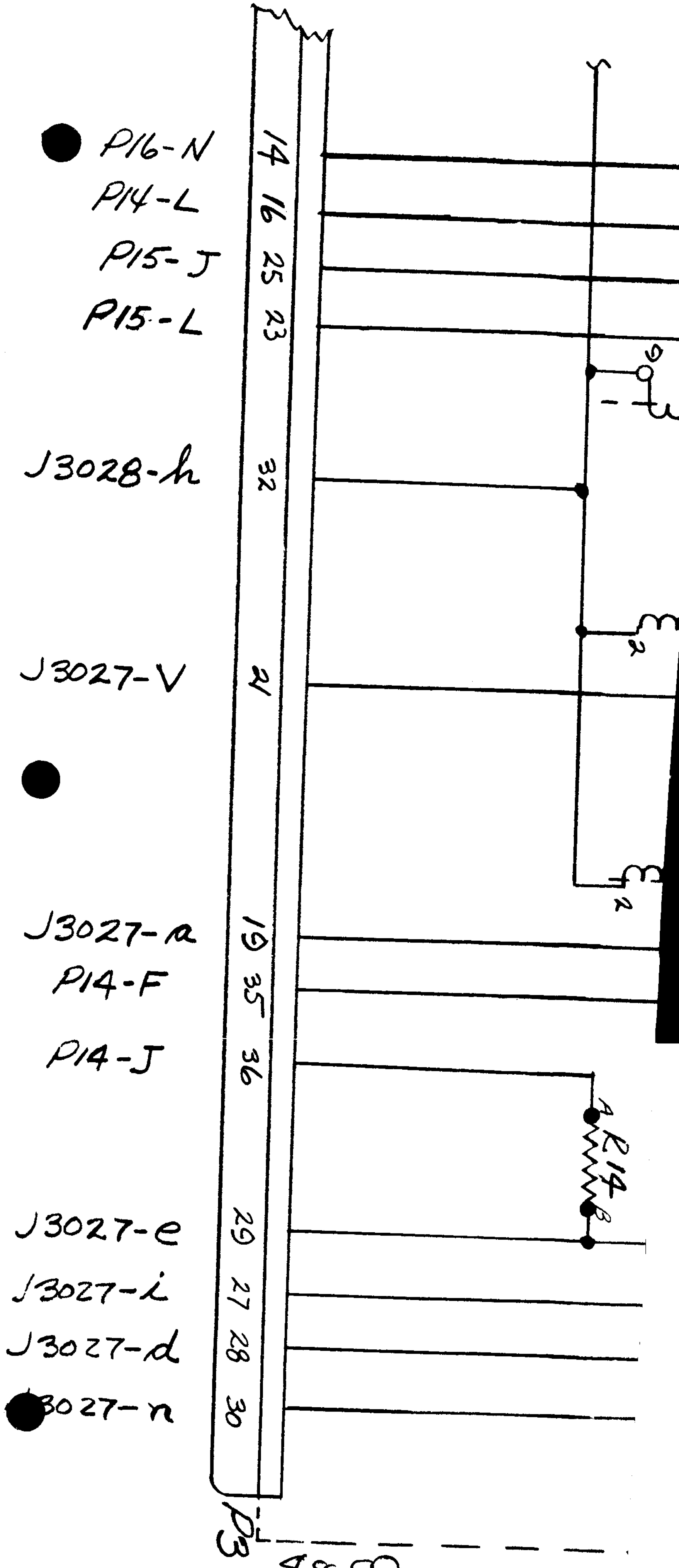
P16-N
P14-L
P15-J
P15-L
J3028-h
J3027-V
J3027-a
P14-F
P14-J
J3027-e
J3027-i
J3027-d
3027-n
14
16
25
23
32
21
19
35
36
29
27
28
30
R14
P3

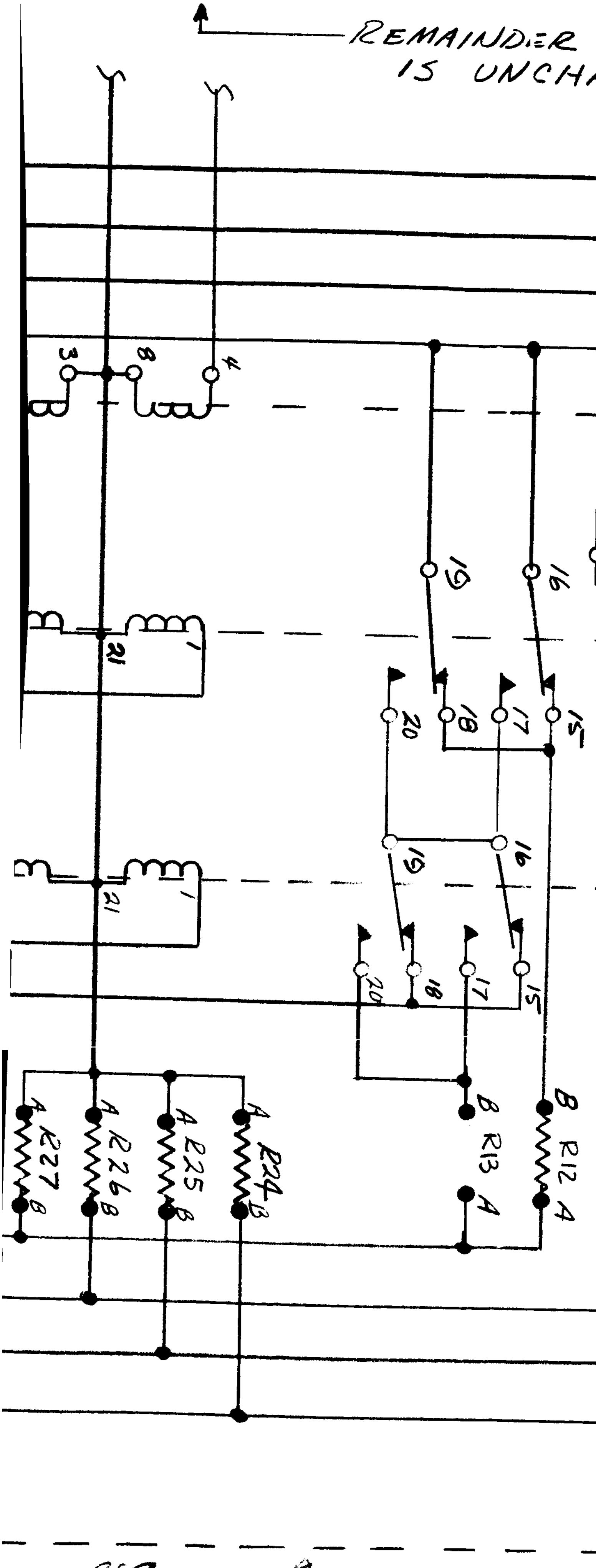
REMAINDER
IS UNCH
R27
R26
R25
R24
R13
R12

OF BOARD
NGED

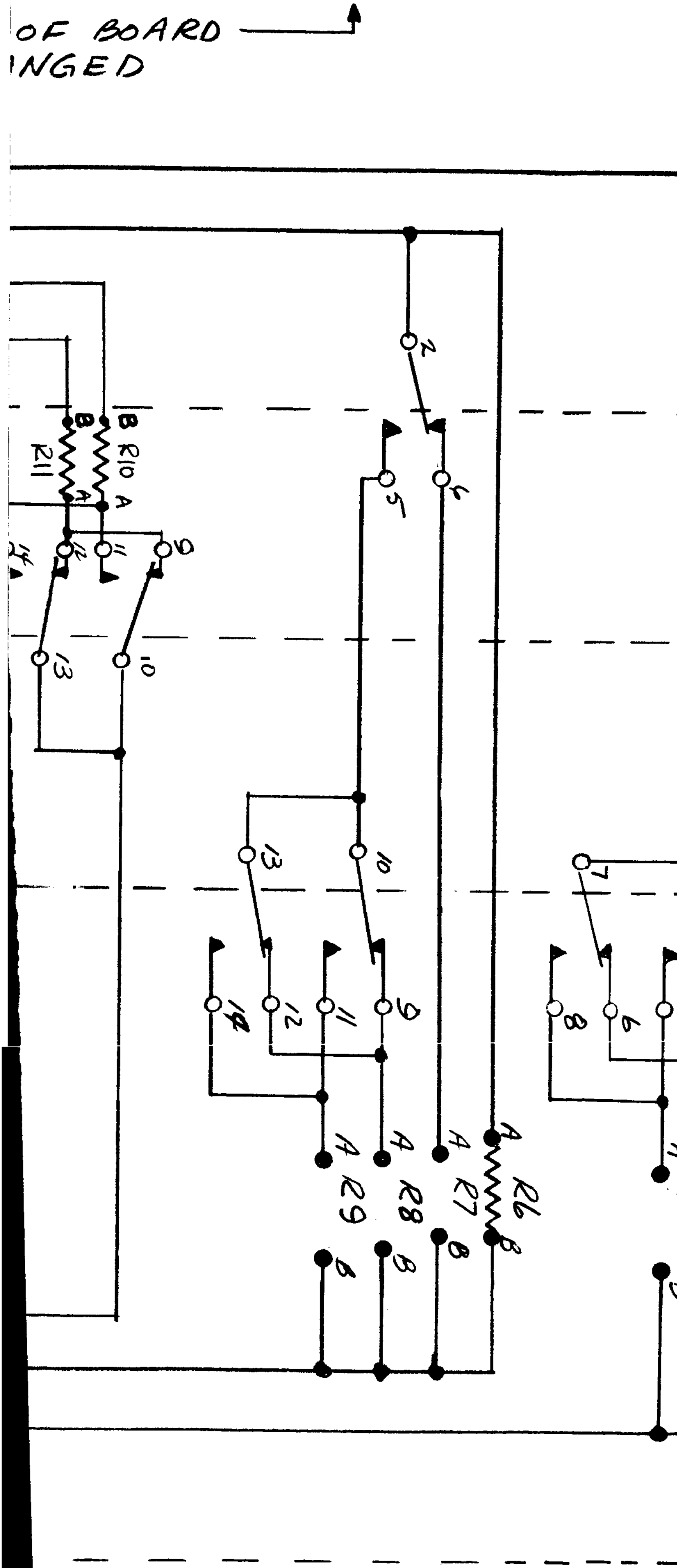

88 3

FIGURE 5.70

UNCONVENTIONAL VEHICLE – SPACECRAFT

IRP GAIN CIRCUIT – UNMODIFIED

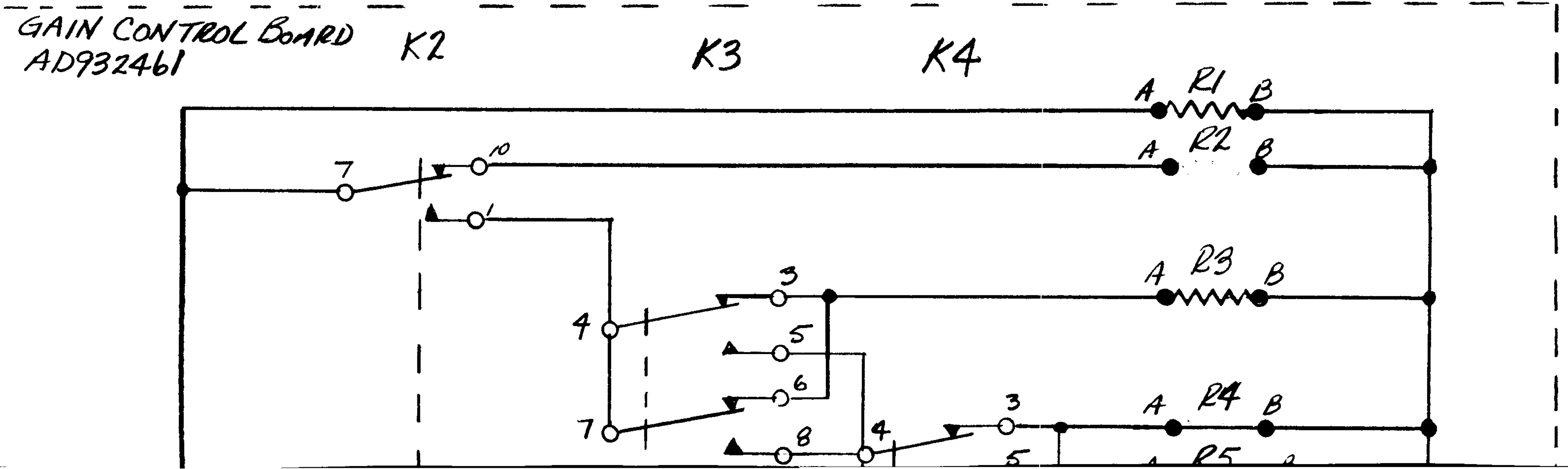

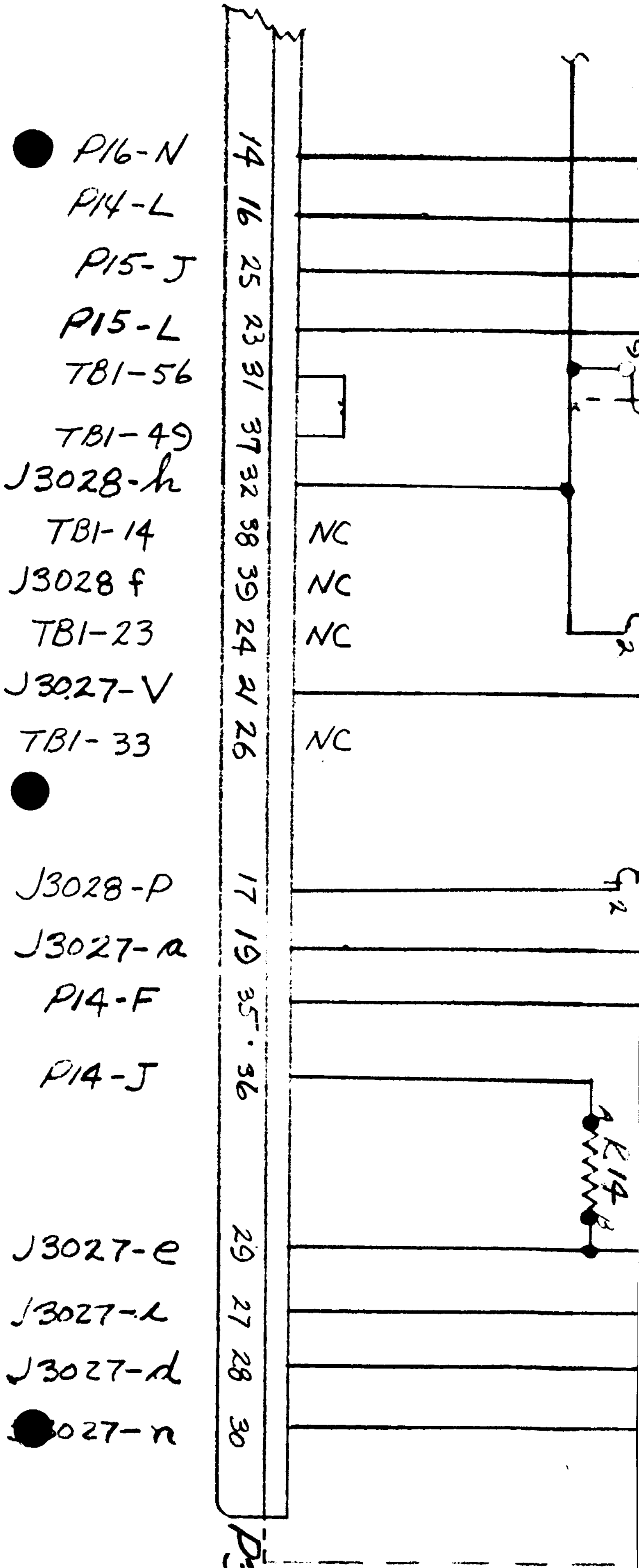

P16-N 14
P14-L 16
P15-J 25
P15-L 23
TB1-56 31
TB1-49 37
J3028-h 32
TB1-14 38 NC
J3028 f 39 NC
TB1-23 24 NC
J3027-V 21
TB1-33 26 NC
J3028-P 17
J3027-a 19
P14-F 35
P14-J 36
K14
J3027-e 29
J3027-l 27
J3027-d 28
027-n 30
P3

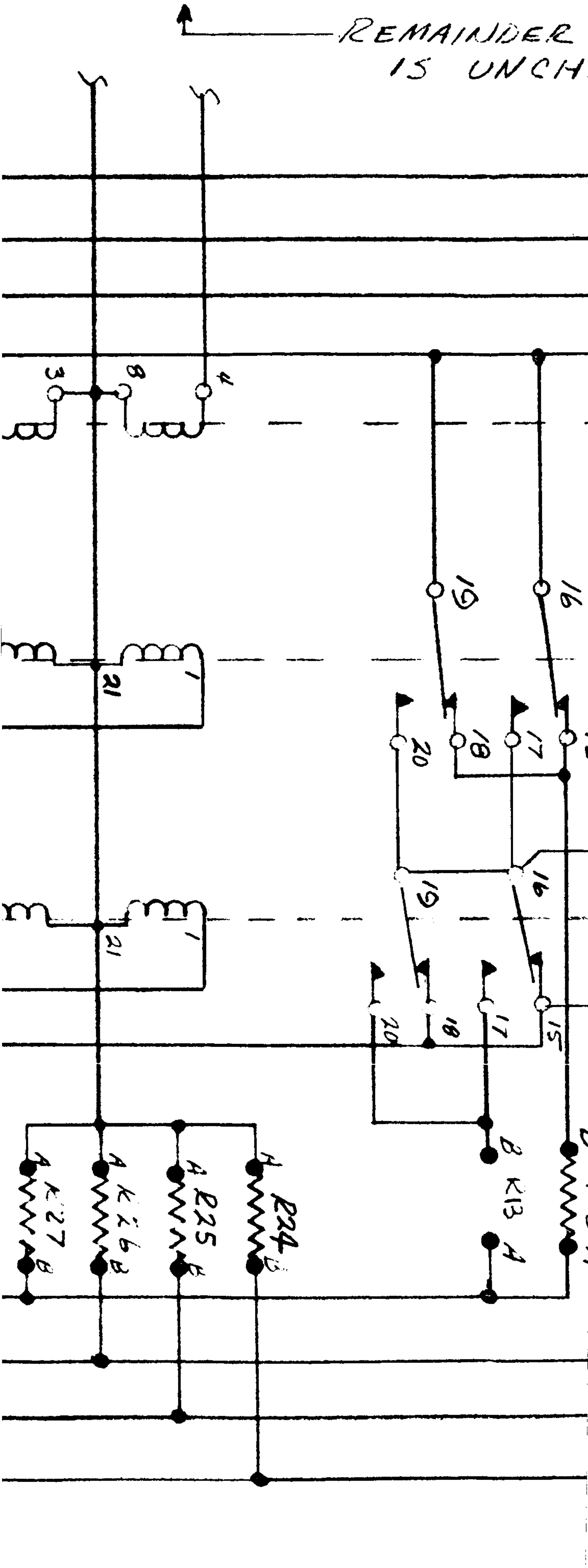
REMAINDER
IS UNCH
3
8
4
19
16
21
1
20
18
17
15
B
K13
A
R27
K26
R25
R24

89 2

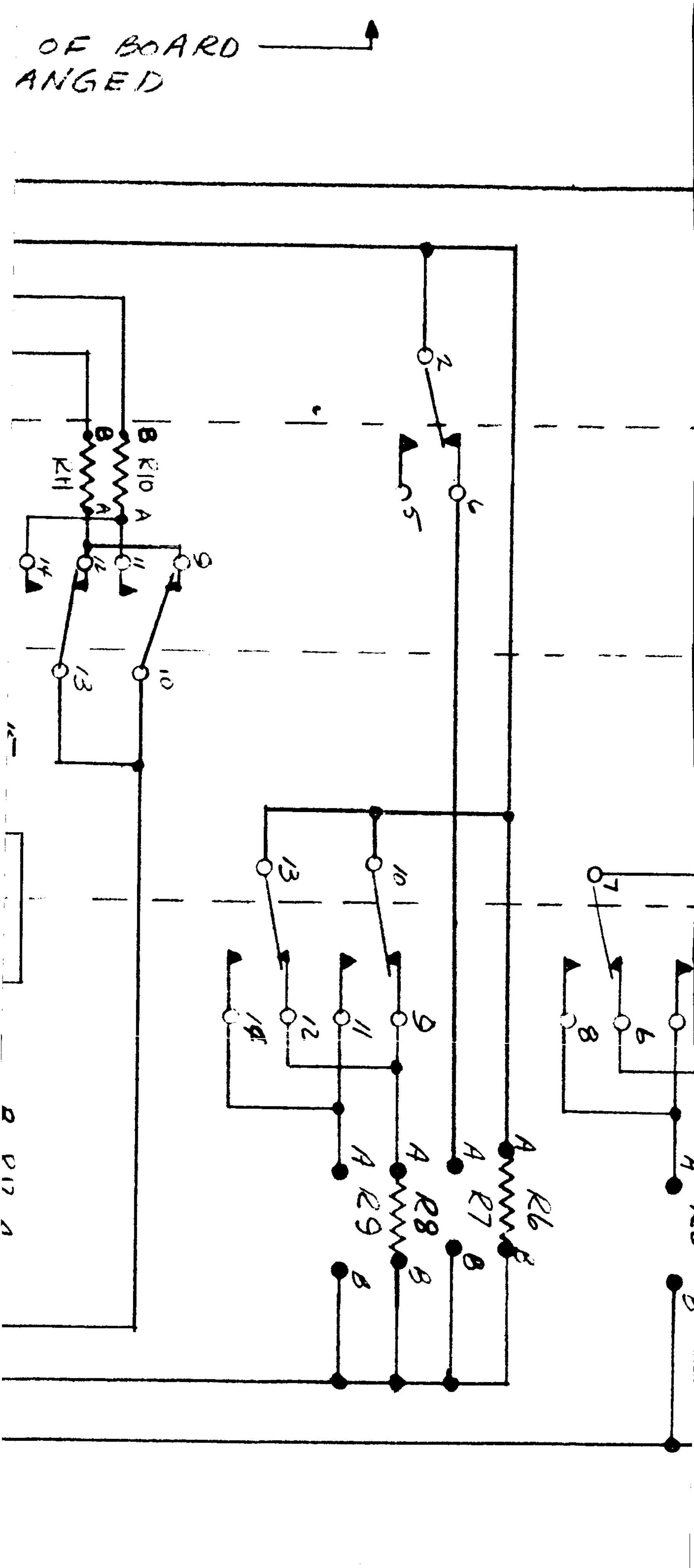

OF BOARD
ANGED
R11
R10
R9
R8
R7
R6

FIGURE 5.71

UNCONVENTIONAL VEHICLE — SPACECRAFT

IRP GAIN CIRCUIT - PITCH & YAW MODIFIED

23.175
5.89

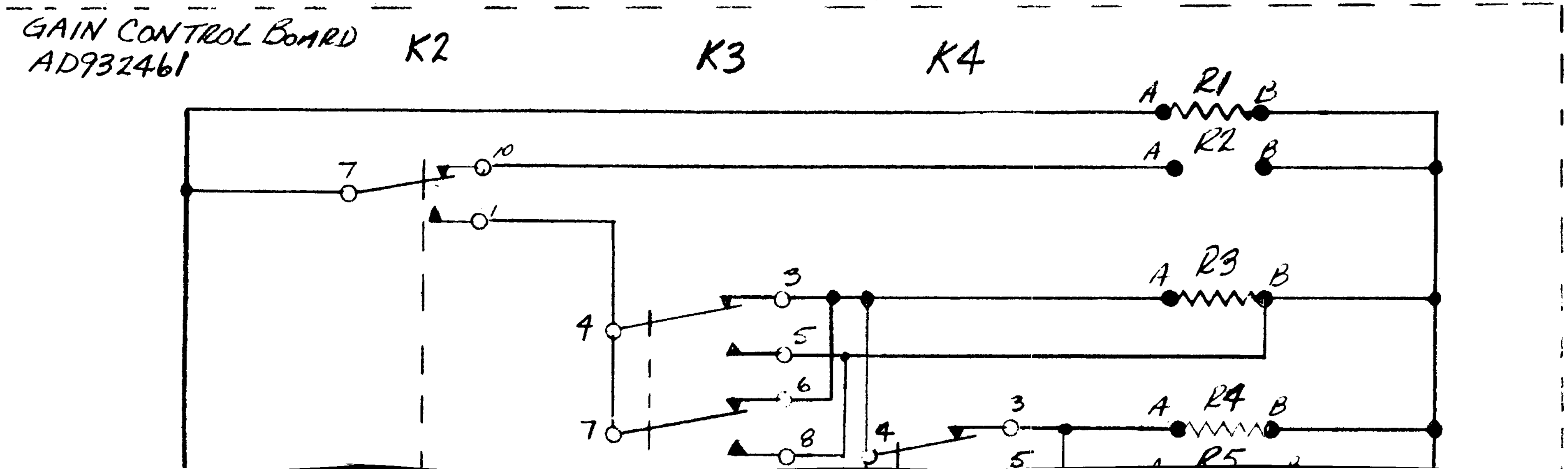

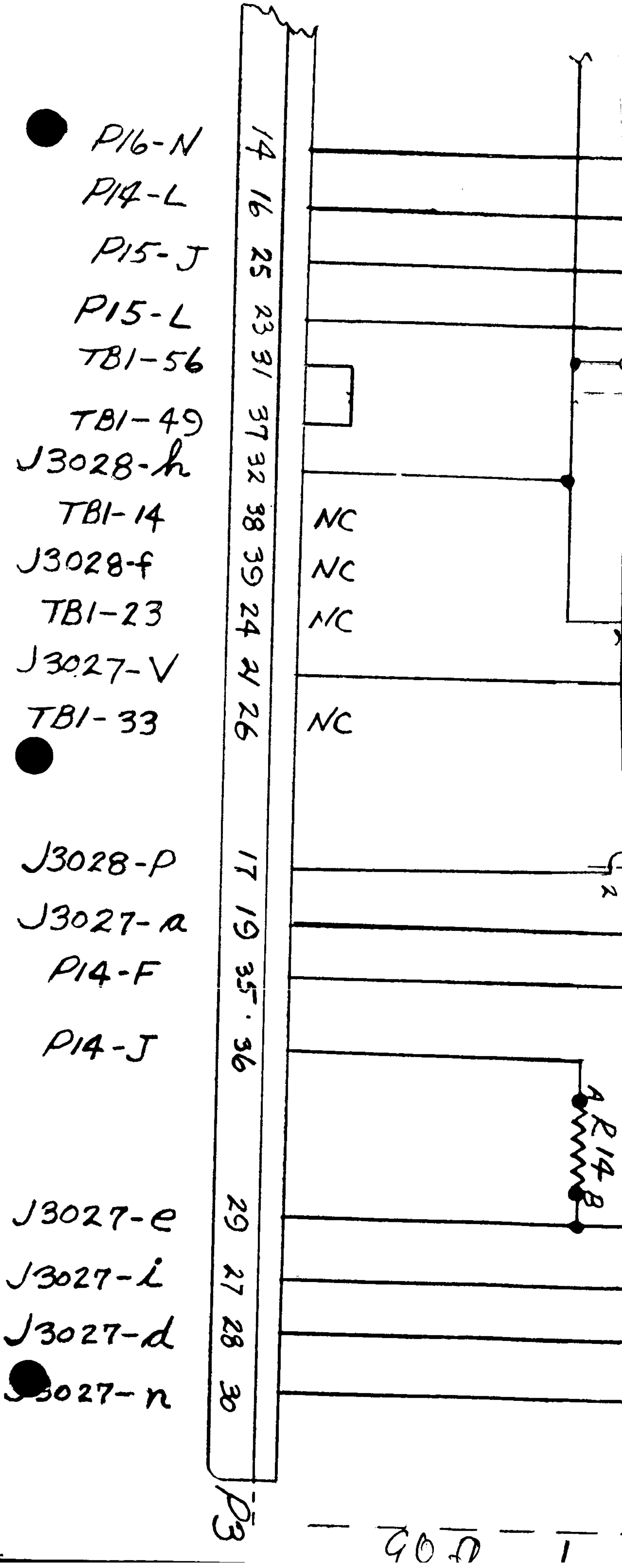
P16-N 14
P14-L 16
P15-J 25
P15-L 23
TB1-56 31
TB1-49 37
J3028-h 32
TB1-14 38 NC
J3028-f 39 NC
TB1-23 24 NC
J3027-V 21
TB1-33 26 NC
J3028-P 17
J3027-a 19
P14-F 35
P14-J 36
A R14 B
J3027-e 29
J3027-i 27
J3027-d 28
J3027-n 30
P3

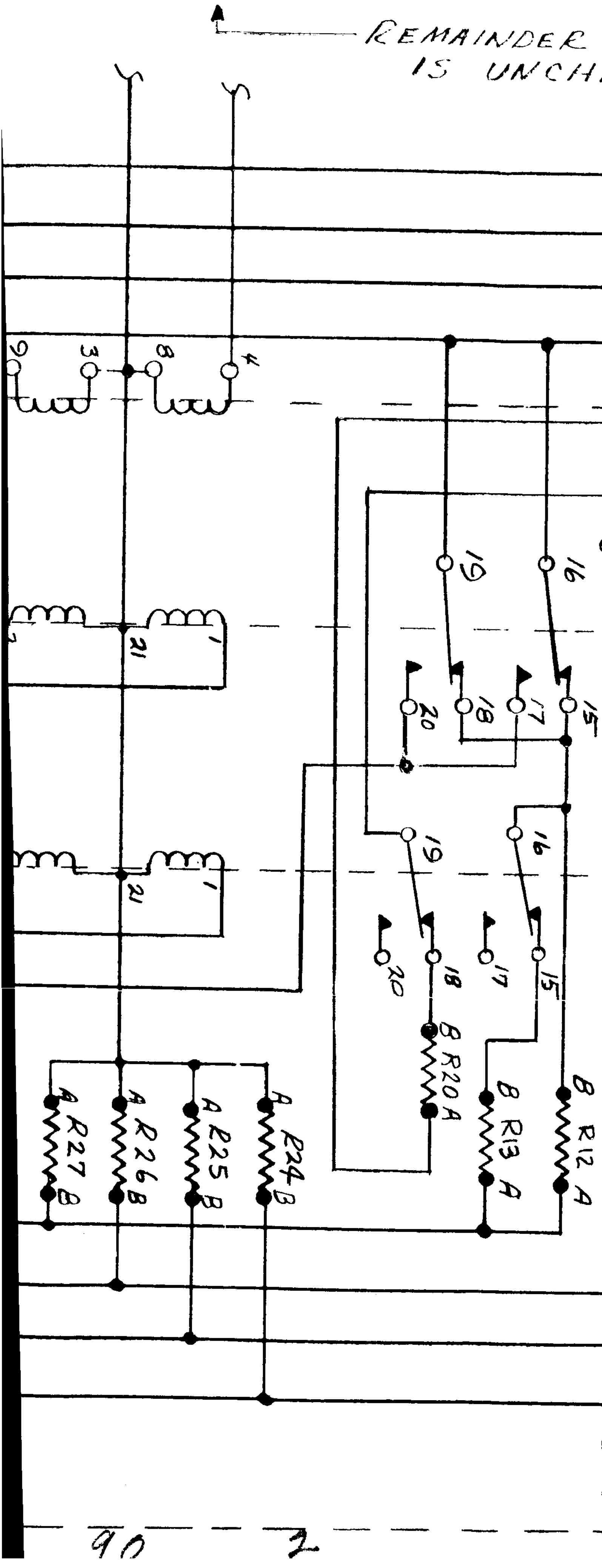
REMAINDER
IS UNCH
A R27 B
A R26 B
A R25 B
A R24 B
B R20 A
B R13 A
B R12 A
21
21
90
2

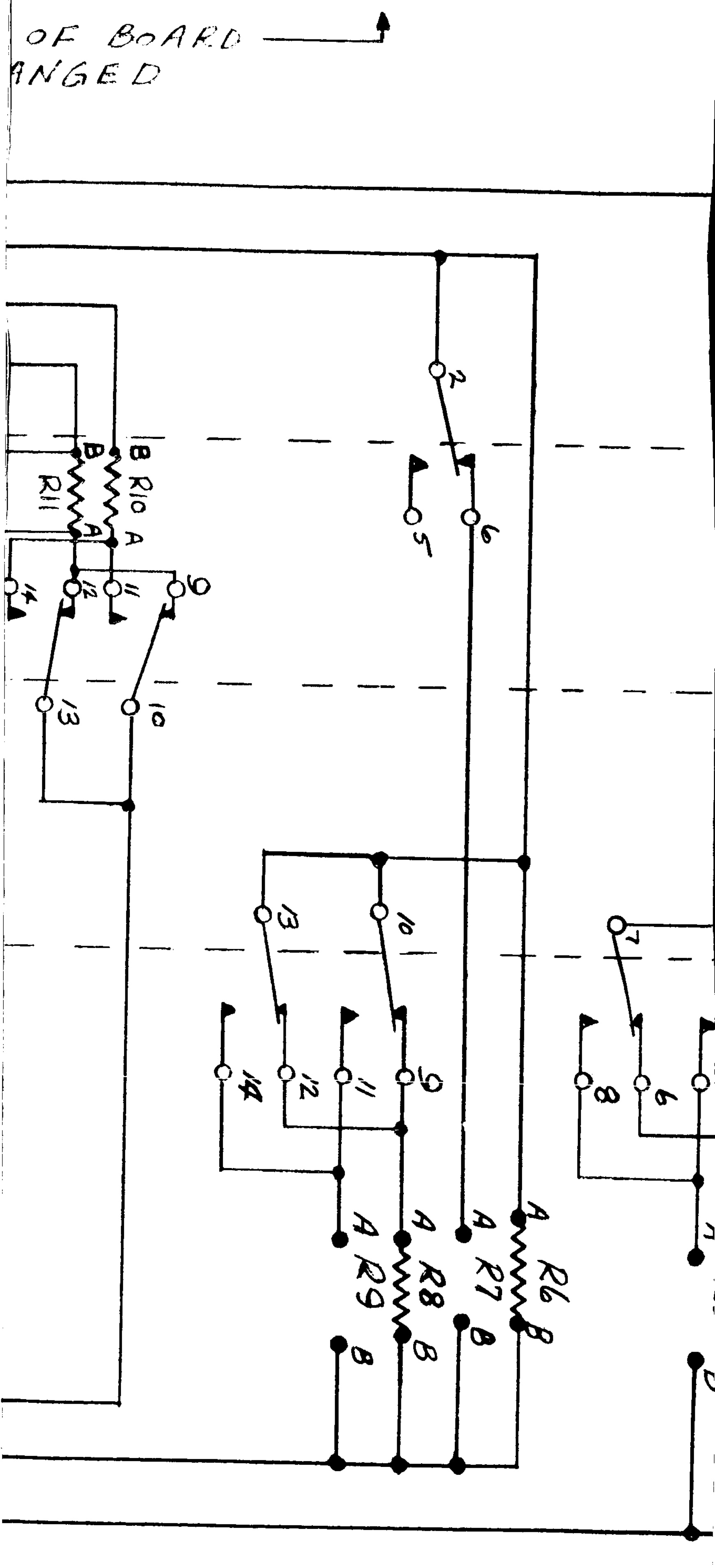
OF BOARD
ANGED
R11
R10
R9
R8
R7
R6

FIGURE 5.72

UNCONVENTIONAL VEHICLE – SPACECRAFT

IRP GAIN CIRCUIT – PITCH, YAW & ROLL MODIFIED

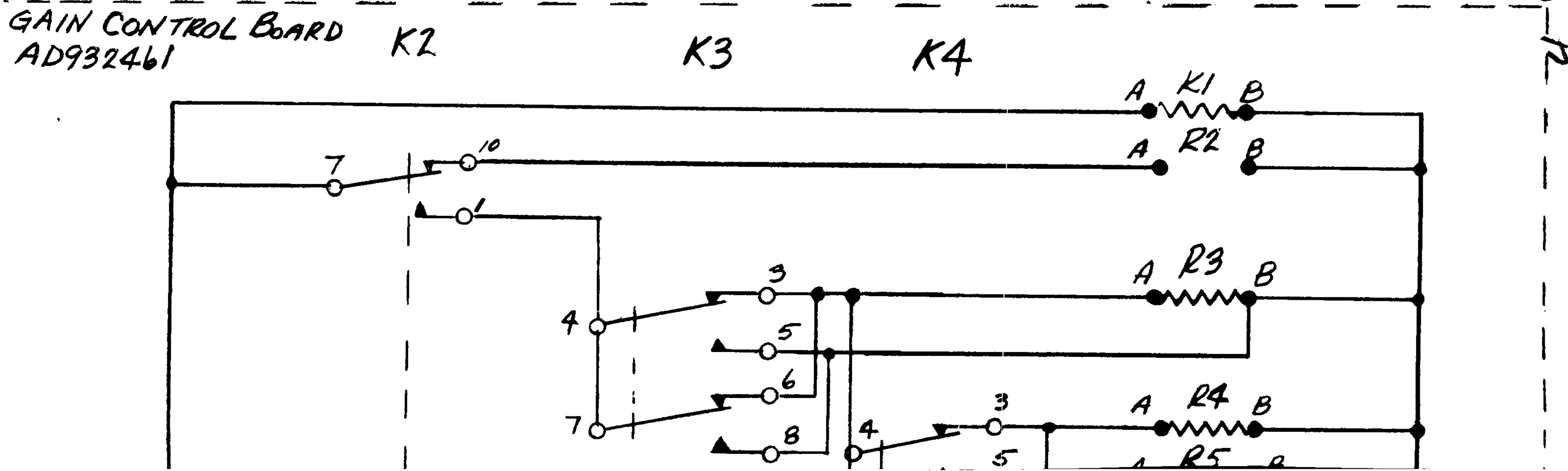

FIGURE 5.73

UNCONVENTIONAL VEHICLE – SPACECRAFT INTERVALOMETER & RELAY INTERCONNECTION

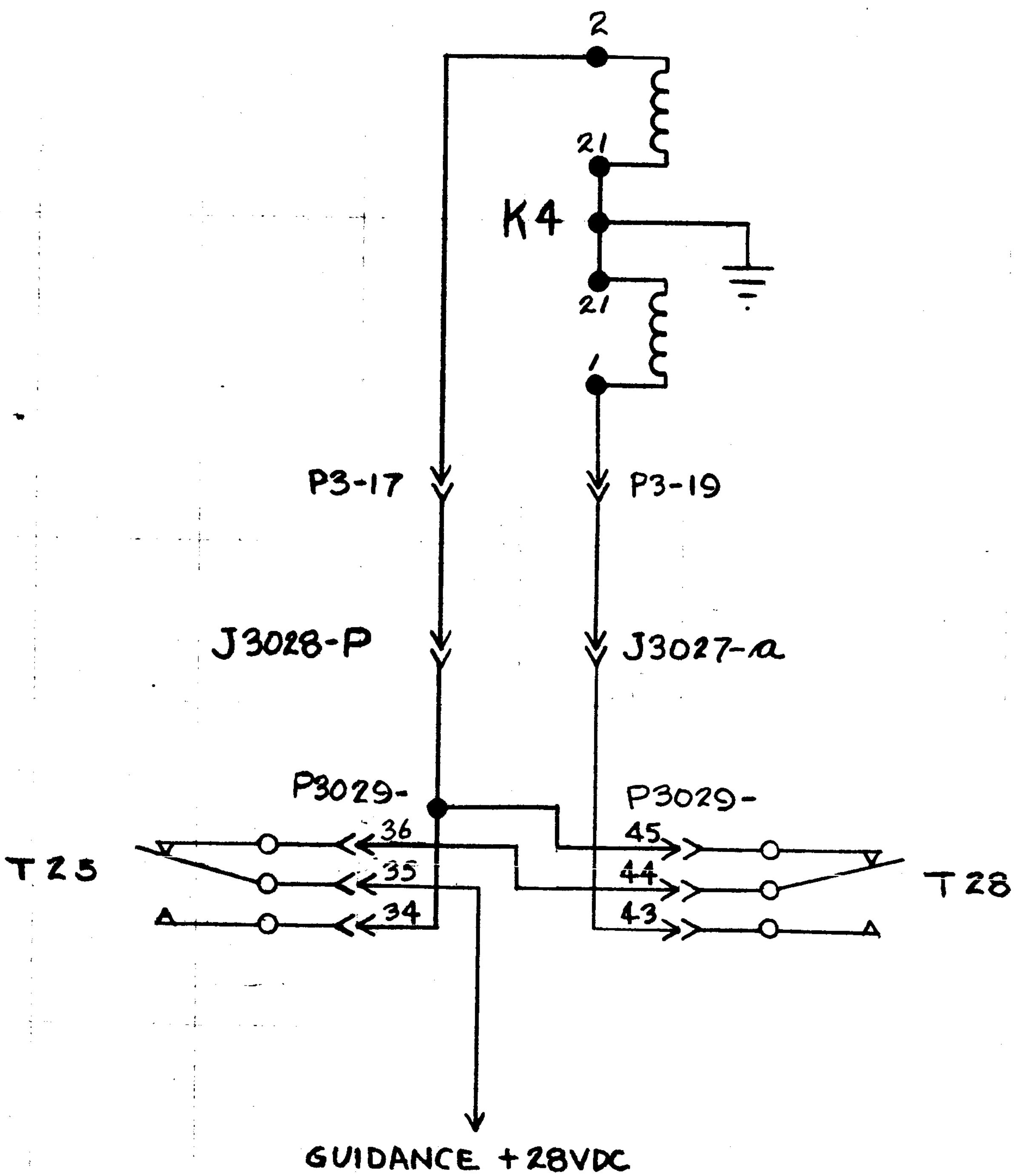

1. T28 – ACTUATES TO CHANGE GAIN FOR 2ND ST. COAST
2. T25 – ACTUATES JUST PRIOR TO 3RD ST. IGN. TO CHANGE GAIN BACK TO THE 2ND ST. BURN GAIN.

STUDY

"Unconventional Vehicle - Spacecraft Configuration"

VEHICLE DESIGN

Prepared by

C. Doucette
C. Doucette

B. J. Curb
B. J. Curb

Reviewed by

M. E. Jarrell
M. E. Jarrell

6.0 VEHICLE DESIGN

Two vehicle configurations of Scout have been developed to accommodate the Hypervelocity Reentry requirements. Case IA configuration has its payload housed within the Fourth Stage heat shield. Case IIA configuration utilizes no heat shield. The general arrangement of these configurations is shown in Figure 6.1.

6.1 CASE IA

This configuration is a standard Scout vehicle with the Fourth Stage removed. Housed within a standard 34" diameter heat shield and attached directly to the fourth stage separation clamp joint is a 300 pound conical reentry payload. Figure 6.2 shows this configuration.

6.1.1 Payload Configuration

The maximum length of a conical payload which can be contained within the heat shield has a forward limit at Scout Station -11.0. For this configuration the aft limit is established by clearance with the separation clamp and by space requirement for attaching the payload to the clamp adapter ring. Scout Station 98.25 has been determined to be the aft limit. The length of the conical portion of the reentry body is therefore set at 109.25 inches.

The base diameter of a cone of this length can be no greater than 24.0 inches. This may be reduced to 22.0 inches if the aerodynamic effects of the clamp adapter ring can be tolerated.

The resulting cone half-angle is 6°16' or 5°45' depending on the base diameter selected.

Provisions must be made on the payload to accommodate the adapter as shown in Section C-C of Figure 6.2.

6.1.2 Vehicle Structure

Case IA requires no major structural modification to the Scout vehicle. The payload will be attached to the existing Fourth Stage separation joint at Station 99.70 by the use of an adapter ring. Installation and removal of the payload will be accomplished by a ring of bolts at Station 98.25. The adapter will be designed to mate with the payload as shown in Section C-C of Figure 6.2.

6.1.3 Heat Shield

A standard Scout heat shield, such as 23-002860-1, can be modified for this configuration.

Modifications will consist of special payload access doors, payload umbilical provisions, and revision to the electrical wire routing to the heat shield. The standard routing of the wiring to the heat shield is through the Fourth Stage Upper "D" Section. Since the payload occupies this space in this configuration, a new routing will be employed as shown in Section C-C of Figure 6.2.

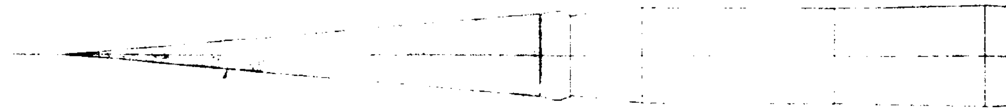

PAYLOAD

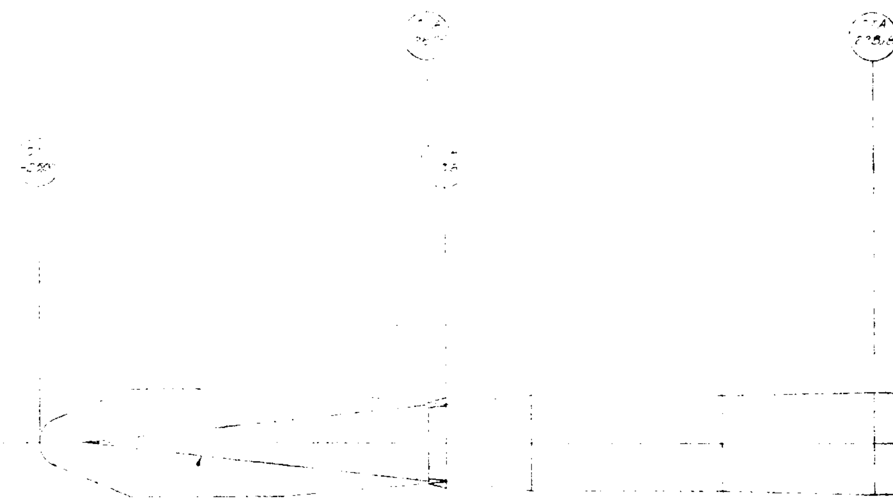

6.2 #1

612 (2)

CONFIGURATION II A

[illegible] PAYLOAD - NO HEAT SHIELD

CONFIGURATION I A

[illegible] PAYLOAD 34 [illegible] HEAT SHIELD

FIGURE

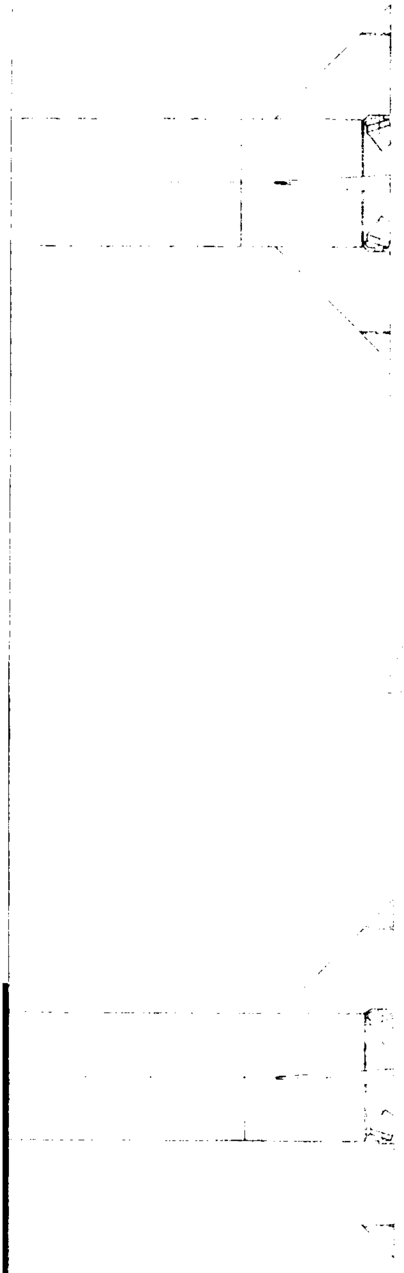

62(3)4

FIGURE 6.1

PROJ ENGR		
STR DSGN		
GR APPD	[illegible]	[illegible]
CHK BY		

GENERAL ARRANGEMENTS
HYPERVELOCITY RE-ENTRY PAYLOAD
SCOUT

6-3 (1)

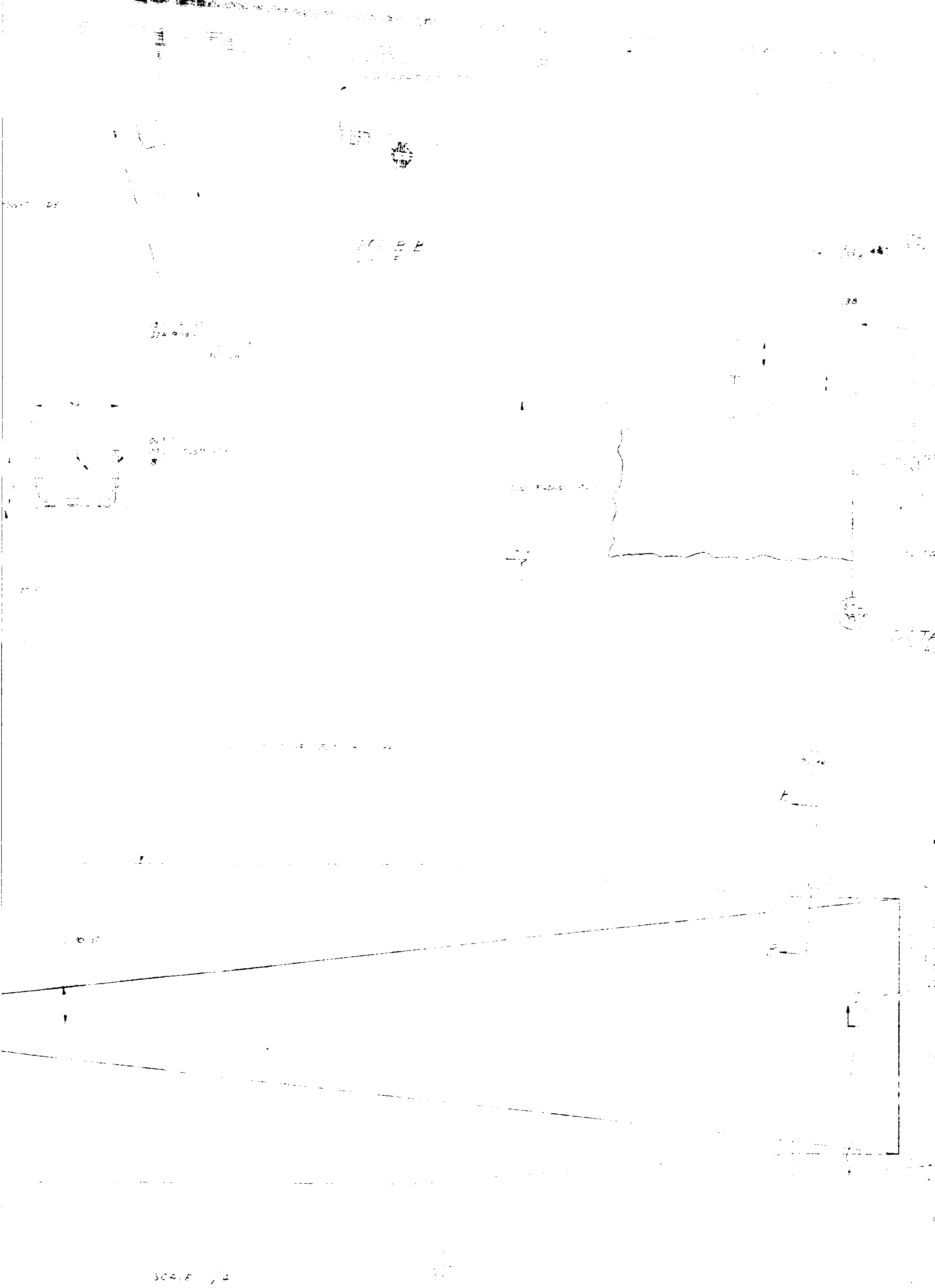

6.3 (2)

FIGURE 6.2

6.3 (3)

PROJ ENGR		
STR DSGN		
GR APPD		
CHK BY		
DRAWN BY		
ENGRG UNIT NO.		

VEHICLE MODIFICATION
CONICAL PAYLOAD INSTL
34 INCH HEAT SHIELD

CODE IDENT NO.	SIZE	
11813		399-998105

Heat shield separation for this mission will be initiated at the end of the Second Stage coast period as is typical on all standard Scout trajectories.

6.1.4 Electrical

The only modification required in the Scout Ignition System is the revision to the Heat Shield and Lower "D" Section wiring harnesses to accomplish the re-routing shown in Section C-C, Figure 6.2.

In the Guidance System a minor rework is required to add one wire between the Timerand the IRP, to add one jumper between two inner channels, and to relocate the power input of one channel to another channel of the Timer. These changes are required to accomplish the dead-band switching required for the long coast period.

No provisions are made for an electrical interface with the payload.

6.2 CASE IIA

This configuration is a Scout vehicle with the Heat Shield and Fourth Stage removed and with a conical payload attached to a modified Spin Table. The modified area is shown in Figure 6.3.

6.2.1 Payload Configuration

This payload is defined as a 5° half-angle cone with a length of 150 inches. The payload weight will be between 300 and 600 pounds.

Provisions must be made on the payload to accommodate an Adapter and a Spin Table fairing as shown in Section A-A of Figure 6.3.

6.2.2 Vehicle Structure

Strucural modifications for this configuration are limited to the area forward of Lower "D" Section. Without the Heat Shield to carry the primary vehicle loads during First and Second Stage operations, the existing Scout spin bearing joint is inadequate to provide proper support for this payload. A completely revised Spin Table Assembly is proposed which will be clamped directly to Lower "D" Section clamp ring. This will provide a load path which by-passes the spin bearing. Explosive bolts remove the clamp to free the section for spin-up. Spin-up and payload separation can then be initiated as in the standard Scout (Ref. Figure 6.3.).

6.2.2.1 Spin Table Assembly

A new assembly is provided to which the payload will be attached at Scout Station 98.25. An adapter ring permits the payload to be clamped to the basic Spin Table structure using a joint similar to the existing Scout "cold-separation joint." Details of the clamp joint will only be changed because of the larger diameter of the section.

A one-piece shell is proposed between the separation joint and the spin bearing. This piece may be machined from a casting or from a roll-ring forging.

6.5 ①

6.5 (2)

6.5 (5) FIGURE 6.3

VEHICLE MODIFICATION
CONICAL PAYLOAD INSTL
NO HEAT SHIELD

CODE IDENT NO. 11813

399-998106

Rings on each end provide for clamping to the "cold-separation" joint and to the existing clamp ring on Lower "D" Section. The aft end of the structure will also serve as a housing for the existing Scout spin bearing.

Spin motor installation will be basically unchanged except that, as a by-product of the redesign, an approximate 10% increase in moment arm is obtained.

The aft clamp assembly will be integrated into a fairing which covers the spin table area.

6.2.2.2 Spin Table Fairing

A fairing is required over the Spin Table area to provide thermal protection for the section during the early part of the flight. This fairing is proposed to be made in two identical segments. It extends from a lip to be provided on the payload to a point on Lower "D" Section. The segments are held in place by virtue of being attached to the band clamp at Station 103.81. The detonation of the explosive bolts on the band clamp frees the segments. Spring ejectors at the separation plane force the segments away from the vehicle in a manner similar to the Scout Heat Shield ejection. The same type explosive bolt will be used on the aft clamp as is used at the payload separation joint.

6.2.3 Electrical

The Scout Ignition system will be modified to accommodate the elimination of the Heat Shield and Fourth Stage ignition functions and the addition of the Spin Table Fairing Clamp separation function.

A schematic representing the vehicle ignition system (power circuit) is shown in Figure 6.4. The Spin Table Fairing Clamp separation requires the use of two additional sets of power control relays. Since no spare relays are available in the present Power Control Relay Assembly (401-10380), a tandum P.C.R. Assembly is required. It will utilize the interlock relays in the present P.C.R. Assembly and will be controlled by two timer channels, which are available in the 28 channel timer. The existing Third Stage Arming Relay Assembly (23-002564) can be used in its present configuration. The Spin Table Fairing Clamp circuit will utilize the 25 Inch Heat Shield (Belly Bands) arming commands, however, the power circuit wiring to the Arming Relay Assembly must be changed to route from the new tandum P.C.R. Assembly instead of being parallel with the 2nd Stage Ignition Circuit. Figure 6.5 shows the tandum P.C.R. Assembly and the wiring changes required for the addition of the Spin Table Fairing Clamp ignition function. Additional wiring is necessary between the Timer and the tandum P.C.R. Assembly for control of the ignition function.

The spring loaded disconnects for electrical separation of the Spin Motor circuit is eliminated. However, the Spin Motor circuit will require resistors to balance the power to the separation bolts should a short occur when the Spin Motors fire.

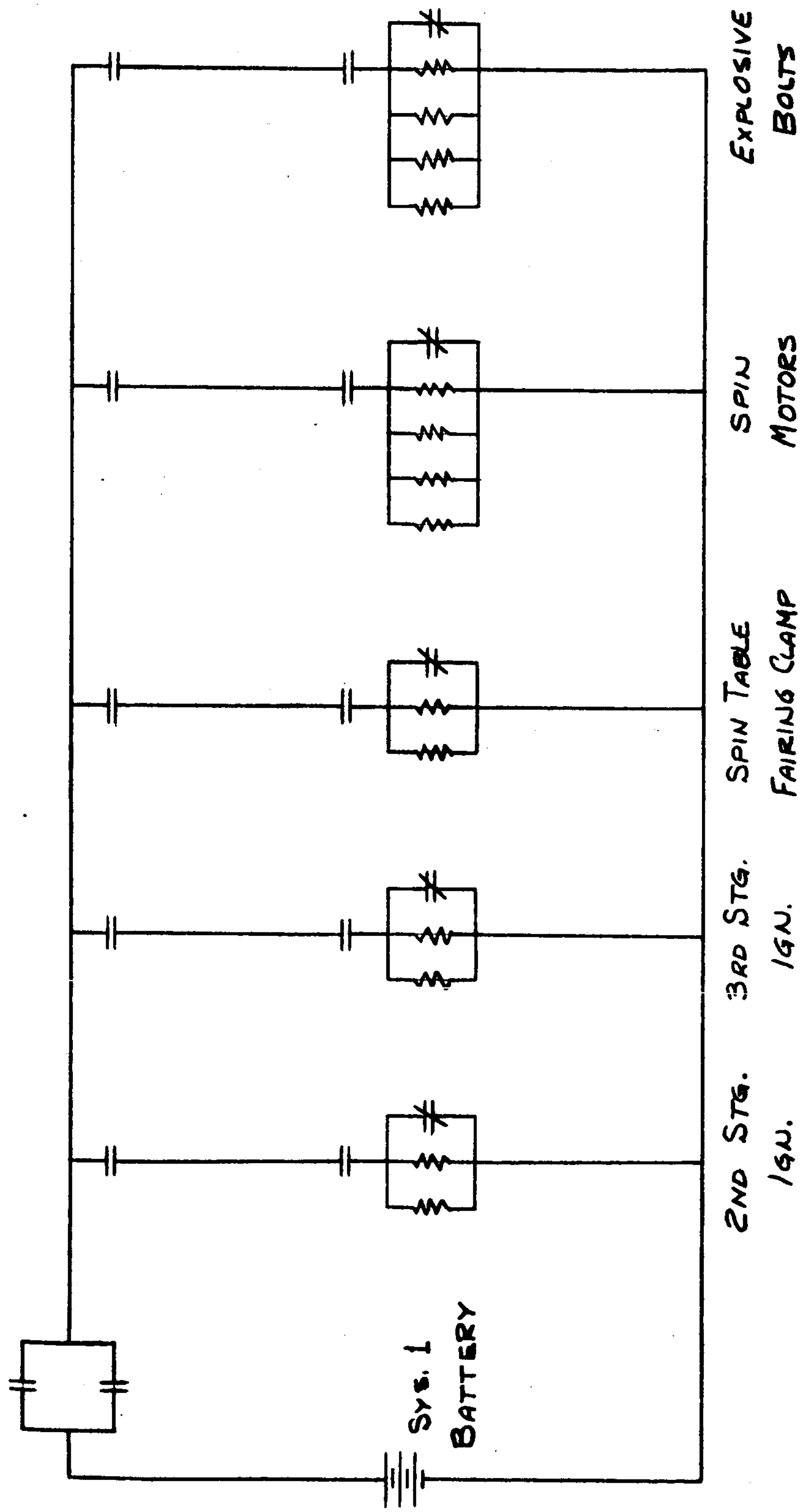

FIGURE 6.4
SCHEMATIC OF IGNITION FUNCTIONS
(SYSTEM 1 ONLY)

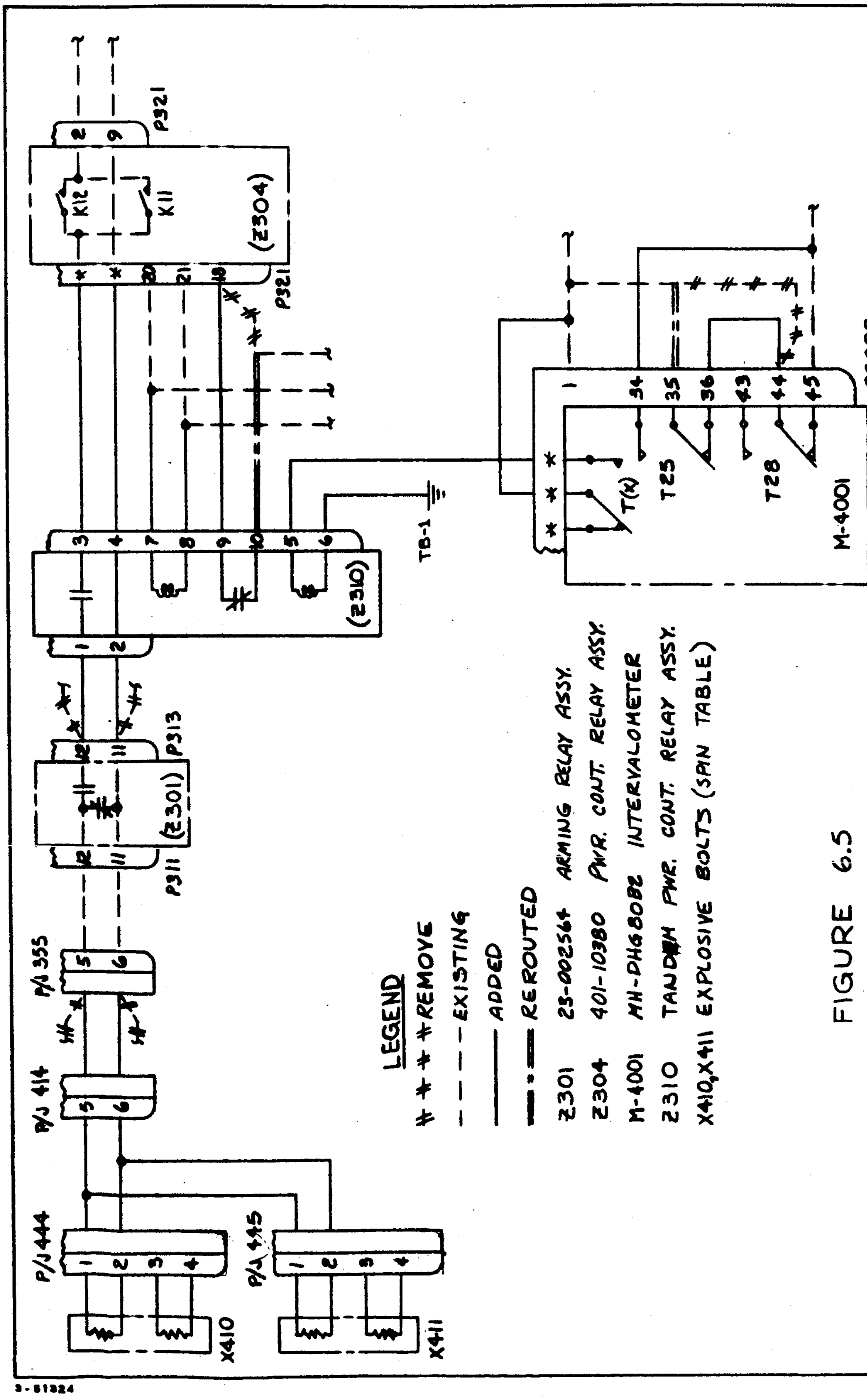

FIGURE 6.5
WIRING DIAGRAM SHOWING IGNITION AND GUIDANCE SYSTEM CHANGES
(SYSTEM 1 ONLY)

The harness routing will be inside the new Spin Table assembly. Holes will be cast 90° apart for mounting connectors on the adapter's external surface. Figure 6.6 shows the approximate harness routing.

In the Guidance System, a minor rework is required to add one wire between the Timer and the I.R.P., to add one jumper between two timer channels, and to relocate the power input of one channel to another channel of the Timer. These changes are required to accomplish the dead-band switching required for the long coast period.

No provisions are made for an electrical interface with the payload.

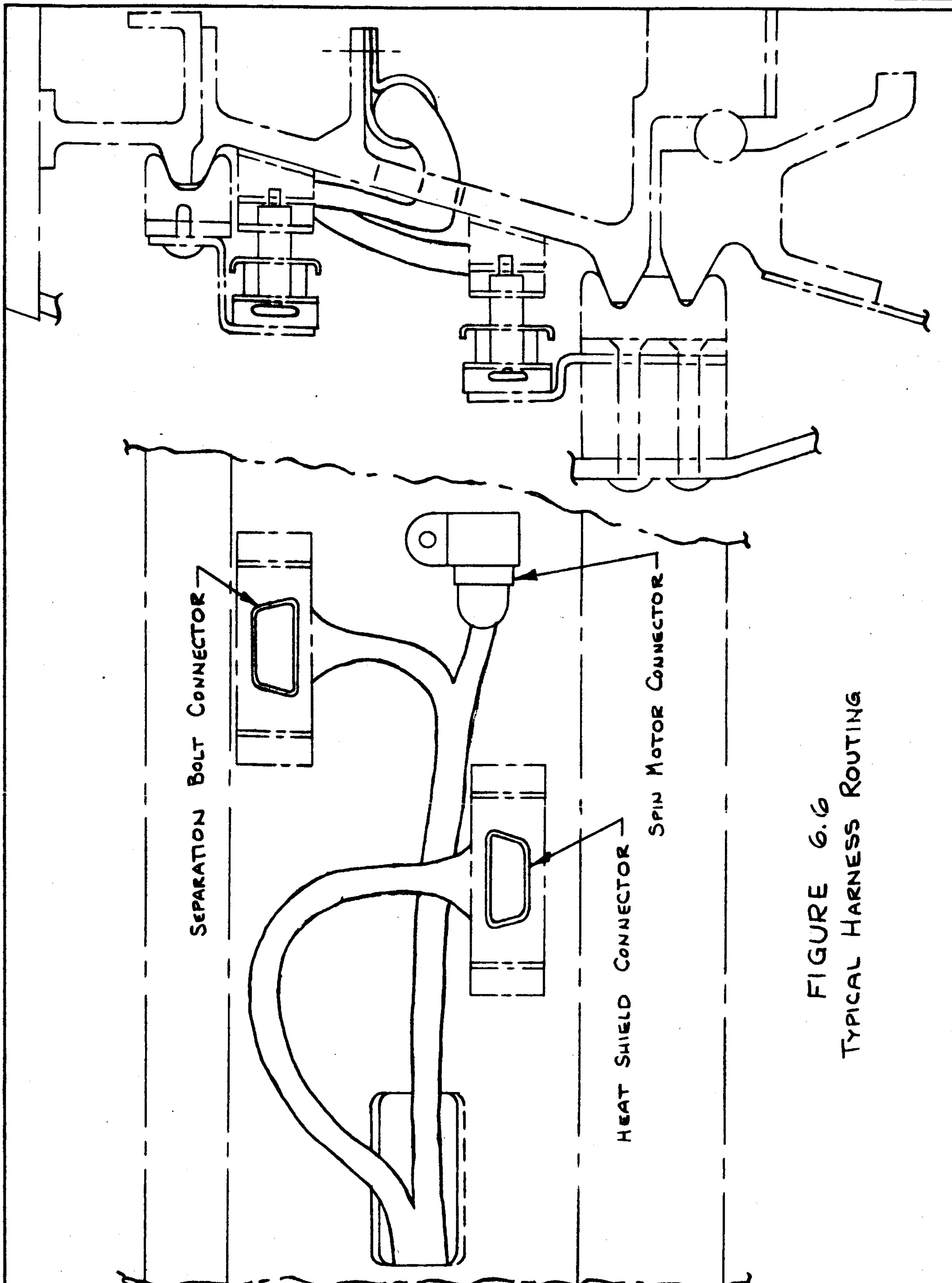

FIGURE 6.6
TYPICAL HARNESS ROUTING

STUDY

"UNCONVENTIONAL VEHICLE - SPACECRAFT CONFIGURATION"

VEHICLE PERFORMANCE

PREPARED BY:

C. O. McGregor

J. J. Banchetti

REVIEWED BY:

J. L. Midgorden

7.1 STUDY OBJECTIVE AND MISSION DESCRIPTION

The objective of the performance portion of this study is to demonstrate the ability of a three stage Scout launch vehicle to provide a specified atmospheric re-entry environment spectrum. The mission spectrum to which this study is addressed is defined as follows:

Re-Entry Altitude	100,000 feet
Re-Entry Velocity	Maximum
Re-Entry Angle	-30 to -60 degrees
Payload Weight	300 to 600 pounds
Range at Re-Entry	Case 1: Unconstrained Case 2: 620 ± 100 n.mi.

A parametric study was conducted to determine the effects of payload weight and re-entry angle in the ranges specified, on re-entry velocity. These effects are presented below under Performance Capability. The Scout launch facilities at Wallops Island, Virginia were assumed and the vehicle trajectories were flown to pass within 90 nautical miles of Bermuda Island, which is the present range safety criteria.

7.2 VEHICLE DESCRIPTION

The performance presented is based on a standard Scout launch vehicle with the fourth stage and associated structural transition sections removed. The conical payload is attached, as described in Section 6.0, to the lower "D" transition section.

7.2.1 MOTOR PERFORMANCE

The thrust and consumed-weight-remaining time histories for the three motors used in this study are presented in Tables 7.1 through 7.3. The Algol IIB used as a first stage is the motor currently being flown as the first stage of Scout. The Castor II data shown in Table 7.2 represents an advanced version, currently under development, of the present Scout second stage. Table 7.3 shows performance data describing the current Scout third stage, the X-259 Antares. These motor data represent nominal performance levels for these three motors.

7.2.2 WEIGHTS

Vehicle weight, center of gravity and inertia data are shown in Section 2.0 and are not repeated here. However, as noted in Section 2.0, two sets of weights data are presented. The performance data presented are based on the preliminary weights since the final weights were not known until the design was completed. The differences are small, the most significant being the 9 pound increase in third stage weight. This increase means the velocity numbers quoted are approximately 30 fps optimistic. This difference was not deemed significant enough to recompute all the performance data.

7.2.3 AERODYNAMICS

The Statement of Work (Reference 1) specifies two basic vehicle configurations. One (Case IA) requires the payload to be contained within the present 34 inch diameter Scout heatshield. The other (Case IIA) specifies that no heatshield be used and the payload be exposed to the free stream during the entire boost phase of the trajectory. The only significant difference between the two cases, from a performance standpoint, is that the no-heat-shield case, because of its reduced drag coefficient, produces a smaller drag loss during first stage operation. The performance shown represents the case with the heatshield on, because at the time this performance was initially determined the drag for the no-heat-shield case was not available. The result is that for the no-heat-shield case the velocity performance shown is approximately 250 feet per second low. This small difference in velocity did not warrant recomputing the entire performance spectrum for the no-heat-shield case.

7.3 BOOSTER STAGING AND TRAJECTORY PROGRAMMING

The spectrum of re-entry missions considered in this study are particularly suited to the three stage Scout vehicle. The majority of the performance information presented represents a booster staging technique in which the first two stages are fired in rapid sequence on the ascent leg of the trajectory, (the second stage is ignited as soon as the dynamic pressure has reduced to 35 psf following first stage burnout) and the third stage is fired on the descent leg, driving the payload back into the atmosphere. The only significant difference between these three stage trajectories and previously flown Scout trajectories is the second stage coast times. The second stage coast times required to provide the necessary re-entry angles specified in this study are from two to three times as long as the present Scout control system operating limit. However, by opening the deadband widths and modifying the control system gains the coast times required can be achieved with only minor modifications to the present system. These control system changes are discussed in detail in Section 5.0.

In addition to the two stage ascent - one stage descent staging arrangement some performance information obtained earlier in the study for a three stage ascent staging is also presented. This technique requires all three stages to be fired in sequence, imparting all the energy of the booster system to the payload in a very short time after launch. These types of trajectories produce ranges at re-entry on the order of 2000 to 4000 nautical miles and third stage coast times in excess of 2000 seconds. These coast times are again beyond the capabilities of the current control system and modifications, similar to those mentioned above, would be required to maintain attitude control during these long coast periods. This technique is presented more for academic interest because the long ranges to re-entry present problems, particularly with respect to down range radar tracking facilities, which are not practical in view of the satisfactory performance achieved by the other staging method.

Performance data are shown below for two cases of the two stage ascent one stage descent booster staging technique. One case represents ballistic trajectory performance for the entire range of entry angles and payload weights. In this case the range to re-entry is not a trajectory constraint and is merely the range consistent with the ballistic performance. However, for the shallow re-entry angles, between -30 and approximately -48 degrees (depending on payload weight), the range to re-entry is too long to provide adequate radar tracking margin from the Bermuda tracking facilities. For this reason a second family of performance data is presented which corresponds to the case in which the range is constrained to a maximum of approximately 700 nautical miles. Adding the additional constraint of range to the trajectory development requires the adoption of shaping techniques. These shaping techniques require the design of an optimum pitch pointing or attitude program in the second and third stage which will result in a foreshortened range. The utilization of this technique requires that the vehicle no longer fly a ballistic trajectory and the performance loss is a function of the severity of the shaping required. The performance penalties resulting from this constrained range case are demonstrated in the data presented.

7.4 PERFORMANCE CAPABILITY

The preceding paragraphs have discussed the mission requirements, vehicle configuration, booster staging and trajectory programming used in this study. The following paragraphs will discuss and present the results for the unconstrained and constrained range cases.

7.4.1 UNCONSTRAINED RANGE CASE

7.4.1.1 Three Stage Ascent Staging

As mentioned in paragraph 7.3, limited performance data were obtained for the three stage ascent staging arrangement. In Figure 7.1 the re-entry velocity and re-entry angle are presented as functions of re-entry range for both 300 and 400 pound payloads. This performance was not extended to encompass heavier payloads because of the extremely long range trajectories resulting from this staging technique. As will be obvious in the two-stage-ascent one-stage-descent data which follows, the velocity performance is comparable for the two methods as long as the range is not constrained. Therefore, if heavier payload performance for this technique should become of interest the velocities shown in Figure 7.3 would be representative. The third stage coast times required to fly these long trajectories are presented in Figure 7.2.

7.3.1.2 Two Stage Ascent One Stage Descent

The basic performance for this staging technique in the unconstrained range case is presented in Figure 7.3. Re-entry velocity is shown as a function of re-entry range for a payload range from 300 to 600 pounds and a re-entry path angle range from -30 to -60 degrees. All re-entry conditions are at an altitude of 100,000 feet. The second stage coast times corresponding to this performance are given in Figure 7.4.

Figure 7.5 presents typical altitude-range profiles for a -30, -45 and -60 degree re-entry angle trajectory. These three profiles are for a 400 pound payload and show graphically the effect of re-entry angle on peak altitude, range and trajectory positioning of the third stage firing. Similarily, the geographical positioning of these trajectories is shown in Figure 7.6. These trajectory ground tracks show the trajectories passing approximately tangent to the 90 nautical mile range safety circle around Bermuda Island.

Time histories of altitude, earth relative velocity, range and path angle for a 400 pound payload for -30, -45 and -60 degrees re-entry angles are shown in Figures 7.7, 7.8 and 7.9, respectively. Figure 7.10 presents a velocity versus altitude plot for the same set of trajectories.

7.4.2 CONSTRAINED RANGE CASE

A nominal range to Bermuda is 620 nautical miles. This study allowed a ±100 nautical mile tolerance on this range. Referring to Figure 7.3 it can be seen that a portion of the shallow re-entry angle performance is outside this range tolerance. As discussed above, shaping techniques were applied to the trajectory development in this region restricting the range to 700 nautical miles. The velocity performance with range constraint is presented in Figure 7.11 as a function of payload weight and re-entry angle. The following table shows a velocity comparison between the constrained range and nonconstrained range cases for a re-entry angle of -30 degrees.

PAYLOAD	BALLISTIC TRAJECTORY	SHAPED TRAJECTORY	SHAPING PENALTY
300	21,480 fps	21,030 fps	450 fps
400	20,870 fps	20,520 fps	360 fps
500	20,260 fps	20,020 fps	240 fps
600	19,750 fps	19,620 fps	130 fps

This trajectory shaping also affects second stage coast time and this effect is shown in Figure 7.12.

7.5 TRAJECTORY LISTINGS

This study also includes one copy of a selected set of the IBM digital computer output listings. This set of listings includes twelve (12) trajectories representative of the unconstrained range case and eight (8) trajectories representative of the constrained range case. The trajectory book contains a detailed index of these trajectories.

TABLE 7.1

FIRST STAGE ROCKET MOTOR PERFORMANCE DATA

ALGOL IIB

CONS WEIGHT = 21458.00
PROP WEIGHT = 21174.00
TOTAL WEIGHT = 23725.0

TOTAL IMPULSE	SPECIFIC IMPULSE	EXIT AREA
5469074.8	258.292	5.647

TIME	JET VANE DRAG	THRUST*	WT. REMAINING
0.00	1212	91942.0	21458.00
0.20	1320	95398.0	21384.50
0.50	1355	102311.0	21268.14
0.70	1433	103793.0	21187.27
1.20	1308	98855.0	20988.50
1.50	1303	96385.0	20873.60
2.70	1284	94904.0	20423.28
5.00	1288	95201.0	19565.52
13.40	1377	101817.0	16318.91
25.40	1414	104583.0	11460.02
34.00	1477	109224.0	7852.86
42.60	1564	115643.0	4059.10
44.00	1564	115643.0	3423.88
48.40	1063	78609.0	1747.15
51.40	516	38118.0	1060.18
54.80	362	26761.0	627.44
56.80	282	20835.0	440.69
59.20	222	16392.0	265.42
66.00	36	2648.0	11.43
68.20	0	0.0	0.00

*Jet Vane Drag has not been subtracted out.

TABLE 7.2

SECOND STAGE ROCKET MOTOR PERFORMANCE DATA

CASTOR II

COMB WEIGHT = 8321.50
PROP WEIGHT = 8210.00
TOTAL WEIGHT = 9707.50

TOTAL IMPULSE	SPECIFIC IMPULSE	EXIT AREA
2337000.0	284.653	8.083

TIME	THRUST	WT REMAINING
0.00	57895.0	8321.50
0.80	53267.6	8163.17
1.40	51007.8	8051.78
2.60	48425.1	7839.35
3.00	48640.4	7770.22
8.00	56280.8	6836.22
10.00	58971.0	6425.84
13.00	62521.5	5776.93
16.00	65858.2	5091.24
20.00	68656.1	4133.29
24.00	69839.8	3146.99
26.00	69839.8	2649.62
28.00	69086.5	2154.94
30.00	68118.0	1666.39
32.00	66503.8	1187.03
34.00	64566.9	720.32
35.00	64351.6	490.79
35.60	62952.7	354.80
36.20	61769.0	221.57
36.50	59724.3	156.68
36.70	58648.0	114.53
37.10	37664.0	45.94
37.40	10761.1	20.08
37.70	5165.4	11.57
38.00	2152.2	7.66
40.00	0.0	0.00

TABLE 7.3

THIRD STAGE ROCKET MOTOR PERFORMANCE DATA

ANTARES X-259

CONS WEIGHT = 2580.00
PROP WEIGHT = 2555.00
TOTAL WEIGHT = 2795.00 *

TOTAL IMPULSE	SPECIFIC IMPULSE	EXIT AREA
712129.6	278.720	4.346

TIME	THRUST	WT REMAINING
0.00	0.0	2580.00
0.21	21680.8	2571.75
1.00	21081.9	2510.56
3.00	20781.9	2358.89
7.00	21900.6	2049.61
10.00	22560.9	1807.99
12.00	22834.2	1643.53
14.00	22987.6	1477.52
16.00	22941.1	1311.12
18.00	22743.1	1145.61
20.00	22185.7	982.84
24.00	21430.4	666.80
26.00	21078.9	512.79
28.00	20534.4	362.03
30.00	19554.3	216.79
30.69	18873.5	168.76
31.57	18008.0	109.97
32.73	15006.3	40.59
33.08	12005.6	23.47
33.52	6002.3	9.11
34.00	991.0	3.03
34.55	499.9	1.55
36.26	0.0	0.00

* Cork insulation - no weight loss during flight.

FIGURE 7.1

Unconventional Vehicle - Spacecraft Configuration Study
Unconstrained Range Case - Three Stage Ascent

RE-ENTRY RANGE AND VELOCITY AS FUNCTIONS OF PAYLOAD WEIGHT AND RE-ENTRY ANGLE

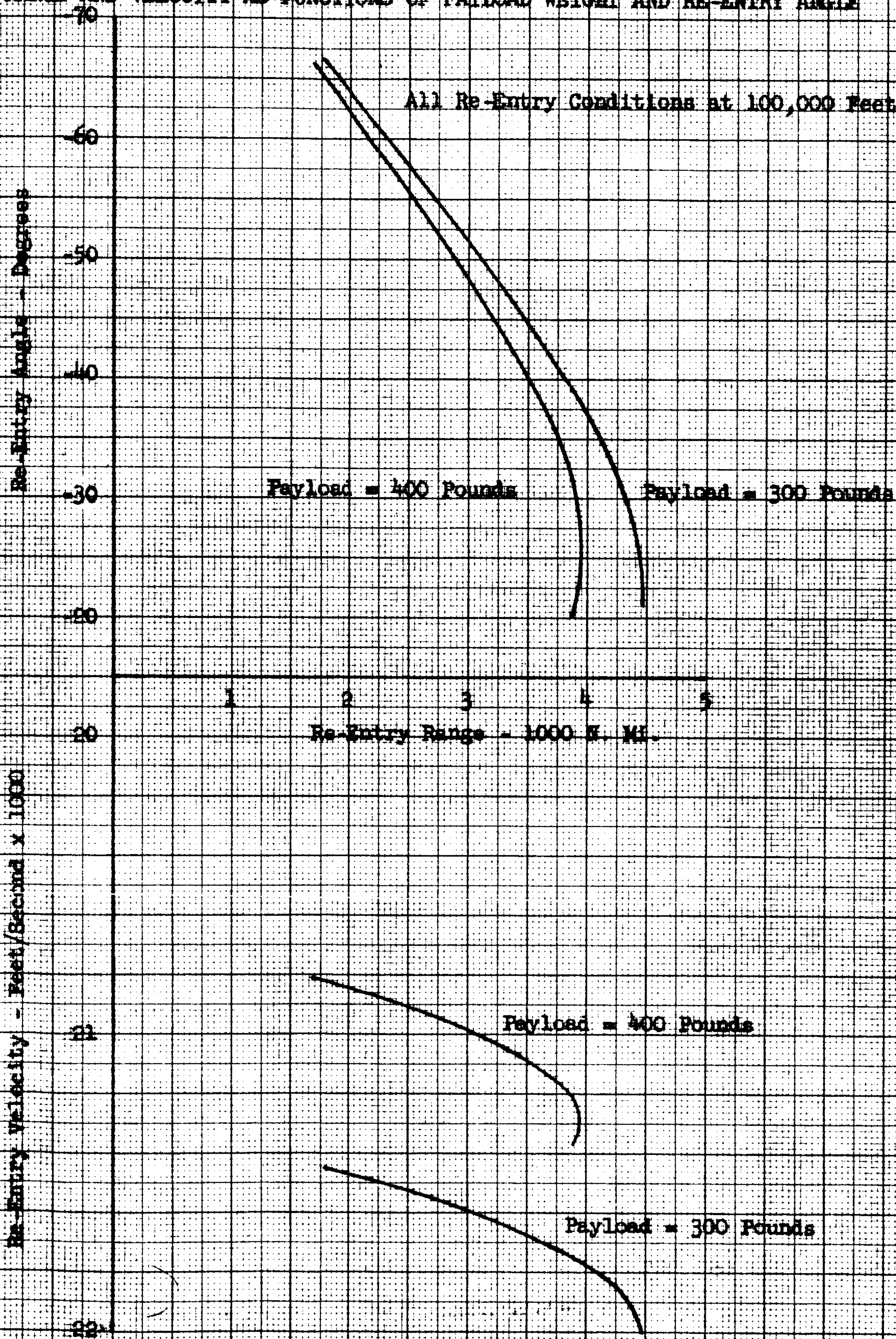

FIGURE 7.2

Unconventional Vehicle - Spacecraft Configuration Study
Unconstrained Range Case - Three Stage Ascent

THIRD STAGE COAST TIME REQUIREMENTS

Notes:

1. Coast Time is From Third Stage Burnout to 100,000 Feet.
2. Re-Entry Conditions at 100,000 Feet.

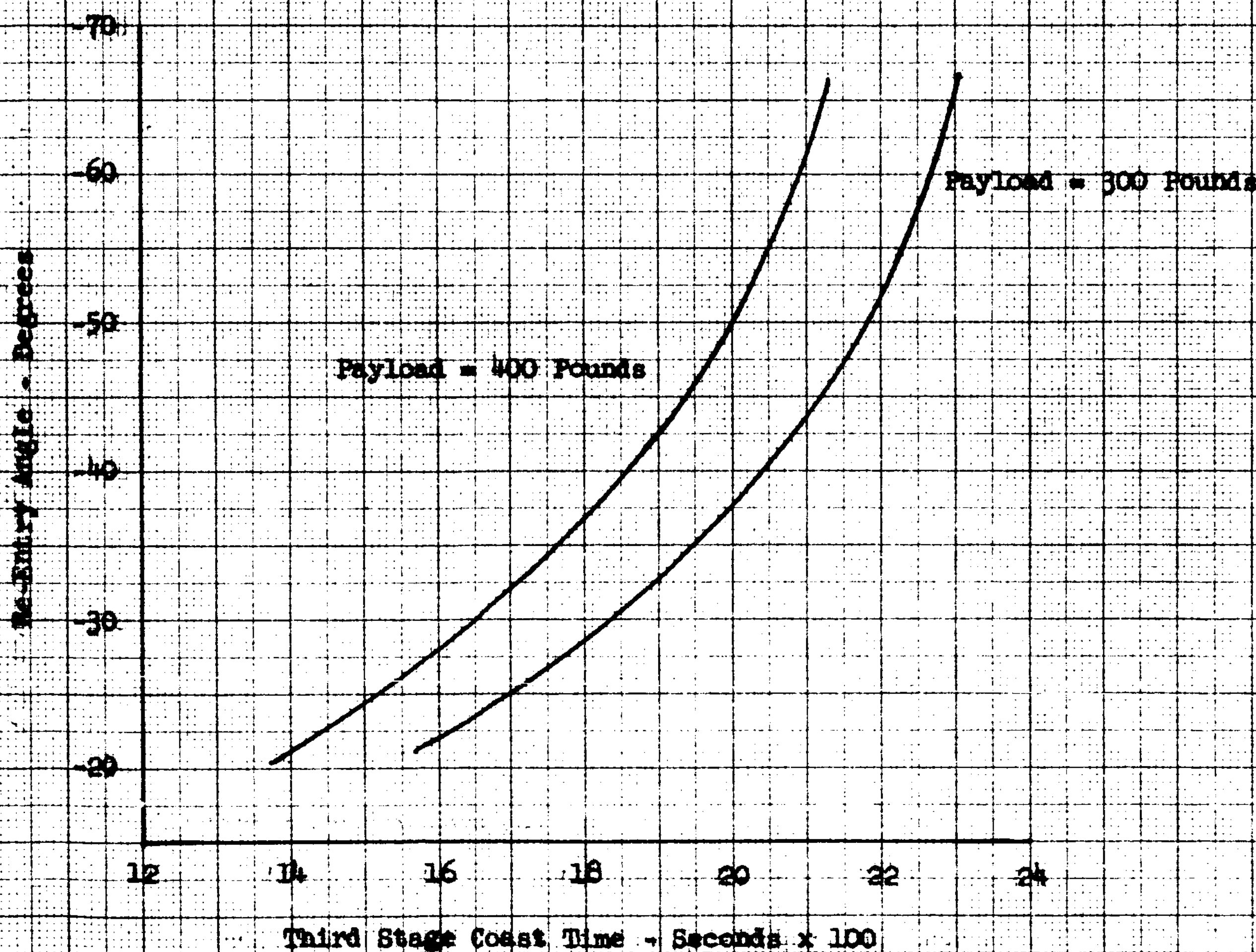

FIGURE 7.3

Unconventional Vehicle - Spacecraft Configuration Study

Unconstrained Range Case - Two Stage Ascent, One Stage Descent

RE-ENTRY RANGE AND VELOCITY AS FUNCTIONS OF PAYLOAD WEIGHT AND RE-ENTRY ANGLE

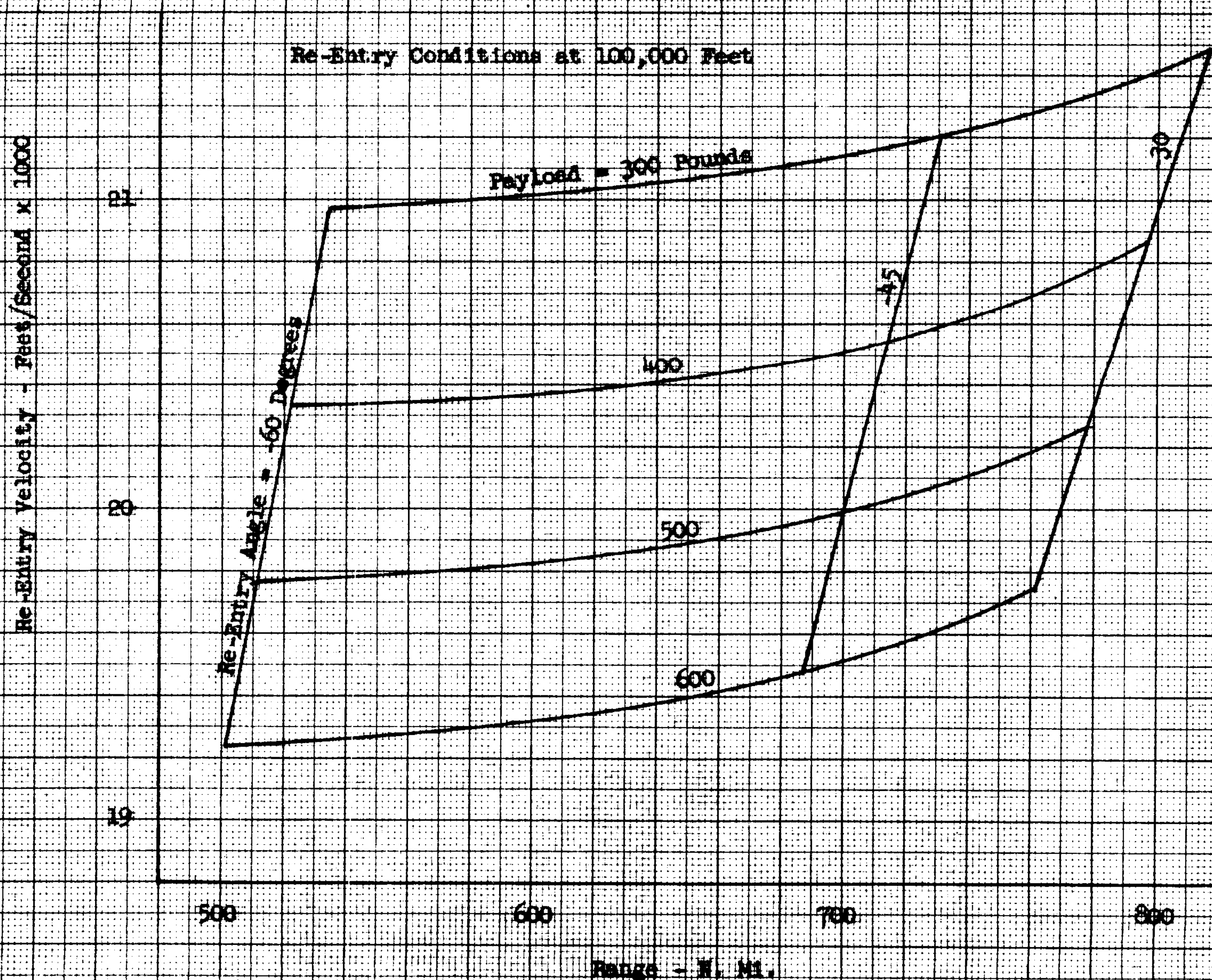

FIGURE 7.4

Unconventional Vehicle - Spacecraft Configuration Study
Unconstrained Range Case - Two Stage Ascent, One Stage Descent

SECOND STAGE COAST TIME REQUIREMENTS

Re-Entry Conditions at 100,000 Feet

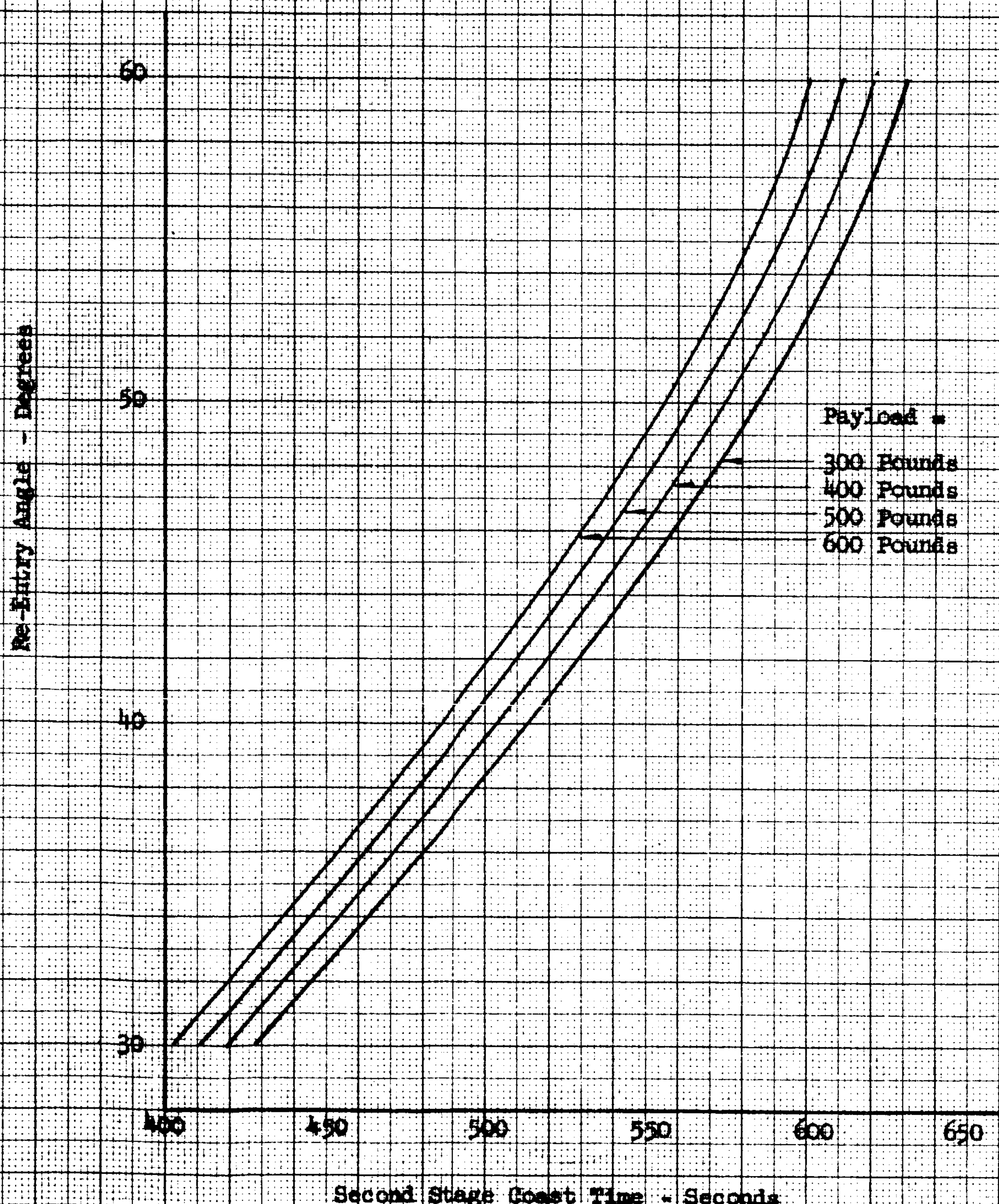

FIGURE 7.5

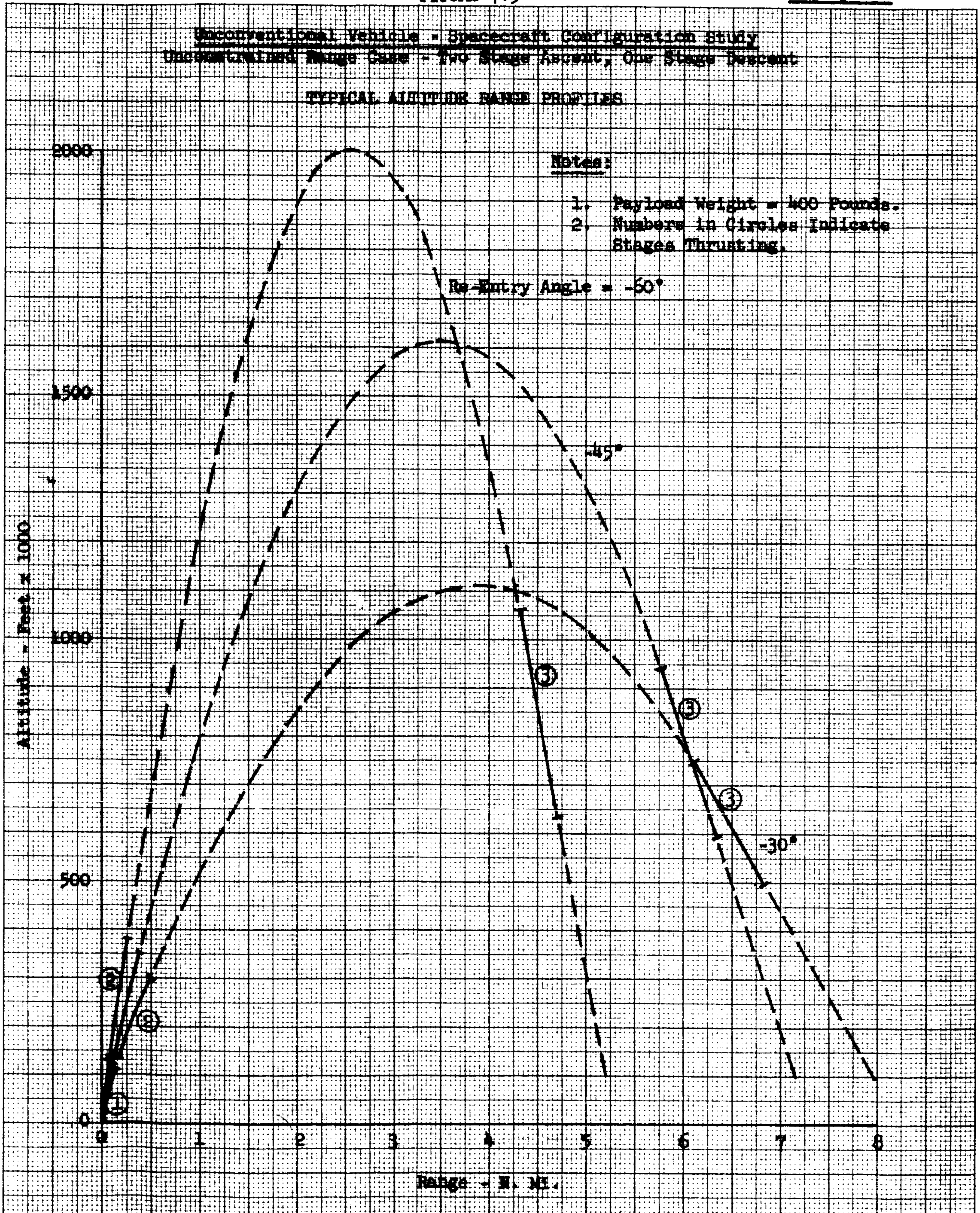
Unconventional Vehicle - Spacecraft Configuration Study
Unconstrained Range Case - Two Stage Ascent, One Stage Descent
TYPICAL ALTITUDE RANGE PROFILES
Notes:
1. Payload Weight = 400 Pounds.
2. Numbers in Circles Indicate Stages Thrusting.
Re-Entry Angle = -60°
-45°
-30°
1
2
3
Altitude - Feet x 1000
2000
1500
1000
500
0
Range - N. MI.
0
1
2
3
4
5
6
7
8

FIGURE 7.6

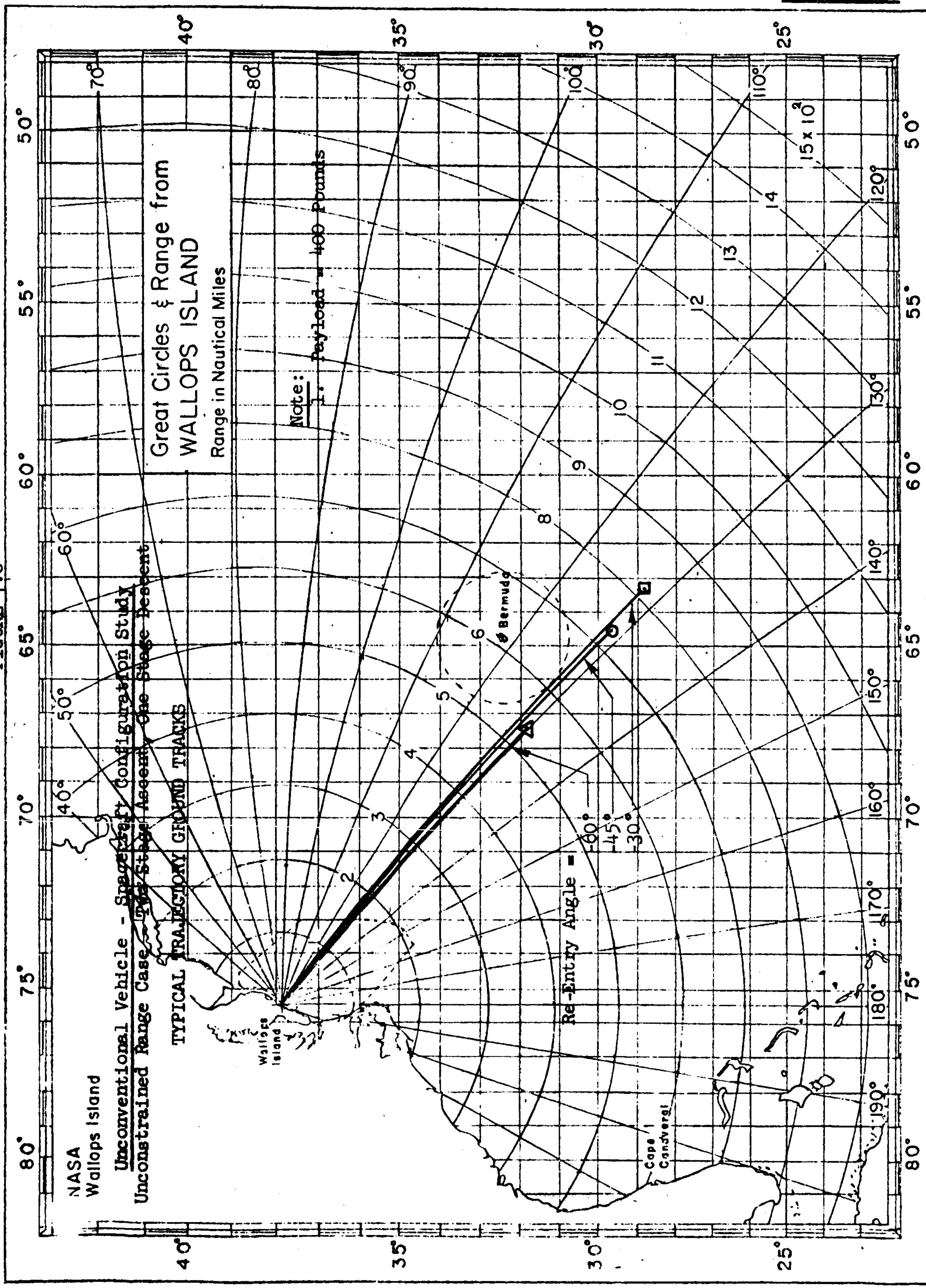
NASA
Wallops Island
Unconventional Vehicle - Spacecraft Configuration Study
Unconstrained Range Case - Two Stage Ascent, One Stage Descent
TYPICAL TRAJECTORY GROUND TRACKS
Great Circles & Range from
WALLOPS ISLAND
Range in Nautical Miles
Note:
1. Payload = 400 Pounds
Re-Entry Angle =
-60°
-45°
-30°
Bermuda
Wallops Island
Cape Canaveral
15×10^2
40°
35°
30°
25°
50°
55°
60°
65°
70°
75°
80°
2
3
4
5
6
8
9
10
11
12
13
14
40°
50°
60°
70°
80°
90°
100°
110°
120°
130°
140°
150°
160°
170°
180°
190°

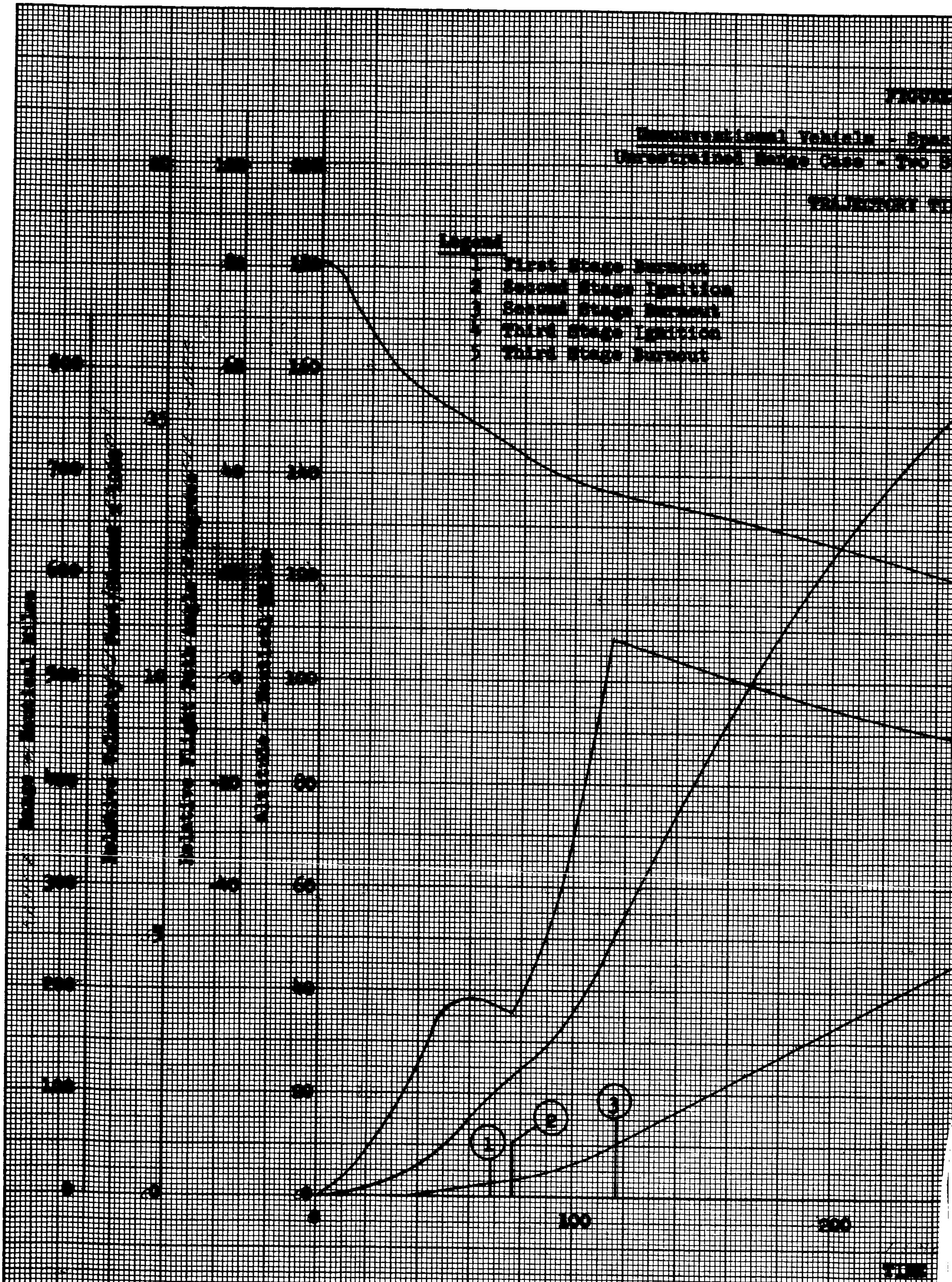
Legend
1 First Stage Burnout
2 Second Stage Ignition
3 Second Stage Burnout
4 Third Stage Ignition
5 Third Stage Burnout
0
100
200

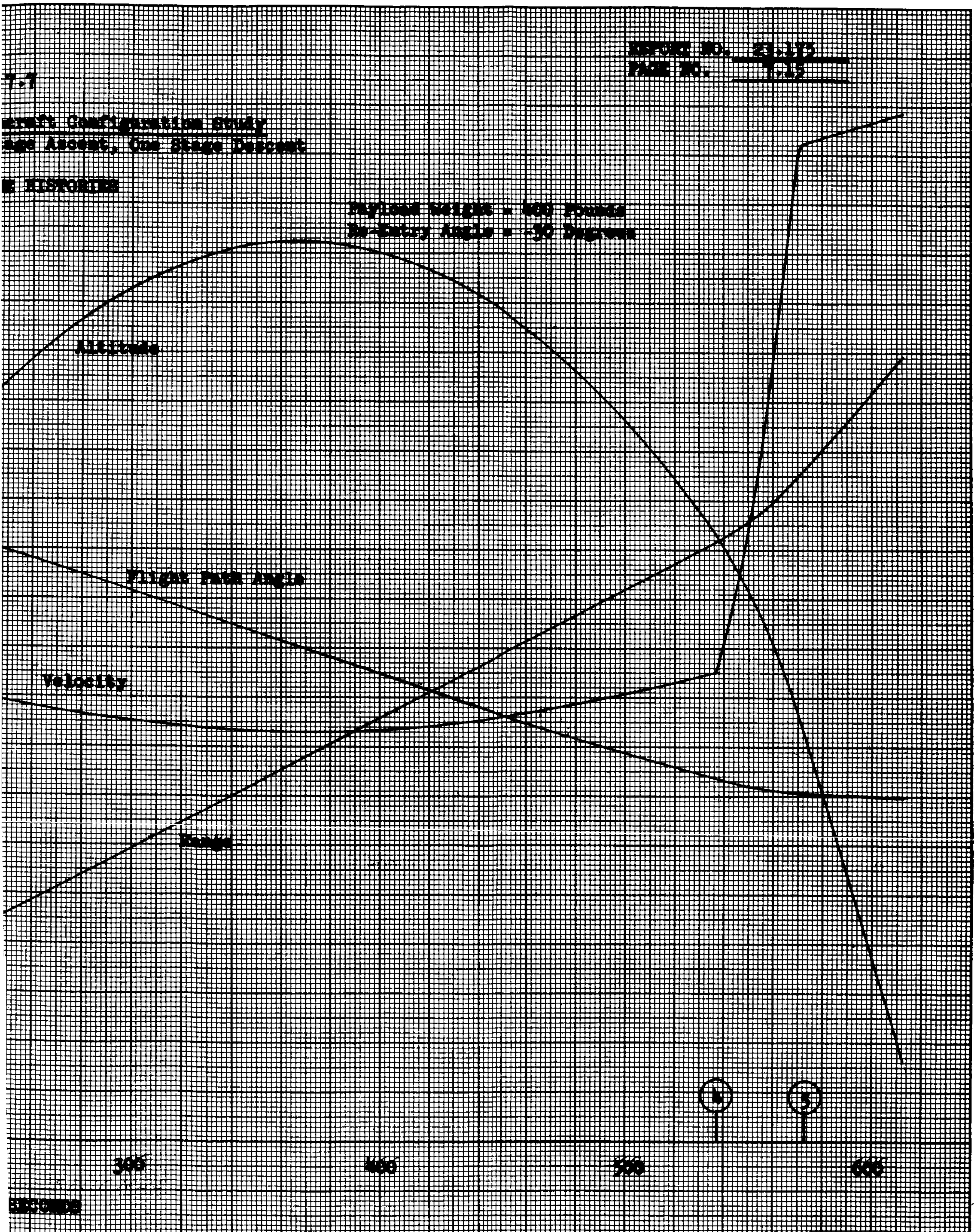

REPORT NO.
PAGE NO.
Craft Configuration Study
Stage Ascent, One Stage Descent
HISTORIES
Re-Entry Angle = -30 Degrees
Altitude
Flight Path Angle
Velocity
Range
4
5
300
400
500
600
SECONDS

15 ②

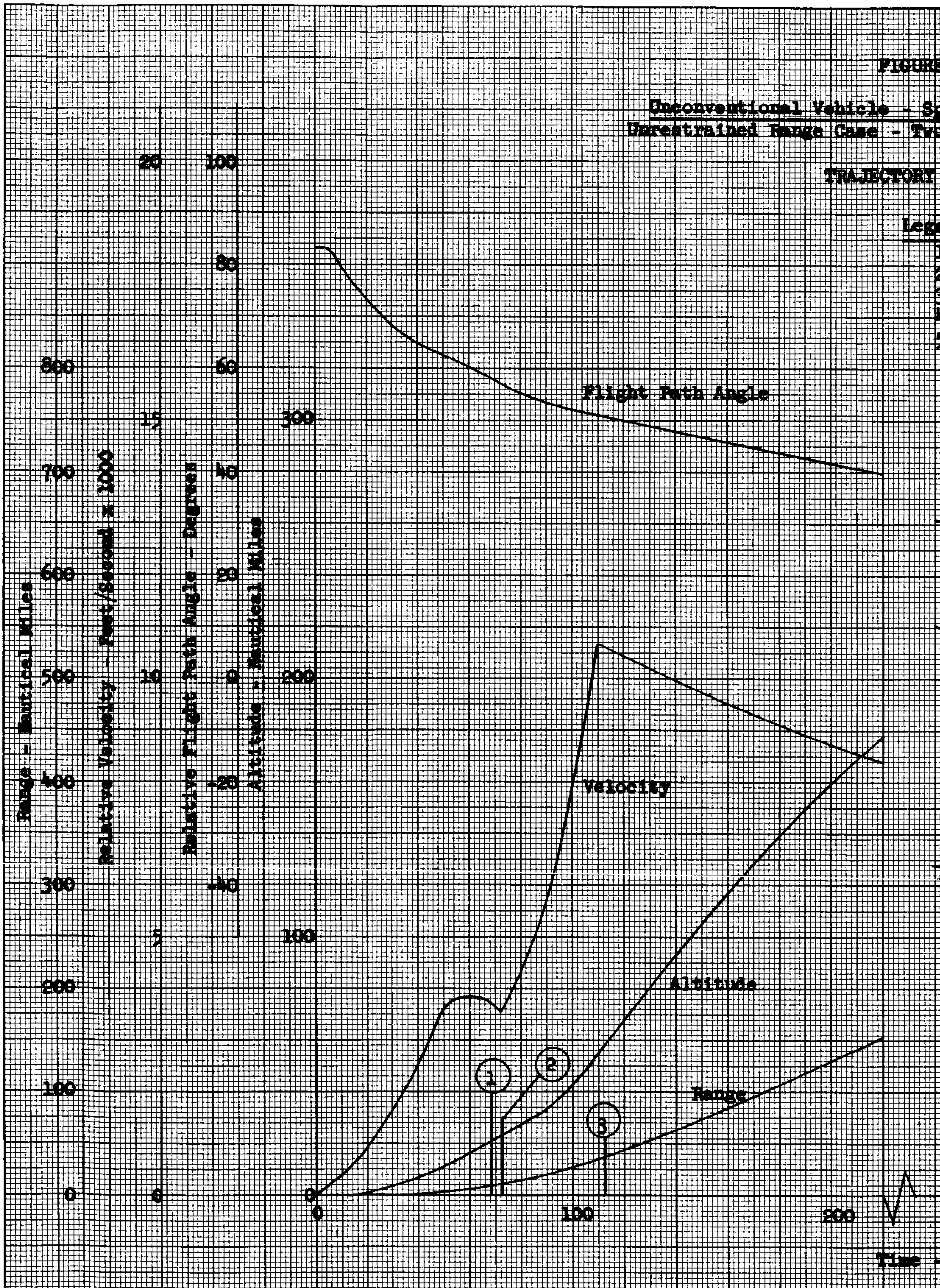
FIGURE
Unconventional Vehicle -
Unrestrained Range Case -
TRAJECTORY
Range - Nautical Miles
Relative Velocity - Feet/Second x 1000
Relative Flight Path Angle - Degrees
Altitude - Nautical Miles
Flight Path Angle
Velocity
Altitude
Range
1
2
3
Time -
0
100
200
800
700
600
500
400
300
200
100
0
20
15
10
5
0
100
80
60
40
20
0
-20
-40
300
200
100
0

7.8

acecraft Configuration Study
Stage Ascent, One Stage Descent

TIME HISTORIES

nd

First Stage Burnout
Second Stage Ignition
Second Stage Burnout
Third Stage Ignition
Third Stage Burnout

Payload Weight = 400 Pounds
Re-Entry Angle = -45 Degrees

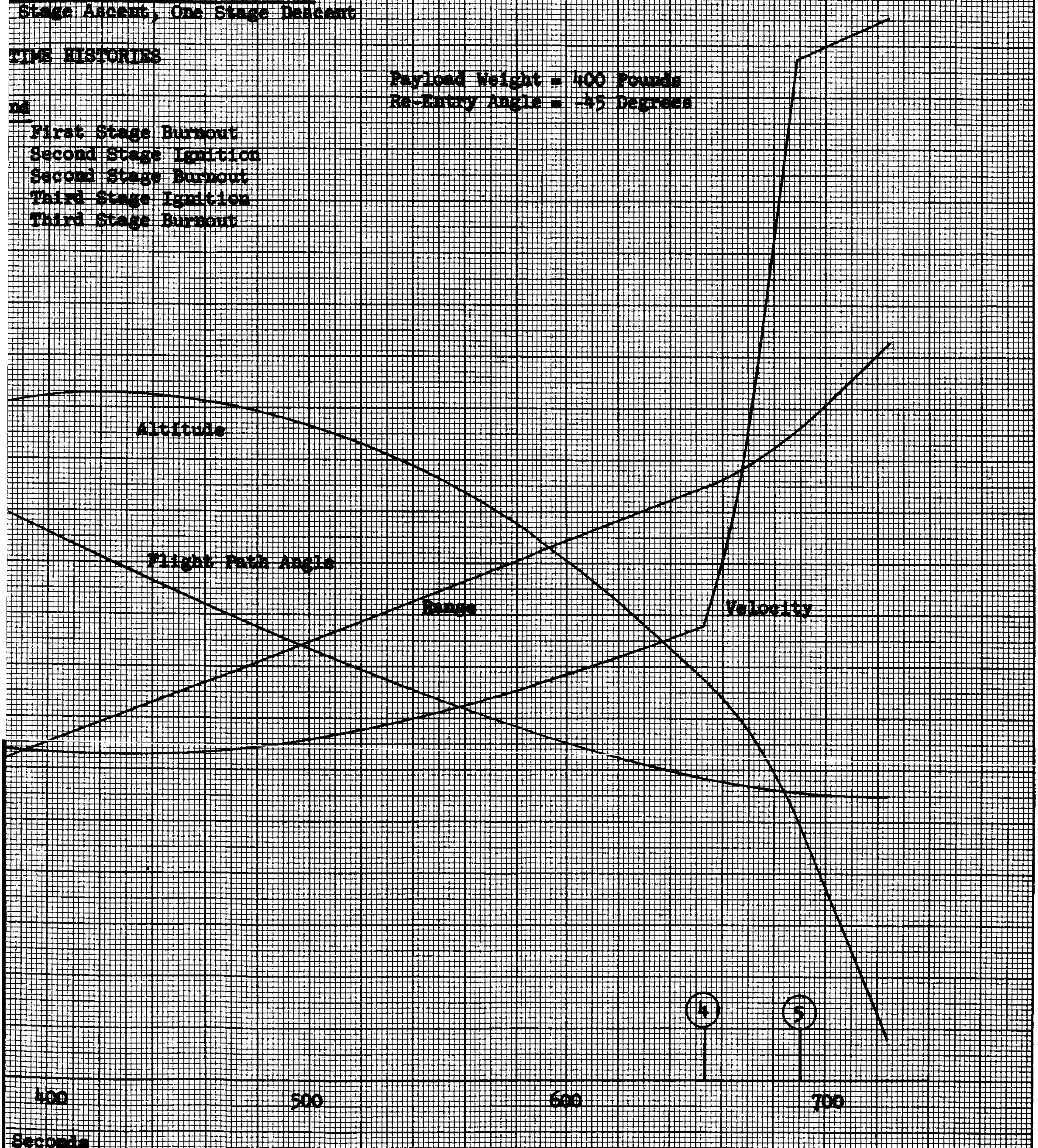

16 (D)

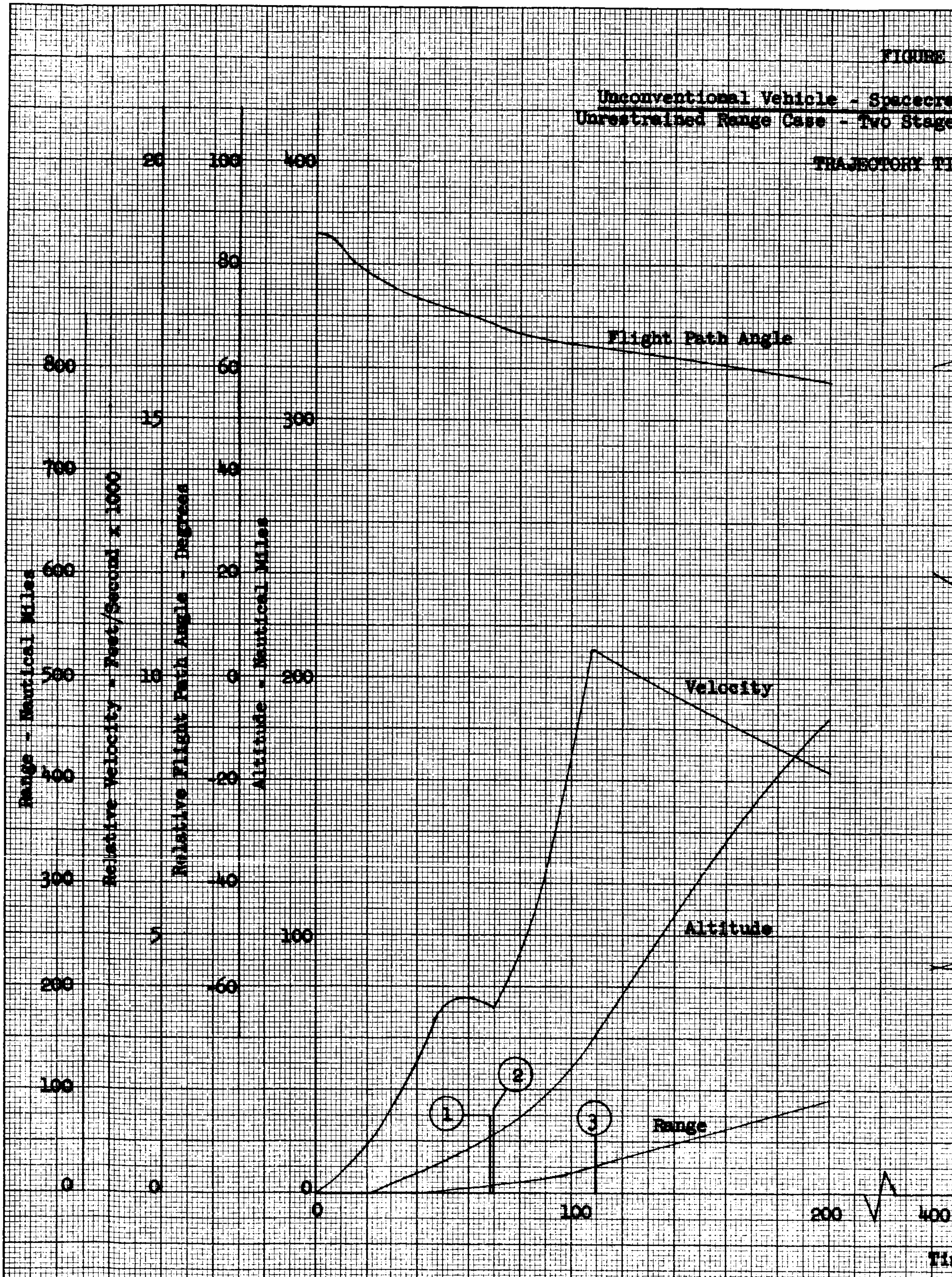
FIGURE
Unconventional Vehicle - Spacecra
Unrestrained Range Case - Two Stage
TRAJECTORY TI
Range - Nautical Miles
Relative Velocity - Feet/Second x 1000
Relative Flight Path Angle - Degrees
Altitude - Nautical Miles
Flight Path Angle
Velocity
Altitude
Range
1
2
3
0
100
200
400
0
100
200
300
400
500
600
700
800
0
5
10
15
20
-60
-40
-20
0
20
40
60
80
100
0
100
200
300
400
Ti

7-9

ft Configuration Study
Ascent, One Stage Descent

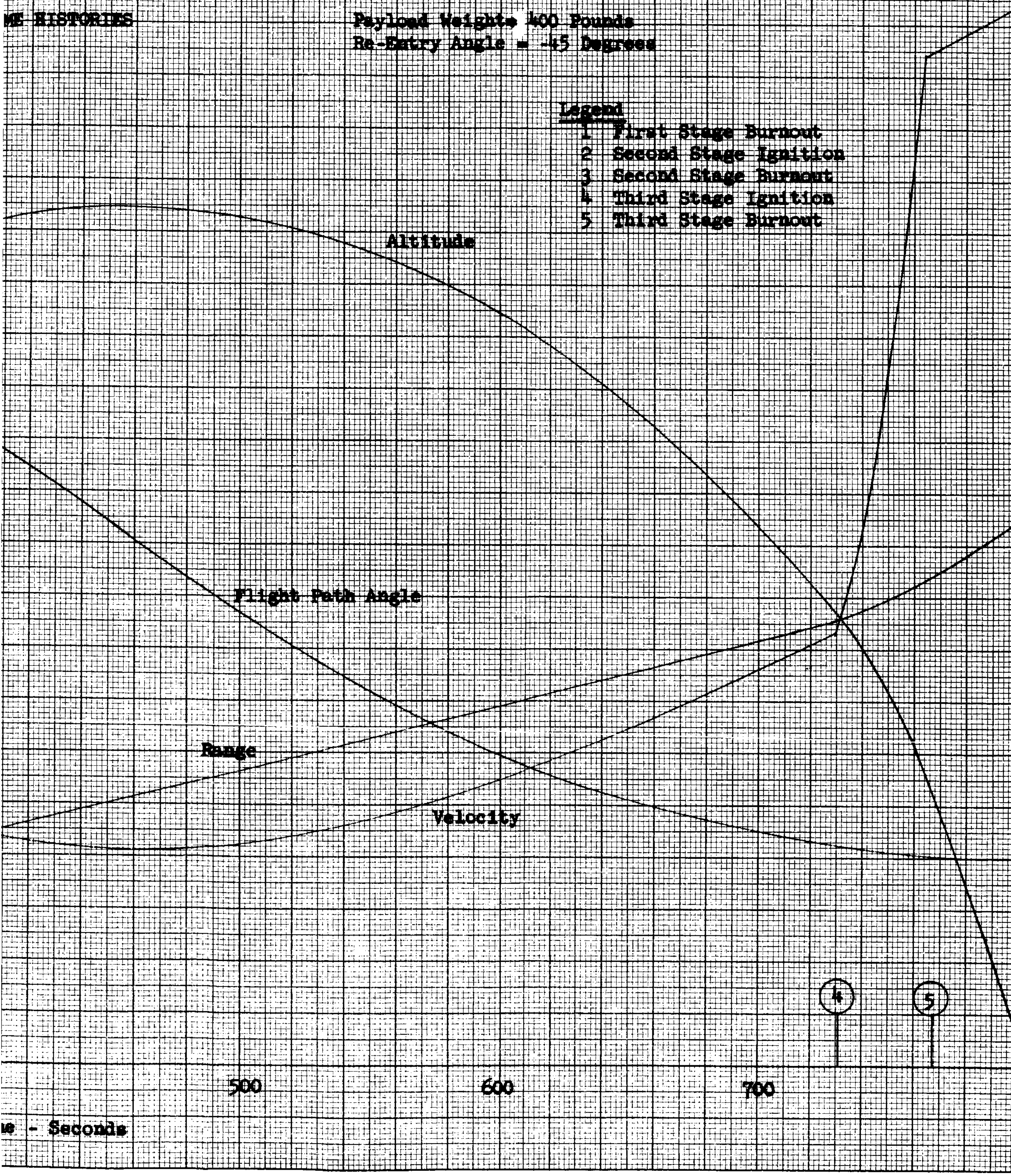

FIGURE 7.10

Unconventional Vehicle - Spacecraft Configuration Study
Unconventional Range Case - Two Stage Ascent, One Stage Descent

ALTITUDE AS A FUNCTION OF VELOCITY

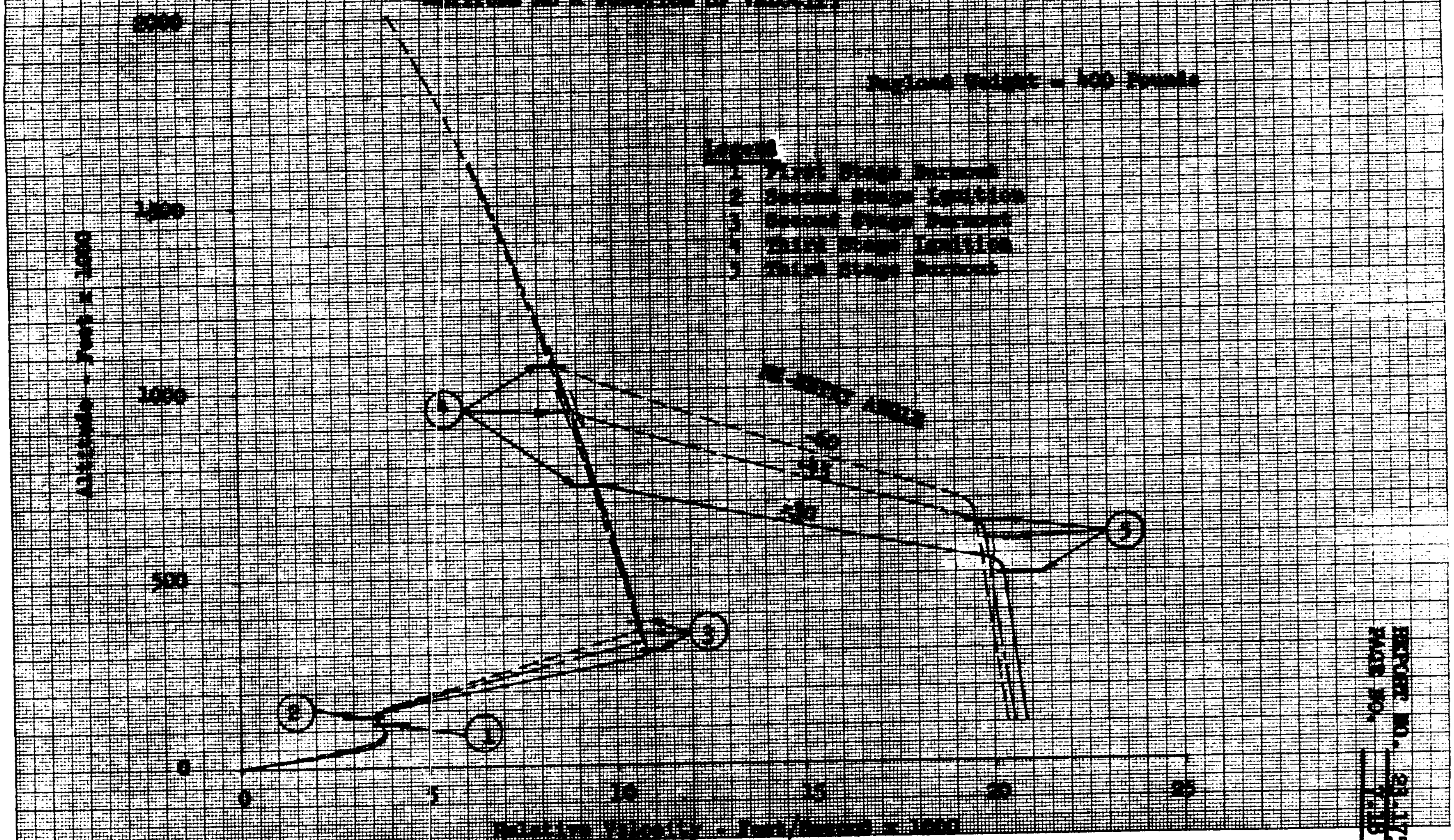

FIGURE 7.11

Unconventional Vehicle - Spacecraft Configuration Study
Restrained Range Case - Two Stage Ascent, One Stage Descent

RE-ENTRY ANGLE AS A FUNCTION OF RE-ENTRY VELOCITY SHOWING PAYLOAD VARIATION AT 700 N.MI.

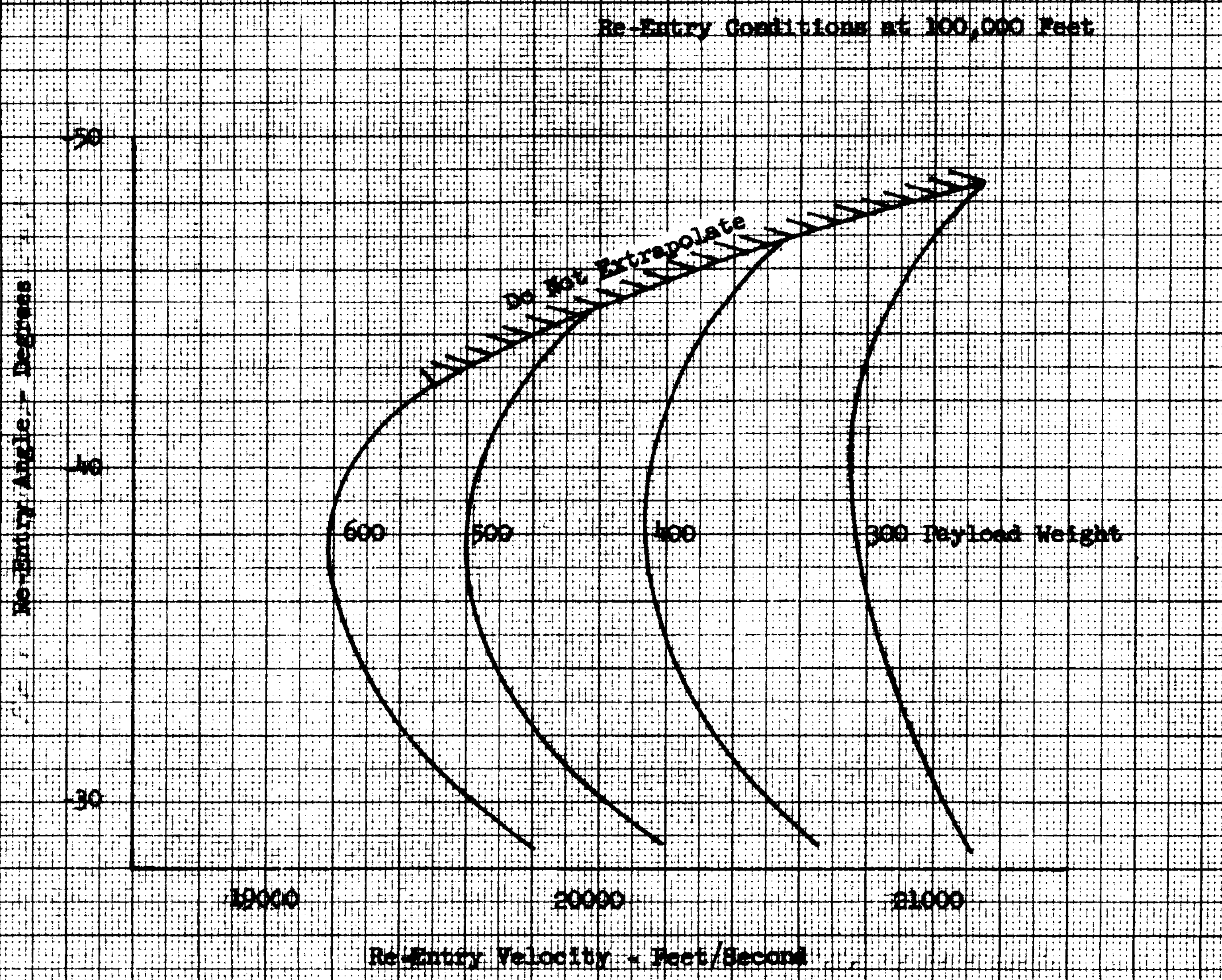

FIGURE 7.12

Unconventional Vehicle - Spacecraft Configuration Study
Restrained Range Case - Two Stage Ascent, One Stage Descent

SECOND STAGE COAST TIME REQUIREMENTS

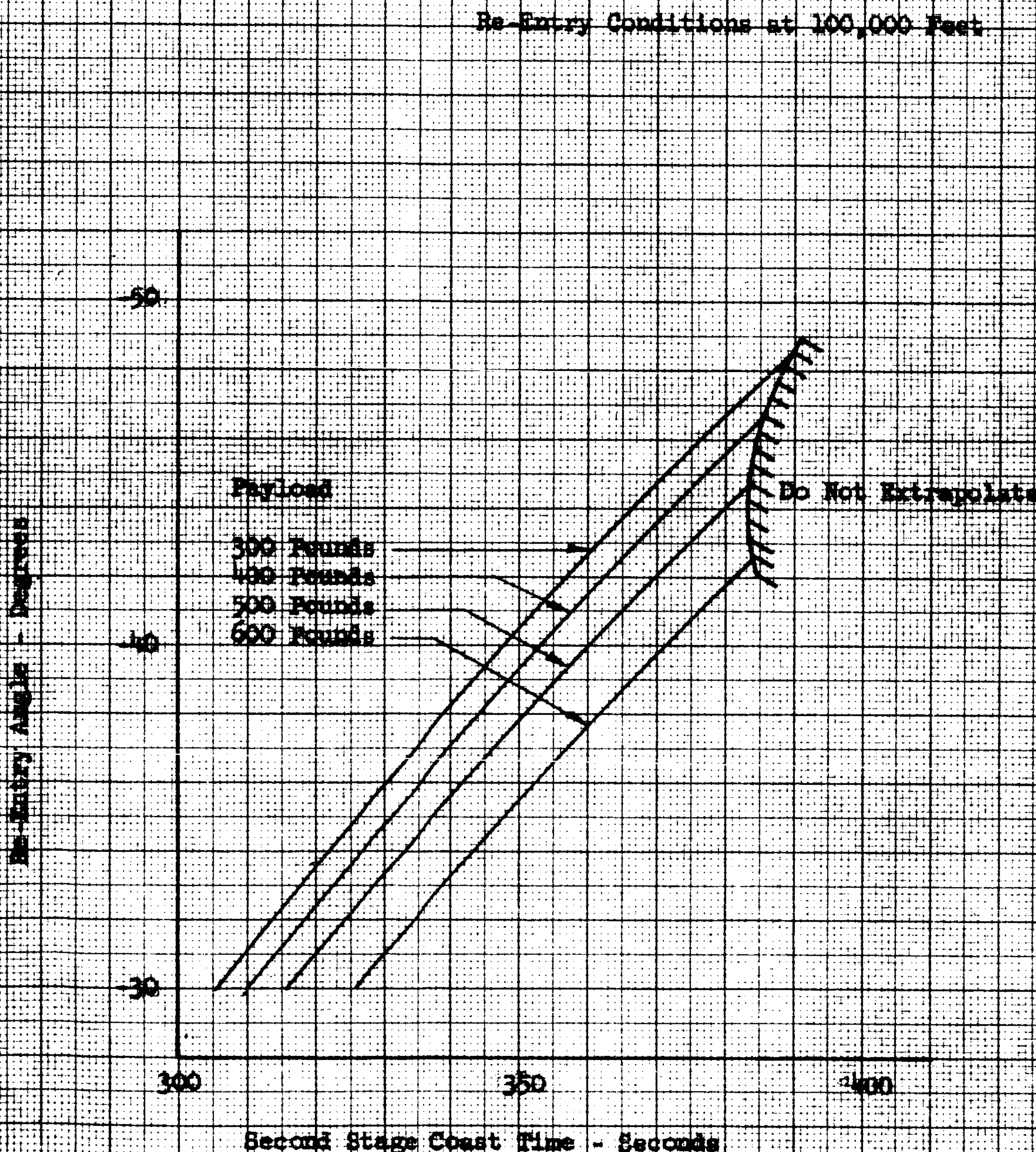

STUDY

"UNCONVENTIONAL VEHICLE - SPACECRAFT"

THERMAL ANALYSIS

Prepared by:

F. K. McGinnis

J. L. Williams

Reviewed by:

D. M. Martin

THERMAL ANALYSIS

8.0 INTRODUCTION

The results of thermal analyses relating to the unconventional vehicle - spacecraft configuration are presented in this section. The effects of the proposed vehicle configuration and trajectory on the heating of structure and internal components aft of Station 106 are determined, and the heating of the new structure forward of Station 106 is investigated.

8.1 ANALYSIS

8.1.1 Aerodynamic Heating Analysis

Aerodynamic heating rate and transient structural temperature calculations were performed using IBM 7090 Routine LVV622 (reference Q). The boost trajectories presented in Section 7 corresponding to entry angles of -30°, -45°, and -60° for a 300 pound payload were used, with local flow conditions determined by standard hand methods (reference R). In determining skin temperatures during the long second stage coast period, solar heating was included.

8.1.2 Internal Heating Analysis

IBM 7090 Routine LVV601 (reference S) was used in computing the component temperatures presented herein.

8.2 RESULTS

8.2.1 Aerodynamic Heating

From the standpoint of aerodynamic heating, the Case I A configuration is identical to the standard Scout vehicle. Thus, the structural temperature data for standard Scout with Castor II motor stack is applicable, and no additional thermal protection is required.

For Case II A-2 the local flow conditions resulting from the 5° half-angle cone are less severe than those resulting from the standard Scout heat shield configuration, thus leading to lower aerodynamic heating rates and correspondingly lower skin temperatures for this case. The computed transition 'D' Section transient skid temperatures for Case II A-2 are shown in Figure 8.1, with the corresponding Case I A temperatures (standard Scout). The peak temperature for Case I A is seen to be 100°F higher than the maximum Case II A-2 value. Upper 'B' Section skin temperatures for Case II A-2 were calculated in support of the internal heating analysis discussed later in this section. Figures 8.2, 8.3, and 8.4 show Upper 'B' inside skin temperature as a function of time for the long coast time trajectories corresponding to entry angles of -30°, -45°, and -60°, respectively.

Another area of concern with regard to Case II A-2 was the spin table fairing located at Station 103.68. Computed temperatures for this fairing and the separation clamp explosive bolt are shown in Figure 8.5. The peak temperature of the explosive bolt is 110°F, well below the allowable limit of 300°F. The fairing temperatures are shown in support of Section 4.

8.2.2 Internal Heating Results

8.2.2.1 Base 'A' and Lower 'B' Sections

The thermal environment encountered by the vehicle skin as stated in Section 8.2.1, for unconventional payload missions, is the same as or less severe than that of the conventional Scout mission. The flight duration is the same for Base 'A' and Lower 'B' Sections for either mission. Therefore, the temperature histories of components located in Base 'A' and Lower 'B' Sections should be the same on unconventional payload missions as on conventional payload missions.

8.2.2.2 Upper 'B' and Lower 'C' Sections

The duration of second stage coast is considerably longer for unconventional payload missions than for the basic Scout design mission (450 seconds as opposed to 180 seconds). This results in increased heating of components located in Upper 'B' and Lower 'C' Sections. The increase in component heating is not significant in Lower 'C' Section. However, the increase in heating is significant in Upper 'B' Section primarily due to the influence of the Castor II nozzle.

The Castor II motor has not been flown to date, and only preliminary information is available on the Castor II nozzle temperature. A preliminary thermal analysis has been made for 'B' Section components with the Castor II nozzle installed. This analysis considers a Scout maximum aerodynamic heating trajectory and a 250 second, second stage coast. The vehicle skin temperature used in this analysis is given on Figure 8.6, along with the Castor II nozzle temperature. The Castor II nozzle temperature was adjusted from atmospheric test conditions to flight conditions.

Results of the analysis are presented on Figures 8.6 through 8.18. As these figures show, there are no component heating problems in 'B' Section with the Castor II motor on basic Scout missions.

The results of the basic Scout mission analysis were extrapolated to apply to unconventional payload Cases I A and II A-2. However, the unconventional payload trajectories provide lower vehicle skin temperatures as well as longer second stage coast intervals than were considered in the basic Scout analyses. Therefore, the most critical components, the hydrogen peroxide and nitrogen supply lines, were analyzed for unconventional payload, Case II A-2 which provides the most severe vehicle skin temperature (Figure 8.2) of the unconventional payload missions. The results of this analysis are presented on Figure 8.19. As this figure shows, no additional insulation is required on either the hydrogen peroxide supply lines or the nitrogen supply lines for the Case II A-2 configuration. Based on this analysis and on the analysis of components for the basic Scout mission, it is concluded that there are no severe component heating problems in 'B' Section during unconventional payload missions. Any problems which exist, such as the overtemperature hydrogen peroxide storage tanks shown on Figure 8.8 , can be solved by addition of local insulation to the component.

8.2.2.3 Upper 'C' Section

The thermal environment in Upper 'C' Section is less severe for the unconventional payload missions than in the basic Scout design mission. The basic design is for no second stage coast and a 600 second third stage coast, during which time the section components are heated by the nozzle. On the unconventional payload missions there is a 450 second, second stage coast during which the third stage nozzle is cold, and there is very little third stage coast. Therefore, no component heating problems are expected in Upper 'C' Section.

8.2.2.4 Transition 'D' Section

The thermal environment in 'D' Section is less severe for unconventional payload missions than for the basic Scout design mission. The aerodynamic heating is less severe, and the mission duration is shorter. Therefore, no component heating problems are expected in 'D' Section.

8.3 CONCLUSIONS

The existing Scout transition sections may be used in the unconventional vehicle - spacecraft configuration without additional external thermal protection. Some internal components located in Upper 'B' Section may require additional insulation as a result of the long second stage coast time, and actual quantities of insulation required will be calculated when further Castor II nozzle temperature data becomes available.

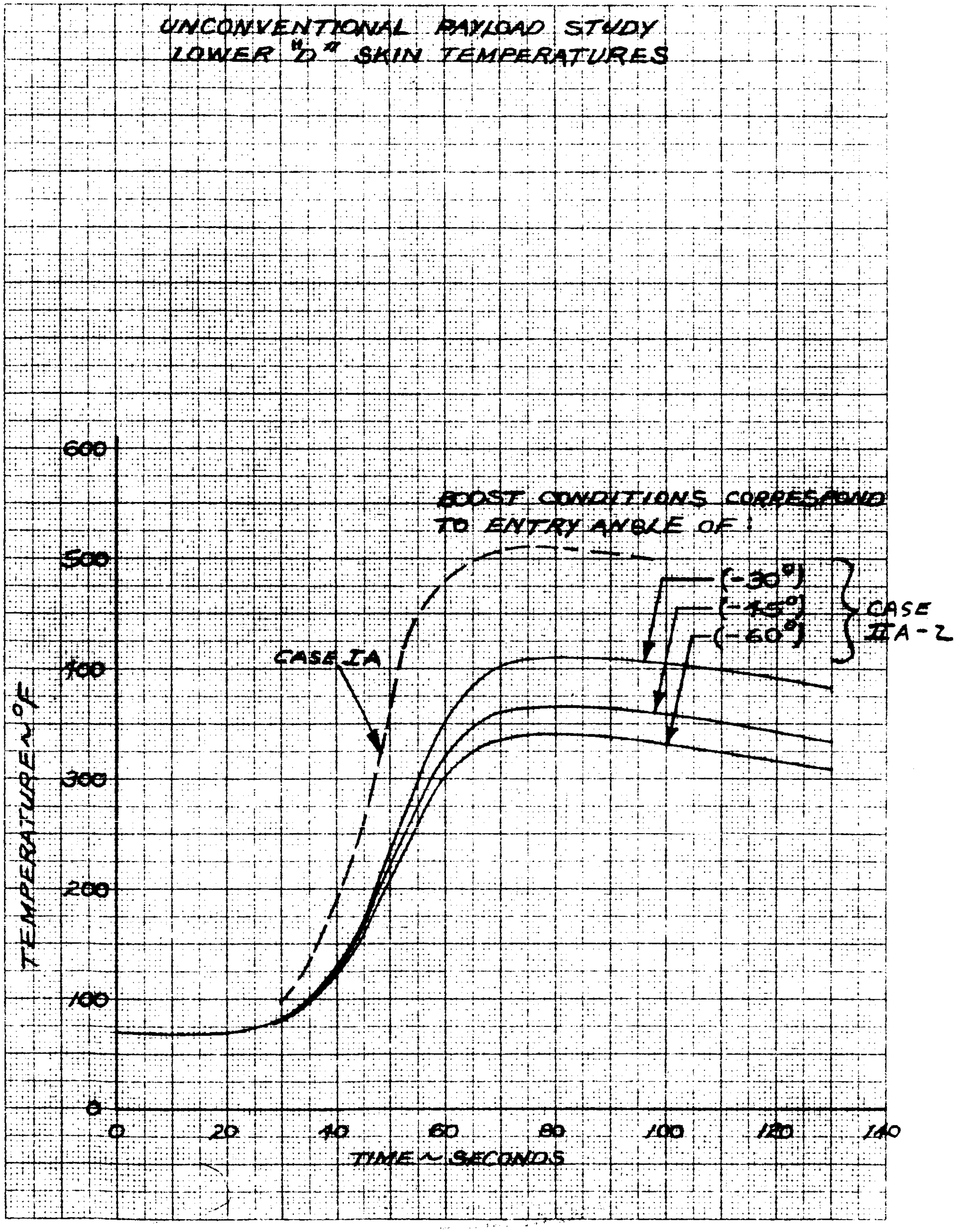
UNCONVENTIONAL PAYLOAD STUDY
LOWER "D" SKIN TEMPERATURES
BOOST CONDITIONS CORRESPOND TO ENTRY ANGLE OF:
(-30°)
(-45°)
(-60°)
CASE IIA-2
CASE IA
TEMPERATURE ~ °F
600
500
400
300
200
100
0
0
20
40
60
80
100
120
140
TIME ~ SECONDS

FIGURE 8.1

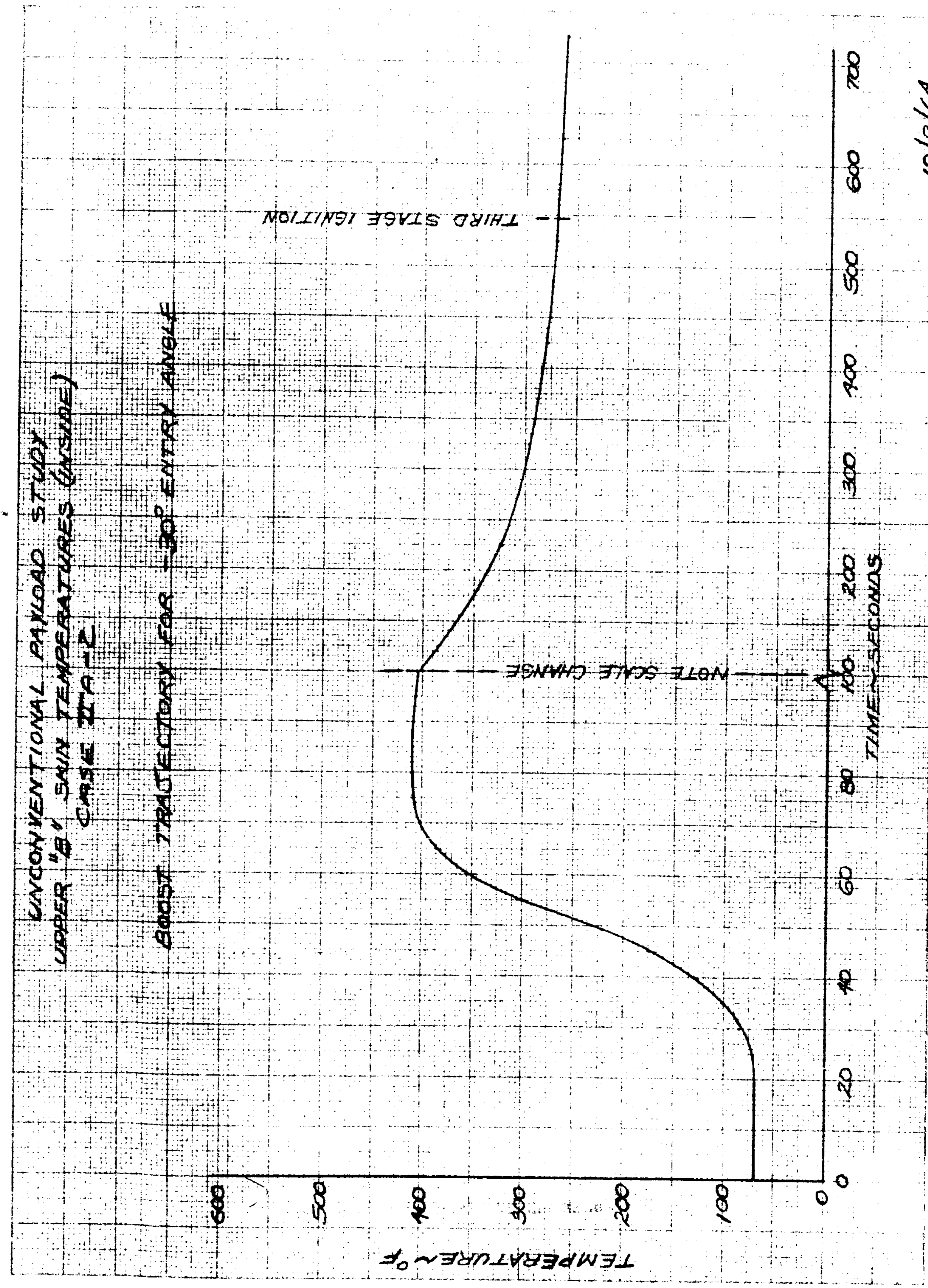

10/8/64

FIGURE 8.2

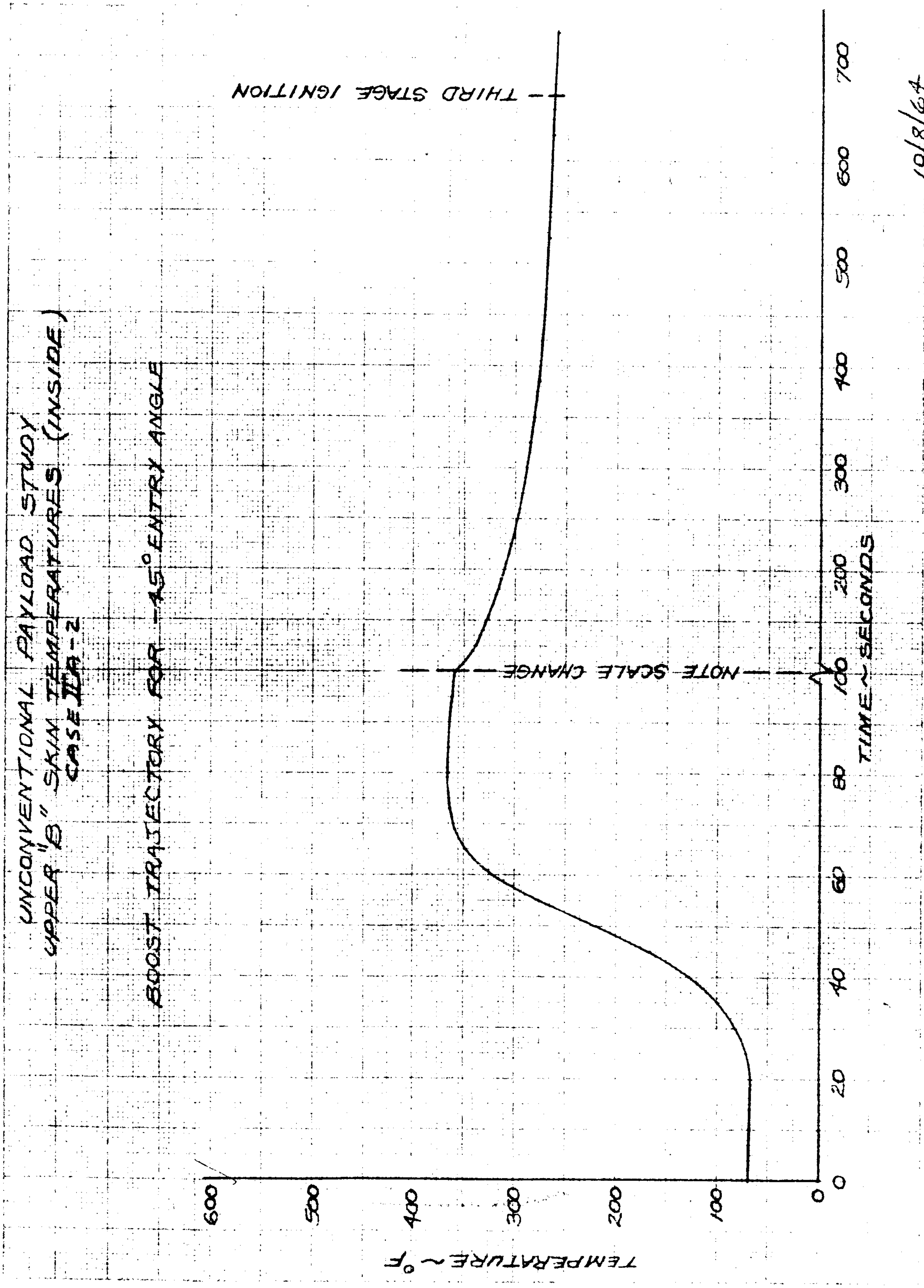
UNCONVENTIONAL PAYLOAD STUDY
UPPER "B" SKIN TEMPERATURES (INSIDE)
CASE IIIA-2
BOOST TRAJECTORY FOR -4.5° ENTRY ANGLE
THIRD STAGE IGNITION
NOTE SCALE CHANGE
TEMPERATURE ~ °F
0
100
200
300
400
500
600
TIME ~ SECONDS
0
20
40
60
80
100
200
300
400
500
600
700
10/8/64

FIGURE 8.3

10/8/64

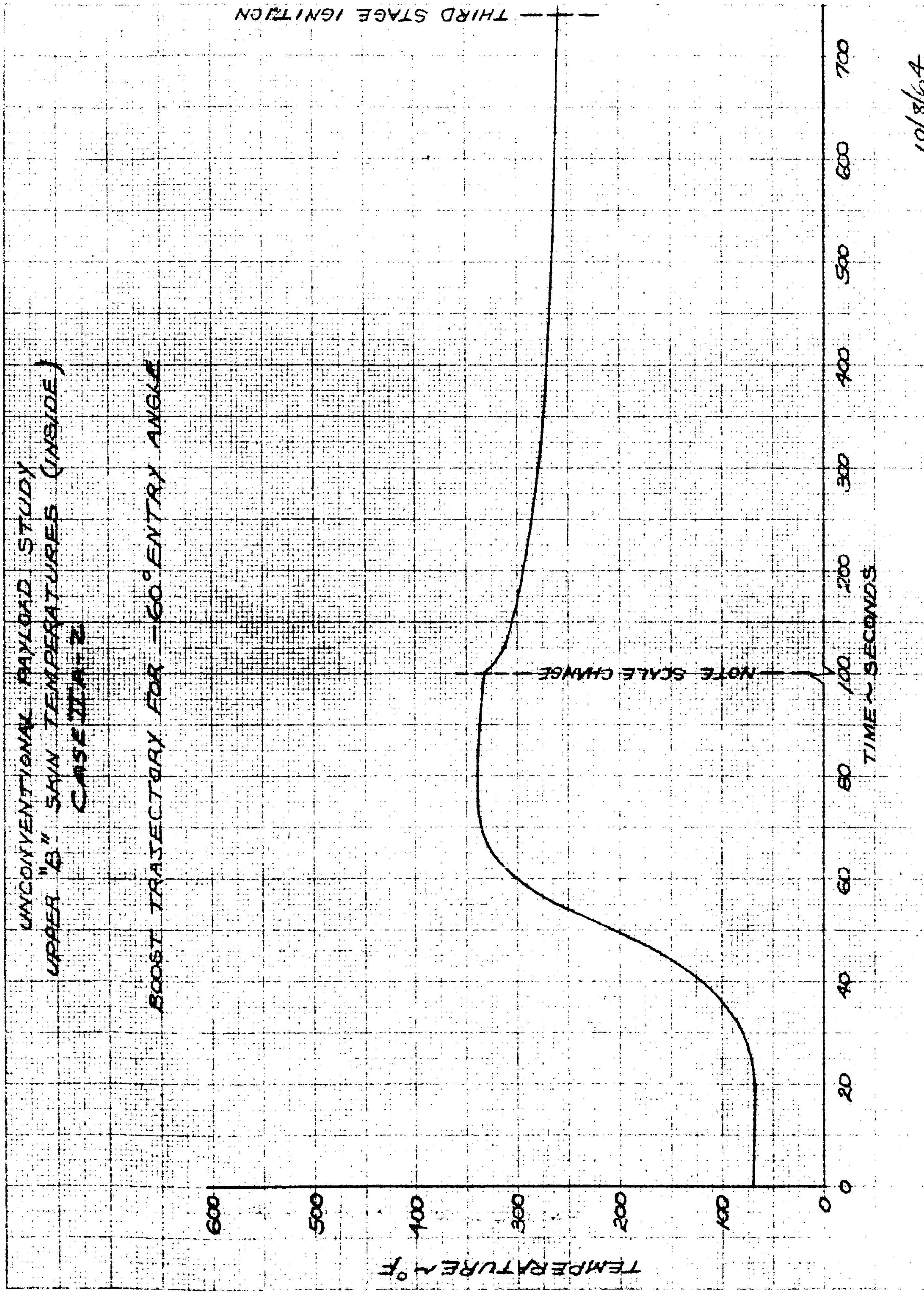

FIGURE 8.4

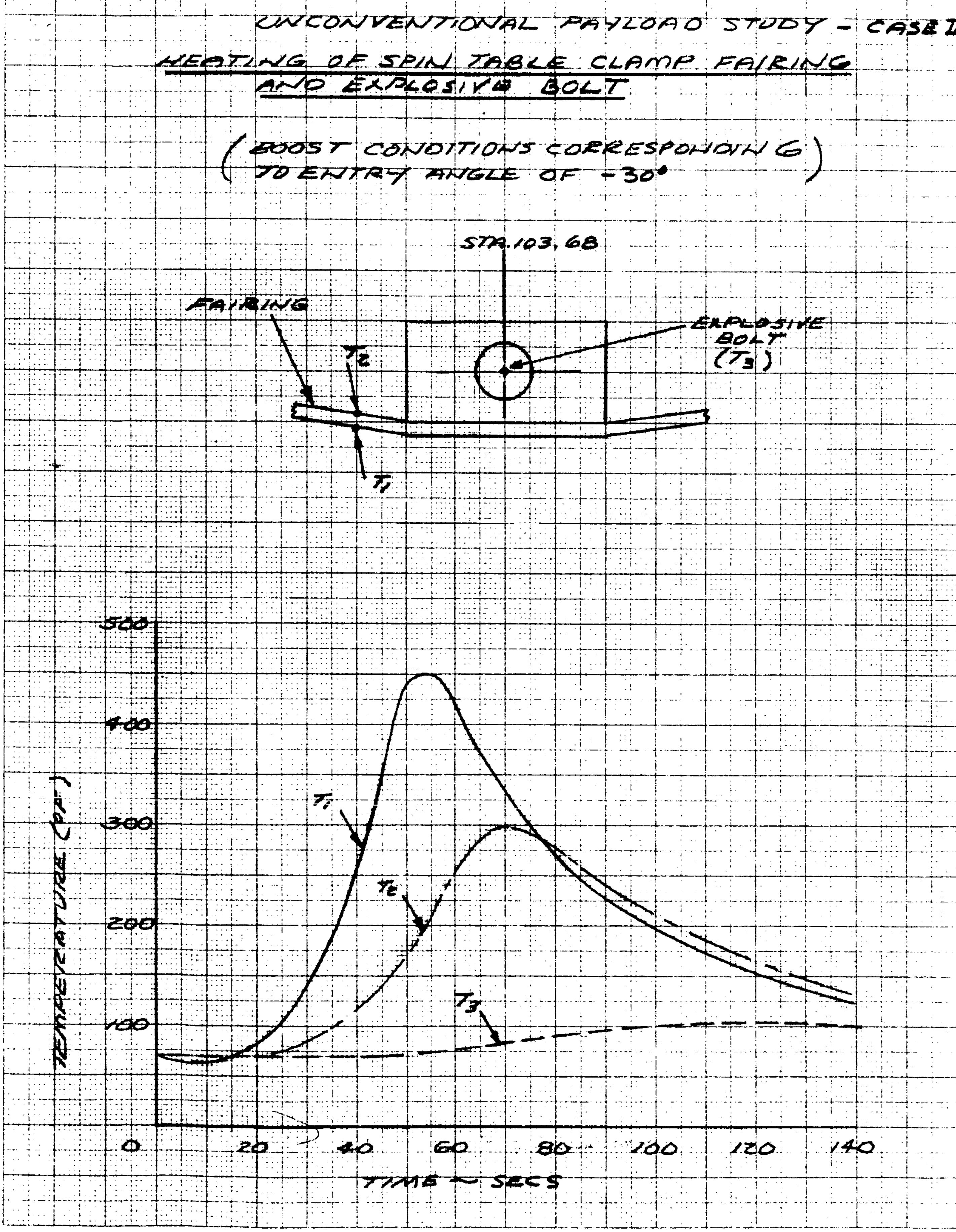
UNCONVENTIONAL PAYLOAD STUDY - CASE IIA-2
HEATING OF SPIN TABLE CLAMP FAIRING AND EXPLOSIVE BOLT
(BOOST CONDITIONS CORRESPONDING TO ENTRY ANGLE OF -30°)
STA. 103.68
FAIRING
T_2
T_1
EXPLOSIVE BOLT (T_3)
500
400
300
200
100
TEMPERATURE (°F)
T_1
T_2
T_3
0
20
40
60
80
100
120
140
TIME ~ SECS

FIGURE 8.5

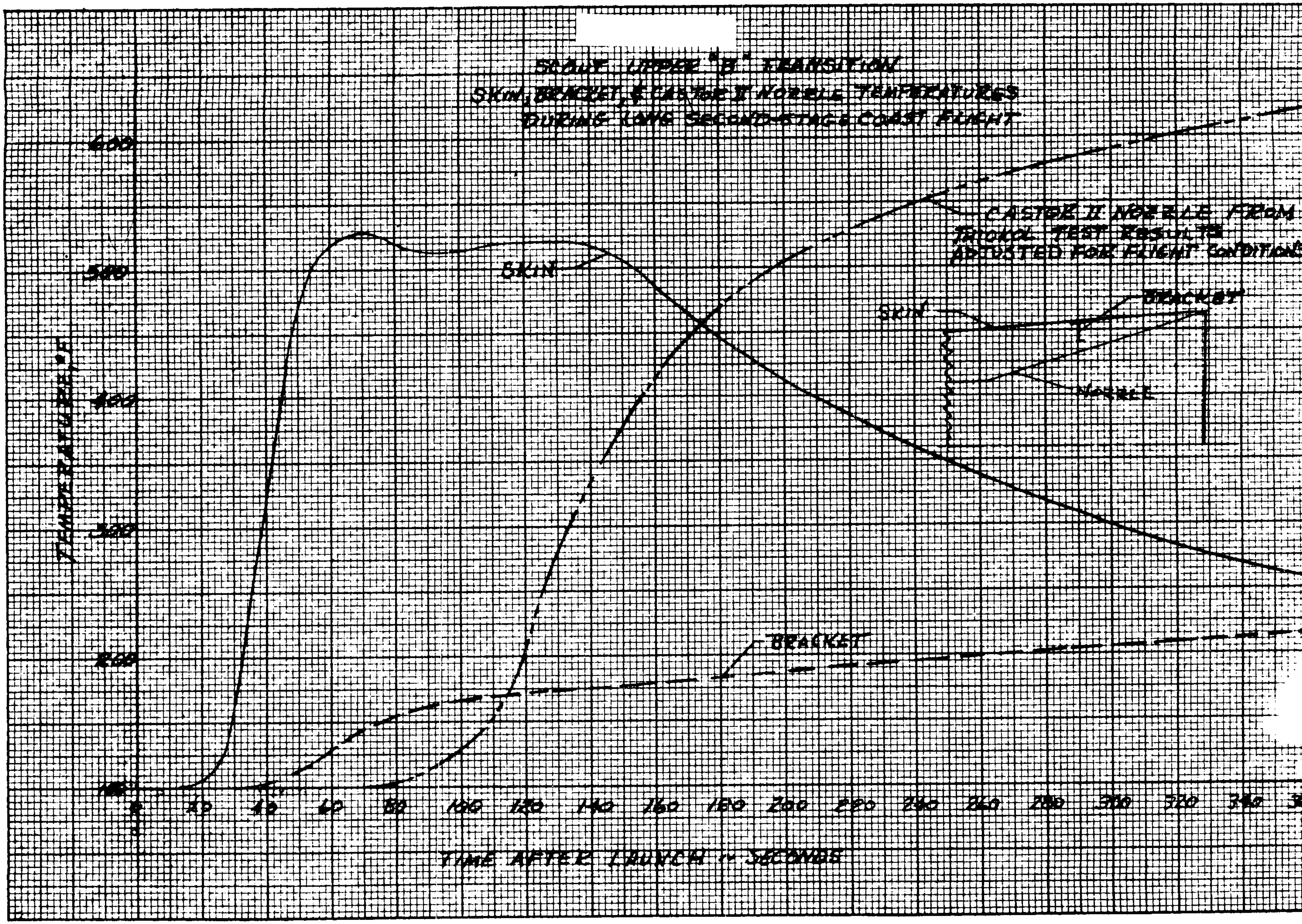
SCOUT UPPER "B" TRANSITION
SKIN, BRACKET, & CASTOR II NOZZLE TEMPERATURES
DURING LONG SECOND-STAGE COAST FLIGHT
CASTOR II NOZZLE FROM
THIOKOL TEST RESULTS
ADJUSTED FOR FLIGHT CONDITIONS
SKIN
BRACKET
NOZZLE
TEMPERATURE, °F
TIME AFTER LAUNCH ~ SECONDS
100
200
300
400
500
600
0
20
40
60
80
100
120
140
160
180
200
220
240
260
280
300
320
340
360

FIGURE 8.0

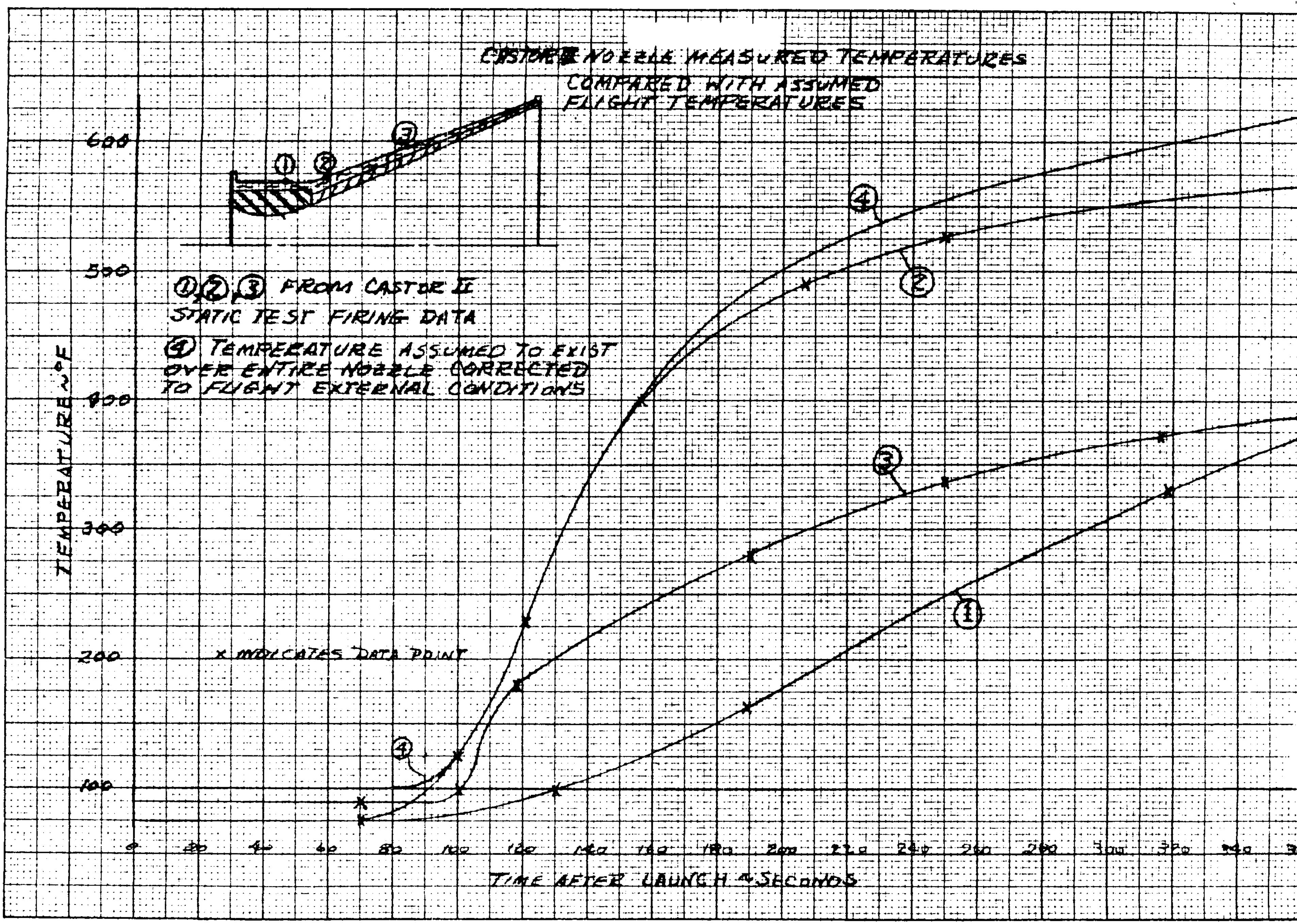
CASTOR NOZZLE MEASURED TEMPERATURES
COMPARED WITH ASSUMED
FLIGHT TEMPERATURES
①②③ FROM CASTOR II
STATIC TEST FIRING DATA
④ TEMPERATURE ASSUMED TO EXIST
OVER ENTIRE NOZZLE CORRECTED
TO FLIGHT EXTERNAL CONDITIONS
x INDICATES DATA POINT
TEMPERATURE ~ °F
600
500
400
300
200
100
0
20
40
60
80
100
120
140
160
180
200
220
240
260
280
300
320
340
360
TIME AFTER LAUNCH ~ SECONDS

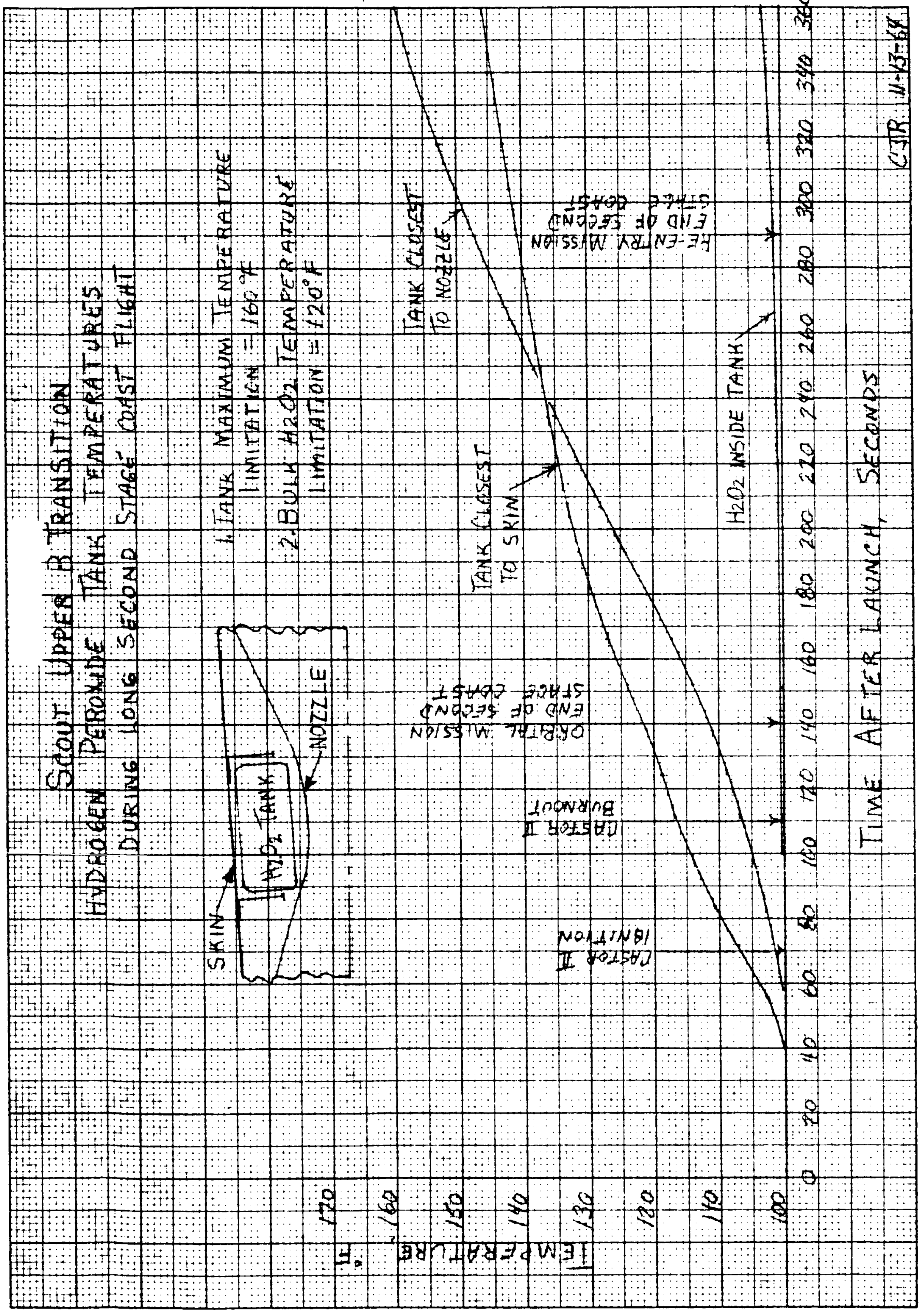
Scout Upper B Transition
Hydrogen Peroxide Tank Temperatures
During Long Second Stage Coast Flight
1. Tank Maximum Temperature Limitation = 160°F
2. Bulk H_2O_2 Temperature Limitation = 120°F
Skin
H_2O_2 Tank
Nozzle
Castor II Ignition
Castor II Burnout
Orbital Mission End of Second Stage Coast
Re-Entry Mission End of Second Stage Coast
Tank Closest to Skin
Tank Closest to Nozzle
H_2O_2 Inside Tank
Temperature °F
100
110
120
130
140
150
160
170
0
20
40
60
80
100
120
140
160
180
200
220
240
260
280
300
320
340
360
Time After Launch, Seconds
CJR 11-13-61

Figure 8.8

K+E 10 X 10 TO ½ INCH 46 1323
KEUFFEL & ESSER CO.

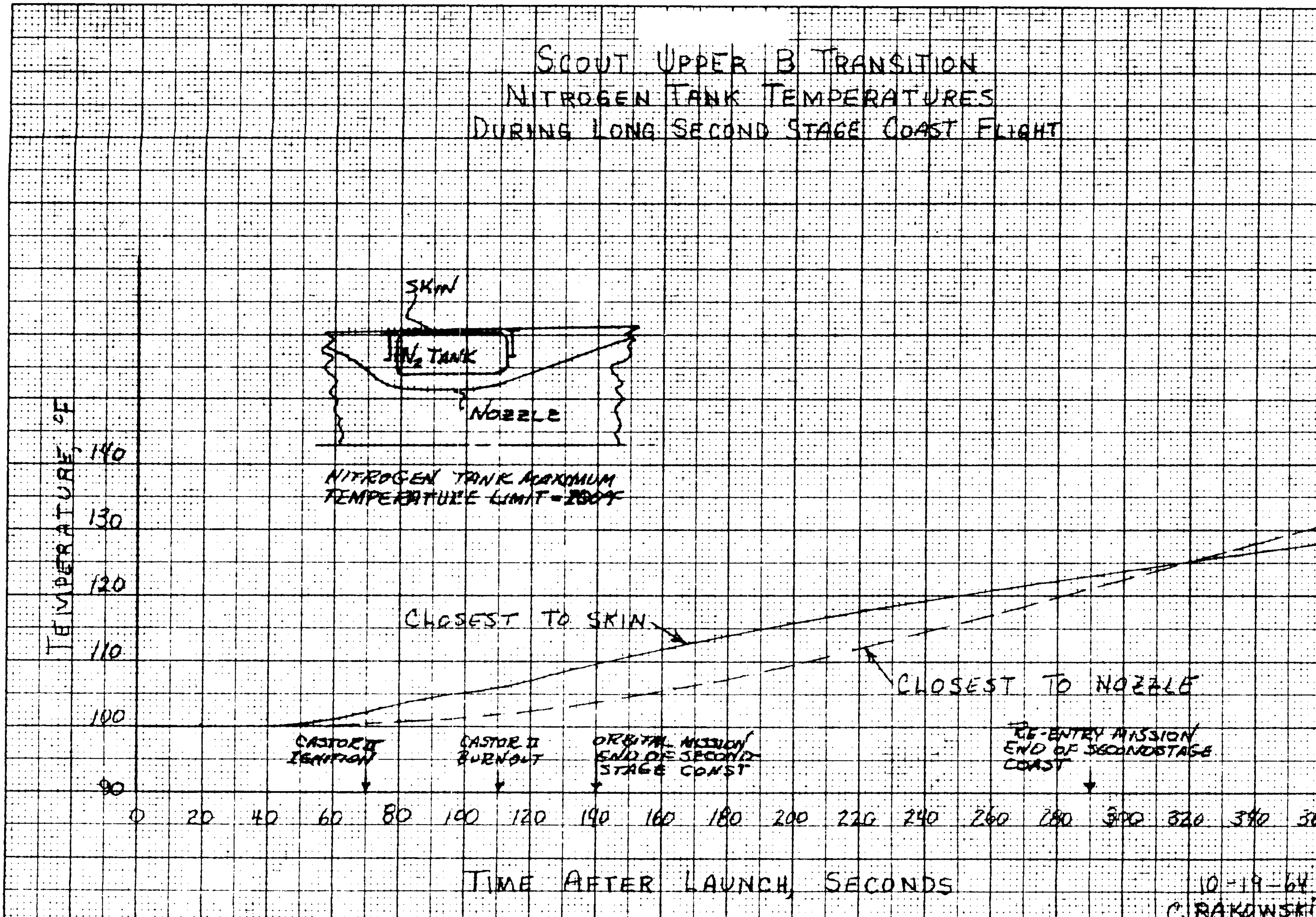

FIGURE 8.9

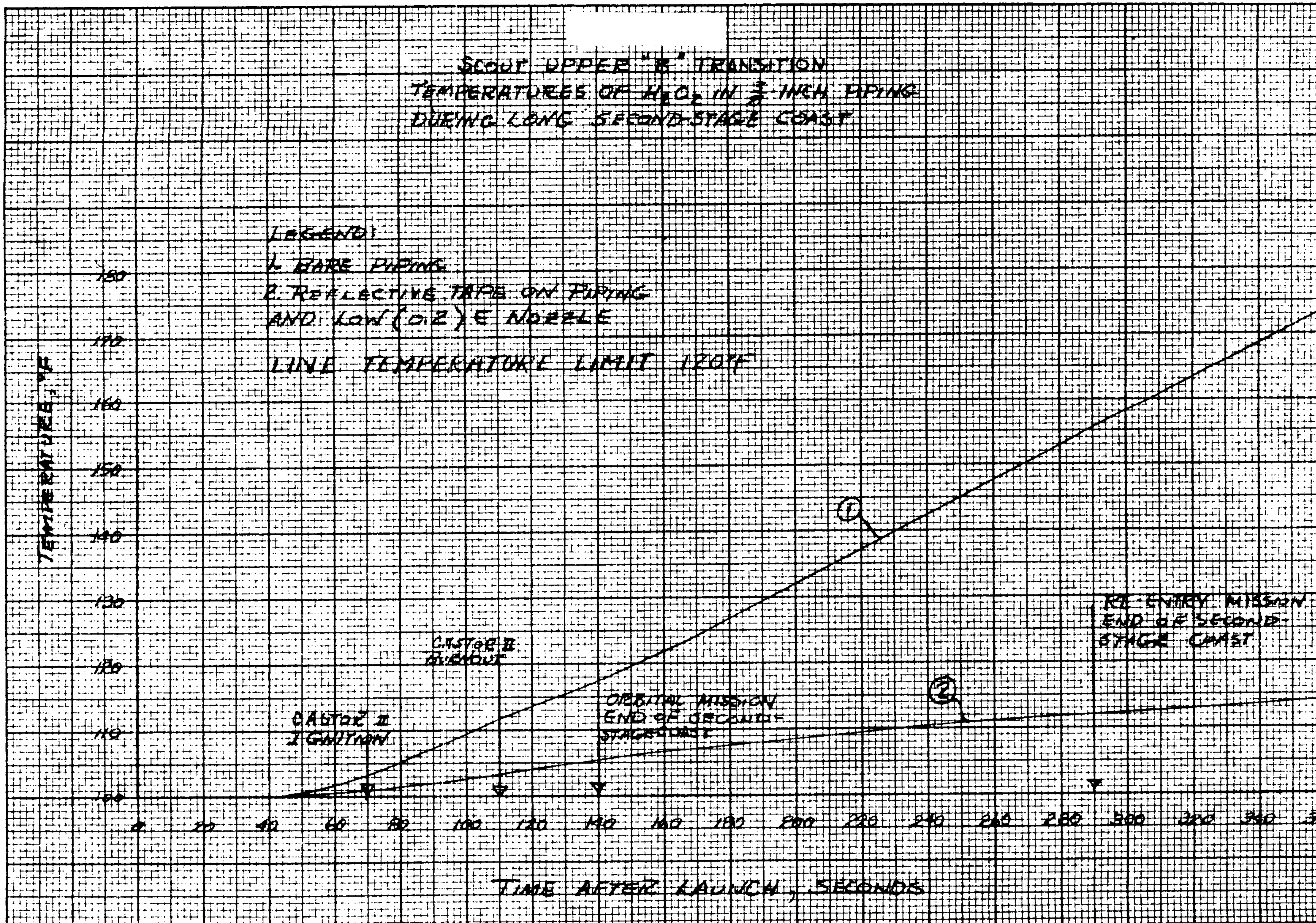
SCOUT UPPER "B" TRANSITION
TEMPERATURES OF H_2O_2 IN $\frac{3}{8}$ INCH PIPING
DURING LONG SECOND STAGE COAST
LEGEND:
1. BARE PIPING
2. REFLECTIVE TAPE ON PIPING
AND LOW (O.Z) E NOZZLE
LINE TEMPERATURE LIMIT 120°F
CASTOR II IGNITION
CASTOR II BURNOUT
ORBITAL MISSION END OF SECOND STAGE COAST
RE-ENTRY MISSION END OF SECOND STAGE COAST
TEMPERATURE, °F
TIME AFTER LAUNCH, SECONDS

FIGURE 8.10

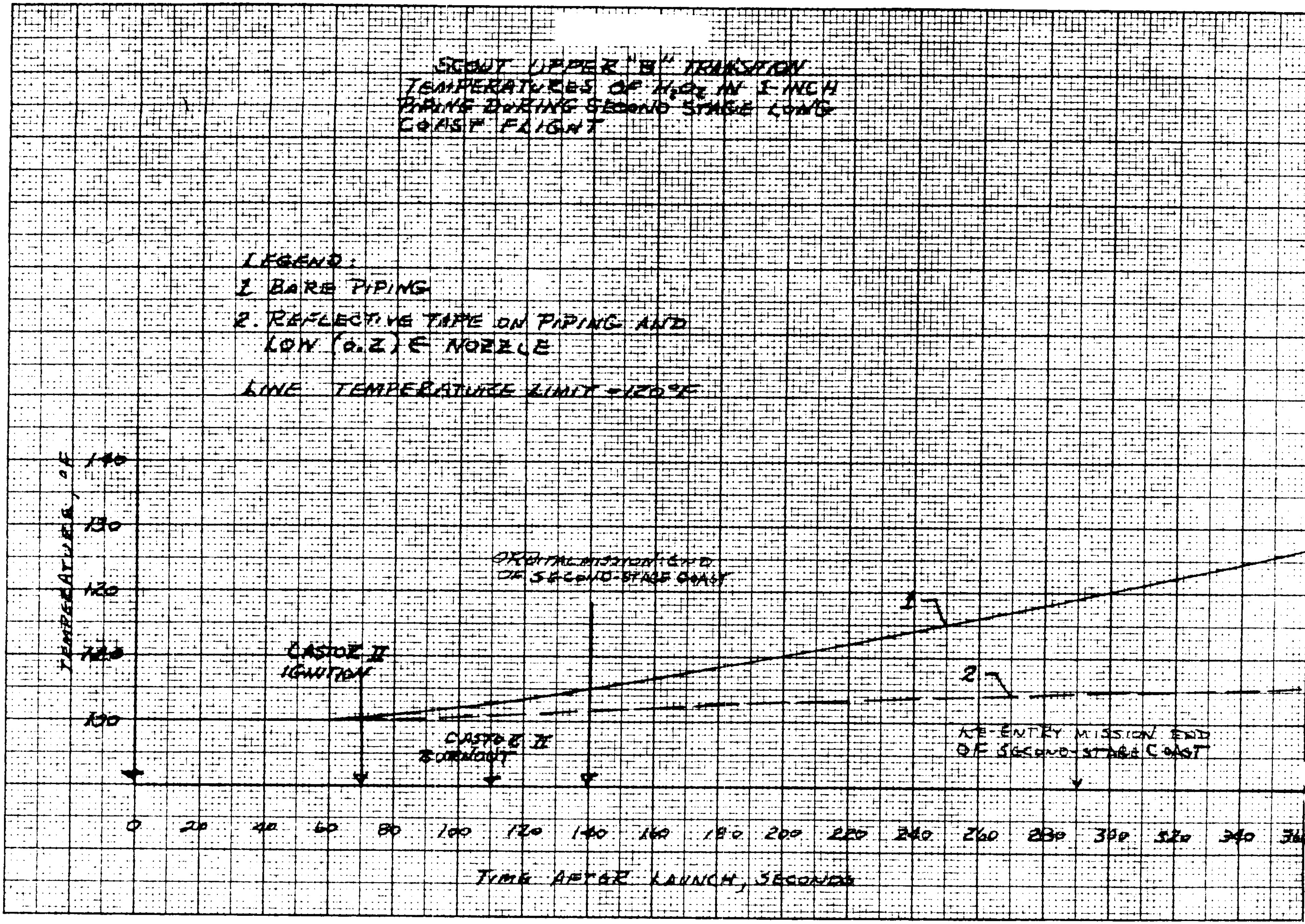
SCOUT UPPER "B" TRANSITION
TEMPERATURES OF H_2O_2 IN 1-INCH PIPING DURING SECOND STAGE LONG COAST FLIGHT
LEGEND:
1 BARE PIPING
2. REFLECTIVE TAPE ON PIPING AND LOW (0.2) ε NOZZLE
LINE TEMPERATURE LIMIT = 120°F
TEMPERATURE, °F
140
130
120
100
CASTOR II IGNITION
CASTOR II BURNOUT
ORBITAL MISSION END OF SECOND-STAGE COAST
RE-ENTRY MISSION END OF SECOND-STAGE COAST
1
2
0
20
40
60
80
100
120
140
160
180
200
220
240
260
280
300
320
340
360
TIME AFTER LAUNCH, SECONDS

FIGURE 8.11

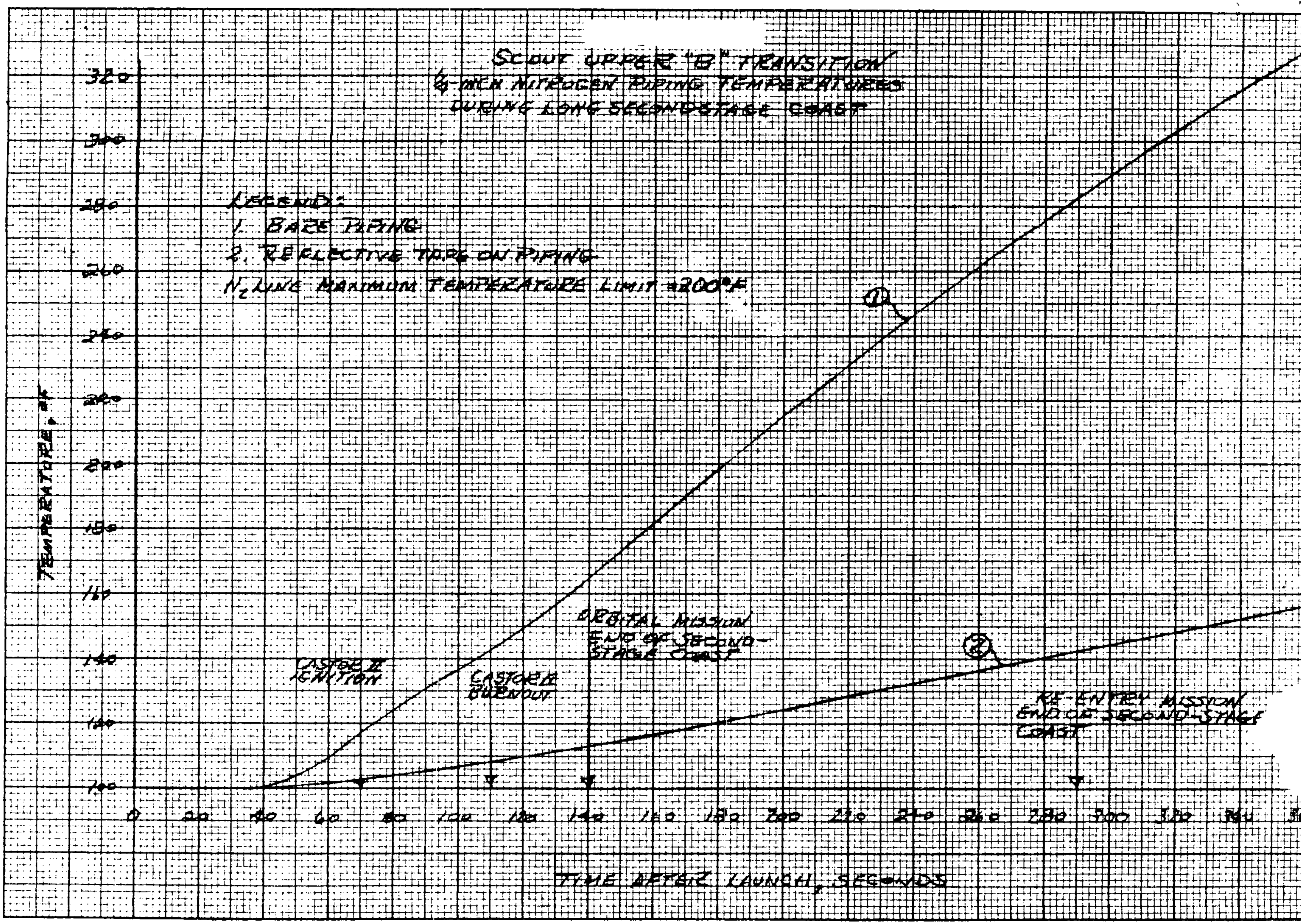
SCOUT UPPER "B" TRANSITION
¼-INCH NITROGEN PIPING TEMPERATURES
DURING LONG SECOND STAGE COAST
LEGEND:
1. BARE PIPING
2. REFLECTIVE TAPE ON PIPING
N_2 LINE MAXIMUM TEMPERATURE LIMIT = 200°F
CASTOR II IGNITION
CASTOR II BURNOUT
ORBITAL MISSION END OF SECOND-STAGE COAST
RE-ENTRY MISSION END OF SECOND-STAGE COAST
TEMPERATURE, °F
TIME AFTER LAUNCH, SECONDS

FIGURE 8.12

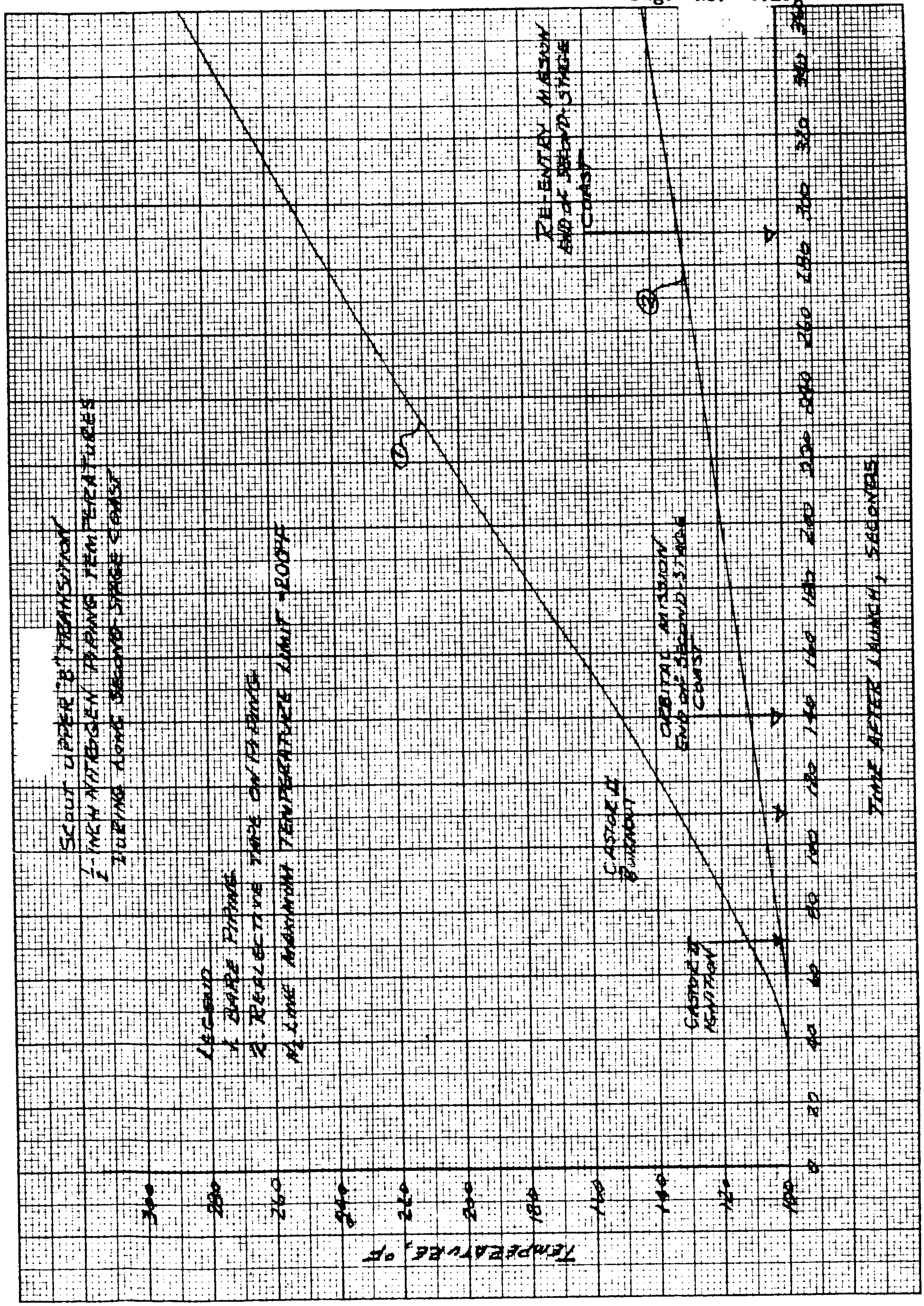
SCOUT UPPER "B" TRANSITION
1/2 INCH NITROGEN PIPING TEMPERATURES
DURING LONG SECOND STAGE COAST
LEGEND
1 BARE PIPING
2 REFLECTIVE TAPE ON PIPING
N2 LINE MAXIMUM TEMPERATURE LIMIT +200°F
CASTOR II IGNITION
CASTOR II BURNOUT
ORBITAL MISSION END OF SECOND STAGE COAST
RE-ENTRY MISSION END OF SECOND STAGE COAST
1
2
TEMPERATURE, °F
100
120
140
160
180
200
220
240
260
280
300
0
20
40
60
80
100
120
140
160
180
200
220
240
260
280
300
320
340
360
TIME AFTER LAUNCH, SECONDS

FIGURE 8.13

Page No. 8.17

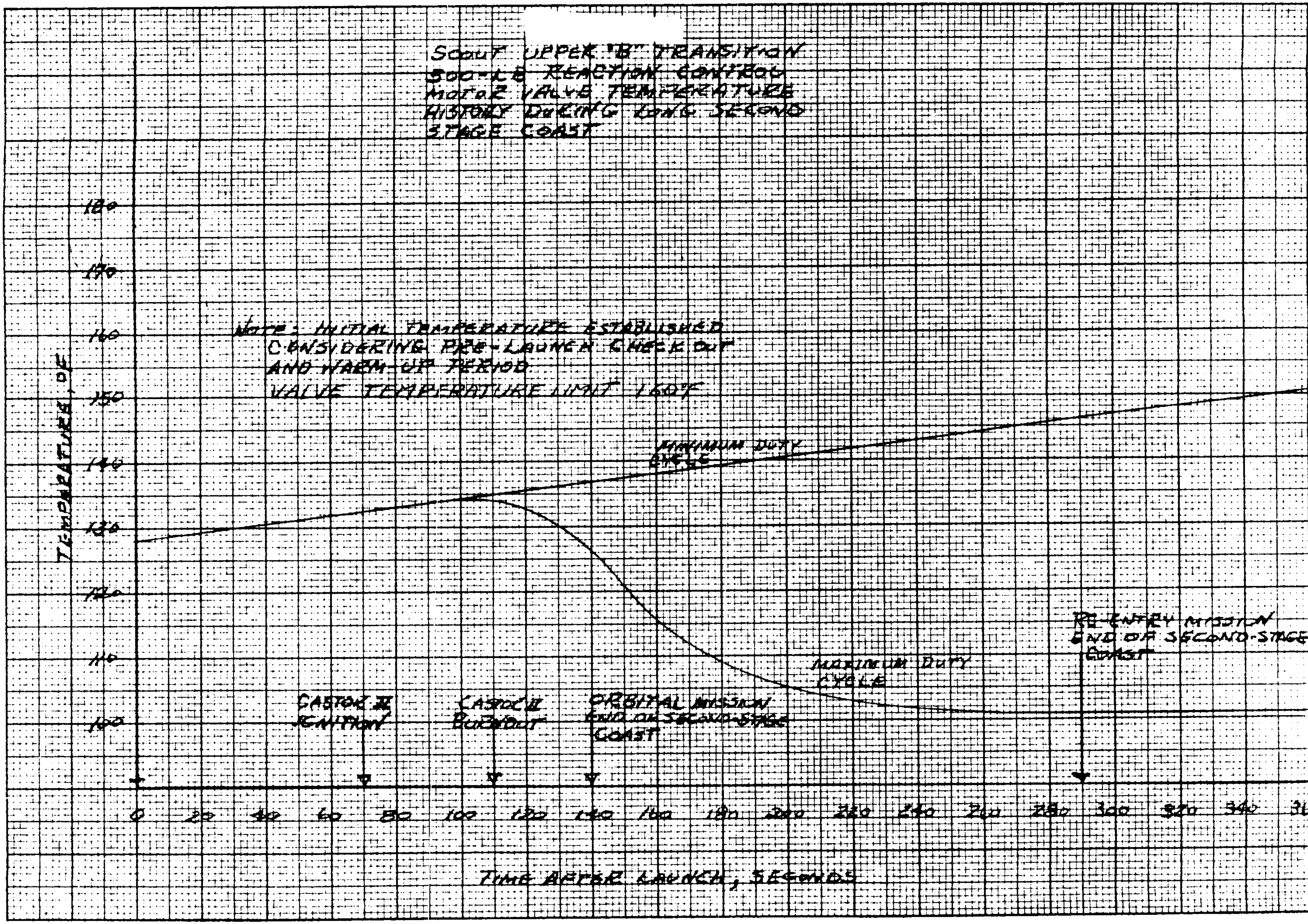

FIGURE 8.14

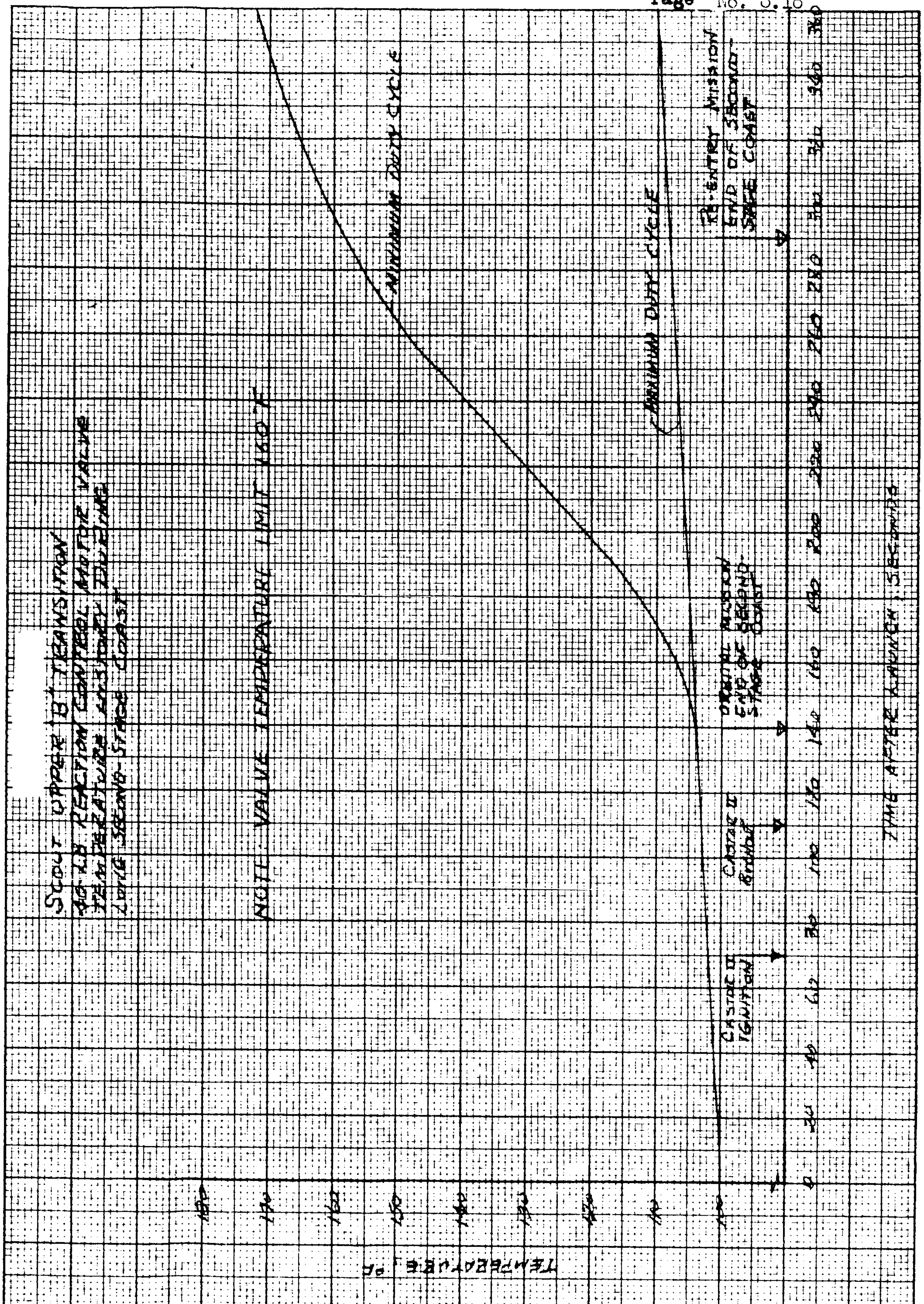
SCOUT UPPER D TRANSITION
40 LB REACTION CONTROL MOTOR VALVE TEMPERATURE HISTORY DURING LONG SECOND STAGE COAST
NOTE: VALVE TEMPERATURE LIMIT 160°F
MAXIMUM DUTY CYCLE
MINIMUM DUTY CYCLE
RE-ENTRY MISSION END OF SECOND STAGE COAST
ORBITAL MISSION END OF SECOND STAGE COAST
CASTOR II BURNOUT
CASTOR II IGNITION
TEMPERATURE, °F
100
110
120
130
140
150
160
170
180
0
20
40
60
80
100
120
140
160
180
200
220
240
260
280
300
320
340
TIME AFTER LAUNCH, SECONDS

FIGURE 8.15

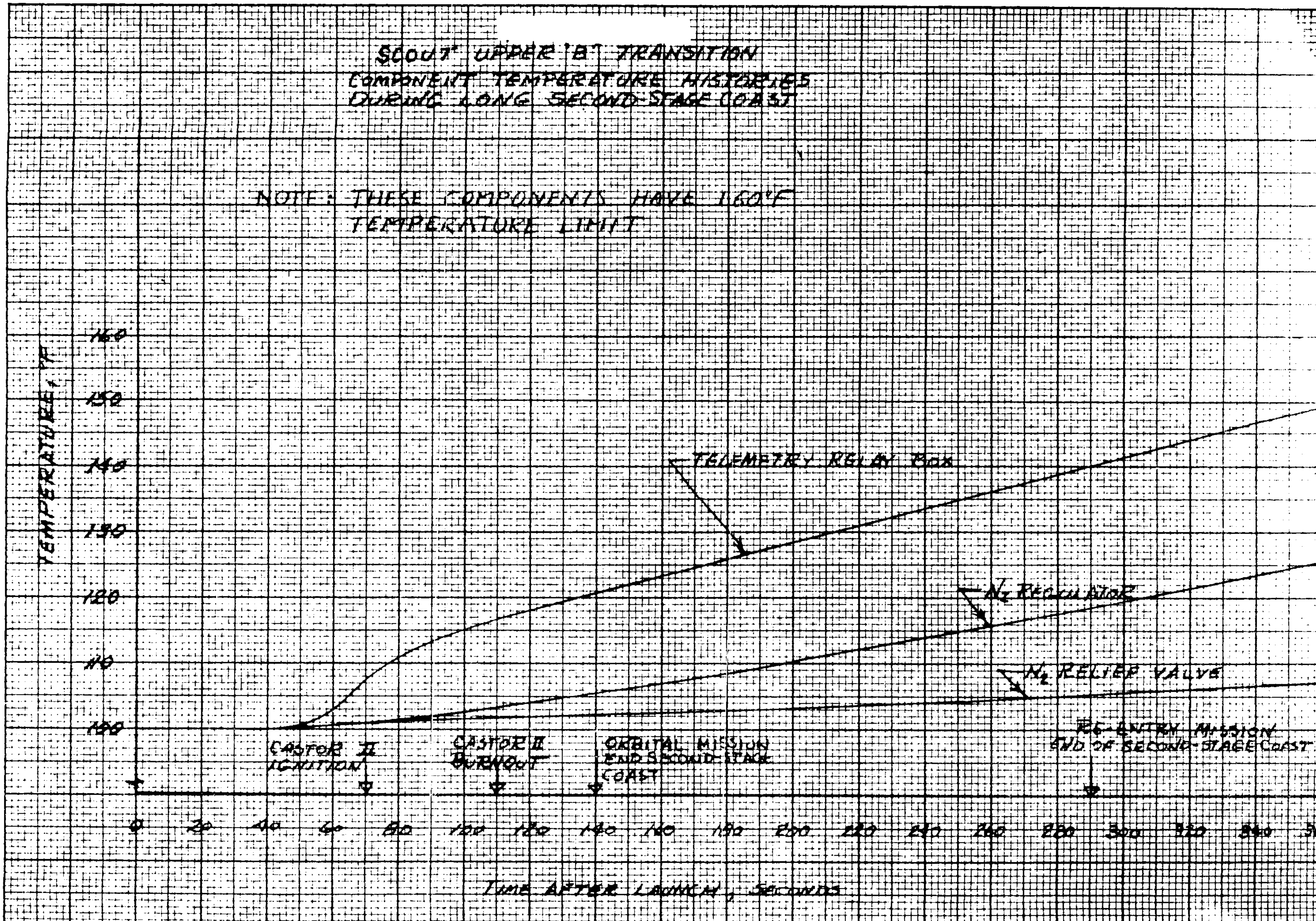
SCOUT UPPER 'B' TRANSITION
COMPONENT TEMPERATURE HISTORIES
DURING LONG SECOND-STAGE COAST
NOTE: THESE COMPONENTS HAVE 160°F
TEMPERATURE LIMIT
TELEMETRY RELAY BOX
N_2 REGULATOR
N_2 RELIEF VALVE
CASTOR II IGNITION
CASTOR II BURNOUT
ORBITAL MISSION END SECOND-STAGE COAST
RE-ENTRY MISSION END OF SECOND-STAGE COAST
TEMPERATURE, °F
160
150
140
130
120
110
100
0
20
40
60
80
100
120
140
160
180
200
220
240
260
280
300
320
340
360
TIME AFTER LAUNCH, SECONDS

FIGURE 8.16

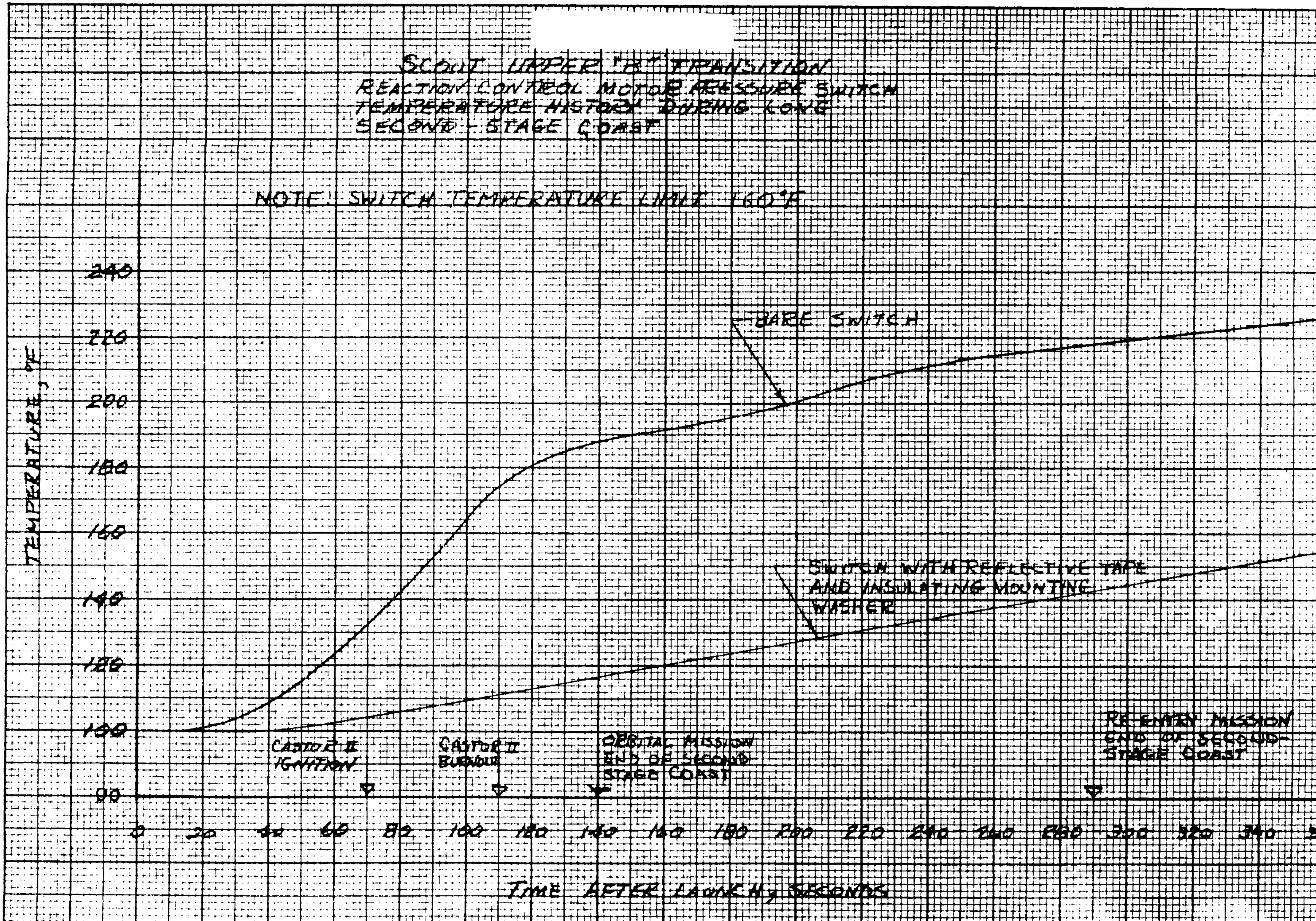
SCOUT UPPER "B" TRANSITION
REACTION CONTROL MOTOR PRESSURE SWITCH
TEMPERATURE HISTORY DURING LONG
SECOND - STAGE COAST
NOTE: SWITCH TEMPERATURE LIMIT 160°F
BARE SWITCH
SWITCH WITH REFLECTIVE TAPE
AND INSULATING MOUNTING
WASHER
CASTOR II
IGNITION
CASTOR II
BURNOUT
ORBITAL MISSION
END OF SECOND
STAGE COAST
RE-ENTRY MISSION
END OF SECOND-
STAGE COAST
TEMPERATURE, °F
240
220
200
180
160
140
120
100
80
0
20
40
60
80
100
120
140
160
180
200
220
240
260
280
300
320
340
360
TIME AFTER LAUNCH, SECONDS

FIGURE 8.17

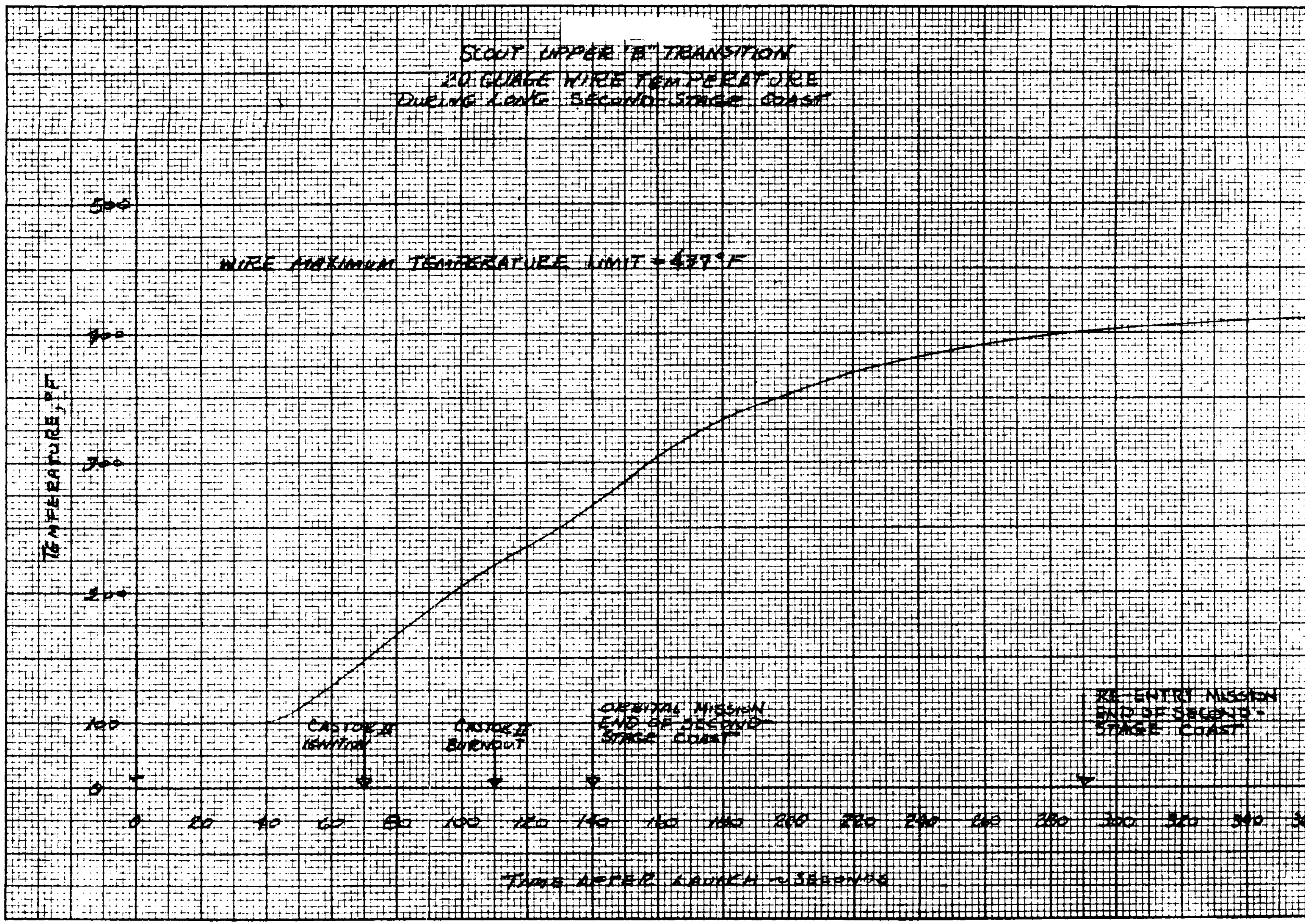
SCOUT UPPER "B" TRANSITION
20 GUAGE WIRE TEMPERATURE
DURING LONG SECOND-STAGE COAST
WIRE MAXIMUM TEMPERATURE LIMIT = 437°F
TEMPERATURE, °F
0
100
200
300
400
500
CASTOR II IGNITION
CASTOR II BURNOUT
ORBITAL MISSION END OF SECOND-STAGE COAST
RE-ENTRY MISSION END OF SECOND-STAGE COAST
0
20
40
60
80
100
120
140
160
180
200
220
240
260
280
300
320
340
360
TIME AFTER LAUNCH ~ SECONDS

FIGURE 8.18

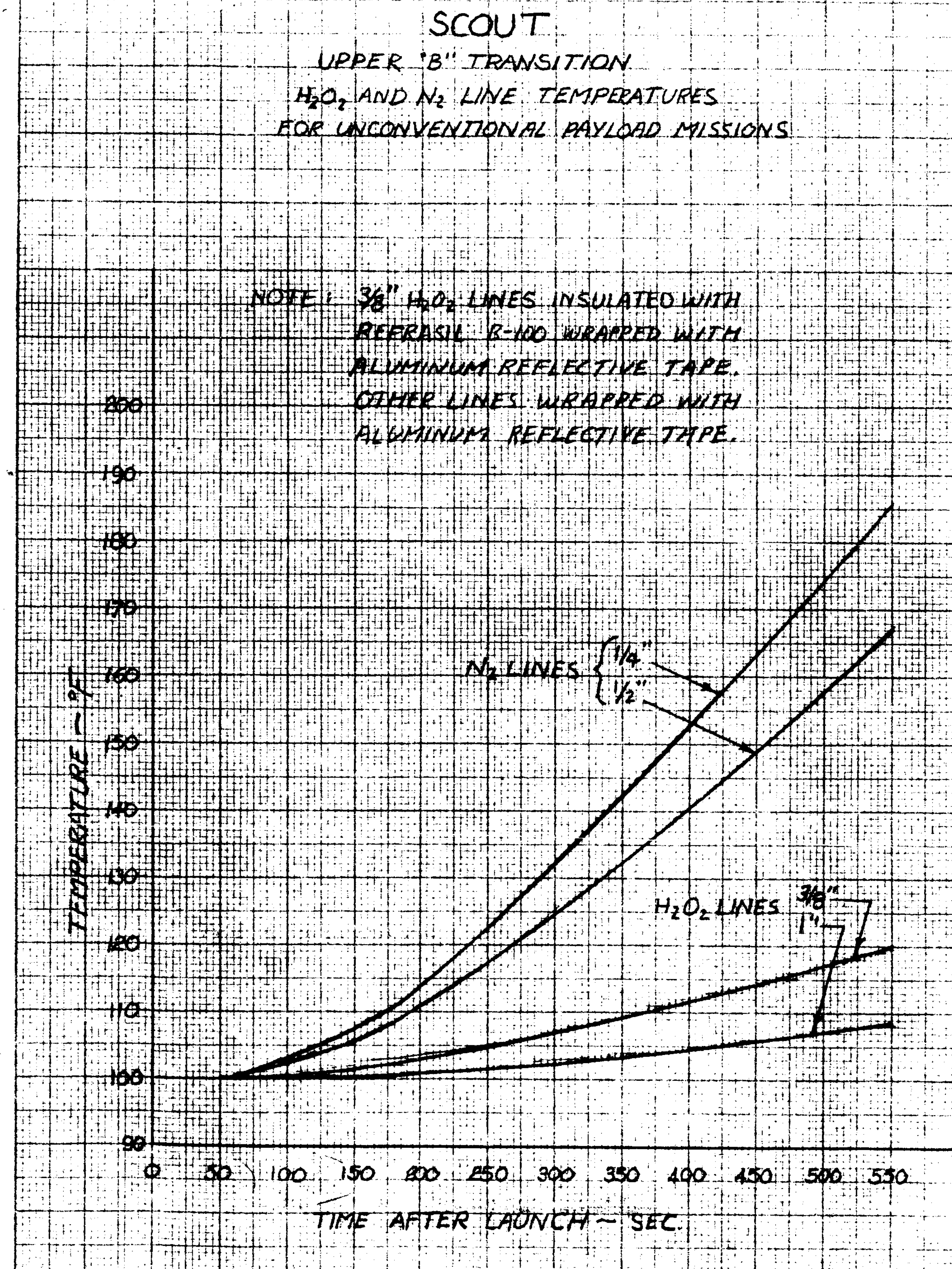
SCOUT
UPPER "B" TRANSITION
H_2O_2 AND N_2 LINE TEMPERATURES
FOR UNCONVENTIONAL PAYLOAD MISSIONS
NOTE: 3/8" H_2O_2 LINES INSULATED WITH
REFRASIL R-100 WRAPPED WITH
ALUMINUM REFLECTIVE TAPE.
OTHER LINES WRAPPED WITH
ALUMINUM REFLECTIVE TAPE.
N_2 LINES
1/4"
1/2"
H_2O_2 LINES
3/8"
1"
TEMPERATURE ~ °F
90
100
110
120
130
140
150
160
170
180
190
200
0
50
100
150
200
250
300
350
400
450
500
550
TIME AFTER LAUNCH ~ SEC.

FIGURE 8.19

REFERENCES

A. Statement of Work "Study to Determine the Effects on the Scout Vehicle Structure Due to Unconventional Vehicle - Spacecraft Configuration" Contract NAS1-3899, Task Order #4.

B. Scout Detail Specification for FY '63, L-2880, 7 January 1963.

C. Report No. 00.138 "An IBM Digital Routine for the Analysis of Flexible Boosters," 20 December 1962.

D. Aerodynamic Design Data Report, AST/EIR-1243, 20 February 1961.

E. A Study of the Stability and Location of the Center of Pressure on Sharp, Right Circular Cones at Hypersonic Speeds, TN D-2283, May 1964, Jim A. Peuland.

F. Equations and Charts for Determining the Hypersonic Stability Derivatives of Combinations of Cone Frustums Computed by Newtonian Impact Theory, TN D-149, November 1959, Lewis R. Fisher.

G. Scout Castor II Stability and Control Evaluation Study, 23 DIR 3-54100/4-07, 5 August 1964.

H. Stability and Control Report, AST/EIR-13381, 2 March 1961.

I. Investigation of the Effects of Elastic Coupling on the Scout Upper Stage Reaction and Control System, Report No. 23.70, 30 April 1963.

J. Study to Determine the Effect on Scout Structure and Stability Due to Payloads in Excess of Current Weight and Center of Gravity Limitations. Report No. 23.144 dated 7 October 1964, LTV Astronautics Division.

K. Military Handbook-5 "Strength of Metal Aircraft Elements" dated August 1962.

L. "Formulas for Stress and Strain" Raymond J. Roark, dated 1954, McGraw-Hill Book Company, Inc.

M. "Advanced Strength of Materials" J. P. Den Hartog, dated 1952, McGraw-Hill Book Company, Inc.

N. "A Summary of Structural Data for Mechanical Fasteners Commonly Used at Chance Vought Aircraft" Report No. 10049, dated 22 December 1955, Chance Vought Aircraft.

O. "Structural Design Manual" Chance Vought Aircraft, December 1955.

P. "Design Data on Low-Pressure Bonded Phenolic-Glass Laminates" Report No. AST/EIR-13501, dated 24 July 1961, Vought Astronautics.

Q. Shields, S. V., "Description and User's Guide to the Thermal Analyzer Routines", LTV Astronautics Report 00.337, December 1963.

R. Martin, D. M., "Recommended Procedures for Analysis of Aerodynamic Booster Components", LTV Astronautics Report 00.302, October 1963.

S. Hansen, C. C., "Thermal Analyzer Routines LVV601 and LVV602", LTV Astronautics AVO 3/52110/62-69, October 1962.